The University Of Sheffield.

Identifying and Characterising Dormancy in Prostate Cancer Cells

Thesis submitted for the Doctor of Philosophy by

Freyja Eve Docherty

Supervised by

Dr Colby Eaton

Department of Human Metabolism
Medical School
University of Sheffield

Submitted November 2014

My studentship was funded by the award of the
Harry Worthington University Prize Scholarship

My research was funded by
Cancer Research UK

Acknowledgements

I wish first and foremost to thank my supervisor Dr. Colby Eaton. I would like to express my gratitude to him not only for the opportunity to conduct this PhD in the first place but also for giving up so much of his valuable time in the pursuit of this work. I thank him for his guidance, support and knowledge. I feel truly lucky to have had him as a supervisor and to have known him as a friend. I am eternally grateful for all he has taught me about research and life in general.

I would also like to thank all the members of the Human Metabolism department and many in Oncology. Too many people to name have offered guidance and support over the part 3 years but I would particularly like to say thank you to Ning Wang and Anne Fowles for sharing their expertise and knowledge, Julia Hough for offering her support and guidance in many a moment of panic and Susan Newton and Kay Hopkinson for putting up with me during all those 6 hour FACS sorts!

I would also like to express my gratitude to my wonderful family, particularly my parents Dinah and Kevin Docherty. There is nothing I could say, do or give you that would equal the lifetime of love and support you have given me but as a small gesture this thesis is in part dedicated to you and the wonderful and inspiring people that you are. Thank you for supporting me in everything I've done and for offering me the guidance I needed to be the best I could be and for making me feel that that would always be good enough.

Finally and significantly, I would like to thank my partner Tim. You have always believed in me, even when I didn't believe in myself and encouraged me to pursue my dreams. Your determination and ambition is an inspiration and I know I would not be here without you. Your patience and kindness is awe-inspiring and I know that I am a better person because you are by my side. This work is dedicated to you as a thank you for who you are and the love you give me.

Declaration

This thesis is a presentation of my original research work under the guidance of my supervisor Dr. Colby Eaton. Wherever contributions of others are involved, every effort is made to indicate this clearly. All the techniques were carried out by myself save all reference to animal work, which was performed by Dr. Ning Wang and Anne Fowles. Fluorescent activated cell sorting (FACS) was performed in the Flow Cytometry Core facility under the assistance of Susan Newton and Kay Hopkinson. Independent scoring of immunohistochemistry was performed by Dr. Colby Eaton and Professor Simon Cross.

List of publications

Papers:

Prostate cancer cells preferentially home to osteoblast-rich areas in the early stages of bone metastasis - evidence from in vivo models.

Wang N, Docherty FE, Brown HK, Reeves KJ, Fowles AC, Ottewell PD, Dear TN, Holen I, Croucher PI, Eaton CL.

J Bone Miner Res. 2014 Jun 23. doi: 10.1002/jbmr.2300

Mitotic quiescence, but not 'stemness', marks the phenotype of bone metastasis initiating cells in prostate cancer.

Wang N, Docherty FE, Brown HK, Reeves KJ, Fowles AC, Lawson M, Ottewell PD, Holen I, Croucher PI, Eaton CL.

In Review

Abstracts:

Identifying Haematopoietic Stem Cell (HSC) Niche Markers in Human Prostate Cancer Cells: Possible Mediators of Dormancy in Metastatic Cancer.

Docherty FE, Wang N, Fowles A, Hough J, Buckle C, Holen I, Eaton CL.

Poster presentation: The 13th International Conference on Cancer-Induced Bone Disease (CIBD 2013), November 2013, Miami, Florida.

Identifying Haematopoietic Stem Cell (HSC) Niche Markers in Human Prostate Cancer Cells: Possible Mediators of Dormancy in Metastatic Cancer.

Docherty FE, Wang N, Fowles A, Hough J, Buckle C, Holen I, Eaton CL.

Oral presentation: The 13th International Conference on Cancer-Induced Bone Disease (CIBD 2013), November 2013, Miami, Florida.

Identifying Haematopoietic Stem Cell (HSC) Niche Markers in Human Prostate Cancer Cells: Possible Mediators of Dormancy in Metastatic Cancer.

Docherty FE, Wang N, Fowles A, Hough J, Buckle C, Holen I, Eaton CL.

Oral presentation: The University of Sheffield Medical school research day, June 2013.

Table of Contents

Summary

Prostate cancer is the second leading cause of cancer death in men in the UK. Around 30% of patients with apparently localized disease at diagnosis and who receive radical surgery to remove the primary tumour, will present with skeletal metastasis, in many cases >5 years after initial treatment. This suggests that prostate cancer cells can persist in a dormant or indolent state, undetected in patients for many years. To investigate states of dormancy in prostate cancer cells, the growth of human prostate cancer cell lines *in vitro* was examined to test the hypothesis that there are sub-populations of dormant cells present even within widely used, rapidly proliferating cell lines. My studies successfully identified these cells, which were then extensively characterised. Parallel studies in our laboratory indicated that these cells had greater potency than other cells in the initiation of metastatic lesions in xenograft models.

To identify dormant cells in three prostate cancer cell lines: PC-3NW1, LNCaP and C42B4, were stained with the lipophilic membrane dye Vybrant DiD. The retention of this dye was used as a marker of dormant or slow-cycling cells. Flow cytometry analysis and fluorescent microscopy identified a dormant cell sub-population in all three prostate cancer cell lines at a frequency of <2% after 14 days in culture. Dormancy was not an intrinsic characteristic of this sub-population, as this phenotype could re-emerge in cultures of separated re-cultured non-dormant cells. The frequency of dormant cells in cultures could be altered by changes in culture conditions and when isolated these cells could be released from dormancy to form colonies. Gene expression profiles for the non-dormant and dormant sub-population were compared by RT-qPCR and a set of differentially expressed, dormancy specific genes identified. Immunofluorescence microscopy was used to assess whether the observed differences in gene expression between populations were reflected in altered specific protein levels. The presence of a specific marker of dormancy, CXCR4, identified by these experiments, was then evaluated in 75 primary patient samples by immunohistochemistry. Elevated CXCR4, as measure by immunohistochemistry, in patient samples correlated to other indicators of poor prognosis but did not independently predict the presence of metastases.

List of common abbreviations

AIPC	Androgen Independent Prostate Cancer
ANOVA	Analysis of Variance
AR	Androgen Receptor
BMP	Bone Morphogenetic Protein
CAB	Complete Androgen Blockade
cDNA	Complementary Deoxyribonucleic acid
Cm-DiI	Chloromethyl-benzamidodialkyl carbocyanine
CRPC	Castration Resistant Prostate Cancer
CSC	Cancer Stem Cell
Ct	Cycle threshed
CTC	Circulating Tumour Cell
CXCL12	C-X-C Motif-Chemokine ligand 12
CXCR4	C-X-C Motif-Chemokine receptor 4
DiD	Vybrant® DiD (CM-DiI derivative)
DiD+	DiD Positive
DiD-	DiD negative
DMEM	Dulbecco Modified Eagle's Medium
DNA	Deoxyribonucleic acid
DTC	Disseminated Tumour Cell
EMT	Epithelial to Mesenchymal Transition
ERG	ETS-related gene
FACS	Fluorescence-activated cell sorting
FBS	Foetal Bovine Serum
GFP	Green Fluorescent Protein

HSC	Haematopoietic Stem Cell
LDA	Low Density Array
mAIPC	Metastatic Androgen Independent Prostate Cancer
MAPK	Mitogen-activated protein kinases
MET	Mesenchymal to Epithelial Transition
ml	Millilitre
MMPs	Matrix metalloproteinases
ng	Nanogram
nl	Nanolitre
nM	Nanomole
NOD/SCID	Non-obese diabetic/severe combined immune-deficient
PBS	Phosphate Buffered Saline
PCa	Prostate Cancer
PCR	Polymerase Chain Reaction
PenStrep	Penicillin Streptomycin
PI	Propidium Iodide
PSA	Prostate Specific Antigen
RFP	Red Fluorescent Protein
RNA	Ribonucleic Acid
RT-PCR	Reverse Transcription PCR
RT-qPCR	Reverse Transcription- quantitative PCR
TGF	Transforming growth factor
TMPRSS2	Transmembrane protease, serine 2
TNM	Tumour Node Metastasis
µg	Microgram
µl	Microlitre

Chapter 1: Introduction

1.1 Background: Prostate cancer

Prostate cancer is the most commonly diagnosed cancer in men in the United Kingdom and is the second most common cause of cancer death (CancerResearchUK, 2011). With effective treatment, the disease has an average 5 year survival rate of around 95% in patients with clinically localized or regionally advanced disease, yet the survival rate of men with distant metastases remains low (Jemal et al., 2008). Prostate cancer commonly metastasizes to bone, most frequently the lower spine, pelvis, and femur. Once established in the bone, disease management is mainly palliative. Metastases to the skeleton cause symptoms such as spinal-cord compression, pathological fracture, bone pain, and anaemia (Logothetis and Lin, 2005).

The prostate itself is a walnut sized gland, which surrounds the upper part of the urethra, below the bladder in men. As a male accessory sex gland, the prostate contributes to seminal fluid with secretions that include a protein called 'prostate specific antigen' (PSA). This protein 'leaks' into the circulation if the prostate is damaged by infection or infarcts, but can also be used as a marker for prostate cancer (Barry, 2001). This is due to the development of cancerous lesions causing damage within the prostate or the presence of PSA producing tumour cells in the circulation (Barry, 2001). A PSA score of between 3-10ng/ml would raise suspicion of prostate cancer potentially confined to the prostate, while a score >10ng/ml carries a 26% chance of a patient having metastatic disease (James Buchanan Brady Urological Institute, 2012). Serum PSA is however a prostate specific rather than tumour specific marker so, when used in prostate cancer diagnosis, it is considered in conjunction with a digital rectal examination followed by a biopsy of prostate tissue to confirm diagnosis (Punglia et al., 2003). The past decade has seen the introduction of Colour Doppler (CD) ultrasound, which uses reflected sound waves to detect blood flow. Brightly coloured areas can indicate the increased blood flow (hyper vascularity) associated with suspected tumours, which then allows for more selective biopsies. However, CD ultrasound is thought to have only a minor advantage over traditional grey scale imaging. Subsequent tests, used to detect metastasis, include an Isotope bone scan, X-ray, MRI, or a CT scan.

Prostate cancer grading and staging are important components of diagnosis due to their prognostic value, and are often used to determine a treatment plan (Humphrey, 2004).

Gleason grading has long been the most commonly used system and involves the histological evaluation of glandular vs. invasive characteristics of tumour cells in prostate biopsies (Gleason, 1988). TNM (tumour, lymph node, and metastasis) staging determines the extent of the cancer and is also used to assign treatment. This system assesses whether the tumour is confined to the prostate, involves the capsule, or extends outside the gland as well as if it has spread to the lymph nodes and finally to the bone and other areas (Sobin, 2001).

Although existing treatments (such as surgery, radiotherapy, and hormone therapy) have radically improved the outcome for prostate cancer patients diagnosed within the early stages of the disease, the prognosis of patients diagnosed with advanced or metastatic prostate cancer remains poor.

1.1.1 Metastasis

Around 80% of prostate cancer patients with metastatic disease respond to androgen ablation and this remains the current first line treatment for advanced/metastatic disease. This is usually accomplished medically via treatment with anti-androgens and/or Luteinizing-hormone- releasing hormone (LHRH) agonists but surgical castration is also still used to remove the major source of circulating androgens in men. Androgen ablation results in immediate relief of symptoms in responding patients and varying periods of disease remission. Combination treatments, of anti-androgens and medical or chemical castration, have also been used together to produce a 'complete androgen blockade' (CAB) (Suzuki et al., 2008). Although this treatment is commonly used, and is an effective strategy to treat advanced stages of the disease, it is not without its drawbacks. Androgen ablation therapy has been reported in several studies to cause osteoporosis, skeletal fracture, and loss of bone mineral density (Daniell, 1997, Diamond et al., 1998), often resulting in a dramatic decrease in the patient's quality of life. Whilst treatment with bisphosphonates limits these symptoms, they are mainly palliative and do not limit the disease (Diamond et al., 1998, Izumi et al., 2009). Bisphosphonates, the most common being Zoledronic acid, can inhibit osteoclast activity and therefore reduce the presence of osteolytic bone lesions. Although they have been shown to reduce pain and skeletal events in advanced androgen independent prostate cancer they can not prevent skeletal metastasis in early stage patients (Saad et

al., 2002). The average duration of disease remission with these treatments is ~2 years after which patients relapse with progressive disease and have an average survival of just 6 months (Whitmore, 1973).

The poor outlook for patients with recurrence of androgen independent prostate cancer (AIPC), following androgen ablation therapy, results from the return of the disease that is often in a more aggressive, rapidly growing form (Abate-Shen and Shen, 2000). This presents a serious clinical problem and has been reviewed by Feldman and Feldman (2001), who explored the mechanisms behind androgen-insensitivity in prostate cancer. The androgen receptor is phosphorylated and dimerizes in response to DHT, which is converted from testosterone, upon cell binding, by 5α-reductase. The phosphorylated AR can then acts as a transcription factor that binds to the androgen response element (ARE) in the promoter region of target genes. This action mediates the activation of downstream genes involved in survival, proliferation and the production of PSA. Feldman and Feldman summarized 5 key pathways by which aberrant activation of the AR could occur: a) hypersensitivity of the androgen receptor (AR): allowing activation by residual low levels of androgen after androgen ablation, b) promiscuity of AR activation: by which ARs lose specificity and are activated by alternative ligands c) the lurker cell theory, d) AR by-pass, and e) the outlaw pathway - in which AR can be activated by the MAPK or AKT pathway via growth factor signalling (Feldman and Feldman, 2001). The latter is highlighted in a study by Kumar et al (2010), who studied the role of the epidermal growth factor receptor (EGFR) in AIPC. Previous research has shown that EGFR gene expression is significantly increased in patients who have undergone hormone therapy (Marks et al., 2008). Indeed, using the androgen-independent cell lines PC-3, DU-145, C4-2B, and the androgen-dependent LNCaP cell line, Kumar and colleagues (2010) found that the natural compound Psoralidin not only inhibited cell growth by blocking EGFR signalling but also induced apoptosis via the activation of the stress mediated protein kinase (SAPK) cascade in AIPC cells. Although Kumar et al. (2010) do not acknowledge the idea that EGFR signalling could be activating the AR in AIPC, they offer strong *in vitro* and *in vivo* evidence that Psoralidin could contribute to the treatment of AIPC (Kumar et al., 2010).

The direct phosphorylation of the androgen receptor by Cdc42-associated tyrosine kinase Ack1 is also proposed to increase progression in AIPC. Mahajan et al. (2007)

indicated a strong correlation between AR phosphorylation and the presence of elevated Ack1 in AIPC tumour samples compared to androgen dependent tumours. The authors also provided evidence that the constitutive activation of Ack1 promotes androgen-independent growth of prostate xenograft tumours (Mahajan et al., 2007). Targeting tyrosine kinase receptors is an attractive candidate for the treatment of AIPC.

Studies have shown that around 50-75% of prostate cancers carry gene fusions (Tomlins et al., 2005) which involves the promoter region of the highly androgen responsive transmembrane protease serine 2 (TMPRSS2) and members of the ETS family of transcription factors (commonly the ERG gene) (Setlur et al., 2008). In 2008, Setlur et al. investigated the relationship between castration-resistant prostate cancer (CRPC) and the androgen responsive TMPRSS2-ERG gene fusion. The presence of this fusion event is associated with increased mortality in prostate cancer (Demichelis et al., 2007) and, although its activity decreases in response to androgen ablation therapy, it has been shown to be reactivated after treatment and contributes to tumour progression (Cai et al., 2009). Although the prospect of AR reactivation is explored in Cai et al., Setlur and colleagues tested the hypothesis that an alternate mechanism is reactivating the TMPRSS2-ERG fusion in CRPC. They found that in AR negative NCI-H660 cells, positive for the TMPRSS2-ERG gene, treatment with the oestrogen receptor α agonist, PPT (propyl pyrazole triol), sustained cell growth and increased TMPRSS2-ERG gene expression. Furthermore, treatment with DRN, an oestrogen receptor β agonist, reduced cell growth (measured by viability assays) and decreased TMPRSS2-ERG expression. Despite the lack of *in vivo* evidence, these results present a novel mechanism by which TMPRSS2-ERG expression is reactivated by the oestrogen receptor α in CRPC. Setlur et al. (2008) suggest the potential treatment of TMPRSS2-ERG positive prostate cancer patients with Toremifene, an oestrogen receptor α antagonist. However, a phase II clinical study conducted in 2001 found no significant reduction in prostate cancer risk when patients were treated with Toremifene (Stein et al., 2001). This suggests that the extent to which TMPRSS2-ERG expression is regulated by the oestrogen receptor α may not be significant enough to be a useful target as a treatment option.

However the results presented in Setlur et al. (2008) do highlight the importance of exploring alternate mechanisms by which androgen-responsive elements can be activated in CRPC and suggest a potential role for oestrogen signalling. The discovery

of the TMPRSS2-ERG fusion, and its association with androgen regulated proliferation in prostate cancer, is an important and evolving field. This data highlights that the ETS proto-oncogene family plays a role in proliferation/survival in these tumours and loss of androgen sensitivity may reflect alternative pathways for ETS/ERG regulation as yet unknown.

The negative side effects and the eventual development of androgen insensitivity, both indicate that androgen ablation therapy does not represent a long-term effective treatment option for advanced prostate cancer. Targeting the earlier stages of metastasis and preventing the dissemination of the disease is likely to provide more effective treatment whilst limiting sequelae. This is particularly relevant with the current trend in clinical practice for earlier diagnosis, when prevention of metastasis is a realistic option.

1.1.2 Current and developing treatments for prostate cancer

Along with osteoclast targeting therapies e.g. Bisphosphonates, radiotherapy remains the first line palliative treatment for castration resistant prostate cancer. While radiotherapy can offer pain relief and a reduction in tumour burden, it often leads to the development of radiation resistant AIPC. A number of new treatments are growing in practice, a selection of these are discussed below.

Sipuleucel-T (Provenge®) is an FDA approved therapeutic cancer vaccine that aims to boost the patient's immune response to prostate cancer cells in AIPC. The potency of this vaccine has been tested in numerous double-blind randomized phase III clinical trials including the IMPACT trial that had a large patient cohort of 512. In the IMPACT 2010 trial, Sipuleucel-T increased the overall survival of patients by an average of 4.1 months compared to placebo treated (Kantoff et al., 2010). However, the patients tested had metastatic AIPC (mAIPC) that was minimally symptomatic. The effects of Sipuleucel-T on advanced mAIPC are currently under evaluation. However a number of other immune based treatments are in Phase II clinical trials, including the vaccine Ipilimumab.

The ability of the angiogenesis inhibitor Ang-(1-7) was assessed in Krishnan et al. (2013). The authors tested the ability of Ang-(1-7) to reduce the incidence of skeletal

metastases in SCID mice following the injection of PC-3 cells into the carotid artery. In mice pre-treated with Ang-(1-7), the authors found a reduction in the incidence of bone tumours when compared to untreated mice (Krishnan et al., 2013). However in the VENICE phase 3, double blind randomised trial the use of an angiogenesis inhibitor in combination with traditional chemotherapy resulted in no improvement in overall survival (OS) in mAIPC patients. The VENICE trial, published in the Lancet Oncology in 2013, tested the ability of the angiogenesis inhibitor Aflibercept, which binds the A and B isoforms of VEGF and placental growth factor to prevent angiogenesis, to increase overall survival in patients with mAIPC. The trial concluded that no improvement in OS of patients treated with Aflibercept compared to placebo was noted and a number of adverse side effects were associated with the drug (Tannock et al., 2013).

As mentioned previously, the aberrant activation of the AR in response to low levels of androgen, or independently of androgens, caused the recurrence of androgen independent prostate cancer (AIPC). The recurrence of AIPC leads to disease progression and poor survival in patients. Tyrosine kinase inhibitors are attractive candidates for the treatment of AIPC as they can prevent the aberrant phosphorylation and activation of the AR following androgen ablation. XL184 (Cabozantinib) is a tyrosine kinase inhibitor that blocks MET and VEGF receptor 2 signalling. In a Phase II randomized discontinuation trial, XL184 was found to increase progression free survival (PFS) after 12 weeks when compared to placebo. In patients with detectable skeletal metastasis, as measured by increased radiotracer uptake in bone scans, XL184 treatment led to an improvement in bone scans compared to placebo. Furthermore, patients with a complete or partial resolution of bone scans, as a result of XL184 treatment, had an increase in PFS after 6 months compared to the placebo (Smith et al., 2013).

A further importance of the development of tyrosine kinase inhibitors is highlighted in Mahajan et al. (2010). The authors provide evidence for the role of Ack1 tyrosine kinase in radiotherapy resistant AIPC; radiotherapy resistant castration-resistant prostate cancer remains an incurable disease. Mahajan et al. provided evidence of the role of Ack1 in the activation of ATM (Ataxia Telangiectasia Mutated) by the binding of phosphorylated AR to the gene promoter region. ATM is involved in the repair of

double strand DNA breaks (DSB) and cell cycle regulation that can occur after radiation treatment. Up-regulation or mutations in this gene are therefore associated with radiation insensitivity. The authors used ChIP-on-chip to demonstrate the recruitment of phosphorylated AR to the ATM promoter in an Ack1 dependent manner and the subsequent increase in ATM mRNA and protein after binding. The authors showed that the Ack1 inhibitor AIM-100 suppressed ATM expression and reduced the repair of DSB following irradiation. AIM-100 was also shown to decrease the growth of irradiated castrate resistant xenograft tumours in mice (Mahajan et al., 2012).

Ski-606 (Bosutinib) is a Src/Abl kinase inhibitor. Rabbani et al. (2010) found that SKI-606 can decrease Src activation and the proliferation and migration of the invasive prostate cancer cell lines PC-3 and DU-145. Interestingly, Rabbani et al. also found that SKI-606 can reduce the volume of skeletal tumours (as measured by micro-computed tomography) in balb/c mice injected intra-tibia with PC-3 cells. The tumour to bone volume ratio was significantly lower in mice treated daily with SKI-606 compared to the vehicle alone (Rabbani et al., 2010). Treatment commenced 3 days post inoculation with PC-3 cells, so although there is evidence that Ski-606 can reduce bone lesions if administered early, the effect on established bone tumours remains to be tested.

In order to target the early stages of metastasis, an understanding of the metastasis initiating cell/cells is required. However, identification and potential drug development for targets in these cells first requires a so far uncharacterised definition of this sub-group.

1.2 Tumour/Metastasis initiating cells

1.2.1 Epithelial to Mesenchymal transition and metastasis

Metastases result when cancer cells are shed from the primary tumour and colonize and grow in distant organs. Metastatic spread is the results of a complex series of events that leads to great attrition between the number of cells that leave the primary tumour and the number of cells that eventually form growing lesions in distant sites. This process involves cell shedding from the primary tumour, invasion of the basement membrane, intravasation into the blood stream and dissemination to distant sites. A small number of

cells will then exit the bloodstream (extravasation) and colonize new organs. This is often referred to as the metastatic cascade.

EMT is a normal process required for embryonic and developmental progression. In cancer it is hypothesised that cancer cells of an epithelial type can hijack this process and revert to a more mesenchymal phenotype. This is characterised by a decrease in the expression of epithelial markers, including E-cadherin, and an increase in mesenchymal cell markers, including vimentin (Tsai and Yang, 2013). This is hypothesised to result in the acquisition of a more migratory phenotype and contribute to the development of metastases. Evidence suggests that EMT induction is caused by the up-regulation of the transcription factors Twist, Snail and Zeb via TGF-β signalling (Tsai and Yang, 2013). Studies suggest that EMT occurs in the early stages of the metastatic cascade, allowing the dissociation of cells from the primary tumour due to loss of cell-cell contact. Cells of a mesenchymal phenotype also produce increased levels of MMPs, which contribute to increased invasion through the basement membrane. EMT is also thought to occur at later stages to allow cell migration into the circulation. Yu et al. (2013), found that circulating tumour cells in advanced-stage breast cancer are characterised by a more mesenchymal phenotype with increased expression of mesenchymal markers including fibronectin by RNA in-situ hybridisation.

In the prostate the androgen receptor, along with TGF- β signalling, is hypothesised to act as an inducer of EMT, as it positively regulates Snail and represses E-cadherin (Grant and Kyprianou, 2013). Aberrant activation of EMT in prostate cancer has been linked to poor prognosis. Gravdal et al. (2007), found that increased N-cadherin and decreased E-cadherin, 'the EN-switch' indicative of EMT, was linked to poor prognosis when identified by immunohistochemistry in tissue microarray samples from patients with known clinical outcome (Gravdal et al., 2007).

Although there is clear evidence that EMT is important in the metastatic cascade, more research is required to understand and exploit this knowledge to aid patient treatment. This is particularly significant as there is evidence that cells of a mesenchymal phenotype have an increased resistance to chemotherapeutics (Hoshino et al., 2009).

1.2.2 Mesenchymal to epithelial transition and metastasis

Mesenchymal to epithelial transition (MET) has recently been implicated as an important mechanism in the later stages of metastasis i.e., the epithelial phenotype is more associated with secondary site colonization while a mesenchymal phenotype, in cancer cells, is linked to increased motility and invasion (Chaffer et al., 2006). Chaffer et al. (2006) examined the frequency of metastasis using a mesenchymal-like bladder cancer cell line, Tsu-Pr1, and two epithelial-like bladder cancer cell lines, B1 and B2, from different sites of inoculation in SCID mice. They found that following orthotopic inoculation mesenchymal-like Tsu-Pr1 cells formed more micrometastasis than B1 and B2 cells but following intracardiac or intratibial inoculation epithelial-like B1 and B2 cells formed more metastases (Chaffer et al., 2006). Chaffer and colleagues argued that these results show that the epithelial phenotype is more associated with the latter stages of the metastatic cascade. Therefore, it is likely that at some point during the metastatic cascade, cells that have undergone EMT need to revert back to an epithelial phenotype by MET in order to expand in the new metastatic site. Indeed in a study by Tsai et al. (2012) using chemically induced squamous cell carcinomas in mice, it was found that carcinoma cells that have undergone irreversible TWIST mediated EMT, had an increased ability to disseminate to the lung. However, the subsequent reduction in proliferation rate of these mesenchymal-like cells resulted in a reduced rate of detectable metastases forming. It was found that reversible TWIST induction was required to allow proliferation and the development of micrometastatic lesions, highlighting the importance of MET in the progression of metastasis (Tsai et al., 2012). However, it is currently unclear whether the induction of MET is required for the reactivation of cell proliferation or whether proliferation induces MET. The processes of EMT and MET and the occurrence of tumour dormancy will be discussed in section 1.4.

1.2.3 Cell fusion

The potential role of cell fusion in the initiation and progression of cancer remains an over-looked and under-researched area. However, studies by Bhatia et al. (2008) isolated and characterised low/non-tumourigenic L-cells from PC-3, DU145 and 293T cell lines and showed how co-injection with senescent normal human prostate (NHP)

epithelial cells increased tumourigenesis *in vivo* compared to injection of L-cells alone. Bhatia and colleagues showed via fluorescent labelling that cell fusion was occurring between these cells. As further evidence, stable NHP6/293T-L hybrid cells were injected into NOD/SCID mice and showed increase tumourigenicity (6/6) compared to the parental cell lines (293T 1/6, NHP6 0/5). However, the role of cell fusion in cancer is controversial as it has been found to be both an indicator of good (Larsson et al., 2007) and poor (Larsen et al., 2009) prognosis in different cancers.

However, evidence that cell fusion contributes to the metastatic phenotype has been proposed in Chakraborty et al. (2001). This research builds on the previous observation that mouse melanoma cells fused to either mouse macrophages or human monocytes had an increased metastatic phenotype, based on increased motility *in vitro* and increased metastatic incidence *in vivo* (Rachkovsky et al., 1998). Chakraborty and colleagues claimed for the first time to show that not only does fusion between human cells and mouse cells occur but, via RT-PCR, the human gene SPARC is expressed in the resulting, metastatic, hybrid. Although good evidence for cell fusion, SPARC is not found to be commonly mutated in human cancer (only one record of a mutation in the Catalogue Of Somatic Mutations In Cancer (COSMIC, 2011) in human glioblastoma (McLendon et al., 2008)) so any contribution it makes to the cancer phenotype is unclear. However, SPARC expression was found to be linked to high-grade tumours in prostate cancer patient samples in a gene expression profiling study conducted by Lapointe et al. (2003). In which, SPARC expression was found to be associated with high grade tumours (classified as a Gleason grade of ≥4+3) from cDNA microarray analysis (Lapointe et al., 2004). However, of the 112 prostate samples taken only 9 were from lymph node metastases and none were from bone metastases so the profile of these tumours cannot be taken as an indicator of osseous metastases. However, these results indicate that SPARC may contribute to tumour progression adding significance to the results found in Chakraborty et al. (2001).

The role of cell fusion in tumour progression in breast cancer has been explored in Jacobsen et al. (2006). In this study a hybrid cell line, BJ3Z, isolated from a human xenograft grown in a nu/nu mouse was shown to be the result of a fusion event as it expressed markers of mouse stromal origin but also contained human chromosomes. Following *in vivo* inoculation, the BJZ3 cell line was found to be highly aggressive and

metastatic. The authors argue that cell fusion between epithelial tumour cells and the host stroma may result in genetic alterations that increase the metastatic potential of the tumour (Jacobsen et al., 2006). Cell fusion may therefore present a mechanism that contributes to the heterogeneity of tumour cells but until definite studies can clarify the frequency of such fusion events it is unclear to what extent fusion can influence cancer phenotype.

1.2.4 Cancer stem cell theory

The theory that there may be a specific sub-set of cells that are solely responsible for the initiation and maintenance of many cancers is receiving world-wide attention (Visvader and Lindeman, 2008). The cancer stem cell (CSC) theory states that cells exhibiting the stem cell-like properties of self-renewal and multi-potency are responsible for the malignant growth of tumours in the body (Reya et al., 2001). This is an attractive concept as it provides for a cellular hierarchy within tumours where CSCs divide asymmetrically, generating the phenotypic heterogeneity observed, but are also themselves able to act as a reserve population. The latter characteristic implies some level of mitotic quiescence or dormancy, which would confer insensitivity to DNA damaging drugs and be a driver of chemo-resistance in tumours (Reya et al., 2001). Originally the CSC theory was documented in acute myeloid leukaemia in which only a single cell population was found to be enriched for clonogenic ability and capable of forming tumours in SCID mice (Lapidot et al., 1994). This population was identified by the cell-surface phenotype CD33+/CD38-.

The use of putative stem cell markers has since led to the identification of potential CSCs in many other cancers including breast (CD44+/CD24-) (Al-Hajj et al., 2003) and pancreatic cancer (CD44+/CD24+/ESA+) (Li et al., 2007). Indeed, despite on going controversy surrounding CSC theory the identification of novel CSCs in multiple cancers is still a lucrative area of research. For example a novel CSC with mesenchymal-like, as apposed to radial glial-like, characteristics was recently identified in primary glioma samples from 20 patients cells (Brennan and Frame, 2014).

It has been hypothesised that a CSC sub-population exists within prostate cancers. Collins et al. (2005) presented evidence for a CD44+/α2β1hi/CD133+ population of

cancer stem cells isolated from human prostate tumours. Collins et al. (2005) demonstrated the heightened ability of these cells to produce colonies, proliferate and survive anchorage independent growth *in vitro* (Collins et al., 2005). Initially it was thought that this sub-population was androgen receptor (AR) negative, however Williamson et al. (2012) used a combination of techniques (flow cytometry, quantitative Real-time PCR and western blot) to show that isolated α2β1hi/CD133+ did express low levels of the AR. It is thought that this may contribute to the development of CRPC from the CSC pool (Williamson et al., 2012). However, Collins et al. (2005) did not demonstrate the ability of this cell sub-population to produce tumours, or an ability to differentiate, *in vivo,* a hallmark of CSCs. Patrawala et al. (2006) however, showed that CD44+ cells isolated from the LAPC-4 prostate cancer xenograft model had an increased tumour incidence (67%) when injected into SCID mice compared to CD44- cells (6%). Further to this, CD44+ cells isolated from LAPC-9 xenograft models (originally extracted from a bony metastasis) showed increased metastasis (33%) *in vivo* following surgical orthotopic implantation (SOI) compared to CD44- cells, also from lapc-9, (0%). However, although LAPC9 was bone derived, the metastases were mainly confined to lumbar lymph nodes and bladder and not to the bone. (Patrawala et al., 2006). The theory that tumour cells use the lymph nodes as a starting point to invade other organs or whether they are merely a 'dead end' in the process of progression (Joyce and Pollard, 2009) remains to be tested in this model. A table summarizing some of the key molecules associated with the prostate cancer stem cell phenotype can be seen in Table 1.1.

Marker	Explanation	Evidence
CD44+	Cell surface glycoprotein	CD44+/α2β1hi/CD133+ prostate cancer cells shown *in vitro* to have an increased ability to produce colonies, proliferate and survive anchorage independent growth *in vitro* (Collins et al., 2005). Furthermore CD44+ cells had an increased tumourigenic ability in SCID mice compared to CD44- cells (Patrawala et al., 2006).
$\alpha2\beta1^{high}$ (integrin)	Transmembrane protein that mediates cellular interactions	As above (Collins et al., 2005), and has previously been characterized as a marker for normal human prostate epithelial stem cells (Collins et al., 2001).
CD133+	Cell surface glycoprotein	As well as characterization *in vitro* in prostate cancer (Williamson et al., 2012) (Collins et al., 2005), CD133+ cells also show stem cell properties and increased tumourigenicity *in vivo* in small and non-

		small cell lung cancer (Eramo et al., 2008).
CD24-	Cell surface glycoprotein	CD44+/CD24- cells display stem cell properties, such as anchorage independent growth, and show high tumourigenesis in SCID mice (with as low as 100 cells) a characteristic of CSC. CD44+/CD24- cells also show an ability to give rise to other cell types, shown by FACS in the tumours removed from SCID mice (Hurt et al., 2008).
ALDH+	Aldehyde dehydrogenase enzyme	When compared to $ALDH^{low}$ cells $ALDH^{high}$ cells produced more colonies and were more motile *in vitro* and produced greater tumour burden and increased bone marrow growth in mouse models (van den Hoogen et al., 2010).
hTERT	Human Telomerase reverse transcription enzyme	The established HPET (human prostate epithelial/hTERT) cell line was shown to express embryonic/progenitor cell markers, such as SOX2 and NANOG. These cells were also shown to re-establish the parental tumour *in vivo* indicating hTERT as a possible prostate CSC marker (Gu et al., 2007).

Table 1.1 A summary of the key markers found to be associated with prostate cancer stem cells.

1.2.4.1 Epithelial to mesenchymal transition as a source of CSCs

Recently Kong et al. (2010) investigated the link between epithelial to mesenchymal transition (EMT) and the CSC phenotype in prostate cancer. Kong et al. (2010) identified prostate cancer cells with the EMT phenotype (PC-3 PDGF (platelet derived growth factor D over expression) and $ARCaP_m$) that also exhibited stem cell-like properties, such as self-renewal and high clonogenic ability. Moreover, PC-3 PDGFD cells showed increased gene expression of stem cell markers such as Sox2 and Oct4 (Kong et al., 2010).

Kong and colleagues did not explicitly suggest that EMT could be a mechanism by which CSCs are generated but this theory is explored in Santisteban et al. (2010). Following EMT via immune-induction in epithelial breast cancer cells, Santisteban and colleagues generated tumour cells with stem cell properties and the breast cancer stem cell surface phenotype (CD44+/CD24-) as proposed in Al-Hajj et al. (2003) (Santisteban et al., 2009). Indeed, this theory is also supported by Mani and colleagues (2008) who, following induced EMT in human mammary epithelial cells (HMLE), produced mesenchymal like cells that expressed stem cell markers and formed mammospheres *in vitro*, a characteristic of breast epithelial stem cells. However,

HMLER cells (HMLE cells transformed with the oncogene V12H-Ras) failed to form tumours *in vivo* unless subject to continuous EMT-induction via Twist or Snail; EMT-inducing transcription factors (Mani et al., 2008).

Without further research it is easy to discount these findings as it is unknown how realistic constant EMT-induction could be in a real cancer scenario. EMT does, however, present an alternate mechanism that seems to contradict the accepted intrinsic theory of CSC origin i.e. from an existing stem or progenitor cell that has undergone oncogenesis. However in a recent review by Chaffer and Weinberg (2011) they speculate that CSCs may originate from both processes and, by the very nature of this, contribute to tumour heterogeneity (Figure 1.1.) (Chaffer and Weinberg, 2011). As prostate cancer is characterised by extreme heterogeneity this is an attractive prospect but requires further research.

1.2.5 CSC and cell fusion

The hypothesis that cell fusion events between a stem cell and an oncogenic somatic cell could represent a source of CSCs (Figure 1.1) was explored in Bjerkvig et al. (2005). Indeed, a recent study by Xu et al. (2014) found that the co-culture of RFP labelled human MSCs with GFP labelled human lung cancer cell lines generated dual labelled heterotypic fused or 'hybrid' cells. They found that these hybrids had several characteristics of mesenchymal cells e.g. increased expression of vimentin and decreased expression of E-cadherin, as well as increased characteristics of stem cells. Hybrids expressed higher levels of stem cell markers by quantitative RT-PCR e.g. SOX2 and NANOG and had an increased ability to form spheres in soft agar, a characteristic of stem cells. These cells were also more tumourigenic in xenograft models than the original parental cell lines (Xu et al., 2014). It is clear that cell fusion events can lead to the development of hybrids with increased stem cell like characteristics and may represent a source of CSCs. However, as with EMT cell fusion may represent only a possible mechanism to generate stem cells and multiple methods may be employed in a tumour to contribute to heterogeneity and spread.

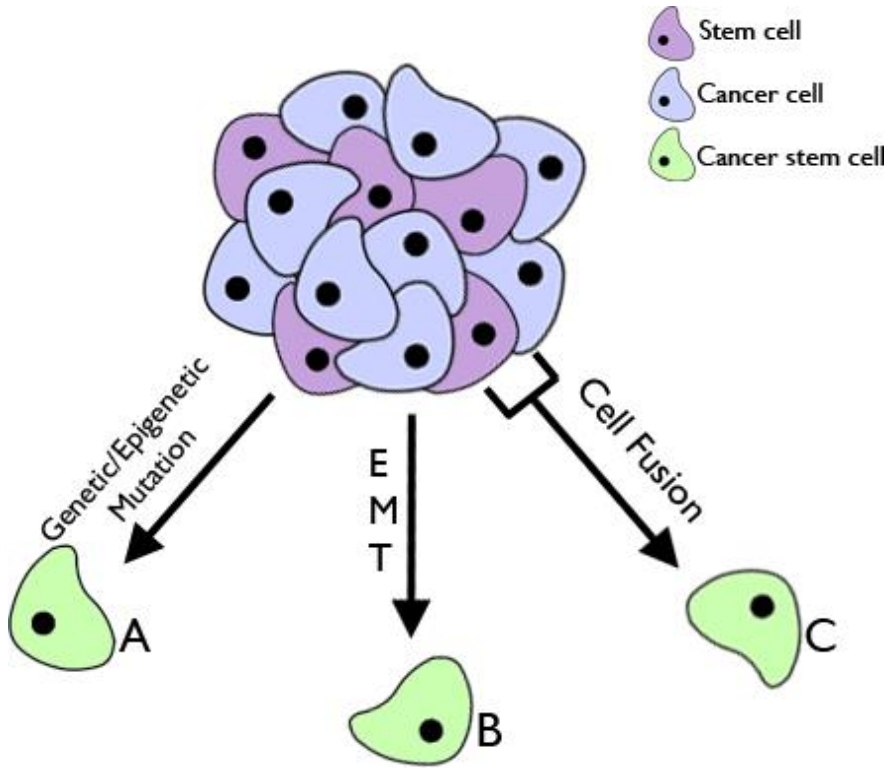

Figure 1.1 The proposed mechanisms of CSC theory. A. An existing stem/progenitor cell receives an oncogenic hit (Chaffer and Weinberg, 2011). B. EMT (epithelial to mesenchymal transition) causes the resulting mesenchymal cell to exhibit stem-cell like properties (Mani et al., 2008, Santisteban et al., 2009). C. Heterotypic fusion of a stem cell to a genetically altered tumour cell can result in a cancer cell with stem cell properties (Xu et al., 2014).

1.2.6 Plasticity of the CSC phenotype

As well as being heterogenic in origin, there is evidence that the CSC phenotype is plastic within cell lines and tumours. The review by Tang (2012) summarises some of the key evidence that supports this notion. Tang mentions that although normal stem cells do not often exhibit plasticity they do retain the potential and in a less stringently organised system, such as a tumour, CSC may be in a fluidic state of differentiation and de-differentiation (Tang, 2012).

Wang et al. (2010) provided evidence that CD133+ Glioblastoma cells (the proposed CSC sub-population in Glioblastoma) have the ability to differentiate into CD133+/CD144+ endothelial cells (Wang et al., 2010). Patrawala et al. (2006) demonstrated that this process can work the other way, in that tumour cells can de-differentiate into CSC. Using the human prostate cancer cell line DU145, the authors showed that CD44- DU145 cells could generate cells that are CD44+ (the proposed prostate cancer stem cell phenotype) when seeded in clonal assays. Tang (2012) also discussed the hypothesis that this de-differentiation of tumour cells into CSC can be

increased by environmental stresses like hypoxia or drug treatment. This highlights the importance of developing novel therapeutics that not only target the bulk tumour population but also de-differentiated CSC.

1.2.7 Alternative interpretations of evidence for cancer stem cells (CSCs)

Despite the growing body of research, CSC theory has come under criticism for, amongst other things, the lack of definitive evidence in many studies that the isolated CSC has an increased ability, *in vivo*, to effectively recreate the original tumour phenotype (Lathia et al., 2010). Furthermore, the use of other *in vitro* assays to distinguish stem-cell like properties, such as sphere formation, have been criticised that the growth conditions used were not analogous to those present in *in vivo* tissues (Lathia et al., 2010). In addition a limitation for one of the key observations in the CSC theory, that only a very small population can initiate tumour growth, was highlighted by Quintana et al. (2008). By optimising xenotransplantation conditions and performing them in increased immuno-deficient mice (NOD/SCID IL2Rγnull), Quintana and colleagues showed an increase in the number of tumourigenic melanoma cells and furthermore, could identify no marker that could distinguish tumourigenic from non-tumourigenic cells (Quintana et al., 2008). The lack of clear markers may however be due to the method of detection used, as Eaton et al. (2010) investigated the expression of markers in the proposed prostate cancer stem cell population and highlighted the difficulty of detecting cell surface markers as well as the potential to miss certain markers due to small numbers of cells or technical complications (Eaton et al., 2010).

Despite the criticisms, the concept that CSCs are present in tumours may yet prove valuable. Treatments targeted at this population could remove the threat of disease relapse that could occur with treatments that leave residual CSCs (Reya et al., 2001). Further characterisation of CSCs in a range of cancers, including prostate cancer, may reveal key traits or mechanisms that can be exploited to eradicate this threat.

1.3 The bone metastatic niche

Despite the advances made in the characterisation of the tumour/metastasis initiating cell, Paget's renowned 'seed and soil' theory states that this is only a partial explanation for the process of malignancy (Ribatti et al., 2006). An understanding of the environment (the 'soil') to which these cells home, is also crucial. In the case of prostate cancer this is the bone microenvironment, a complex site of resorption and remodelling, which has been an active area of research for many years.

1.3.1 The 'vicious cycle'

It is now widely accepted that the frequent metastasis of prostate cancer to bone is due to interactions between these cells and a 'bone metastatic niche', which creates a favourable environment for attachment and growth. Indeed it has been suggested that these interactions create a 'vicious cycle' that leads to, not only tumour growth in bone but, damage and destruction of bone tissue. The healthy bone environment depends upon a balance of bone resorption (mediated by osteoclasts) and bone formation (by osteoblasts) (see Figure 1.2). However, during tumour metastasis to bone this normal process is disrupted, resulting in the symptoms previously mentioned, such as pathological fracture. Prostate cancer bone metastases are frequently characterised as osteoblastic (or osteosclerotic), which results in increased bone formation and the development of osteoblastic lesions. Breast cancer metastases, on the other hand, are frequently osteolytic resulting from increased bone resorption. However, these processes are not distinct in the patient and a mixture of bone formation and resorption is likely to contribute to metastasis resulting in both osteolytic and osteosclerotic features with the phenotype dependent on the balance between resorption and bone formation (Mundy, 2002). The precise location and characteristics of the bone metastasis niche to which prostate cancer (PCa) cells home is still unknown however, several studies have investigated the role of osteoblast and osteoclast bone cells, as well as the tumour cells themselves, and their contribution to this environment.

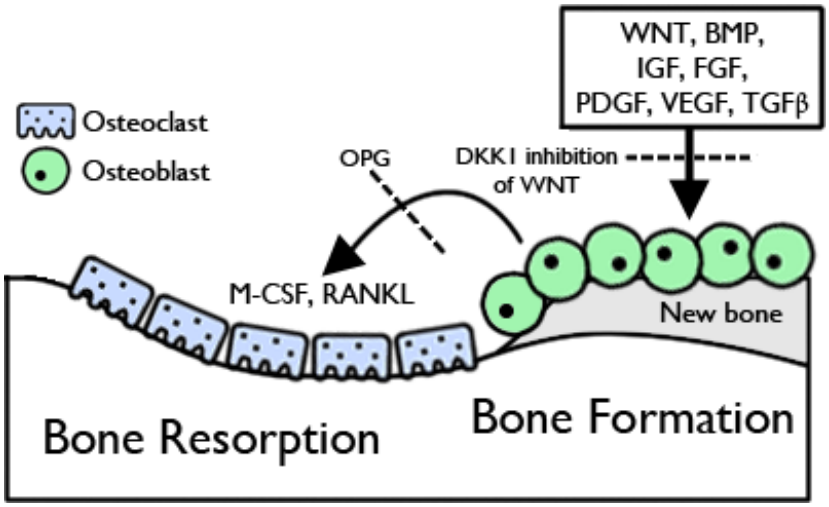

Figure 1.2. A simplified diagram of the remodelling process in bone.
A variety of growth factors stimulate the differentiation of osteoblasts that lay down the new bone surface. This process is also stimulated by WNT signalling which, itself, can be inhibited by Dickkopf-related protein 1 (DKK1) (Logothetis and Lin, 2005). Osteoblasts in turn stimulate osteoclast differentiation and maturation, via receptor activator of nuclear factor kappa-B ligand (RANKL) which binds to receptor activator of nuclear factor kappa-B (RANK) on the surface of pre-osteoclasts, and osteoclast proliferation, via macrophage colony-stimulating factor (M-CSF) (Sims and Gooi, 2008). Osteoprotegrin can act as a decoy receptor for RANKL causing osteoclastogenesis to be inhibited (Sims and Gooi, 2008).

1.3.2 Characteristics of the niche

1.3.2.1 Osteoblasts

During metastasis to bone, prostate cancer cells increase the activity of osteoblasts via the secretion of a variety of growth factors. These can act directly, and include fibroblast growth factor (FGF), Platelet derived growth factor (PDGF) and bone morphogenetic protein (BMP), or indirectly, (PSA and uPa) by modifying the bone environment and existing growth factors (Guise et al., 2006, Logothetis and Lin, 2005). Further to this endothelin-1 (ET-1) secreted by tumour cells was found to stimulate osteoblast activity, via the endothelin-1 A receptor (ETAR), in breast cancer cell lines (Yin et al., 2003). Suppression of ET-1 via Atrasentan (an ETAR antagonist) was also shown to reduce bone remodelling in prostate cancer, however the results of this clinical trial were accumulated from 74 different medical centres introducing a possible sampling bias effect (Nelson et al., 2003). Tumour cell Wnt signalling has also been shown to stimulate osteoblastic activity in prostate cancer *in vitro* and *in vivo* (Hall et

al., 2005). In this study Dickkopf-related protein 1 (DKK1), an inhibitor of Wnt signalling, was shown to decrease osteoblastic activity which the authors postulate may contribute to the osteolytic lesions seen in prostate cancer.

1.3.2.2 Osteoclasts

Increased osteoclast activity has also been shown to contribute to bone metastasis in prostate cancer, resulting in osteolytic lesions (Mundy, 2002). In a study by Zang et al. (2001), the authors demonstrated that PCa cells induce osteoclastogenesis by the production of receptor activator of nuclear factor kappa-B ligand (RANKL). This induces pre-osteoclast to differentiate into mature osteoclast via interactions with its surface receptor, RANK (Zhang et al., 2001). In subsequent research, Roato at al. (2008) compared the levels of osteoclastogenesis in blood samples from metastatic, non-metastatic prostate cancer patients and healthy controls and found increased osteoclast numbers in metastatic patients compared to the other two sample groups. The authors also found that RANKL was increased in this group. Despite this interesting finding the sample size was small (only 46) and all the patients were in the early stages of diagnosis with newly forming bone metastases so any role of osteoclasts in the later stages of metastasis was not explored.

The role of RANKL in osteoclastogenesis and prostate cancer bone metastasis can be an effective target from treatment. Denosumab is a human monoclonal antibody that binds RANKL and reduces osteoclast differentiation, survival and activation. Denosumab has been shown to reduce the risk of osteoporotic fractures in men with prostate cancer in a phase III randomised control trial (Smith et al., 2009). However, as with bisphosphonates, Denosumab is mainly used to limit symptoms and not prevent disease progression.

In Lu et al. (2007), monocyte chemotactic protein-1 (MCP-1) from prostate cancer cells was shown to mediate bone resorption via osteoclast stimulation. MCP-1 (with IL-8) stimulated human bone marrow mononuclear cells (HBMC) to differentiate into osteoclast-like cells. However, MCP-1 was not shown to induce bone resorption in the absence of IL-8, but when it is neutralised resorption does decrease. This suggests that MCP-1 produced by prostate cancer cells works with IL-8 to induce osteoclastogenesis and subsequent bone resorption. Although these results are only shown *in vitro* the

potential influence of MCP-1 on osteolysis does offer an explanation for the low level of RANKL observed in PCa cells, in this study and previous work (Zhang et al., 2003), as the two may work together with IL-8 to induce bone loss via osteoclast stimulation (Lu et al., 2007).

It is proposed that the production of osteoblastic and osteolytic lesions in metastasis have a positive effect on cancer cells. Growth factors released by the bone matrix and mature osteoblasts, such as TGF-β, are thought to increase tumour cell proliferation and support growth in bone (Buijs and van der Pluijm, 2009). Recently, osteoprotegrin (OPG) has been implicated in the survival of prostate cancer cells at the bone metastatic site (Holen et al., 2002). As previously mentioned OPG can influence bone remodelling by acting as a decoy receptor for RANKL (a stimulator of osteoclastogenesis) (Sims and Gooi, 2008). However Holen et al. (2002) suggest that perhaps more importantly OPG may act to suppress tumour necrosis factor-related apoptosis-inducing ligand (TRAIL) induced apoptosis and therefore promote tumour cell survival in bone. Holen et al. (2002) demonstrated that PC3 cells, which express high levels of endogenous OPG, were protected from TRAIL induced apoptosis (measured by DAPI staining) by recombinant OPG *in vitro*. Furthermore, endogenous OPG also successfully inhibited apoptosis when challenged with TRAIL *in vitro*. As higher levels of OPG are associated with bony metastases in prostate cancer, compared with primary tumours or non-bone metastases (Brown et al., 2001), OPG may present a further factor that promotes the growth of prostate cancer cells in the bone by offering protection from apoptosis. However, as shown in Holen et al. (2002), sRANKL can inhibit OPG and therefore reduce the protection of cancer cells against apoptosis. As prostate cancer cells have also been shown to produce high levels of RANKL (Zhang et al., 2001), it raises the question of how these factors interact to promote PCa cell survival in the bone metastatic niche. Perhaps further investigation is needed to elucidate the mechanism by which these factors are regulated. A summary of the processes and the factors involved in PCa bone metastasis are shown in Figure 1.3 and Table 1.2.

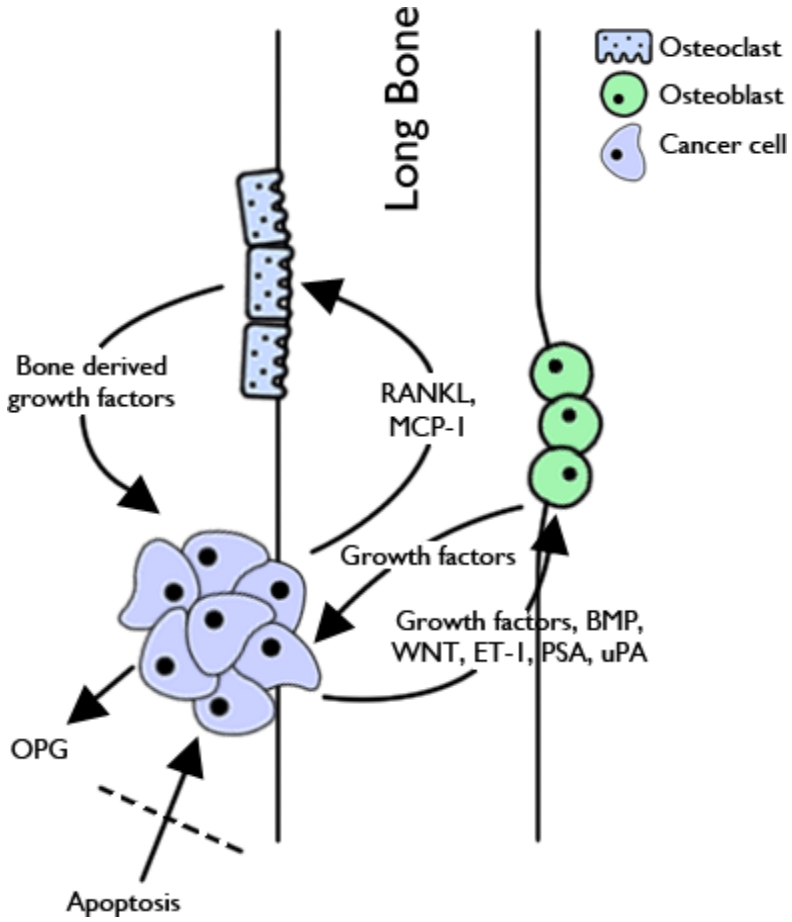

Figure 1.3. The 'vicious cycle' of osteoblastic and osteolytic bone metastases.
Prostate cancer cells that arrive in the bone secrete growth factors, such as FGF, as well as other factors, such as ET-1, that that can stimulate osteoblast activity (Guise et al., 2006, Logothetis and Lin, 2005, Nelson et al., 2003). This induces increased bone formation and the accumulation of osteoblastic lesions. This process can stimulate tumour growth by the release of growth factors from mature osteoblasts (Buijs and van der Pluijm, 2009). PCa cells can also stimulate osteoclast activity via the release of RANKL (Zhang et al., 2003) and MCP-1, which has been shown to work with IL-8 to induce osteoclast differentiation (Lu et al., 2007) . This results in osteoclast-mediated breakdown of the bone surface causing osteolytic lesions. The release of bone derived growth factors from the mineralised bone matrix can then stimulate the proliferation and growth of PCa cells (Buijs and van der Pluijm, 2009). OPG released by tumour cells may also promote survival by inhibiting TRAIL induced apoptosis of cancer cells (Holen et al., 2002).

Factor	Origin	Effect
Bone Morphogenetic Proteins (BMP)	Prostate cancer cells	Stimulates osteoblast proliferation (Logothetis and Lin, 2005).
Bone derived growth factors	Mineralized bone matrix	Stimulated tumour proliferation (Buijs and van der Pluijm, 2009).
Endothelin-1 (ET-1)	Prostate cancer cells	Binds to ETAR and promotes osteoblast growth (Nelson et al., 2003).
Fibroblast growth factor (FGF)	Prostate cancer cells	Stimulates osteoblast proliferation (Logothetis and Lin, 2005).
Insulin-like growth factor (IGF)	Prostate cancer cells	Stimulates osteoblast proliferation (Logothetis and Lin, 2005).
Interleukin-8 (IL-8)	Prostate cancer cells	Acts with MCP-1 to promote osteoclastogenesis (Lu et al., 2007).
Monocyte chemoattractant protein-1 (MCP-1)	Prostate cancer cells	Promotes osteoclastogenesis with IL-8 (Lu et al., 2007).
Osteoblast derived growth factors	Mature osteoblasts	Promote tumour cell growth and proliferation (Buijs and van der Pluijm, 2009).
Osteoprotegrin (OPG)	Prostate cancer cells	In vitro evidence shows that recombinant and endogenous OPG produced by PC-3 cells can protect from TRAIL induced apoptosis (Holen et al., 2002).
Platelet-derived growth factor (PDGF)	Prostate cancer cells	Stimulates osteoblast proliferation (Logothetis and Lin, 2005).
Prostate-specific antigen (PSA)	Prostate cancer cells	Acts indirectly to modify the bone environment and activate growth factors to stimulate osteoblasts (Logothetis and Lin, 2005).
Parathyroid hormone related peptide (PTHrP)	Prostate cancer cells	Stimulates osteoblast proliferation (Logothetis and Lin, 2005).
Receptor activator of nuclear factor-κB ligand (RANKL)	Prostate cancer cells	Binds to RANK on the surface of pre-osteoclasts to promote differentiation (Zhang et al., 2001).
Transforming growth factor (TGF)	Prostate cancer cells	Stimulates osteoblast proliferation (Logothetis and Lin, 2005).
Urokinase-type plasminogen activator (uPA)	Prostate cancer cells	Acts indirectly to modify the bone environment and activate growth factors to stimulate osteoblasts (Logothetis and Lin, 2005).
Vascular endothelial growth factor (VEGF)	Prostate cancer cells	Can act directly or indirectly to either promote osteoblast proliferation or increase bone angiogenesis (Logothetis and Lin, 2005).
Wingless and Int-1 (Wnt)	Prostate cancer cells	Wnt signalling activates downstream targets that induce osteoblast proliferation (Logothetis and Lin, 2005).

Table 1.2. A summary of key factors involved in the formation of prostate cancer bone metastasis.

1.3.3 Clinical relevance of the vicious cycle

Research has increased our understanding of the vicious cycle and the discovery of a number of agents that target this process, for example Denosumab, has led to the considerable pain relief of patients with skeletal metastasis. However, once established in the bone skeletal tumours can grow independently of growth signals from the environment therefore agents that target the vicious cycle may only be effective on early stage metastases.

Nevertheless, the use of Fc-OPG (OPG fused to Fc) has been show to reduce the progression of established bone lesions in mouse xenograft models. Armstrong et al. (2008) provided evidence that fc-OPG alone can reduce bone resorption and the progression of osteolytic lesions when administered up to 20 days after intratibial injection of PC-3 cells (Armstrong et al., 2008).

1.3.4 Osteomimicry

A proposed feature of bone metastasis is the process of osteomimicry; by which cancer cells become more 'bone-like' by taking on the properties of osteoblasts in order to thrive in the bone niche (Koeneman et al., 1999). The expression of osteomimetic markers such as osteocalcein and osteoprotegrin in prostate cancer cell lines has been shown to be linked with increased bone metastatic ability (Dorai et al., 2004). Zayzafoon et al. (2004) offer a potential mechanism by which osteomimicry is induced in osteoblastic prostate cancer cell lines. The authors investigated the link between Notch expression, which is involved in signalling events that determine cell fate, and osteomimicry. Using RT-PCR Zayzafoon and colleagues showed that *notch1* expression is 5x greater in the osteoblastic PCa cell lines C42B and MDA PCa 2b compared to nonosteoblastic LNCaP and DU145 lines. It was also shown that C42B cells, that express both the Notch 1 receptor and the DII 1 ligand, have increased ability to produce calcium deposits following osteogenic induction, a feature of osteoblast-like bone formation. These cells also express RUNX2, an important transcription factor for osteoblast differentiation, in a Notch and ERK dependent manner (Zayzafoon et al., 2004). Building on this observation, Yuen et al. (2008) found that RUNX2 was also positively regulated by TWIST expression. Following osteogenic induction, expression

of the transcription factor TWIST was up-regulated in the 22Rv1 prostate cancer cell line. This matched the expression of RUNX2 at the protein and RNA level and when TWIST expression was reduced, by short hairpin RNA, RUNX2 expression also decreased. These results suggest PCa cells can be induced to become more 'osteoblast-like' via the expression of RUNX2, induced by Notch and TWIST factors.

Although both papers provide evidence for the importance of RUNX2 in osteomimicry, and the factors that regulate it, neither paper presents a mechanism by which either Notch signalling or TWIST transcription is activated in the bone niche i.e., which stromal/bone cells are involved. In order to target osteomimicry as a potential therapy for advanced prostate cancer an understanding of this process is key. Moreover, the 22Rv1 cell line was isolated from an organ-confined prostate cancer so further research is needed in metastatic cell lines, such as PC3, to confirm the significance of TWIST and osteomimicry in metastasis.

1.3.5 The hematopoietic stem cell (HSC) niche and tumour metastasis

Further research to characterise the metastatic niche has led to the identification of several HSC markers that are expressed by metastatic prostate cancer cells. These include CXCL12 (Taichman et al., 2002) and, recently, annexin II (ANXA2) (Shiozawa et al., 2010). It is hypothesised that these markers allow the cancer cells to home to the bone by targeting the HSC niche. However, Shiozawa et al. (2011) claim to be the first to show evidence that prostate cancer cells directly target, and even compete with HSC for, the endosteal niche. Using HSC engraftment in NOD/SCID mice to test this theory, Shiozawa and colleagues demonstrated that engraftment was significantly reduced in mice injected with metastatic PC3 and C42B cells compared to non-metastatic transformed prostate epithelial (NMPE) cells or surgical controls. The authors argue that this shows direct competition between PCa cells and HSC for the niche and go on to further characterise this niche by using multi-photon microscopy to show that HSC and PCa cells co-localise (within a 5-cell distance) to the endosteal niche. In addition, the mobilization of PCa cells out of the HSC niche and into the circulation was demonstrated using the known HSC mobilizes; AMD3100 and G-CSF. Both agents target interactions between HSC and their niche, interfering with CXCR4/CXCL12 signalling in the case of AMD3100 and decreasing levels of CXCL12 in the case of G-

CSF. This, therefore, not only offers a potential treatment to decrease PCa cells in the niche, but provides further evidence to the shared characteristics of HSC and metastasising PCa cells (Shiozawa et al., 2011a). In a following review Shiozawa et al. (2011b) discuss the potential to target HSC niche-tumour interactions in cancer therapy and the need for further study.

The HSC niche has also been implicated in controlling HSC quiescence, the avoidance of apoptosis and the maintenance of HSC numbers via Tie2-Ang-1 signalling (Arai et al., 2004). As research has also implicated tumour cell dormancy as a factor in chemotherapeutic resistance (Naumov et al., 2003) insights into the effects of the HSC niche on cancer cell quiescence may open up therapeutic targets (Shiozawa et al., 2011b). Future perspectives should look to further characterise the HSC niche and the direct components that the tumour cells target in order to exploit this process for treatment.

1.4 Dormancy in prostate cancer

Prostate cancer is often characterised as a slowly advancing disease, where often the prescribed treatment is 'active monitoring' rather than a radical drug or radiotherapy regimen. However, even when the disease is diagnosed at an early stage, when confined to the prostate, patients that receive radical prostatectomy and deemed to be in remission can still relapse with aggressive skeletal tumours. The time taken from radical prostatectomy to the development of skeletal metastasis has been reported to take up to 10 years. Around 30% of patients that are diagnosed with early stage disease (T1-T2), in which the cancer appears to be confined to the prostate, develop skeletal metastases many years after treatment despite having a clear bone scan at diagnosis. We now think that up to 60% of these early stage patients have circulating tumour cells at diagnosis (Ruppender et al., 2013). However there is an obvious lack of accord between this number of patients and the 30% that go on to develop delayed bone metastases. The difference between circulating tumour cells (CTCs) and disseminated tumour cells (DTCs) is important here. CTCs are present in the blood but may never find a favourable environment to grow. However, DTCs have by definition migrated to an environment where they may form metastases. DTCs can be found in the bone marrow of prostate cancer patients without evidence of disease after surgery (Morgan et al.,

2009). Although many will not go on to form metastases, the sub-set of patients in which these DTCs are triggered to grow will eventually develop incurable bone tumours. This period of dormancy and the possible survival advantage that cellular quiescence may provide in the bone marrow has been an on-going area of interest in prostate cancer.

Recently several biomarkers have been hypothesised to be linked with dormancy in metastatic prostate cancer. Kobayashi et al. (2011) established a link between tumour cell senescence and the bone morphogenetic protein, BMP7. Initially conditioned media (CM) collected from human bone marrow stromal cells (HS5) was found to have an inhibitory effect on the growth of multiple prostate cancer cell lines, including PC-3 and DU145. The authors concluded that it was the action of BMP7 in CM that was inducing cell senescence in these cells via the activation of P37, P21 and P27 cell cycle proteins. They went on to show that in mouse xenograft models in which PC-3 cells were injected directly into the tibia, treatment with BMP7 could suppress the development of bone tumours. Several other groups have used cell lines and xenograft models to investigate metastasis and dormancy in prostate cancer.

1.4.1 Models of metastasis and dormancy

1.4.1.1 Prostate cancer cell lines

Unlike many other cancers there is a relative paucity of human prostate cancer cell lines available to study prostate cancer. Those that are available can roughly be divided into two groups, those that are androgen dependent e.g. LNCaP, VCaP and DuCaP and those that are androgen independent e.g. PC-3, DU145 and the LNCaP variants C4. Several *in vitro* assays exist to characterise cells that may have a more metastatic phenotype. For example, a migration assay using a Boydon chamber can be used to test the migratory/invasive potential of a cell that may correlate to metastasis ability.

Cell lines have also been used to study dormancy. An example of this was shown in Li et al. (2014), who authors showed that when DU145 cells were treated with the chemotherapeutic Docetaxel, chemo-resistant cells were present after the 4 day treatment period and these cells had a dormant phenotype. The chemo-resistant cells were found to be less proliferative than the parental cells, as measured by thymidine

uptake, and had higher levels of p21 protein, as measured by Western blot. After harvesting and re-plating, the dormant chemo-resistant cells were found to resume proliferation and formed colonies (Li et al., 2014). Interestingly, these 'recurrent' colonies were even more resistant to Docetaxel than the parental strain, an observation which mimics the chemo-resistance of recurrent tumours in patients.

Although there are several obvious advantages to using *in vitro* models to study dormancy, i.e. low cost, less time consuming, mouse xenograft models remain the 'gold standard' to more accurately recapitulate human disease.

1.4.1.2 Mouse xenograft models

The androgen independent cell lines PC-3 and DU145 are most commonly used *in vivo* to study metastasis as they are more comparable to the castration resistant disease that occurs in patients. Although, there are *de novo* mouse models of prostate cancer metastasis i.e. Mice carrying the TRAMP (Transgenic Adenocarcinoma of Mouse Prostate) transgene which develop progressive forms of prostate cancer with distant site metastasis, these are often confined to the lymph nodes or lung. Therefore to study skeletal metastases, xenografts into immuno-compromised mice must be used. The most common strain used in our lab is Balb/s nude, an immune-deficient strain that lacks a thymus. Human prostate cancer cells can be inoculated directly into the tibia of these mice to study the development of skeletal tumours. However, most frequently cells are injected intracardiac into the left ventricle of mice to study the later stages of the metastatic cascade (extravasation, homing, survival and growth in distant sites) to monitor the development of bone lesions.

Xenograft models of tumour dormancy and recurrence often involve a lengthy procedure of primary tumour growth, resection, delay and study of either DTCs or subsequent recurrent tumour growth. Marsden et al. (2012) however, used a method to isolate dormant DTCs in the bone marrow of xenograft mice in order to test their tumourigenic ability in naïve mice. Marsden et al. cultured tumourspheres isolated from primary breast cancer patients and injected them into the fat pads of nu/nu mice. They found that up to 12 months after injection DTCs were present in the bone marrow of animals without skeletal lesions. The presence of these cells was assessed by

immunohistochemistry for the human specific HNA (human nuclear antigen). The authors found that these dormant DTCs had acquired a more aggressive phenotype as when injected into the fat pad of naïve mice, DTCc from whole bone marrow flushes formed more tumours than bone marrow flushes from mice without DTCs. These cells also formed more metastases however, the majority where found in the lungs and livers of injected mice and not the bone (Marsden et al., 2012).

1.4.1.3 The use of cellular dyes to track dormancy

Fluorescent cell dyes can be used to track dormant cells *in vitro* and *in vivo* due to their ability to bind to the cell and be diluted by distribution to daughter cells at each division. Cells that retain a high intensity of these dyes over long periods of culture are thought to be mitotically dormant or at least very slow cycling.

Carboxyfluorescein succinimidyl ester (CFSE) is a fluorescent cell staining dye that is usually purchased as carboxyfluorescein diacetate succinimidyl ester (CFDA-SE). CFDA-SE diffuses into the cell where is reacts with intracellular esterases to form the fluorescent ester, CFSE, by the removal of acetate groups. CFSE is covalently bound to the cell and is divided equally amongst daughter cells upon division. The advantage of CFSE is that when analysed by flow cytometry, subsequent generations of cells can be visualised by the amount of fluorescence (shown as individual peaks on the histogram) that they retain. CFSE was originally used to track the division of lymphocytes . Today CFSE is predominantly used in immunology and not to study cancer dormancy. This could be due to high toxicity and its use in studying cycling cells is limited as it can only trace around 7-8 cell divisions before it is lost.

PKH fluorescent dyes are vital dyes that consist of a fluorophore attached to an aliphatic carbon back- bone. These can irreversibly bind to the lipid bilayer on cell membranes and so can be equally partitioned among daughter cells upon cell division. Due to low toxicity, PKH labelling enables the monitoring of live cells and can be used to isolate slow-cycling cells for subsequent analysis. The PKH dye PKH67 was used by Kusumbe and Bapat (2009) to identify dormant cells in the ovarian cancer cell line A4. A4 cells stained with PKH67 were injected subcutaneous into NOD/SCID mice and, after tumour formation, were collected, retrieved by digestion of the tumour and analysed by

flow cytometry. These studies found that within a tumour a gradient of PKH67 was present with three sub-sets of cells evolving, $PKH67^{High}$, $PKH67^{Low}$ and $PKH67^{Negative}$. Clonogenic analysis revealed that the $PKH67^{High}$ sub-population were more clonogenic than $PKH67^{Low}$ or $PKH67^{Negative}$ cells. It was also found that the $PKH67^{High}$ cells were more tumourigenic *in vivo* when injected into NOD/SCID mice compared to $PKH67^{Low}$ or $PKH67^{Negative}$ cells. The authors hypothesised that these slow-cycling $PKH67^{High}$ cells represent a CSC sub-population, as they had significantly higher expression of the stem cell markers Oct4, Nestin, Nanog, and Bmi compared to $PKH67^{Low}$ or $PKH67^{Negative}$ cells (Kusumbe and Bapat, 2009).

CM-DiI and DiD are further class of lipophilic cell dyes. These intercalate with the cell plasma membrane by the presence of a thiol-reactive chloromethyl moiety that allows the dye to form covalent bonds with cellular thiols. (Andrade et al., 1996). When excited, Cm-DiI and DiD emit a red (emission 565 nm) and far red fluorescence (emission 665), respectively. Fluorescence can be monitored by flow cytometry or fluorescent microscope. As with other membrane dyes, fluorescence fades during cell division as the cell label is diluted at each division by ≈50% (Haldi et al., 2006). In this way the presence of non-dividing, or dormant, cells can be identified by a persistent bright red signal *in vivo* (using multi-photon imaging) and *in vitro*.

In our laboratory, we have used these dyes to provided evidence that prostate cancer human cell lines can persist in a mitotically dormant state in the bone marrow of mouse xenograft models. By using the lipophilic cell membrane dyes Cm-DiI and Vybrant®DiD (DiD), dye retaining and therefore non-dividing cells can be observed by multiphoton imaging in the mouse bone marrow up to 8 weeks after intracardiac injection. The frequency of tumour formation in the bones of these animals is >80%, with the majority of tumours being detected by bioluminescence imaging (IVIS®, In Vivo Imaging systems) at 3 weeks after injection. However, tumours can begin to develop up to 12 weeks after injection (unpublished).

These dyes are an attractive candidate to explore dormancy at a cellular level. The use of the lipophilic cell membrane dyes Cm-DiI and Vybrant®DiD to characterise dormancy *in vitro* will be explored in the current thesis.

1.5 Conclusions

The high prevalence of prostate cancer in the United Kingdom (CancerResearchUK, 2011) and the poor survival rate of patients with distant metastases (Jemal et al., 2008) highlights the need to develop an understanding of the processes involved in the development of metastases and progression of the disease. Although androgen ablation remains the first line treatment for advanced prostate cancer, the development of androgen insensitivity and the return of advancing disease is a serious clinical problem. Other existing treatments for advanced prostate cancer, mentioned earlier in this thesis, mainly target bone resorption but do not limit the disease. Furthermore, the negative side effects associated with androgen ablation, and the dose related complications of some bisphosphonates, suggests a need to develop alternative therapies that target the early stages of prostate cancer spread. This requires a better understanding of the tumour/metastasis initiating cell population.

As discussed, tumour dormancy and recurrence is a common theme in prostate cancer. Detection of the presence and defining the importance of dormant tumour cell populations has been possible due to the use of mouse xenograft models and by the use of cellular dyes. We have identified a dormant cell population in the bone marrow of mice xenograft models using the lipophilic dye DiD. Work presented in this thesis will use *in vitro* techniques to investigate and characterise dormancy in human prostate cancer cell lines.

1.6 Aims, Hypothesis and Objectives

1.6.1 Aims

The body of work present in this thesis aims to use *in vitro* models to investigate and characterise dormancy in human prostate cancer cell lines.

To address these aims the following hypotheses will be tested.

1.6.2 Hypotheses

1. A dormant cell sub-population exists in human prostate cancer cell lines
2. This sub-population will allow the identification of conditions that regulate dormancy
3. The dormant cell sub-population is phenotypically distinct re: gene and protein expression and certain markers define a dormant phenotype
4. These markers identify dormant cells in patients where their presence is linked to poor prognosis.

1.6.3 Objectives

To test the above hypotheses the following objectives will determine whether:

1. Vital lipophilic membrane dyes can be used to identify slow/non-dividing cells.
2. Dormancy is subject to changes from the environment that can modulate entry and exit from this state
3. RT-qPCR methods can identify gene expression alterations in the dormant cell sub-population compared to the bulk population.
4. Changes at the RNA level are also observed at the protein level.
5. Immunohistochemistry for these protein markers can be used to identify these cells in patient biopsies.
6. The presence of these cells correlates to the presence of metastases in these patients.

Chapter 2. Materials and methods

2.1 Cell culture techniques

2.1.1 General cell culture materials

Reagent	Supplier
70% Industrial methylated spirits	Fisher scientific (Loughborough, UK)
Dulbecco's Modified Eagle Medium (DMEM), + GlutaMax 1x, + 4.5g/L Glucose, - Pyruvate	Gibco® (Paisley, UK)
DMSO	Invitrogen™ (Paisley, UK)
Foetal Bovine serum	Sigma-Aldrich® (Dorset, UK)
Haemocytometer	Weber Scientific Int. (New Jersey, USA)
Isoton Solution	Beckman Coulter Inc. (High Wycombe, UK)
Penicillin-Streptomycin	Gibco® (Paisley, UK)
Phosphate buffered saline (PBS)	Gibco® (Paisley, UK)
Trypsin/ Ethylenediaminetetraacetic acid (EDTA)	Gibco® (Paisley, UK)

Table 2.1. The reagents and suppliers used in standard tissue culture techniques

Material	Supplier
Cryovials, 1.5 mL	Nalgene Nunc Ltd. (New York, USA)
Disposable Pipettes (5, 10 and 25mL)	Corning Costar® (Tewksbury, USA)
Disposable Tips (10, 200 and 1000µL)	Corning Costar® (Tewksbury, USA)
Eppendorf Tubes (0.5 and 1.5mL)	Starstedt Ltd. (Beaumont Leys, UK)
Flasks (T25, T75, T175)	Nalgene Nunc Ltd. (New York, USA)
Multi Well Plates (6, 12, 24, 48, 96 wells)	Nalgene Nunc Ltd. (New York, USA)
Petri Dishes (60 and 100mm)	Nalgene Nunc Ltd. (New York, USA)
Tubes and Bijou (5, 15, 25, 50mL)	Starstedt Ltd. (Beaumont Leys, UK)

Table 2.2 The disposable materials and suppliers used in general tissue culture techniques

2.1.2 Cell lines

Cell line	Source	Description	Reference
PC-3	American type culture collection (ATCC)	Isolated from a bone metastasis from a stage IV prostatic adenocarcinoma by ME Kaighn. PC-3 cells are androgen receptor negative and insensitive to androgens.	**(Kaighn ME, 1979)**
PC-3GFP	Dr. Niel Cross, *Sheffield Hallam University* (From the original ATCC PC-3)	A derivative of the PC-3 line transfected with green fluorescent protein.	**(Cross, 2008,)**
PC-3RFP	From the original ATCC PC-3 strain, transfected Dr. Giancarlo Pesce	A derivative of the PC-3 line transfected with red fluorescent protein.	**n/a**
PC-3NW1	Transfected by Dr. Ning Wang from the original PC-3 line (ATCC)	The result of a stable transfection of the PC-3 cell line with firefly luciferase gene. These cells are routinely used *in vivo* as they can be easily imaged by IVIS *(In Vivo Imaging System)*.	**(Wang et al., 2014)**
LNCaP	American type culture collection (ATCC)	The LNCaP cell line was originally derived from a patient's lymph node metastasis. Unlike the PC-3 cell line, LNCaP cells are androgen-sensitive	**(Horoszewicz et al., 1980)**
C42B4	Generous gift from Professor George Thalmann, *University Hospital Bern*	The original C4-2 cell line was an androgen insensitive sub-strain of LNCaP, derived from a tumour grown from LNCaP cells in castrated mice. The C42B4 cell line was derived from an osseous tumour in a castrated mouse model following orthotropic injection of the C4-2 cells.	**(Thalmann et al., 1994)**

Table 2.3. The main cell lines used for *in vitro* experiments during the project

2.1.3 Maintenance of cell cultures

All cells were routinely grown in T75 sterile tissue culture flasks in DMEM plus 10% foetal bovine serum (FBS) and 1% (5 ml of a 10,000 units/ml added to 500 ml media) Penicillin-Streptomycin (Pen-Strep) with the exception of PC-3RFP/GFP cells which were grown in 5% foetal bovine serum. Cells were grown in an incubator at 37 degrees Celsius (°C) supplied with 5% CO2 and 95% humidity.

Cells were passaged every 3 days or between 80 and 60% confluence, as assessed by Olympus CK2 Inverted microscope at 10x magnification.

2.1.4 Cell harvesting

To harvest cell cultures for either sub-culturing ('passaging') or counting to set up experiments, the media was eluted from the well or flasks, washed with a specific volume of PBS (As defined in **Table 2.4**) and subject to 0.25% Trypsin/EDTA for 5 minutes at 37°. Trypsin was then neutralized with an appropriate volume of standard media. The resulting cell suspension was either counted or centrifuged at 300 x *g* for 5 minutes, at room temperature, and the resulting cell pellet re-suspended in 10 ml of media, with either 1 ml (1in10 split) or 2 ml (1in5 split) added to a further 10 ml of media in a sterile T75 flask.

Flask type	Vol. PBS wash/ml	Vol. trypsin/ml	Vol. neutralisation media/ml
T175	10	5	15
T75	6	2	8
T25	4	1.5	3.5

Table 2.4 The reagent volumes required in standard passage

2.1.5 Cell counting by Haemocytometer

For routine cell counting a Haemocytometer was used. This consists of a thick microscope slide with two laser etched counting grids scored in the centre of the slide. The indentation either side and between the two counting grid allows a capillary space,

of 0.1 mm depth, to be created when a cover slid is applied to the Haemocytometer slide.

To count cells, 10 µl aliquots of cell suspensions were injected into the capillary space in each counting grid by pipette and counted, using a clicker counter, under a 10x optical zoom on the Olympus CK2 Inverted microscope. The number cells in all 8 of the 1 mm^2 squares (the blue box indicates one 1 mm^2 square, **Figure 2.1**) were counted and the resulting tally divided by 8 to get the average cell number per 1 mm^2 square. As each 1 mm^2 square holds 100 nl of liquid the number of cells per ml in the cell average was calculated by multiplying by 10,000.

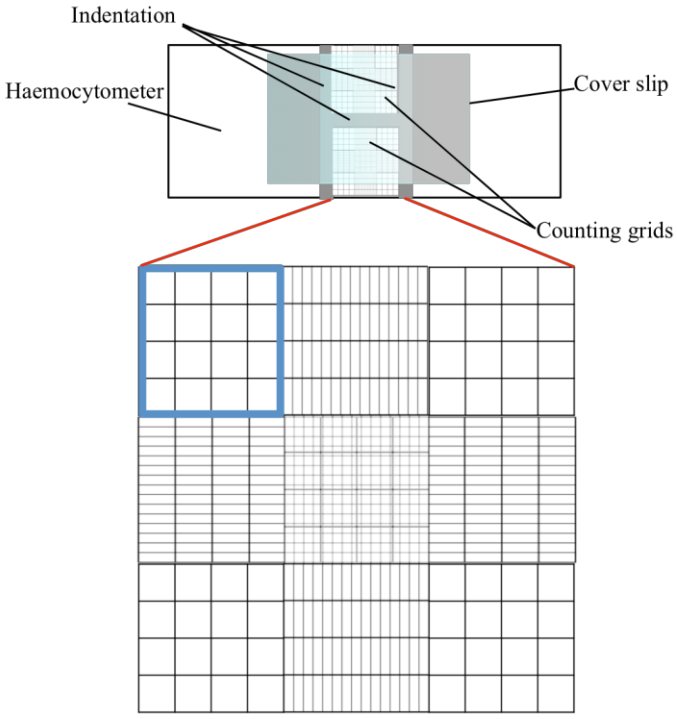

Figure 2.1 Schematic representation of a Haemocytometer
The parts of the Haemocytometer are illustrated in the top diagram. The grid below represents one of the laser etched counting grids. In which, the blue outlined square represents a 1 mm^2 area which holds 100 nl.

2.1.6 Cell counting by Coulter Counter

The Z2 Coulter particle count and size analyser from Beckman Coulter (High Wycombe, UK) was developed to measure the number of cells or particles in a 10 ml suspension by using a sensitive electrical probe. As the cell suspension passes through the probe the electrical conductance is altered which gives a measure of the number of cells or particles present.

The probe can be set to measure particles of a particular diameter e.g. between 10-25 μm for PC-3 cells and sub-strains. The Coulter counter measures 0.5 ml of the cell suspension and therefore, the total in a 10 ml suspension was calculated by multiplying by 20. All cultures were collected into a 10 ml volume for controlled counter analysis. Two measurements were taken per sample and the average was calculated.

2.1.7 Growth curves in routine serum concentrations

To establish the base line growth of cell lines in standard conditions, growth curves were generated over 12 days for all human prostate cancer cell lines used. Cells were harvested from 60-80% confluent flasks by trypsinisation and counted using a Haemocytometer. Cells were then centrifuged and the resulting cell pellet was made up to a $1x10^6$ cell suspension by adding the appropriate volume of standard media and counted again to ensure the suspension was accurate. A 1 in 100 dilution was performed to acquire 25 ml of a $1x10^4$ cell suspension. 1 ml of solution was added, per well, into a 12 well plate to equal 10,000 cells per well.

Cells were counted every other day for 12 days using the Z2 Coulter particle count and size analyser from Beckman Coulter (High Wycombe, UK). The plates were subject to media change on day 2, day 6 and day 10. On each count day the media was removed from each of the 4 replicate wells and added to a 15 ml falcon tube. The wells were washed with 1 ml of PBS, which was also added to the tube. 0.5 ml of trypsin/EDTA was added and the plate was incubated at 37° for 5 minutes and viewed under a microscope to ensure all the cells had detached. 0.5 ml of standard media was added to neutralize, and the cell suspension was added to the falcon. The resulting 3 ml cell suspension was made up to 10 ml with the addition of 7 ml of Isoton II Diluent (purchased from Beckman Coulter). The tube was inverted several times and added to a 25 ml Accuvette and counted using the Z2 counter. Each growth curve was repeated three times.

2.1.8 Determining the exponential growth phase

The exponential growth phase was determined for all cell lines from growth curves generated in routine serum. Following guidelines outlines in the ATCC® ANIMAL

CELL CULTURE GUIDE tips and techniques for continuous cell lines the lag, exponential and stationary growth stage could be identified (**Figure 2.2**).

The lag phase was characterised as the time taken from initial seeding (day 0) to the time that the cells reach linear/exponential growth. The exponential phase was defined as the steep increase in cell number after the lag phase until growth begins to plateau as cells reach the non-exponential/stationary phase, defined as the time after exponential growth when cell division slows down. These stages could be easily defined as long the growth curves followed a sigmoidal or 'S-shaped' curve which allowed these stages to be easily discernable.

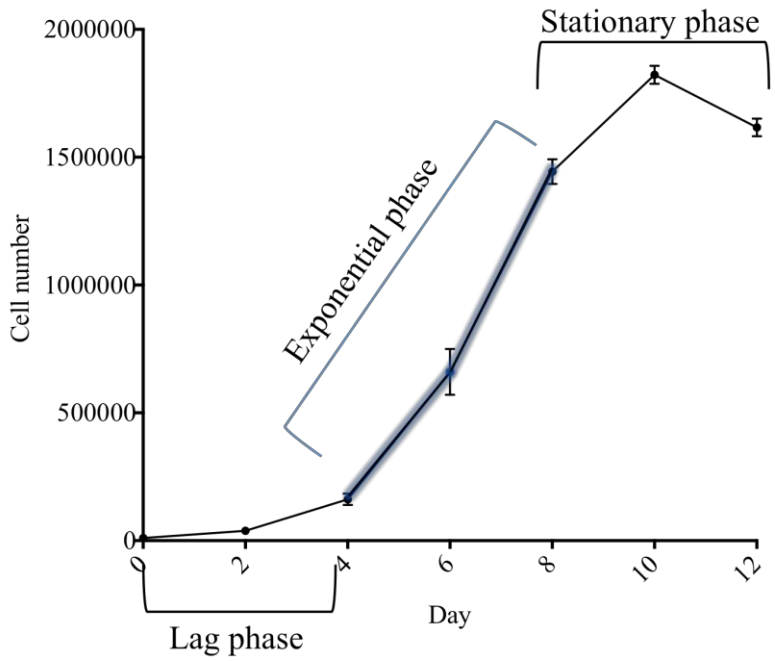

Figure 2.2 Determining the stages of growth

The lag phase is characterised as the time taken from initial seeding to the time that the cells reach exponential growth. The exponential phase is the steep increase in cell number after the lag phase until growth begins to plateau as cells reach the non-exponential /stationary phase, defined at the time after exponential growth when cell division slows down.

2.1.9 Determining the effect of serum on exponential cell growth; serum titration experiments

An assessment of how serum concentration affects growth in mid-exponential growth (as defined by the guidelines above from growth curves in routine serum) was performed. FBS was added to standard DMEM + Pen-Strep to make nine different concentrations, 0%, 1%, 2%, 4%, 6%, 8%, 10%, 12% and 15%. Cells were seeded into

12 well plates at a density of $1x10^4$ cells per well, as described above, in standard media. At day 2 the media was removed and the wells were washed once with 1 ml of PBS. 1 ml of new media, of each of the designated serum concentrations, was added to well plates in replicates of 4. At the point of mid-exponential growth the cell number was determined by Coulter counter, in all four replicate wells for each serum concentration.

2.1.10 Growth curves in FBS concentrations for ½ maximum proliferation

The ½ maximum growth condition was determined from serum titration experiments and a growth curve was performed. The half maximum growth condition was defined as the serum concentration that stimulates a 50% reduction in growth (measured by cell number) compared to growth in optimum serum concentrations during mid-exponential growth. To determine the ½ maximum growth conditions, the cell number at day 6 (mid-exponential growth) in optimum serum was halved. This number was then referred to the serum titration graph and the FBS concentration that best produced this number was taken as the ½ maximum. To perform a growth curve in the ½ maximum conditions, $1x10^4$ cells were plated per well into 12 well plates in 10% FBS DMEM+PenStrep. On day 2 the media was removed, wells were washed with 1ml PBS, and 1ml of the ½ maximum serum media was added. The cells were cultured for a further 10 days in the new media and counted by Coulter Counter every other day. The media was refreshed on day 6 and day 10.

2.1.11 Clonogenic assays in monolayer

To assess the cloning ability of cell lines, cells were seeded at clonal density in 60mm petri dishes and cultured for 14 days. Clonal density is defined as the minimal cell seeding density that produces colonies that can be detected by the Biocount colony counter; for the prostate cancer cell lines this is $1x10^3$ cells/60mm dish. Prostate cancer cell lines were harvested from 60-80% confluent flasks and counted by Haemocytometer. A $1x10^3$ cells per ml suspension was made by serial dilution. 1 ml of this suspension was added to 5 ml of DMEM + PenStrep, with multiple FBS concentrations, in a 60mm diameter sterile petri-dish. Dishes were prepared in quadruple replicate for each treatment/ cell type to be analysed. After 14 days of

incubation the dishes were removed from culture. The media was removed and the dishes were washed with 5 ml PBS. Dishes were left to air dry for 5 minutes and cells were 'fixed' by the addition of 2 ml of 100% methanol for 5 minutes. This was removed and the dishes were air dried for 5 minutes. 2 ml of Giemsa stain solution (Purchased from VWR International Ltd. (Poole, UK)) was added to the dish for 5 minutes then removed and washed twice with distilled water and left to air dry overnight.

The number of colonies was determined from images of the dishes taken by the Biocount colony counter, which were converted to greyscale images for analysis by GeneTool software (**Figure 2.3**). This software allows a region of interest to be selected (red circle) in which individual colonies are highlighted (yellow circles) and counted. The generation of false positives is reduced by the exclusion region function, which allows the user to highlight areas of shadow or non-specific stain (yellow cross region).

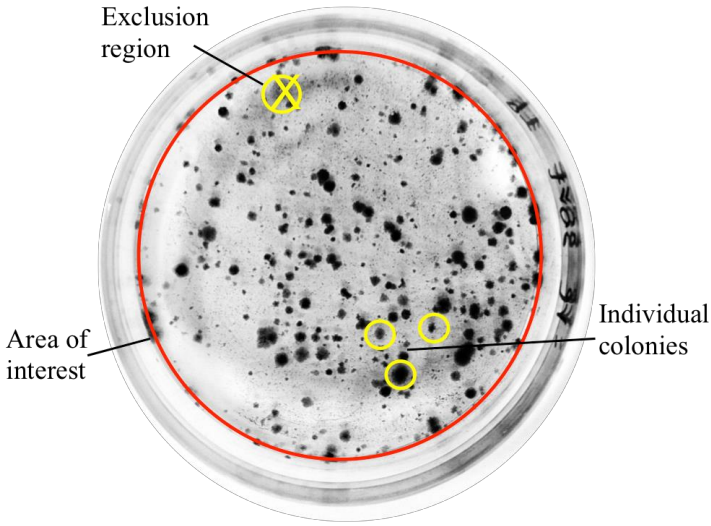

Figure 2.3 Colony number analysis by GeneTool software
The area of interest (red circle) defines the boundaries of the plate. The colonies are highlighted (yellow circles) which allows any false positives to be excluded by the user (yellow circle with cross) and number of colonies is calculated.

2.1.12 Conditioned media

Conditioned media was generated over rapidly growing cell cultures to act as a stimulant for dormant cells. To ensure consistency across replicates, $3.5x10^5$ cells were seeded into T175 flasks to replicate the seeding density in growth curves. Flasks were cultured for 6 days in 10% FBS media, after which the media was removed and the cells were washed with PBS. 20 ml of DMEM containing 1% FBS was added to the flask and cultured for 24 hours.

After 24 hours the conditioned media was removed and centrifuged to remove any detached cells. The media was also sterile filtered through a 0.2 µm mesh to further ensure the media was free of contaminating cells. This medium was then directly applied to experimental plates without freezing.

2.2 Lipophilic membrane dyes

CellTracker™ CM-DiI and Vybrant® DiD cell-labelling solutions (detailed in **Table 2.5**) were purchased from Life Technologies Ltd. (Paisley, UK).

	Molecular formula	**Excitation (nm)**	**Emission (nm)**	**Working concentration**
CellTracker™ CM-DiI	$C_{68}H_{105}Cl_2N_3O$	549	565	10 µM
Vybrant® DiD	$C_{67}H_{103}ClN_2O_3S$	644	665	5 µM

Table 2.5 The specifications of the lipophilic membrane dyes utilised in experiments

2.2.1 CellTracker™ CM-DiI staining method

Prostate cancer cell lines were harvested from 60-80% confluent flasks and counted by Haemocytometer. After centrifugation, cell suspensions of $1x10^6$ cells per ml in Hank's Balanced Salt Solution (HBSS) from GIBCO (Paisley, UK) were prepare in 25 ml tubes. 10 µl of CM-DiI per $1x10^6$ cells was added and the tube was wrapped in foil and placed in a 37°C incubator for 5 minutes. Tubes were then transferred to an ice bucket for 15 minutes. Suspensions were centrifuged at 300 x *g* for 5 minutes and re-suspended in 5ml of ice cold PBS. Cells were re-pipetted/ re-suspended 3 times as above to remove unbound dye. Before the final wash, the cell suspension was counted using a haemocytometer and the final cell pellet re-suspended in standard media to make a $1x10^5$ cells/ml suspension. $1x10^5$ cells were seeded into 5, T25 flasks in 6ml of 10% DMEM plus 1% Pen-Strep. These flasks were cultured for 21 days. The percentage of CM-DiI positive cells was assessed by BD FACS calibur (BD Biosciences (San, Jose, USA)) flow cytometer analysis and Leica fluorescent microscopy at time points; 0, 3, 7,

10, 14 and 21 days. Cells were allowed to grow and kept at high density following the protocol in **Table 2.6.**

2.2.2 Vybrant® DiD staining method

Cell lines were harvested from flasks of between 60-80% confluence and counted by Haemocytometer. Cells were re-suspended in serum-free DMEM to make $1x10^6$ cells/ml suspensions in 25 ml tubes. The suspension was stained with 5µl of DiD per $1x10^6$ cells. The tube was wrapped in foil and placed in a 37°C incubator for 20 minutes. Suspensions were centrifuged at 300 x *g* for 5 minutes and washed 3 times as in 2.2.1 with 5 ml of serum-free media instead of PBS. Before the final wash, the cell suspension was counted using a haemocytometer and the final cell pellet re-suspended in standard media to make a $1x10^5$ cells/ml suspension. $1x10^5$ cells were seeded into 5, T25 flasks in 6ml of 10% DMEM plus 1% Pen-Strep. These flasks were cultured for 21 days. The percentage of DiD positive cells were assesses by BD FACS calibur (BD Biosciences (San, Jose, USA)) flow cytometer analysis and Leica fluorescent microscopy at time points: 0, 3, 7, 10, 14 and 21 days. Cells were allowed to grow and kept at high density following the protocol in **Table 2.6.**

Day	Procedure
0	Cell stain 5x T25 flasks set-up, FACS Calibur analysis.
3	FACS Calibur analysis of 1x T25 flask, remaining 4 undisturbed in culture
7	FACS Calibur analysis 1x T25, transfer of remaining 3 flasks to T75 flasks.
10	FACS Calibur analysis 1x T75 flask, transfer remaining 2 flasks to T175 flasks.
14	FACS Calibur 1x T175 flask, split the remaining T175 flask into 3 x T175 flasks
17	Split one T175 flask 1in4
21	FACS Calibur 1x T175 (if applicable FACS Aria sort 3x T175 flasks).

Table 2.6 The protocol followed for all long-term culture and analysis of cells stained with lipophilic membrane dyes

2.2.3 Mitomycin C treatment of Vybrant® DiD /CM-DiI cells

Mitomycin C is an anti-neoplastic antibiotic that can be used to generate mitotically inactive cells. It acts as an inhibitor of DNA synthesis and nuclear division by producing DNA inter-strand cross-links. Mitomycin C was used to arrest the division of

stained cells in order to assess dye retention in a known dormant state. Mitomycin C was purchased from Sigma-Aldrich (Dorset, UK). PC-3-NW1 cells were stained and seeded as in methods 2.2 and allowed to grow for 24 hours. The media was then removed and 6 ml of a 5 µl/ml solution of Mitomycin C (concentration 5mg/ml) in standard media was added. After 3 hours, the media was removed; flasks were washed with 6 ml of PBS and replenished with 6 ml of fresh standard media. The percentage of CM-DiI or DiD positive cells over 21 days was assessed as above.

2.3 Flow cytometry techniques

2.3.1 Flow cytometry (FACS Calibur) to determine CM-DiI and DiD positive percentages

The principles of FACS calibur flow cytometer are shown in **Figure 2.4**. To determine the percentage of CM-DiI or DiD positive cells in culture, one flask at each time point was trypsinised and centrifuged at 300*x g* for 5 minutes at room temperature. A negative sample of PC-3-NW1 cells without the dye was also prepared in this way. The resulting cell pellet was re-suspended in 0.5 ml of PBS. 2µl of TO-PRO-3 (for CM-DiI stained cells) or Propidium Iodide (PI) (for DiD stained cells) viability dye was added to each sample. TO-PRO-3/PI identifies any non-viable cells by entering through the disrupted membrane of dead cells. TO-PRO-3 is a long wavelength dye (Max. emission 657 nm) and so can be separated from the CM-DiI signal whereas PI emits at 617 nm and so can be separated from the DiD signal.

The FACS calibur has two lasers, of wavelength 488 nm and 633 nm. These lasers allow excitation of fluorescent proteins. The emission wavelength of fluorescent cell dyes or flurophores is detected by the individual channel detectors. This information is analysed by an attached computer using the Cell Quest software package. The percentage of viable CM-DiI retaining cells was detected by the FL-2 channel and the percentage of viable DiD positive cells was detected by the FL-4 channel.

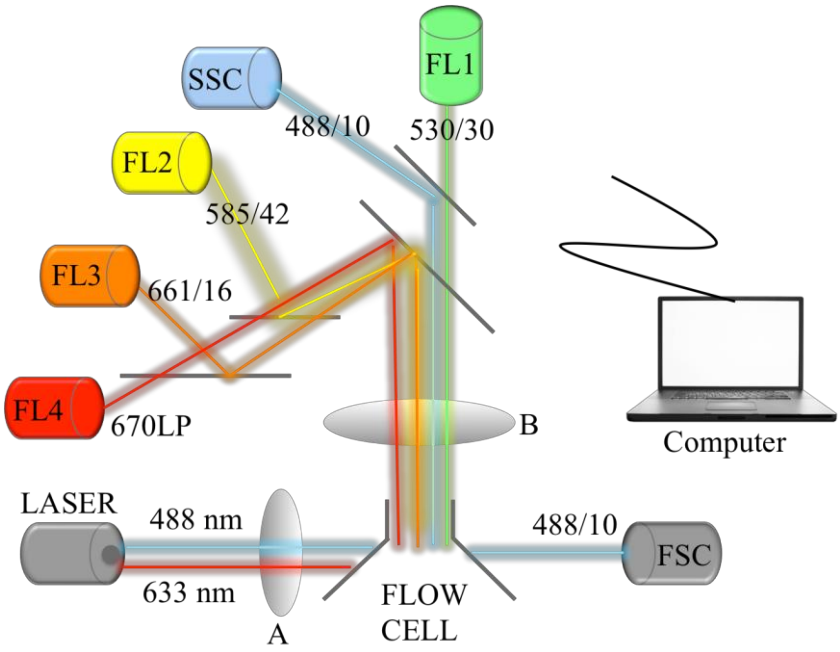

Figure 2.4 The principles of FACS Calibur.

The cell sample is analysed through the flow cell by two lasers: 488 nm (blue) and 633 nm (red). 488 nm detects forward (FCS) and side scatter (SSC) as well as channels FL-1, FL-2 and FL-3. The 633 nm laser detects the FL-4 channel. The laser beam passes through a focusing lens (grey oval A), through the flow cell and up through the fluorescent collection lens (grey oval B) Cells carrying a fluorescent signal, conjugated to an antibody or as a cellular dye, are excited by these lasers and their emission wavelength is reflected by a series of mirrors to the channel detectors (coloured cylinders). The detectors feed to a connected computer to allow analysis by specialized software.

2.3.2 Fluorescent activated cell sorting (FACS Aria)

In order to perform downstream experiments such as RT-qPCR the DiD stained cells were also sorted by BD FACS Aria (BD Biosciences (San, Jose, USA)) on day 14. This allowed the isolation of DiD positive cells, which would represent the dormant sub-population. The principles of FACS Aria are shown in **Figure 2.5**.

The FACS Aria uses a tri-laser system to detect fluorescence from mixed populations of cells. A cell that emits fluorescence upon excitation by these lasers, feeds back to the photomultiplier and is given a positive, negative or no charge based on which channel the signal is detected in. In this way fluorescent signals in multiple channels can be detected and sorted allowing for the separation of multiple cell types (only two populations shown for ease in **Figure 1.2**). The effective sorting of different cell sub-

populations depends on calibrating the Aria to produce a single droplet from the high pressure nozzle, allowing a single cell at a time to be analysed and sorted. After sorting the separate collection tubes can be removed and centrifuged to retrieve the cells.

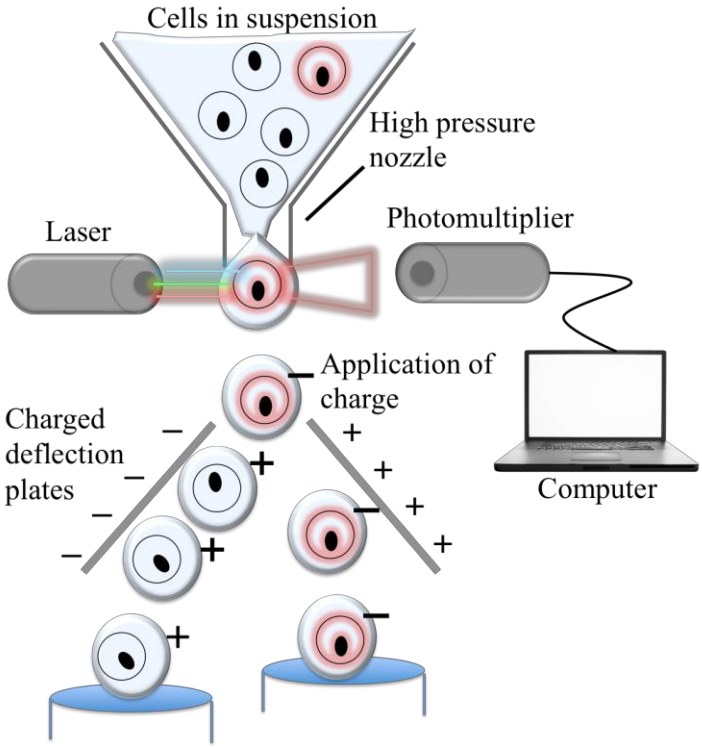

Figure 2.5 The principles of FACS Aria.
The FACS Aria consists of three lasers: 405 nm, 488nm and 633nm. These lasers are focused onto a stream of cells released from a high-pressure nozzle that forms droplets of single cells allowing them to be analysed individually. Cells carrying a fluorescent tag are excited by these lasers and emit light, which is detected by the photomultiplier. This feeds to the computer that signals a charge to be added to the cell, which is then deflected by charged electrodes into the designated collection tube.

2.4 Imaging techniques

2.4.1 Fluorescent imaging

Fluorescent cell imaging was performed using the Leica AF6000 Automated Inverted Microscope. The Leica features a fluorescence axis and enables the excitation of a range of flurophores from UV to far red (**Table 2.7**).

Filter cube	Excitation	Emission	Colour
A4	BP 360/40	BP 470/40	UV
L5	BP 480/40	BP 572/30	Blue
N3	BP 600/40	BP 600/40	Green
Y5	BP 700/75	BP 700/75	Cy5 Red (Far Red)

Table 2.7 The filter cubes and excitation/emission ranges featured on the Leica AF600.

2.4.2 Colour image analysis

To perform real colour imaging, for use in detecting Beta-galactosidase activity and biotinylated antibodies, the Inverted widefield fluorescence microscope Leica DMI4000B was used with the assistance of Colin Gray.

2.5 Cell cycle experiments

2.5.1 Ki-67 flow cytometry assay

14 days after DiD staining, PC-3NW1 cells were harvested and counted by haemocytometer. $1x10^6$ cells were fixed in formalin for 20 minutes at room temperature. The cells were centrifuged for 5 minutes at 300 x g and non-specific binding blocked in 10% goat serum in 0.5% BSA for 1 hour on ice. The cells were permeabilised by the addition of 300 µl of 1x BD Phosflow™ perm buffer solution (purchased from BD Biosciences), made up in distilled water from the 10x stock, per $1x10^6$ cells for 10 minutes at room temperature. The cells were pelleted (300 x g), re-suspended in perm buffer twice and separated into $1x10^5$ cell aliquots for application of the antibody. The AlexaFluor® 488 Mouse anti-human Ki-67 was purchased from BD Pharmingen™. For experiments the aliquots consisted of a no-treatment control, two replicates of a 1:20 concentration of the antibody and two replicates of a 1:20 concentration of the isotype control (Mouse IgG1 *k*, purchased from BD Pharmingen™).

The cells were incubated with treatments (isotype, no-treatment or Ki-67 antibody) diluted in 10% goat serum PBS for 30 minutes at 4° C. The cells were then centrifuged at 300 x g for 3 minutes and pellets re-suspended/washed 3 times in PBS, centrifuged at 300 x g between washes. After the final wash the cells were re-suspended in 300 µl of PBS and analysed by FACS Calibur flow cytometer. A positive and negative control of DiD stained and unstained PC-3NW1 cells was used to set the gate to determine DiD positive dormant cells. The isotype and no-treatment control were used to set the gate to determine KI-67 positive cells. 10,000 events (cells) were analysed per sample.

2.5.2 KI-67 immunofluorescence (chamber slide method)

KI-67 status was also qualitatively analysed by immunofluorescence. $1x10^6$ PC-3NW1 cells were stained with DiD following methods 2.2.2. After serial dilution 300 stained cells/well were added to an 8 well Permanox® microscope chamber slide in 300 µl of 10% FBS DMEM+Penstrep. Cells were cultured for 14 days, after which the chambers were prepared for immunofluorescence. On ice the media was removed from each well by pipette and the wells were washed with 300 µl ice cold PBS twice. The cells were fixed in 300 formalin µl/well for 20 minutes at room temperature Non-specific binding was blocked by addition of 300 µl of 10% goat serum in 0.5% BSA per well for 1 hour on ice. The cells were washed in 300 µl PBS twice. The cells were permeabilised with 300 µl 0.1% triton in PBS for 10 minutes at room temperature and washed twice with PBS. 300 µl of a 1:20 dilution of AlexaFluor® 488 Mouse anti-human Ki-67 (purchased from BD Pharmingen™) or matched Mouse IgG1 *k* isotype (purchased from BD Pharmingen™) diluted in 10% goat serum in PBS was added to each well in replicates of four. The chambers were incubated overnight at 4°C. After incubation the treatment was removed and the chambers were washed twice with 300 µl PBS. The chamber was then carefully removed and the slides were mounted in VECTASHIELD Mounting Medium with DAPI (purchased from VECTOR laboratories, Peterborough, UK) onto coverslips for imaging.

2.5.3 Propidium Iodide (PI) assay

$1x10^6$ PC-3NW1 cells 14 days after DiD staining were harvested and centrifuged for 5 minutes at 300 x g to pellet. The pellet was resuspended and fixed in 1 ml of 70% ice-cold ethanol, applied drop by drop whilst the cells were gently vortexed. The cells were incubated in ethanol for 5 hours at 4°C. The cells were then washed by adding 5 ml PBS to the tube and centrifuged for 10 minutes at 300 x g. This wash step was repeated. 300 µl (50 µg/ml) of PI and 5 µl (2 mg/ml) of RNAse were added and the cells were incubated overnight at 4°. FACS Caibur analysis was the performed to assess the cell cycle status of DiD positive cells. A DiD positive and negative control of stained and unstained PC-3NW1 cell was used to set the DiD positive gate. A no treatment control was used to ensure no cross over from the FL-4 DiD channel and the FL-2 PI channel.

2.5.4 Senescence assay

The Senescence Detection kit from Abcam® was used to perform a senescence assay. The kit distinguishes cells in a senescent state by the development of a blue stain, which is detected upon the hydrolysation of X-gal into galactose and 5-bromo-4-chloro-3-hydroxyindole when senescent associated beta-galactosidase enzyme is active. It is based on the observation that senescent cells have higher endogenous lysosomal beta-galactosidase which makes the enzyme active in acidic conditions (Lee et al., 2006). SA-beta-Gal represents an accumulation of beta-Gal in senescent cells as opposed to a unique enzyme. Therefore, when performed at pH 6.0, the kit allows the identification of senescent cells by the hydolysis of X-gal under acidic conditions.

The kit components are listed in **Table 2.8**. PC-3NW1 cells that had been stained with DiD and cultured for 14 days were harvested and counted by Haemocytometer. $1x10^5$ cells were seeded in triplicate into a 6 well plate and left to attach overnight. The media in each well was carefully eluted and washed with PBS. 1 ml of the provided Fixative solution was added to each well and incubated for 10 minutes at room temperature. The fixative was removed and the wells were washed twice with 1 ml of PBS. For each well 1 ml of Staining Solution mix was prepared in an eppendorf by mixing 470 µl of 1x Staining solution to 5 µl of 100x Staining Supplement and 5 µl of the prepared X-gal solution. The plate was covered in foil and incubated overnight at 37°C. The presence of blue colour was assessed by Leica DMI4000B colour imaging with fluorescence to detect the DiD channel.

Item	Preparation
1x Fixative solution	**n/a**
X-Gal (150 mg, Lyophilized)	**20 mg X-gal dissolved in 1 ml DMSO**
1x Staining solution	**n/a**
100x Staining Supplement	**n/a**

Table 2.8 The items supplied in the Abcam® Senescence detection kit

2.6 Molecular biology techniques

2.6.1 RNA extraction

RNA extractions were performed using the ReliaPrep™ RNA Cell Miniprep System from Promega. The components supplied are listed in **Tables 2.8 and 2.9**. Reagents supplied by the user include isopropanol, 95% Ethanol and centrifuge. Following preparation the cell pellet was washed once with 5 ml of ice cold PBS and centrifuged for 5 minutes at 300 x g. 100-250 µl of BL buffer plus 1-Thioglycerol was added to the pellet (100 µl 1 $x10^2$ to 5 $x10^5$ cell, 250 µl >5 $x10^5$ to 2 $x10^6$ cells) to effectively lyse the cells. The pellet was re-suspended by pipetting 7-10 times to shear genomic DNA and transferred to a 1.5 ml sterile eppendorf tube. 35-85 µl of ice cold 100% isopropanol was added to the tube and vortexed for 5 seconds (35 µl 1 $x10^2$ to 5 $x10^5$ cell, 85 µl >5 $x10^5$ to 2 $x10^6$ cells). The lysate was transferred to the Minicolumns provided which were then placed in Collection tubes and centrifuged for 30 seconds at 12,000 x *g*. The Minicolumn is designed to capture nucleic acids due to the presence of chaotropic salts in the resin matrix situated at the base of the tube. Centrifugation and subsequent wash steps are designed to remove contaminating proteins and DNA whilst retaining RNA in the matrix. After centrifugation the elution volume was discarded. 500 µl of the provided RNA wash solution was added to the Minicolumn which was then centrifuged for 30 seconds at 12,000 x *g* and the elution volume discarded. At this stage a DNase treatment was performed by the addition of 24 µl of yellow core buffer, 3 µl of $MnCl_2$ and 3 µl of DNase enzyme per sample and left at room temperature for 15 minutes to remove contaminating genomic DNA.

Columns were washed with 200µl column wash solution and centrifuged for 15 seconds at 12,000 x *g*. A second RNA wash was performed with a further addition of 500 µl of RNA wash solution and centrifuged for 30 seconds at 12,000 x *g*. The eluted liquid was discarded and the Minicolumn transferred to a new Collection tube. A final RNA wash step was done, 300 µl of RNA was solution was added and the tubes were spun for 2 minutes at 12,000 x *g*. The Minicolumn was transferred to an Elution tube to allow the release of the bound RNA from the Minicolum matrix by the addition of Nuclease free water. 15 µl of Nuclease free water was added to elute 1 $x10^2$ to 5 $x10^5$ cell, 30 µl was added to elute >5 $x10^5$ to 2 $x10^6$ cells. After the addition of Nuclease free water the tubes were centrifuged for 1 minute at 13,000 x *g* and the resulting elution liquid

containing the released RNA was retained in the Elution tube for analysis by Nanodrop.

Reagent	Description	Preparation prior to use
DNase I	DNase I is a DNA denaturing enzyme that reduces DNA contamination during RNA extraction. The potency of this enzyme is greatly dependent on the reaction buffer. Therefore exact quantities of MnCl2 and yellow core buffer are required for its action.	Add 275µl of Nuclease-Free Water (provided) and mix gently to dissolve. Store 10-20 µl aliquots at –20°C. DNase is mixed with MnCl and yellow core buffer to make the complete reaction mix.
BL Buffer	The BL buffer is made up of 4M Guanidine thiocyanate and 0.01M Tris (pH 7.5). The buffer is made up to 2% 1-Thioglycerol, upon addition. Guanidine thiocyanate is a strong protein denaturant and is used to lyse cells.	Add 325µl of 1-Thioglycerol to 32.5ml of BL Buffer and store at 4º for up to 30 days
MnCl2, 0.09M	In the presence of Manganese (Mn) the DNase enzyme produces double strand DNA 'nicks' allowing potent degradation of contaminating DNA.	n/a
Nuclease-Free Water	Nuclease-free water is autoclaved and sterile filtered water. It is RNase and DNase free.	n/a
RNA Wash Solution	A mixture of potassium acetate and 27.1mM Tris-HCl (pH 7.5 at 25°C). (The specific action of this buffer is not described. However, the known action of potassium acetate is to precipitate dodecyl sulfate (DS) and DS-bound proteins. It is also used as a salt for the ethanol precipitation of DNA. It is therefore likely that this buffer acts as a purifying wash to remove DNA and proteins at each RNA purification step).	Add 60ml of 95% ethanol and swirl to mix prior to first use (stable indefinitely at room temperature)
Column Wash	(The components of this buffer are not listed on the protocol. However, as the Column wash step is performed after the DNase treatment and at no other time I would assume that this buffer contains a DNase inhibitor to effectively stop the reaction. This would most likely be a chelating agent such as EDTA or SDS due to the presence of Manganese).	Add 7.5mlof 95% ethanol and swirl to mix prior to first use (stable indefinitely at room temperature)
Yellow Core Buffer	Yellow core buffer is a mixture of 0.0225M Tris (pH 7.5), 1.125M NaCl and 0.0025% yellow dye (w/v). (Little information is available about this buffer but as the activity of DNase is greatly altered by the ionic strength of the reaction buffer, the presence of NaCl may regulate this). The Yellow dye is used to ensure complete coverage of the RNA capture membrane	n/a
1-Thioglycerol	Is added to the BL buffer in order to inhibit ribonuclease activity and preserve RNA integrity upon cell lysis.	n/a

Table 2.8 The reagents supplied in the ReliaPrep™ RNA Cell Miniprep System

Material	Description
Collection Tubes	The collection tube is a small plastic tube that holds the Minicolumn and captures the elution waste after centrifugation, which is then disposed.
Elution Tubes	After the final wash step the RNA that is bound to the Minicolumn is eluted into the elution tube with nuclease free water. The elution tubes can then be stored at -20 to -80°C
Mini-columns	The Minicolumn comprises of a small plastic tube with a tapered end holding a membrane designed to capture RNA. The membrane comprises of a resin matrix that favours the capture of nucleic acids due to the presence of chaotropic salts. These salts disrupt the structure of larger molecules such as proteins. The Minicolumn sits within the collection tube and allows the elution of proteins and the retention of RNA before its final elution with nuclease free water.

Table 2.9 The materials supplied in the ReliaPrep™ RNA Cell Miniprep System

2.6.2 Nanodrop analysis of extracted RNA

The NanoDrop 2000 from Thermo Scientific was used to assess RNA quantity and quality after extraction. The Nanodrop is a spectrophotometer device that uses the absorbance of ultraviolet light, at a wavelength of 260 nm, to detect RNA/DNA purity. 0.5-2 ul of sample is pipetted onto the pedestal containing the lower optical surface and the arm is lowered to contact the upper and lower optical surfaces to create a sample column for analysis. Prior to use and before each sample, the upper and lower optical surfaces were wiped with a lint free cloth before the sample was pipetted. 1 ul of nuclease free water was used to 'blank' the machine prior to use. A measurement of nuclease free water was taken before the samples to ensure that the machinery was working properly and to check that there was no RNA/DNA contamination in the nuclease free water used for eluting. The RNA was then gently mixed and 1 ul per sample was loaded onto the machine. Two readings per sample were recorded and the average was taken. A sample with a 260/280 ratio close to or equal to 2.0 and a 260/230 between 2.0-2.2 was considered high quality RNA suitable for down stream experiments.

2.6.3 TapeStation

A further measure of RNA quality was performed using the 2200 TapeStation from Aligent technologies. This was particularly useful when optimising the RNA

ReliaPrep™ system. The TapeStation gives a measurement of RNA integrity, the RNA integrity number equivalent or RIN^e. The RIN^e is calculated based on the ratio of 28s:18s species in the RNA sample as well as the level of degradation in the form of small RNA products following gel electrophoresis. Unlike traditional methods this ratio is calculated objectively and automatically from a full electropherogram using an established algorithm.

It is important to ensure that the same quantity of RNA is loaded per sample into the TapeStation, therefore samples of high concentration must first be diluted with nuclease free water. 2 µl of R6K Sample Buffer (purchased from Aligent technologies) was added to each sample in a 0.2 ml tube. The tubes were vortexed and 'pulsed' on the centrifuge. The tubes were heated to 72°C for 3 minutes using a hot block. They were then transferred to an ice bucket for 2 minutes. The tubes were 'pulsed' on the centrifuge and loaded into the TapeStation with the R6K screentape. The R6K screentape platform (purchased from Aligent technologies) consists of a multi-channelled well plate into which the RNA samples are automatically loaded. The TapeStation automatically analyses the samples and produces the RNA integrity number equivalent (RIN^e). The RIN^e is used as a measure of the amount of RNA degradation between 1 and 10, where a RIN^e value of 10 is completely intact RNA. After the sample is run on the screentape system the system produces an image of the electrophoresis gel and also an electropherogram, which displays the 18s and 28s peaks and any 'ripples' between the peaks which would indicate degraded RNA. The software then calculates the RIN^e by the rRNA ratio and also the concentration of the RNA.

2.6.4 Reverse transcriptase-quantitative PCR (RT-qPCR): General principles

The polymerase chain reaction (PCR) allows the amplification of a small amount of DNA, in the presence of Taq polymerase and DNA oligonucleotides (or DNA primers), to produce vast quantities of specific transcripts. Reverse transcriptase PCR generates cDNA (complementary DNA) from extracted RNA to allow amplification. qPCR, often referred to as Real-time PCR, allows the amplification and simultaneous detection of a specific transcript allowing the relative expression level of specific genes to be quantified. The TaqMan® assay system, which was used is all experiments, involves

the use of sequence-specific DNA probes to detect the level of gene expression based on the intensity of a fluorescent signal. TaqMan® primers or 'assays' include a gene specific oligonucleotide sequence that has a reporter dye at the 5' end and a quencher attached to the 3' end. When the primer is initially attached to the specific cDNA sequence the quencher prevents the reporter emitting a fluorescent signal. However, when the probe is displaced/cleaved during PCR amplification, the reporter is released and emits a fluorescent signal. The amount of a specific cDNA transcript is measured by Ct (cycle threshold) value, which is the number of PCR cycles required for the emitted fluorescent signal to pass a threshold. The TaqMan® probes used in all experiments consist of the 6-carboxyfluorescein (FAM) reporter and minor groove binder (MGB) non-fluorescent quencher.

2.6.4.1 Reverse transcription

The materials and reagents for reverse transcription are listed in **Table 2.10**. All the pipettes, tips and tubes as well as the DEPC water were subject to irradiation by U.V light for 20 minutes prior to the start of experiments. As it is important to load the same amount of RNA into each reaction, the RNA yield (as indicated by Nanodrop) was used to calculate the appropriate volume of RNA to add to DEPC water to equal the same amount in ng in a total of 11 µl volume. For each sample a Superscript negative control was carried out, therefore each sample was prepared in two replicate tubes. A tube containing DEPC water only was also prepared to ensure no contamination in the diluent.

Item	**Supplier**
DEPC-treated Water	BIOLINE (London, UK)
dNTP mix (100mM)	BIOLINE (London, UK)
DTT (0.1M)	Invitrogen (Paisley, UK)
First strand buffer	Invitrogen (Paisley, UK)
Oligo (dt) Primers	Promega (Southampton, UK)
Random Primers	Promega (Southampton, UK)
RNase free 0.5 ml eppendorfs	Alpha Laboratories Ltd (Hampshire, UK)
RNasIN recombinant RNase Inhibitor	Promega (Southampton, UK)
SuperScript III	Invitrogen (Paisley, UK)

Table 2.10 The materials and reagents for reverse transcription

2 µl of Reverse transcription (RT) mix I (prepared as in **Table 2.11**) was added to each sample and the reaction was heated to 65ºC for 5 minutes using a Thermocycler and cooled to 4ºC for at least 1 minute.

7 µl of RT mix II Negative (prepared as in **Table 2.11**) was added to half of the tubes to make up a total volume of 20 µl to serve as the RT free control. 7 µl of RT mix II Positive (prepared as in **Table 2.11**) was added to the remaining tubes, including the water control, to allow the generation of cDNA from these samples. The reaction was heated to 50ºC for 60 minutes, 70ºC for 15 minutes and cooled to 4ºC. The resulting cDNA was directly processed in qPCR or stored at -20ºC or -80ºC for long-term storage.

RT Mix	Components (Volume required per reaction)
RT Mix I	DEPC-treated Water (0.5 µl) Oligo (dt) Primers (0.25 µl) Random Primers (0.25 µl) dNTP (1 µl) } Total volume 2 µl + 11 µl RNA
RT Mix II Positive	First strand Buffer (4 µl) DTT (1 µl) RNaseIn (1 µl) Superscript III (1 µl) } Total volume 7 µl
RT Mix II Negative	First strand Buffer (4 µl) DTT (1 µl) RNaseIn (1 µl) DEPC-treated water (1 µl) } Total volume 7 µl

Table 2.11 The components and volume required for reverse transcription reactions.

2.6.4.2 qPCR using individual TaqMan® assays

The primers used for individual TaqMan® assay qPCR are listed in **Table 2.12**. Prior to the start of experiments, all the pipettes, tips and tubes as well as the RT-PCR water and the 384 well plates were subject to irradiation by U.V light for 20 minutes.

3 µl of each 20 µl sample of cDNA, that was generated as described in the previous section, was required for a single TaqMan® assay. As multiple assays were investigated per sample, a 1in4 dilution with RT-PCR water was made to allow enough volume. 0.5 µl of TaqMan® assay, 5 µl of TaqMan® Universal PCR Master mix (purchased from Applied Biosystems) and 1.5 µl of RT-PCR Grade water (from Ambion®) was added to each well of the plate with 3 µl of the diluted cDNA.

The plate was sealed with BioRad Microseal® 'B' seal and analysed using the 7900HT Real-Time PCR system from Applied Biosystems with SDS software Standard Core 2.4.1 for analysis.

Gene name	**Product Code**
Beta-Actin (ACTB)	Hs1060665_g1
Gapdh	Hs02758991_g1
HPRT1	Hs02800695_m1
Angiopoietin 1 (ANGPT1)	Hs00375822_m1
Chemokine (C-X-C Motif) Ligand 12 (CXCL12)	Hs00171022_m1
Chemokine (C-X-C Motif) Receptor 4 (CXCR4)	Hs00976734_m1
Endothelial Tyrosine Kinase (TEK).	Hs00945146_m1
Jagged 1 (JAG1)	Hs01070036_m1
N-cadherin (CDH2)	Hs00983056_m1
Notch-1 (NOTCH1)	Hs01062014_m1

Table 2.12 The primers used for individual TaqMan® assay qPCR all purchased from life technologies™.

2.6.4.3 qPCR using custom designed Low density Array cards

Two custom designed TaqMan® Array micro Fluidic or Low density Array (LDA) cards were designed to cover a broad range of genes of interest. The LDA card consists of 12-384 pre-loaded TaqMan® assays which enables the analysis of multiple samples (1-8) when loaded through the 8 fill reservoirs.

The TaqMan® low density array cards were stored at 4°C. As the cards must reach room temperature before the experiment is started, they were removed from the fridge

at least 15 minutes before cDNA is added. cDNA was prepared from isolated RNA as described in section 2.6.4.1. 30-1000 ng of cDNA sample is required per fill reservoir. cDNA samples were diluted in nuclease-free water to make up a volume of 50 µl of a set concentration to be kept consistent between samples and replicates. This was mixed by pipette with 50 µl of TaqMan® Universal Master Mix before adding to each fill port.

The cards were centrifuged using a Sorvall® Centrifuge complete with Sorvall® Custom bucket and card holder for 331 x g for 1 minute, followed by a rest and repeat 331 x g for 1 minute (Up ramp rate 9, down ramp rate 9). The cards were sealed using the TaqMan® Array Micro Fluidic Card Sealer to seal off the main fluid distribution channels. The cards were loaded on to the 7900HT Real-Time PCR system from Applied Biosystems with SDS software Standard Core 2.4.1 for analysis.

2.7 Immuno-staining techniques

2.7.1 Cytospinning method

To perform Immunofluorescence on cells in culture, detached cell were cytospun onto slides. Cytospinning involves the adhesion of cells from suspensions onto a microscope slide by centrifugation. Following typsinisation, cell preparations were counted and $1x10^6$ cells per cell type were fixed in formalin for 10 minutes at room temperature. The cells were washed twice in PBS and separated into $1x10^5$ cells/ 100 µl aliquots per treatment (usually consisting of a no-treatment control, isotype control and antibody). This was added to a funnel attachment to a superfrost microscope slide (Thermo scientific) separated by a blotting paper and centrifuged, using the Shandon CytoSpin III , for 5 minutes at 'medium' speed with 'medium' acceleration.

The cells form a tight circle after cytospinning and can be encircled using a ImmEdge hydrophobic barrier pen (Vector Laboratories) to allowing immunostaining.

2.7.2 Standard Immunofluorescence protocol

After cytospinning the slides were transferred to an immunostaining tray and non-specific binding of anti-bodies blocked in 10% goat serum in PBS for 1 hour at room

temperature. The cells were permeabilised by washing in PBS with 0.1% Tween (PBS-T) twice for 5 minutes on a shaker. The slides were blotted dry and the appropriate volume of primary antibody or matched isotype control was added. The concentrations and volumes used for all antibodies utilised is shown in **Table 2.12**. The slides were incubated at 4°C overnight. The slides were washed 3 times in PBS-T. If no secondary was required the slides were mounted with VECTASHIELD Mounting Medium with DAPI onto coverslips for imaging. If a secondary antibody was required this was added to the slide after washing and incubated for 1 hour at room temperature. The slides were then washed twice in PBS-T and mounted with VECTASHIELD onto coverslips for imaging.

Antibody	**Conc.**	**Isotype**	**Secondary**	**Conc.**
Monoclonal mouse Anti-human CXCR-4-Phycoerythrin (R&D Systems®)	1:50	Mouse IgG2A-Phycoerythrin (R&D Systems®)	n/a	n/a
Monoclonal mouse Anti-human DKK1 (Abcam®)	1:200	Mouse IgG2b (Abcam®)	Goat Anti-mouse IgG (AlexaFluor® 488) H&L (Abcam®)	1:200
Monoclonal mouse Anti-human FST (Abcam®)	1:100	Mouse IgG2 (Abcam®)	Goat Anti-mouse IgG (AlexaFluor® 488) H&L (Abcam®)	1:200
Rabbit monoclonal anti-Hif1α (life technologies™)	1:200	Rabbit IgG (life technologies™)	Goat Anti-rabbit IgG (AlexaFluor® 488) (life technologies™)	1:200
Monoclonal mouse Anti-human MMP3 (Abcam®)	1:100	Mouse IgG2b (Abcam®)	Goat Anti-mouse IgG (AlexaFluor® 488) H&L (Abcam®)	1:200

Table 2.12 Details of the antibodies and isotypes used for immunofluorescence.

2.7.3 ImageJ analysis

ImageJ software was used to quantitatively assess the intensity of fluorescent staining following immunofluorescent studies. ImageJ was used to analyses original TIFF images taken from the fluorescent microscope, which were stacked to produce tiles of

the individual channels (Phase contrast, DiD, DAPI and AlexaFluor 488 and/or Phycoeerythrin), which allowed the intensity of each channel to be assessed per cell. A cell was defined by the region of interest tool. All DiD positive cells per frame were analysed with an equal number of DiD negative cells analysed. A background reading was taken for each channel to be subtracted from the intensity value to ensure each image could be compared to the next.

2.7.4 Immunohistochemistry

The reagents and suppliers for immunohistochemistry are listed in **Table 2.13**. The method and Mouse monoclonal anti human CXCR4 antibody concentration were optimised by Jenny Down (Eaton et al., 2010). This concentration was also optimised by myself using the purchased test arrays. Primary human prostate cancer arrays were purchased from Biomax (PR752). Two test plates were also purchased from Biomax to test the staining protocol (T195b).

Item	Supplier	Preparation
Anti-mouse biotinylated IgG	Vector Laboratories (Peterborough, UK)	n/a
10x Casein solution	Vector Laboratories	n/a
Elite ABC kit	Vector laboratories	2 drops solution A to 5 ml PBS-T, mix and add 2 drops solution B. Leave to stand for 30 mins
Immpress DAB substrate	Vector Laboratories	To 1 ml Immpress diluent, add 1 drop DAB chromagen substrate
3% Hydrogen Peroxide in methanol or water	VWR International Ltd.	Add 6 ml of the supplied 30% Hydrogen Peroxide solution to 200 ml Methanol
Mouse monoclonal anti human CXCR4 (2µg/µl)	R&D Mab 170	n/a
Mouse IgG2A Isotype Control (Clone 20102)	R&D Mab 003	n/a
Normal horse serum	Vector Laboratories	n/a

PBS with 0.1% Tween	Oxoid Ltd. (PBS tablets) Fisher Scientific (Tween® 20)	10X PBS tablets to 1 L distilled water with 1 ml Tween
10mM Tri-sodium Citrate pH6	Sigma Aldrich	4.41 g of sodium citrate to 1.5 L distilled water and adjust to pH6

Table 2.13 The reagents and suppliers for immunohistochemistry

The sections were dewaxed and hydrated to 70% alcohol. These were then incubated with hydrogen peroxide solution for 15 minutes and washed in water followed by distilled water. Antigen retrieval was done by Pre-treatment (PT) module heating in 1.5 L of 10mM Tri-sodium Citrate for 10 minutes at 80°C. The slides were washed for 5 minutes in PBS-T. The slides were blocked in 10% casein with 2% normal horse serum in PBS-T for 20 minutes at room temperature. The slides were then blotted and incubated with the primary mouse monoclonal CXCR4 antibody or matched isotype (diluted 1:500 in 2% casein with 2% normal horse serum) overnight at 4°C.

After incubation, the slides were washed twice in PBS-T for 10 minutes each wash. They were then incubated with Biotinylated anti mouse IgG 30 minutes at room temperature and then washed twice with PBS-T for 10 minutes. The slides were incubated with ABC reagent for 30 minutes at room temperature. This was washed off, twice in PBS-T for 10 minutes per wash. The slides were incubated in Immpress DAB for 5 minutes at room temperature and washed in water for 5 minutes. The slides were counterstained with haematoxylin for 10-15 seconds and washed in water, dehydrated and mounted.

2.7.5 Pathological analysis

Pathological analysis of the immunohistochemical stain was conducted by Dr. Colby Eaton and Professor Simon Cross.

2.8 Miscellaneous techniques

2.8.1 Mouse bone marrow flush to capture metastasising human cells after intracardiac injection

$1x10^5$ DiD labelled PC-3NW1 cells were injected intracardiac into athymic nude mice by Dr Ning Wang and Anne Fowles. After 3 days the mice were culled and the hind legs of mice were dissected for flushing. Both the femurs and the tibias were cut at both ends to expose the bone marrow. A 23 gauge needle and 10 ml syringe were used to flush each bone with 10 ml PBS or until the bone marrow was fully clear (indicated by a complete loss of pink colour from the bone). This made up Fraction 1. Any bone aggregate was disturbed with the needle and the cell flush was centrifuged for 3 minutes at 1500 rpm. The supernatant was discarded and the pellet was retained. 500 µl of 1x red blood cell (RBC) lysis buffer (purchased as part of the Whole blood erythrocyte lysing kit from R&D) was used to re-suspended the cell pellet. The suspension was incubated at room temperature for 15 minutes and vortexed vigorously. The suspension was centrifuges for 3 minutes at 1500 rpm. The supernatant was discarded and the pellet was retained for re-suspension in 1 ml RBC wash buffer (purchased as part of the Whole blood erythrocyte lysing kit from R&D). After re-suspension the cells were washed a further two times with 1 ml RBC wash buffer. After the final wash the pellet was re-suspended in 500 µl of 10% FBS in PBS and filtered through a 70 µm pore cell strainer.

Fraction 2 was made from the remaining bone after flushing. The tibias and femurs were sliced into small fractions (1-2 mm in length) using a scalpel. The bone chips were then incubated in 2 ml Trypsin-EDTA for 10 minutes at 37°C, voretexing periodically. The Trypsin-EDTA solution was then filtered through a 70 µm pore cell strainer to remove the bone chips and the resulting cell suspension was centrifuges at 1500 rpm for 3 minutes. The supernatant was discarded and the resulting cell pellet was re-suspended in 500 µl of 10% FBS in PBS and added to Fraction 1. The cells were then analysed and sorted, based of DiD retention, by FACS Aria.

Chapter 3: Characterising the growth of prostate cancer cell lines and defining the presence of a dormant sub-population

3.1 Introduction

In our laboratory, Vybrant® DiD and CM-DiI were originally used as an addition to GFP and RFP transfected cells to track cells injected *in vivo* due to their high fluorescent intensity and ease of discriminating from auto fluorescence in tissues. When using the PC-3GFP cell line it was observed that over long periods of time, dye retaining cells persisted in the bone marrow of mice while other cells expanded and lost the CM-DiI fluorescent signal whilst retaining GFP (to make certain of their human origin). When using the PC-3NW1 cell line, Vybrant® DiD retaining cells have been identified in the bone marrow of mice up to 8 weeks after injection. Both Cm-DiI and Vybrant® DiD (referred to as DiD hereafter) are lipophilic cell membrane dyes that are split between daughter cells as the cell divides and therefore red/far-red fluorescent signal is lost upon multiple divisions. We proposed the hypothesis that dye retaining cells are mitotically quiescent or 'dormant' and studied the retention of dye by cells *in vitro* to test the hypothesis that a dormant cell sub-population is present in prostate cancer cell lines. This is of particular significance since the clinical features of prostate cancer in patients are periods of latency that proceed skeletal metastases, implying dormant status where tumour cells are present but remain undetected.

'Dormancy' can be defined as a period of inactivity or latency in growth and development. In a cellular sense, we define dormancy as the reversible arrest of the cell cycle at any stage through G0-M phase. This is to say that during dormancy the potential for activity or activation is not reduced. Therefore, it is important to distinguish dormancy from either quiescence (cells in G0) or senescence (irreversible cell cycle arrest).

In order to study 'dormancy' in more detail several human prostate cancer cell lines will be utilised. The cell line predominately used in these studies will be PC-3NW1, which is most commonly used in *in vivo* experiments in the research group in Sheffield. PC-3NW1 has been engineered to express luciferase which can be used to detect cells after there have been injected into immunocompromised mice. After injection these cells will begin to form tumours which, when luciferin is injected intraperitoneal, will produce bioluminescence upon metabolization by the presence of high luciferase at the site of lesions. The luciferase gene was stably transfected into the PC-3 cell line by

electroporation and expressing cells were selected for by Geneticin resistance. This was done ‘in house’ by Dr. Ning Wang in 2011 and named PC-3NW1.

This chapter tests the hypothesis that there is a dormant cell sub-population in human prostate cancer cell lines. Both the lipophilic cell membrane dyes Cm-DiI and Vybrant® DiD were used to detect dormant cells in otherwise rapidly dividing cell populations by fluorescent microscopy and flow cytometry technology. Due to the low cytotoxicity of these dyes we can trace cell dormancy over long periods of time and can use dye retention to isolate these cells for further study. These features make these dyes attractive candidates to investigate dormancy.

In these experiments cells referred to as DiD negative (DiD-) identifies the bulk population of cells that divide normally and lose the dye in culture. We refer to dye retaining cells as dormant or Cm-DiI /DiD positive (DiD+) as they retain dye over long periods in culture due to a lack of division. These cells are not quiescent in the traditional sense and are not senescent. The characteristics we ascribe to dormancy are assessed in detail.

3.2 Chapter Aims, Hypothesis and Objectives

3.2.1 Aims

The aim of this study is to functionally characterise the growth of several human prostate cancer cell (PCa) lines and to explore the use of vital lipophilic membrane dyes to determine the presence of a dormant cell sub-population within them.

To address these aims the following hypothesis will be tested.

3.2.2 Hypothesis

Human prostate cancer cell lines contain a dormant cell sub-population of dye retaining cells that persist amongst rapidly dividing cells.

3.2.3 Objectives

To test the above hypotheses the following objectives will determine whether:

1. Vital lipophilic membrane dyes can be used to identify slow/non-dividing cells.
2. Multiple human PCa cell lines contain a small sub-population of slow/non-dividing cells.
3. These cells are identified in cell cycle or in G0.
4. Dye retaining cells exist in a dormant rather than senescent state

3.4 Results

3.4.1 Characterisation of the growth of human prostate cancer cell lines in monolayer cell cultures

In preliminary studies the basic growth characteristics of the PC-3 cell line and sub-strains as well as the human PCa cell lines LNCaP and C42B4 were determined by the evaluation of growth over 12 days in serum concentrations routinely used in the laboratory to grow these cells (PC-3, PC-3RFP, PC-3GFP, 5%, PC-3NW1, LNCaP and C42B4, 10%). All growth curves were done as described in Methods 2.1.7. These growth curves were used to determine the time of onset and the duration of exponential growth for each cell line. This information was used to test the effects of different serum concentrations during mid-exponential growth, referred to as a serum titration study (Methods section 2.1.9). The half maximally effective serum concentration for the PC-3 cell line and sub-strains was calculated as the FBS concentration that stimulated a growth rate 50% of that produced by its maximally effective concentration. Growth curves were then done in the half maximally effective serum concentration (the half maximum) and in 1% serum. These growth curves were done to determine whether cells retained the ability to generate curves at these serum concentrations. The results were entered into Prism 6 for Mac OS X (GraphPad Software, Inc.). Cell number on the Y-axis represents the average number of cells per well vs. day on the X-axis.

The standard (5% FBS) growth curve for the PC-3 cell line exhibited the classic sigmoidal growth characterisation, consisting of an early lag phase followed by an exponential and a final stationary phase as outlined in the ATCC® ANIMAL CELL CULTURE GUIDE tips and techniques for continuous cell lines. These stages were defined following these guidelines and outlined in Methods 2.1.8. The exponential growth stage for PC-3 cells begun at day 4 and ended at day 8 at all serum concentrations (**Part A, Figure 3.1**). Mid-exponential growth at day 6 was used as the appropriate time point to carry out serum titrations (**Part B, Figure 3.1**). The half maximum serum concentration was determined as 2%. The doubling time in exponential growth in 5% FBS was 28.55 hours, this increased to 30.79 in the half maximum and 31.50 hours in 1% FBS.

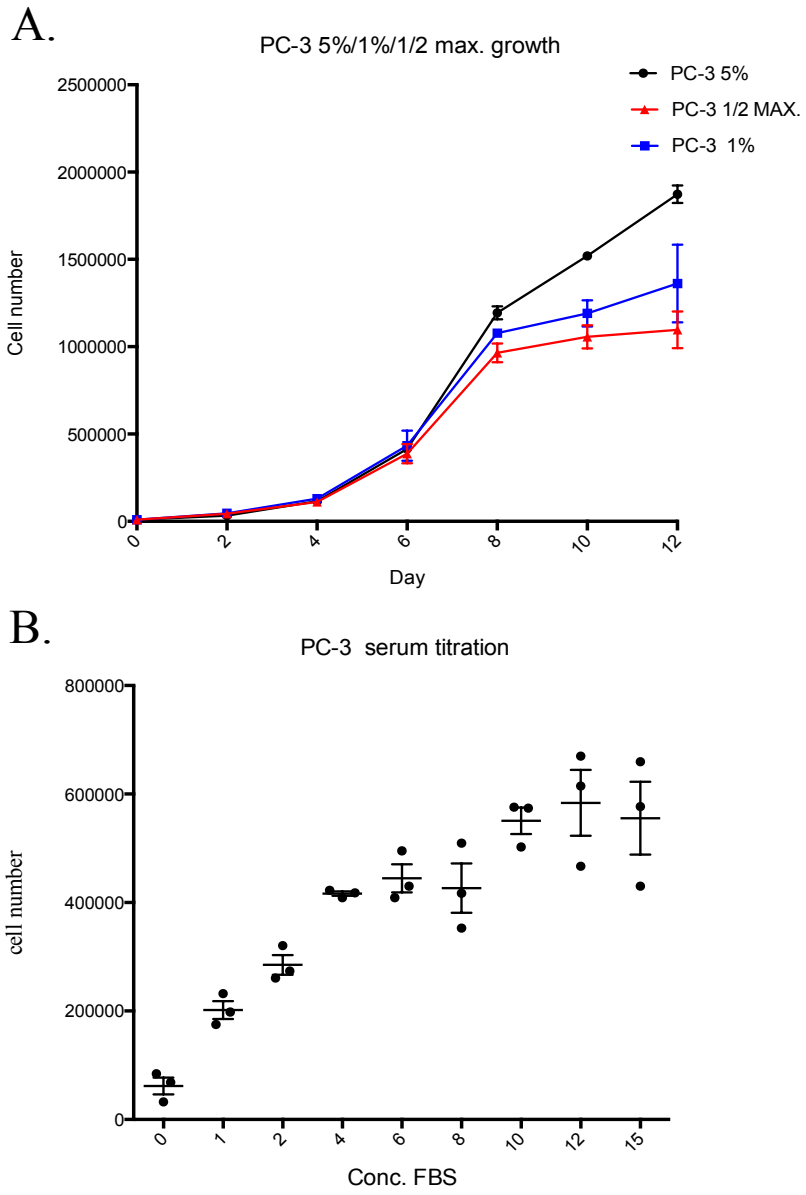

Figure 3.1 Characterisation of the growth of the PC-3 Parental cell line
A. Growth curves for the PC-3 parental line in the routinely used 5% FBS in black. The half maximum growth curve in 2% FBS in red and a low serum growth curve (1% FBS) in blue. Days after seeding is presented on the X-axis and cell number (number of cells per well) on the Y-axis. The curve follows the classic sigmoidal growth trend. **B.** The graph shows the PC-3 serum titration study showing cell number on the Y axis 6 days after seeding in varying percentages of FBS (X axis) in DMEM. For all experiments N = three biological repeats. The average cell number of 4 replicate wells is plotted for each repeat at each time point. Error bars represent the standard deviation.

It was important to determine the growth characterisation of the PC-3NW1 cell strain as this is the most commonly used *in vivo* by the group. This strain was transfected in house by Dr. Ning Wang with a luciferase gene to allow imaging by IVIS upon the addition of luciferin (see Introduction for more detail). In our experience the PC-3NW1 line has a high tumourigenic potential *in vivo* and readily forms skeletal tumours (including in the long bones) following intra-cardiac injection into immunocompromised mice. Due to this PC-3NW1 will be investigated in the most detail in the following results chapters.

A classic sigmoidal growth curve was observed for the PC-3NW1 cell line. Exponential growth begun on day 4 and ended on day 8 at all serum concentrations used (**Part A, Figure 3.2**). The serum titration done on day 6 determined 2% as the half maximally effective serum concentration (**Part B, Figure 3.2**). The doubling time in exponential growth of the PC-3NW1 cell line in 10% serum was 27.25 hours, reducing to 33.72 hours at the half maximum and 31.08 hours in 1% FBS.

The fluorescently labelled PC-3 sub-strains PC-3RFP and PC-3GFP were also used in subsequent experiments, so the growth of these cell strains in standard conditions and in response to varying serum concentrations was determined. The RFP variant was produced, 'in house', by Giancarlo Pesce via a stable transfection of the RFP gene into the parental PC-3 cell line, originally from the ATCC. The GFP variant was produced by Dr. Neil Cross (Sheffield Hallam University).

The doubling time of the PC-3RFP cell line was 31.36 hours in standard (5% FBS) media, 28.95 hours in the half maximum (calculated as 2% FBS by the serum titration **Part B, Figure 3.3**) and 31.58 hours in 1% serum (**Part A, Figure 3.3**). The PC-3GFP cell line had the slowest doubling time of the PC-3 sub-strains, 32.30 hours in standard 5% serum, 31.41 hours at the half maximum (2%) serum concentration and 37.22 hours in 1% serum. Although the growth curve in 5% FBS was sigmoidal as expected, due to the low growth rate the curve in 2% is only weakly S-shaped and in 1% FBS the curve does not reach a clear 'plateau' (**Part A, Figure 3.4**). Despite this doubling time in the 'exponential' phase was calculated between day 4 and day 8 for consistency. The serum titration showed that 2% remained the half maximum (**Part B, Figure 3.4).**

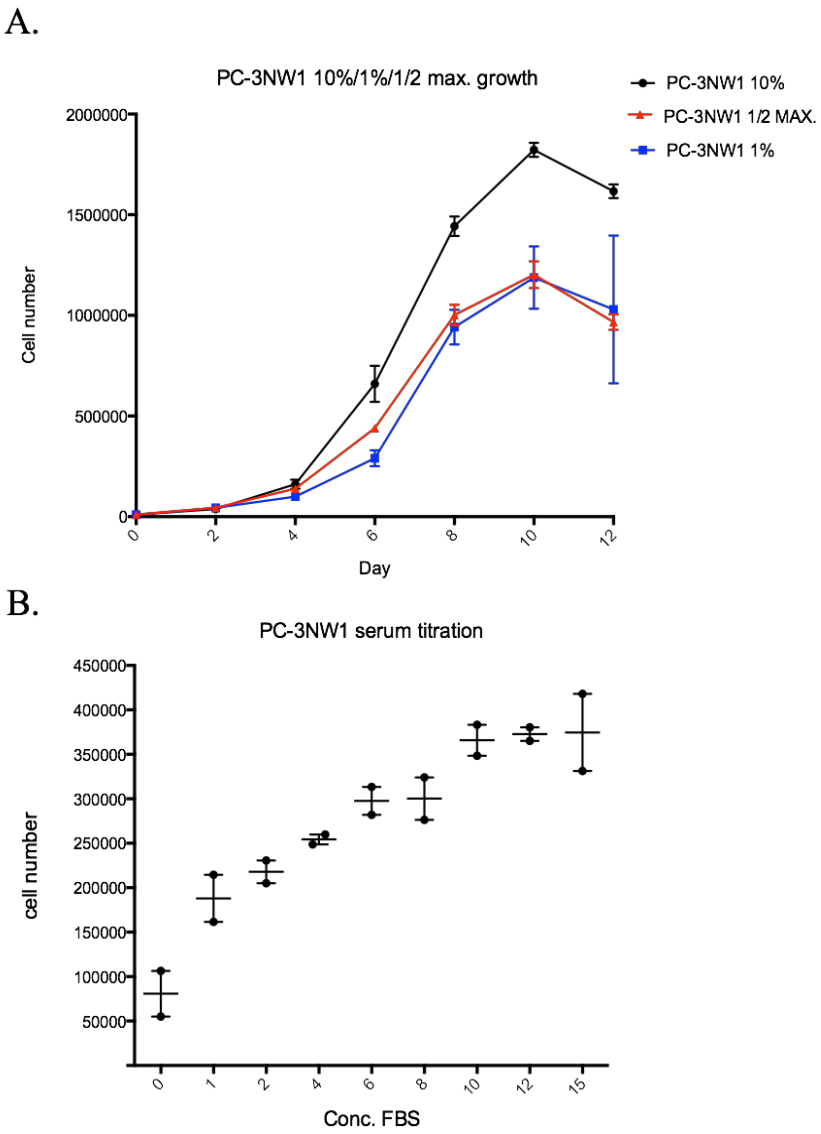

Figure 3.2 Characterisation of the growth of the PC-3NW1 cell line
A. Growth curves for the PC-3NW1 cell line. The standard growth curve in 10% FBS in black. The half maximum growth curve in 2% FBS in red and a low serum growth curve (1% FBS) in blue. All curves follow the classic sigmoidal growth trend. **B.** The PC-3NW1 serum titration study presents the cell number (the number of cells/well) (Y axis) 6 days after seeding in varying percentages of FBS (X axis) in DMEM. For all growth curves and serum titrations N = three biological repeats. The average of 4 replicate wells is plotted for each repeat at each time point. Error bars represent standard deviation.

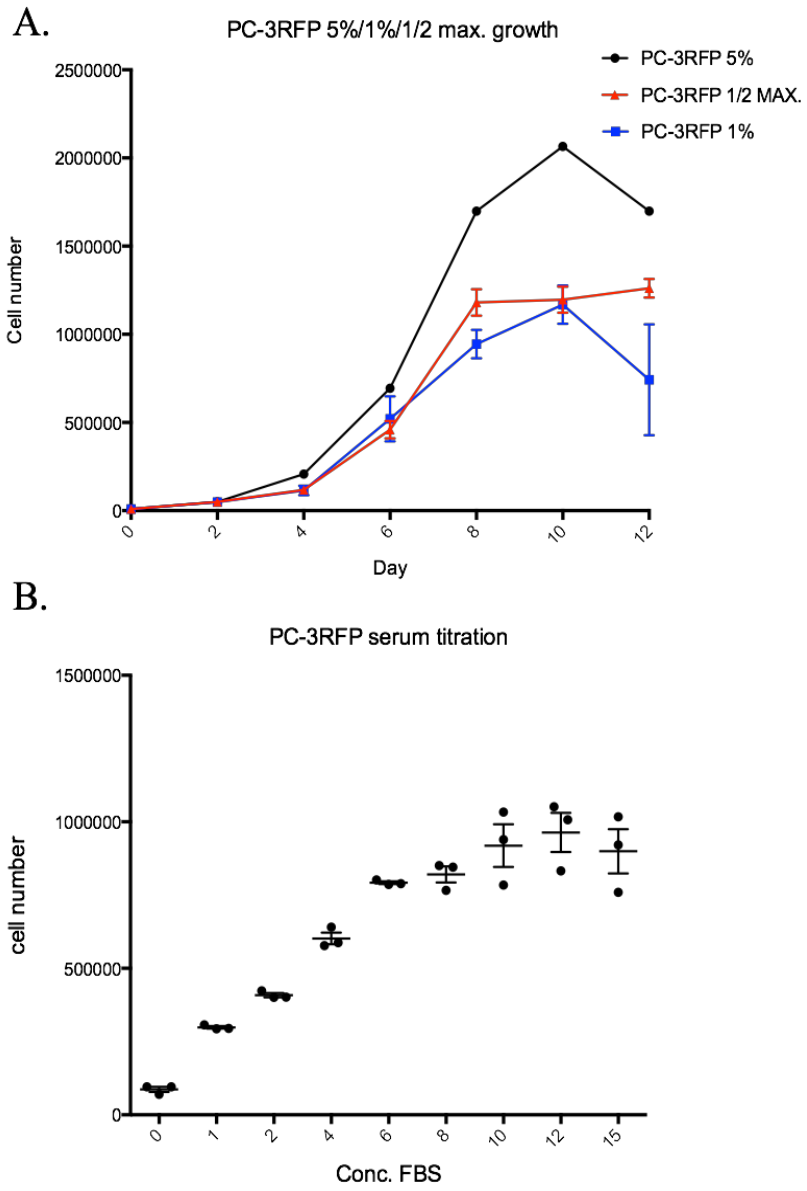

Figure 3.3 Characterisation of the growth of the PC-3RFP cell line

A. The growth curves of the PC-3RFP strain. The standard growth curve in 5% FBS in black, the half maximum growth curve in 2% FBS in red and a low serum growth curve (1% FBS) in blue. The curve follows the classic sigmoidal growth trend. **B.** The PC-RFP serum titration study presents the cell number (number of cells/well) (Y axis) at day 6 after seeding in varying percentages of FBS (X axis) in DMEM.

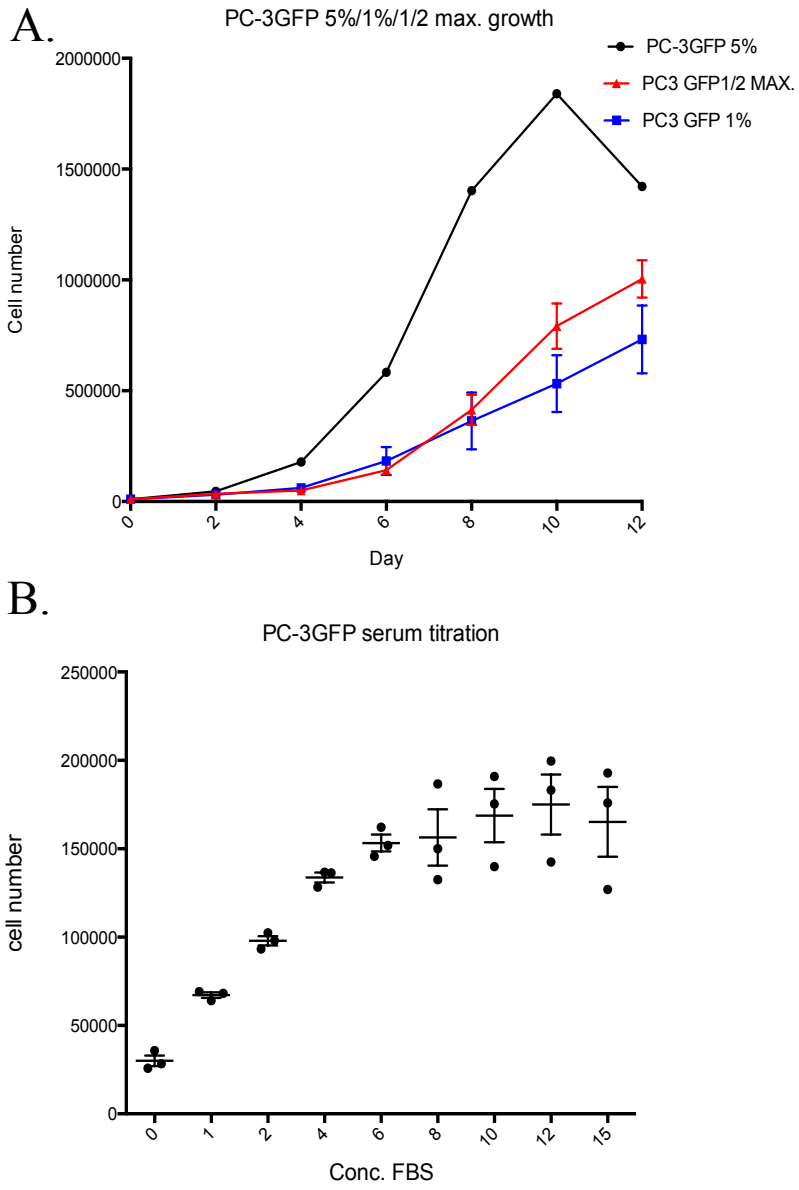

Figure 3.4 Characterisation of the growth of the PC-3GFP cell line
A. The growth curves of the PC-3GFP strain. The standard growth curve in 5% FBS in black, the half maximum growth curve in 2% FBS in red and a low serum growth curve (1% FBS) in blue. **B.** The PC-3RFP serum titration study presents the cell number (number of cells/well) (Y axis) at day 6 after seeding in varying percentages of FBS (X axis) in DMEM.

A standard growth curve in 10% FBS for LNCaP (**Part A, Figure 3.5**) and C42B4 (**Part B, Figure 3.5**) as well as response to low serum (1% FBS) was also done. Neither the LNCaP or C42B4 cell lines exhibited the sigmoidal shaped growth curve seen in the PC-3 sub-strains. In standard media with 10% FBS they exhibited a clear exponential

phase starting at day 6 but did not reach a stationary phase within 12 days. Due to this, the doubling time in 10% and in 1% FBS was calculated between day 6 and day 12. Cell doubling time increased from 43.90 hours for LNCaP in 10% serum to 126.93 hours in 1% FBS. Cell doubling for C42B4 increased from 54.33 hours in 10% FBS to 146.18 hours in 1% FBS.

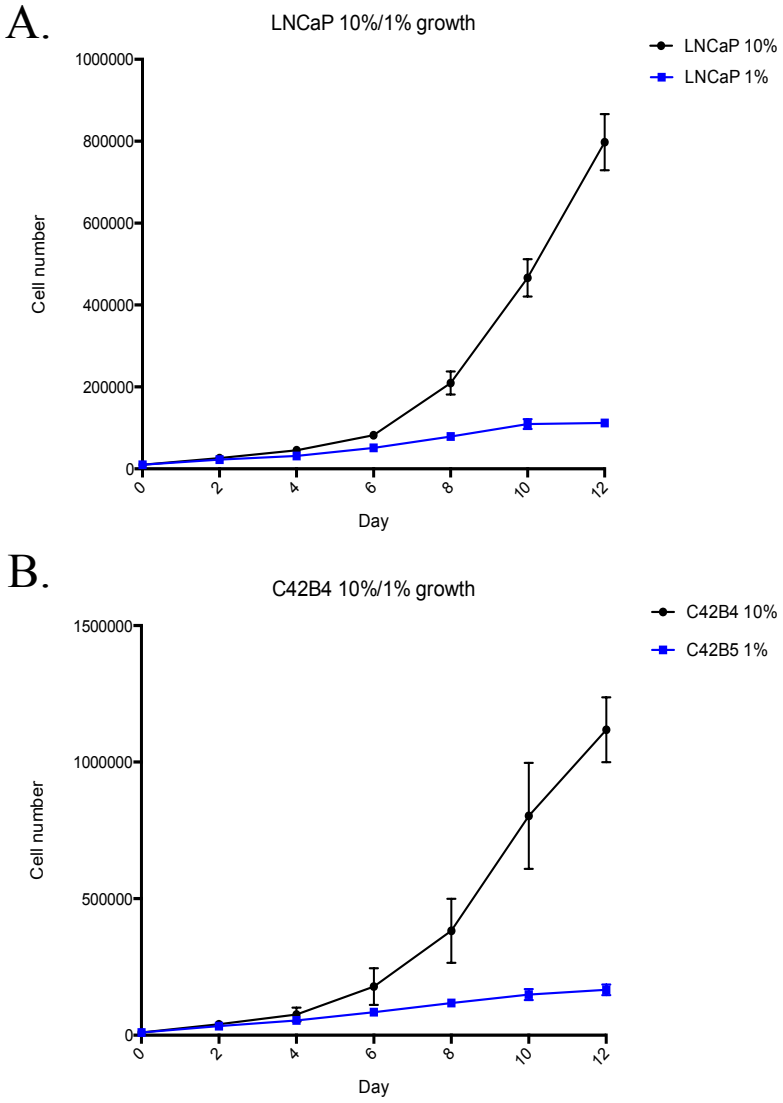

Figure 3.5 Characterisation of the growth of the LNCaP and C42B4 cell lines

A. LNCaP standard growth curve in 10% FBS in black and in response to low serum (1% FBS) in blue. **B.** The C42B4 standard growth curve in 10% FBS in black and in response to low serum (1% FBS) in blue Both cell lines do not reach a stationary phase or 'plateau' within the time of the experiment. N = three biological repeats. The average of 4 replicate wells is plotted for each repeat at each time point. Error bars represent standard deviation.

3.4.2 Identification of dormant cell sub-populations in the PC-3NW1 cell line and other sub-strains

Retention of lipophilic dyes DiD and Cm-DiI can be used as a marker of cell division or low levels of division in tumour cell populations. As discussed in the Introduction these fluorescent dyes become part of the cell membrane and divide amongst daughter cells on division so their fluorescent intensity per cell decreases as the cells proliferate. To investigate whether a dye retaining and therefore dormant sub-population was present in prostate cancer cell lines, $1x10^6$ PC-3NW1 cells were prepared and stained as in Methods 2.2.1 and 2.2.2 and cultured for 21 days in standard 10% FBS DMEM + PenStrep. Analysis of dye retention by flow cytometry using a FACS Calibur flow cytometer took place following the procedure in Methods **Table 2.6**, at each time point (day 0, 3, 7, 10, 14 and 21) a single flask of cells was typsinised, neutralised with media and pelleted by centrifuge. The resulting pellet was re-suspended in PBS and 100,000 events (each event being a single cell) were analysed for dye retention.

The FACS Calibur uses Cell Quest software system which can be used to generate FACS data plots or 'dot plots' which allowed the gating of the CM-DiI or DiD positive population at each time point based on a negative control of unstained cells and a positive control of freshly stained cells on day 0 (DiD used as an example **Parts B and C, Figure 3.6**). At each time point the negative control was analysed prior to the sample to ensure the efficiency of the software and machinery this allowed the percentage of dye positive dormant cells within the population as a whole to be determined. A representative FACS plot at day 14 and the resulting statistics is shown (**Part D Figure 3.6**). Three biological repeats were done and the data was entered into GraphPad Prism 6.

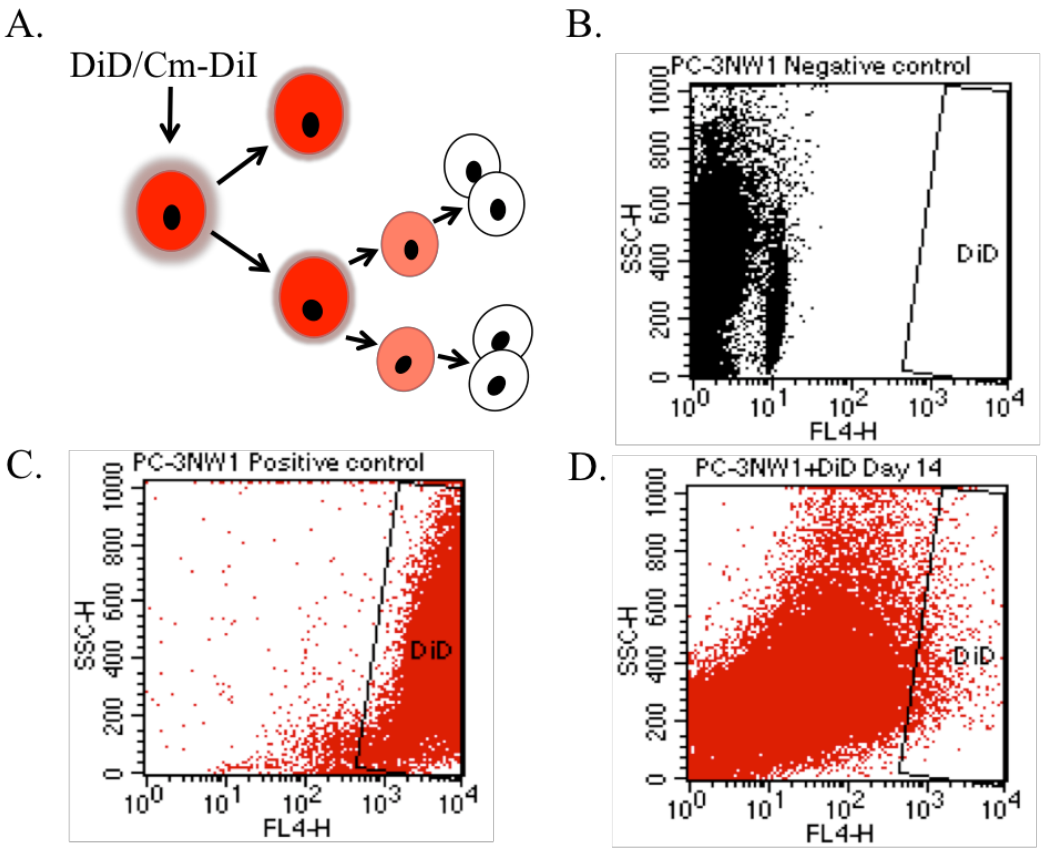

Figure 3.6 Identification of a dye retaining population in PC-3NW1 cells by flow cytometry A. Illustration to show the principles of dye retention. Cells were stained with DiD or Cm-DiI which is incorporated into the cell. As the cell divides the dye is lost. A cell representing the non-dividing dormant sub-population is circled. **B.** 100,000 unstained PC-3NW1 cells acts as a negative control. **C.** 100,000 PC-3NW1 stained with DiD acts as a positive control that sets the gate for dye retaining cells at later time points. D. A representative dot plot at day 14.

At day 0 on average 96.8% and 97.7% of the population were positive for CM-DiI and DiD respectively, representing a successful stain (**Part A, Figure 3.7**). A steep drop occurred at day 7, and this decline continued with the dye retaining sub-population reducing steeply until at day 21, only 0.04% and 0.37% of the population remained CM-DiI and DiD positive, respectively. The X Geometric mean is an indicator of the intensity of the stain per cell in the gated positive region (**Part B**, **Figure 3.7).** No significant reduction in intensity occurred over the 21 day time period in the population that retained CM-DiI or DiD. The intensity of the DiD stain was significantly higher (Unpaired T-test, P value= <0.0001) than the CM-DiI stain overall. On this basis Vybrant® DiD was used to determine dormancy in future experiments. Each experiment was repeated three times.

Fluorescent images were taken of the DiD stained PC-3NW1 cell line, at each time point (days 0, 7 and 14 shown), using the Leica DMI4000 B Automated Inverted Microscope (**Part C, Figure 3.7**). Phase contrast images in grey were layered with a fluorescent image taken by the Y5 (far red) filter cube which excited the DiD at 644 nm.

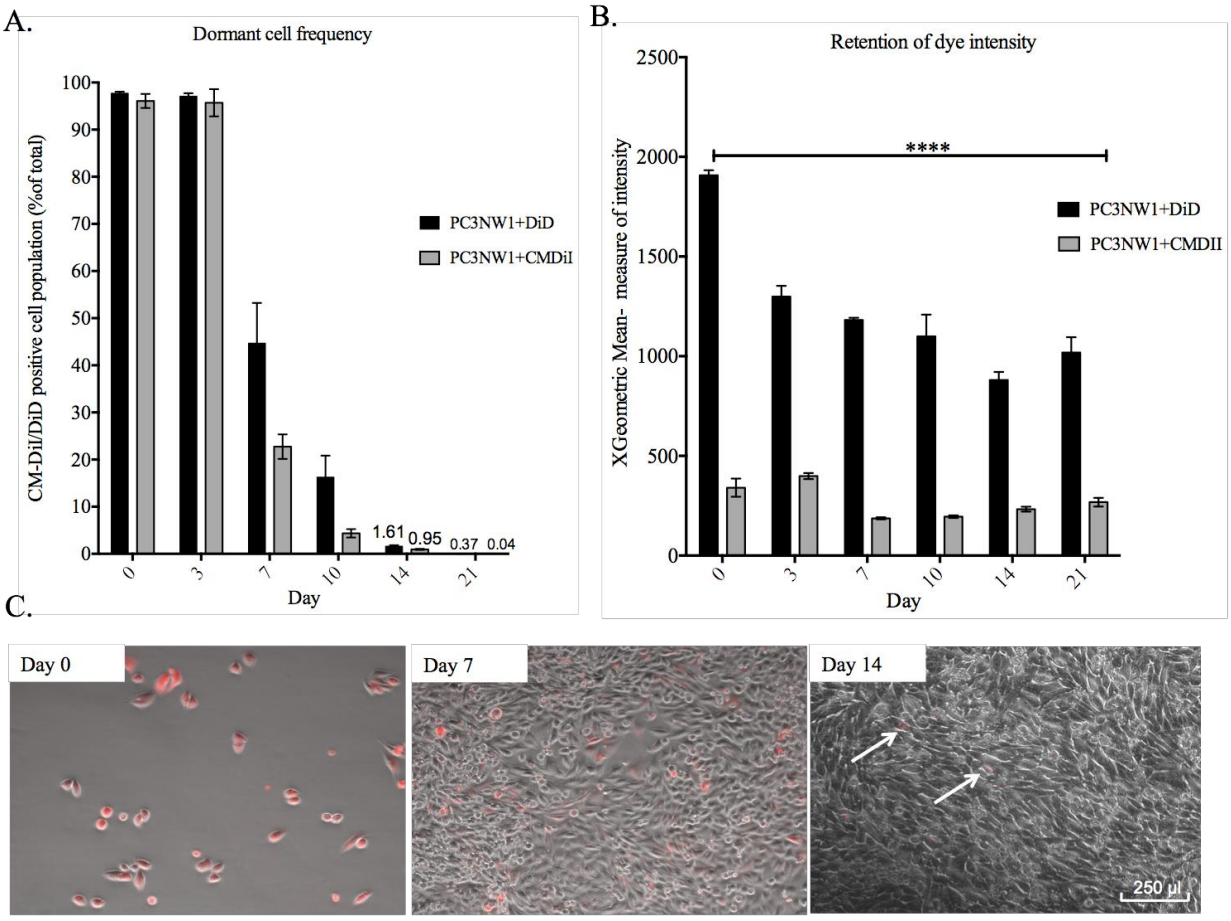

Figure 3.7 Determination of the dormant cell frequency in the PC-3NW1 cell line
A. The bar graph shows the mean percentage of DiD positive cells (Y-axis) at each time point on the X-axis. The error bars show the standard deviation of the mean of three biological repeats. CM-DiI percentages in grey, DiD percentage in black. **B.** The bar chart shows the average dye intensity of a gated DiD positive cell population (Y axis) against time (X-axis). The average intensity of the DiD stain is significantly higher than that of CM-DiI (Unpaired T-test, PC-3NW1+CmDiI vs. PC-3NW1+DiD P=<0.0001). **C.** Representative fluorescent images taken of cultures of PC-3NW1 cells stained with DiD and maintained in 10% FBS DMEM on day 1 (24 hours after staining), day 7 and day 14 (white arrows indicate the small percentage of dye retaining cells at day 14).

The presence/frequency of dormant, DiD positive, sub-populations were also determined for the PC-3 parental cell line and the sub-strains PC-3RFP and PC-3GFP. These cell lines were stained and cultured in 5% FBS DMEM + PenStrep for 21 days and analysed following the same procedure as that used for PC-3NW1. At day 21 the DiD positive fraction was identified as 0.07 for PC-3, 0.15 for PC-3RFP and 0.19 for PC-3GFP (**Figure 3.8**).

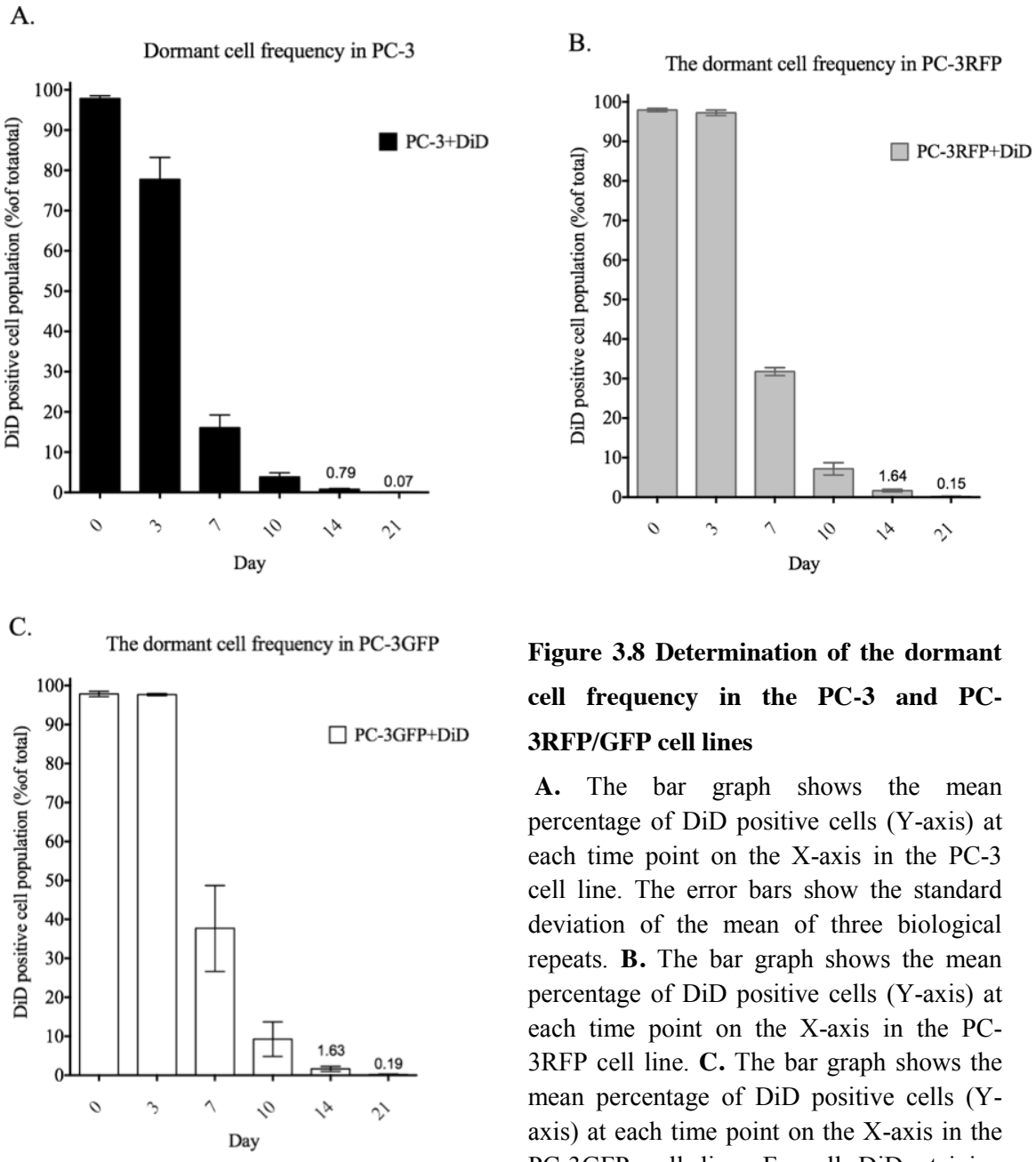

Figure 3.8 Determination of the dormant cell frequency in the PC-3 and PC-3RFP/GFP cell lines

A. The bar graph shows the mean percentage of DiD positive cells (Y-axis) at each time point on the X-axis in the PC-3 cell line. The error bars show the standard deviation of the mean of three biological repeats. **B.** The bar graph shows the mean percentage of DiD positive cells (Y-axis) at each time point on the X-axis in the PC-3RFP cell line. **C.** The bar graph shows the mean percentage of DiD positive cells (Y-axis) at each time point on the X-axis in the PC-3GFP cell line. For all DiD staining experiments N = three biological repeats.
The error bars represent standard deviation.

3.4.3 Identification of dormant cell sub-populations in LNCaP and C42B4 cell lines

The human PCa cell lines LNCaP and C42b4 were also analysed for the presence of a dormant sub-population. Cells were stained and cultured as outlined in Methods section 2.2.2 The dormant cell fraction was evaluated for 21 days by FACS Calibur.

3.4.3.1 A dormant cell sub-population was identified in the LNCaP cell line

LNCaP is an androgen sensitive human prostate cancer cell line with weak tumourigenicity *in vivo*. The LNCaP cell line was stained with DiD (as in Methods 2.2.2) and cultured for 21 days *in vitro* following the standard protocol to analyse dye retention outlined in **Table 2.6**. Although the growth rate is much lower than that of the PC-3 cell lines (the doubling time in 10%= 46.45 hours for LNCaP, 27.25 hours for PC-3NW1), the same passage times were kept to reduce variables when comparing to the PC-3 cell line.

The DiD positive cell fraction was 1.49% on day 14 and 0.06% on day 21 (**Part A, Figure 3.9**), a comparable result to PC-3NW1. Fluorescent images were also taken of the DiD stained LNCaP cell line, at each time point (days 0, 7 and 14 shown) using the Leica DMI4000 B Automated Inverted Microscope (**Part B, Figure 3.9**).

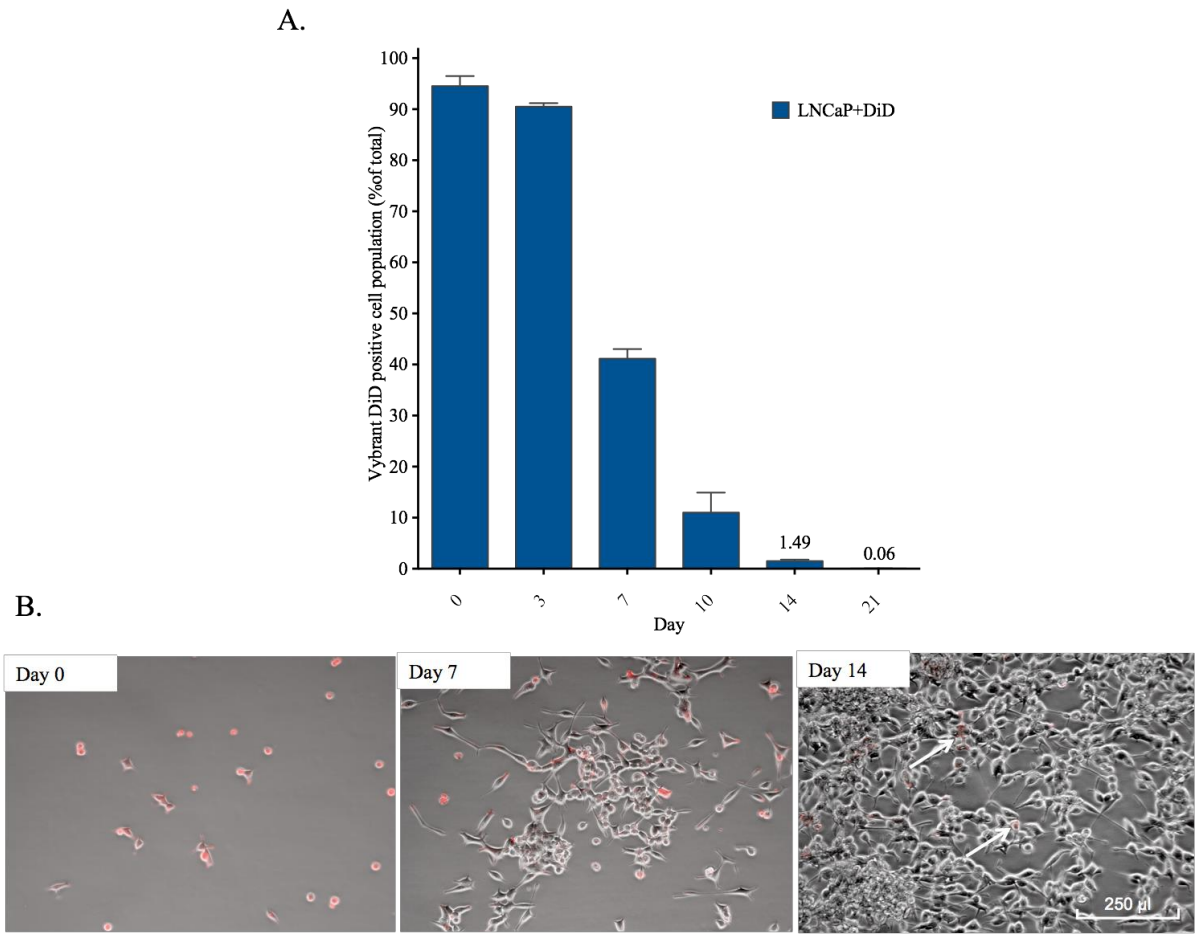

Figure 3.9 Determination of a dormant cell frequency in the LNCaP cell line
A. The bar graph shows the mean percentage of DiD positive cells (Y-axis) at each time point on the X-axis in the LNCaP cell line. The error bars show the standard deviation of the mean of three biological repeats. **B.** Representative fluorescent images taken of cultures of LNCaP cells stained with DiD and maintained in 10% FBS DMEM on day 1 (24 hours after staining), day 7 and day 14 (white arrows indicate the small percentage of dye retaining cells at day 14).

3.4.3.2 A dormant cell sub-population was identified in the C42B4 cell line

C42B4 is an androgen insensitive sub-strain of LNCaP that has a higher metastatic potential than its parental strain. The C42B4 cell line was stained with DiD (as in Methods 2.2.2) and cultured for 21 days *in vitro* and analysed at routine time points to track dye retention. Again despite the reduction in growth rate compared to the PC-3 strains, (the doubling time in 10%= 49.31 hours for C42B4, 27.25 hours for PC-3NW1), the same passage times were kept to reduce variables when comparing to the PC-3 cell line.

The DiD positive cell fraction was 0.74% on day 14 and 0.02% on day 21. Fluorescent images were taken of the DiD stained C42B4 cell line, at each time point (days 0, 7 and 14 shown) using the Leica DMI4000 B Automated Inverted Microscope (**Figure 3.10**).

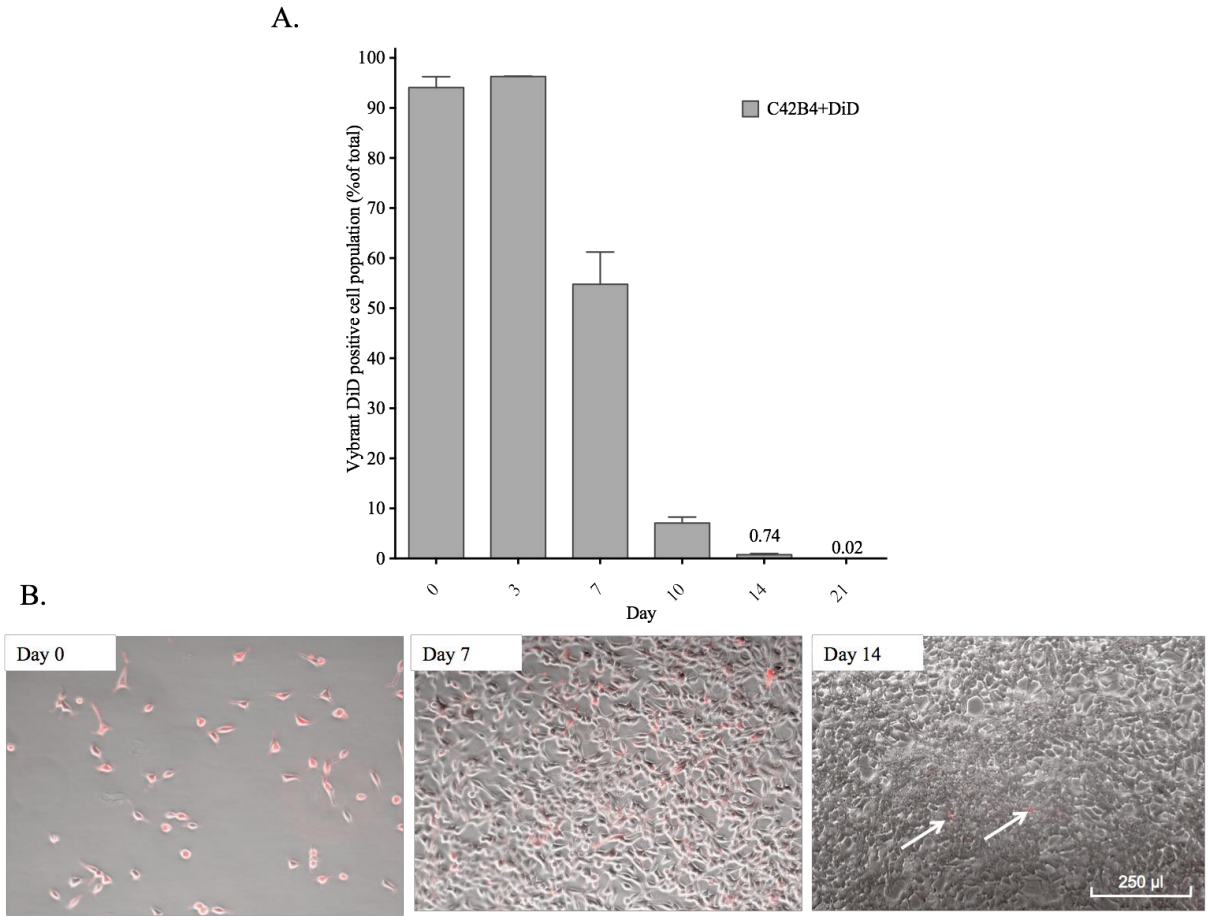

Figure 3.10 Determination of the dormant cell frequency in the C42B4 cell line
A. The bar graph shows the mean percentage of DiD positive cells (Y-axis) at each time point on the X-axis in the C42B4 cell line. The error bars show the standard deviation of the mean of three biological repeats. **B.** Fluorescent images taken of cultures of C42B4 cells stained with DiD and maintained in 10% FBS DMEM on day 1 (24 hours after staining), day 7 and day 14 (white arrows indicate the small percentage of dye retaining cells at day 14).

3.4.4 Lipophilic dyes were retained in a high proportion of cells after growth arrest using Mitomycin C

To test that DiD retention was a result of non-division of cells, PC-3NW1 cells were stained with DiD and growth arrested by Mitomycin C. FACS Calibur analysis and fluorescent microscopy showed that a high number of cells retained DiD as a result of mitotic suppression by Mitomycin C (**Part A, Figure 3.11**). In fact at day 21, 66.89% of cells remained DiD positive suggesting that dye retention is a valid marker of non-dividing cells. The fluorescent image (**Part B, Figure 3.11**) shows the high proportion

of DiD positive cells. The cells are also bigger than usual, an indicator of protein accumulation due to growth arrest. The retention of CM-DiI was also assessed following Mitomycin C treatment and similar results were found (**Part D, Figure 3.11**).

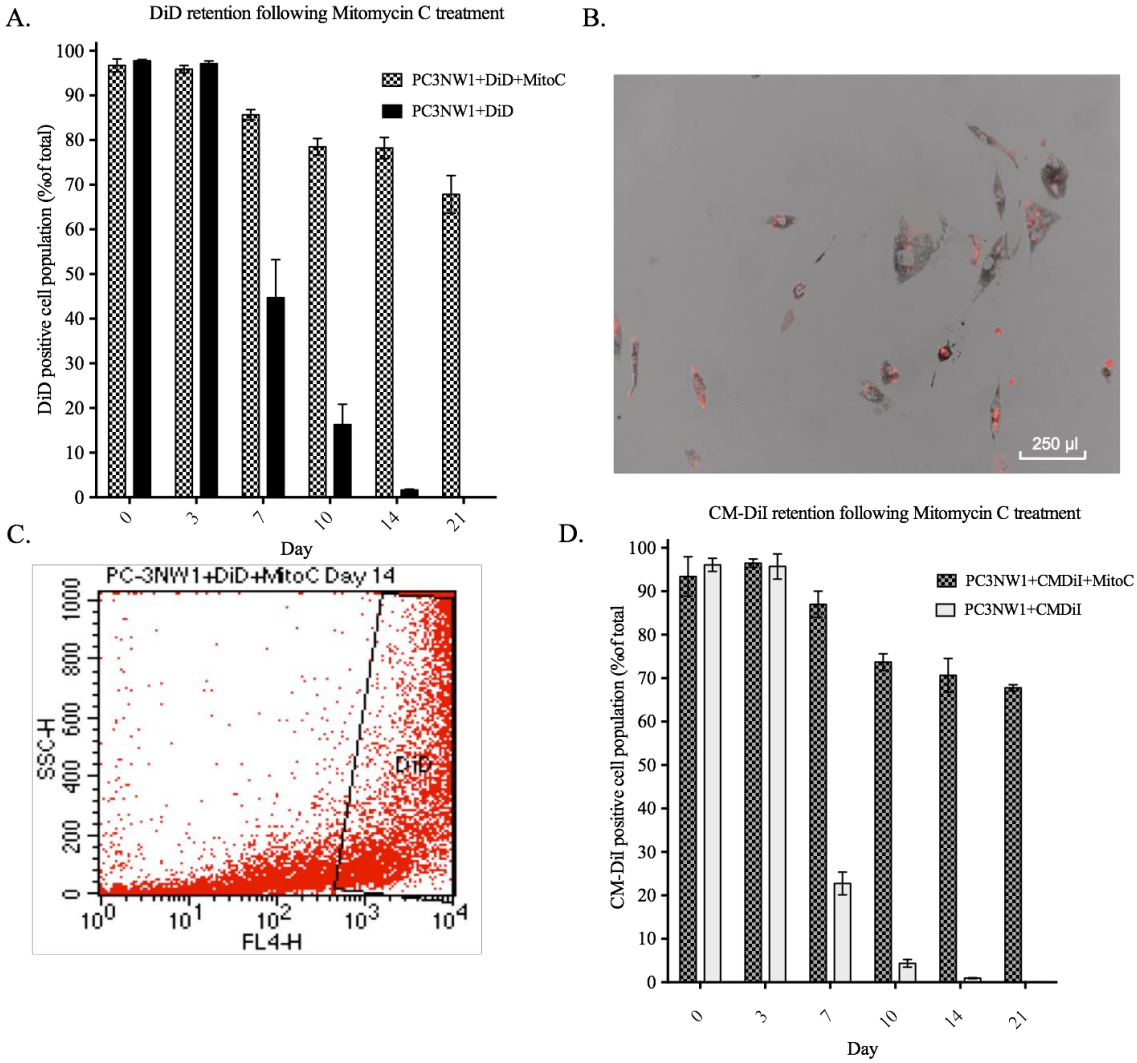

Figure 3.11 Dye retention following a growth arrest treatment

A. A bar graph to show DiD retention over 21 days following growth arrest treatment with Mitomycin C. A high percentage of cells retain the DiD stain long term after Mitomycin C treatment (black bars) compared to untreated control stained cells (grey bars). The graph shows the mean percentage of DiD positive cells on the Y-axis at each time point on the X-axis. The error bars show the standard deviation of the mean of three biological repeats. **B.** A fluorescent image taken on the Leica DMI4000 B Automated Inverted Microscope at day 21. **C.** The dot plot shows the high number of cells that are DiD positive 21 days after staining with the growth arrest. **D.** CM-DiI is retained at high frequency after a growth arrest, compared to untreated CM-DiI stained cells.

3.4.5 The addition of DiD has no effect on PC-3NW1 growth rate or colony forming ability

To determine if the addition of either CM-DiI or DiD had an effect on PC-3NW1 cell growth a growth curve following dye addition was done under standard conditions (10% FBS DMEM + PenStrep) (**Part A, Figure 3.12**). There was no significant change in growth with CM-DiI or DiD dye addition (one-way ANOVA P=0223). Any changes in the ability to form colonies in monolayer was tested by comparing the cloning efficiency of PC-3NW1 cells with and without the addition of DiD following Methods section 2.1.10 Briefly 1,000 cells were seeded per 60mm petri dish in quadruplet and cultured in 10% FBS DMEM + PenStrep for 14 days in a 37° 5% CO_2 incubator. The colonies were stained with Giemsa and imaged using the BioCount Colony Counter. The number and size of colonies was then measured by the GeneTool software system. No significant difference in colony number was seen (Paired T-test P=0.217) (**Part B, Figure 3.12**). A representative comparison is shown in **Part C, Figure 3.12**.

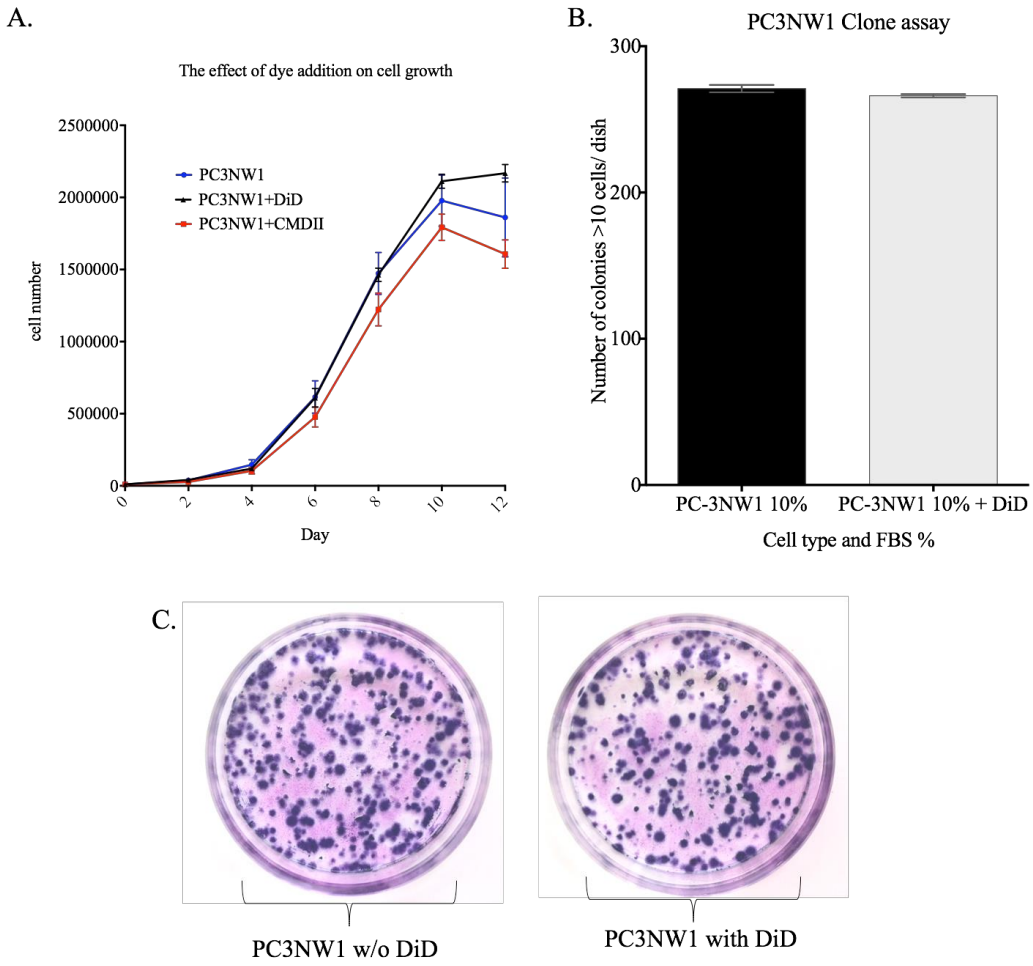

Figure 3.12 Dye addition does not affect the growth characteristics of the PC-3NW1 cell line

A. Comparison growth curves of the unstained PC-3NW1 cell line (blue line), CM-DiI stained PC-3NW1 cells (red line) and the DiD stained cell line (black) shows no significant difference in growth upon either dye addition (one-way ANOVA P=0.223). **B.** Clonal growth in monolayer showed no significant change in cloning ability between control PC-3NW1 cells (black bar) and PC-3NW1 cells stained with DiD (grey bar) (Unpaired T-test, P=0.217). **C.** A representative comparison image of the Giemsa stained clone assays. PC-3NW1 on the left compared to PC-3NW1 cells with DiD on the right.

3.4.6 Dormant cells were more resistant to the chemotherapeutic drug Doxorubicin

Doxorubicin treatment was used to test whether dormancy could protect cells from a chemotherapeutic agent that targets dividing cells. At 14 days post-DiD staining, cultures of PC-3NW1 cells were seeded into a 6 well plate at a density of $1x10^5$ /well in triplicate. Doxorubicin was administered every 48 hours for 14 days at concentrations

1μm, 100nm and 10nm. The percentage of DiD positive and DiD negative cells was compared to an untreated control after 14 days of treatment. Plates were imaged every 48 hours by fluorescent microscopy. 1μm of Doxorubicin appeared to be the optimum dose and is given as an example in **Part A Figure 3.13**.

At the end time point of 14 days the numbers of DiD positive and DiD negative cells were counted. To work out the percentage survival of each group the numbers of cells in the no treatment control were counted and the percentage of DiD positive cells assessed by FACS Calibur. The average of 3 wells in 3 biological repeats was taken. 14 days after set up there were 1.34 $x10^6$ cells per well in the no treatment control with a DiD positive fraction of 0.01% (equal to 134 cells/well). After 14 days of treatment with 1μm Doxorubicin there were on average 62.55 DiD positive cells per well, which shows a 46.47% survival rate. Only 96.33 DiD negative cells/well survived after 14 days of 1μm Doxorubicin treatment (0.007% survival rate) which was significantly lower than that of the DiD positive cells (Unpaired T-test, P= 0.0002) (**Part B Figure 3.13**). This suggests that the DiD retaining dormant sub-population confers a resistance to traditional cancer treatments.

A.

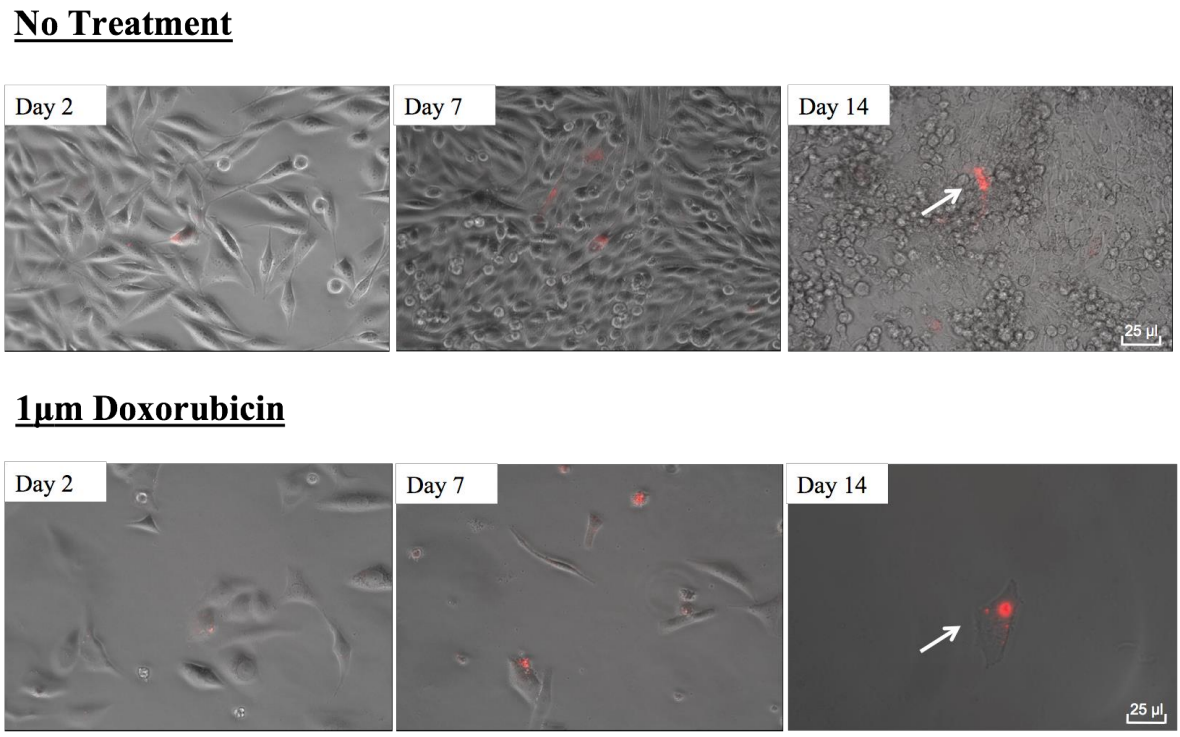

B.

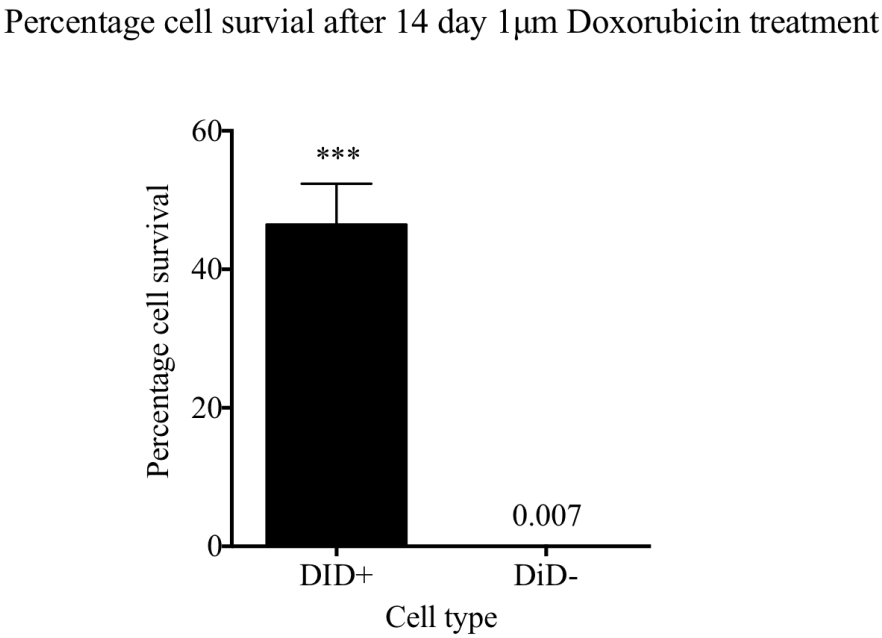

Figure 3.13 DiD positive dormant cells were more resistant to Doxorubicin treatment
A. After 14 days of Doxorubicin treatment a higher percentage of DiD positive cells have survived (lower panels). The upper panel shows the no treatment control (white arrows indicate the presence of dye retaining cells at day 14). **B.** After counting and comparing to the no treatment control, the percentage survival of each cell type after treatment showed that a significantly higher percentage of DiD positive cell were resistant to Doxorubicin (Unpaired T-Test, P= 0.0002) N= 3 biological repeats.

3.4.7 Assessment of the cell cycle status of the dormant cell sub-population

The previously reported experiments confirmed that DiD and Cm-DiI could be used to identify non-dividing or slowly dividing cells (Mitomycin C experiments, see **Figure 3.11**). FACS Calibur analysis showed that there is a dye retaining sub-population present in multiple prostate cancer cell lines. To assess the definition of these cells as dormant (as stated in the chapter introduction) an investigated their cell cycle status was peformed.

3.4.7.1 Senescence assay

The Senescence Detection Kit from Abcam® showed that the DiD positive dormant cells were not positive for senescence associated (SA) -beta-galactosidase activity and were therefore not senescent. SA-beta-galactosidase is active at pH 6.0 and is identified as a senescent marker based on the observation that senescent cells have higher endogenous levels of this enzyme activity in acidic conditions. Increased SA-beta-gal represents an accumulation of beta-galactosidase as opposed to being a unique enzyme marker of senescence. The kit was used to histochemically detect senescent cells by a positive blue stain for SA-beta-gal activity under pH 6.0. Active SA-beta-galactosidase hydrolyses the substrate 5-bromo-4-chloro-3-indolyl-β-D-galactopyranoside (X-gal) to yield galactose and 5-bromo-4-chloro-3-hydroxyindole (visible as a blue stain). In this way cells that are senescent appear as blue stained cells.

On day 14 after DiD staining $1x10^5$ PC-3NW1 cells were seeded in triplicate into a 6 well plate. The cells were fixed with the provided 'Fixative solution' and were stained overnight at 37°C with the prepared X-gal solution (Methods 2.5.4). A qualitative assessment of blue stain was done by fluorescent microscopy (to detect DiD) and colour camera microscopy. This experiment was repeated 3 times and visual assessment showed that DiD positive cells were not positive for SA-beta-Gal activity. A representative image at 10x magnification is shown in **Figure 3.14**.

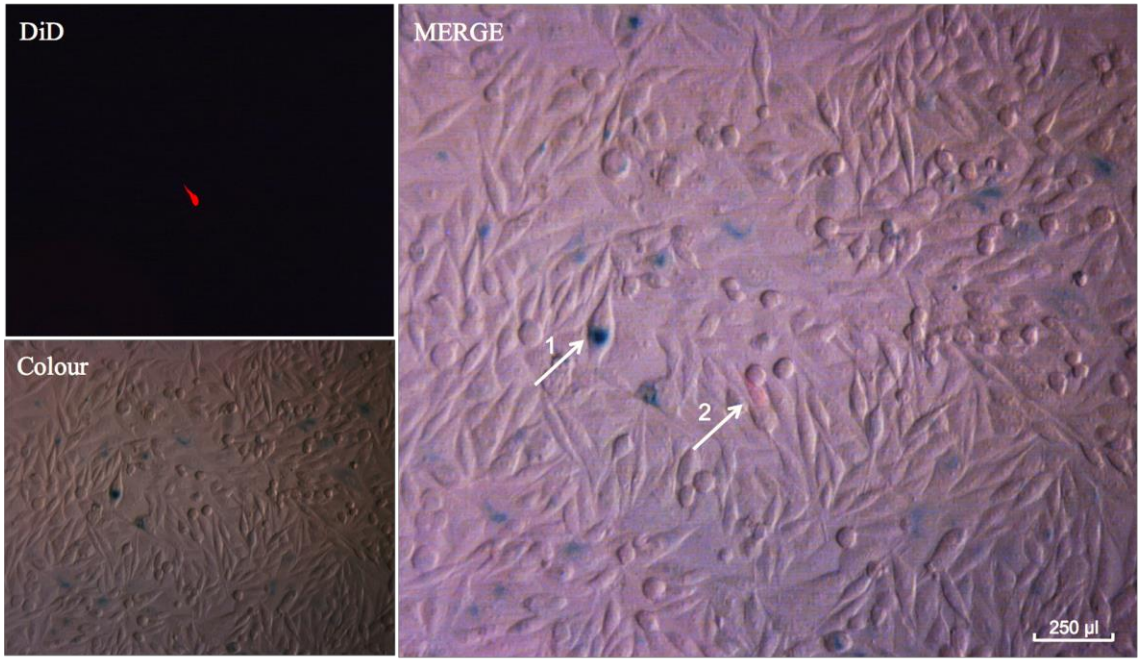

Figure 3.14 Dormant cells were not senescent by assay for SA-beta-Gal activity
A representative image (10x magnification) of the DiD far-red Y5 channel (top-left) and the colour camera image (lower-left) with the merged image. The senescence detection kit showed that at day 14 after DiD staining, DiD positive dormant cells were not positive for blue stain (indicated by arrow 2) although other cells were positive for the blue stain and considered to be senescent (arrow 1).

3.4.7.2 KI-67 assay

Ki-67 protein is present in the nucleus of cells at all active stages of the cell cycle (G1, S, G2 and M-phase) but absent from G0. It is therefore identified as a positive marker of cell proliferation.

The Ki-67 status of DiD positive cells on day 14 after staining was determined by flow cytometry using BD FACS Calibur and CellQuest™ software. Cells were prepared as in Methods section 2.5.1 and 10,000 events (cells) were analysed for their Ki-67 status using an Anti-Human mouse monoclonal antibody to Ki-67 that is conjugated to AlexaFluor 488 (BD Pharmingen™). Gating of the DiD positive population was based on a positive control (PC-3NW1 cells stained with DiD and immediately analysed. **Part A, Figure 3.15**). A negative control of untreated PC-3NW1 cells (not shown) and a matched isotype control were used to gate the KI-67 negative population (**Part B, Figure 3.15**). The upper left (UL) quadrant shows DiD positive cells which were not Ki-67 positive whereas the upper right (UR) shows the shift of DiD positive cells into Ki-67 positivity. The lower left (LL) quadrant shows DiD negative, rapidly diving cells

which were Ki-67 negative whereas the lower right (LR) quadrant represents cells that were DiD negative and KI-67 positive.

10,000 PC-3NW1 cells were analysed 14 days after staining, a representative dot plot and the accompanying statistical output are shown in **Part A, Figure 3.16.** 90.18% of the DiD negative, rapidly dividing population were Ki-67 positive. This is significantly higher than the percentage of DiD positive cells that were KI-67 positive cells on day 14 (61.07%) (Unpaired T-test, P=0.015). A significantly higher percentage of DiD+ cells were KI-67 negative on day 14 (38.92%) compared to DiD negative cells (9.80%) (Unpaired T-test, P=0.015). The bar chart represents the mean value from three biological repeats. The error bars represent standard deviation (**Part B, Figure 3.16**).

A.

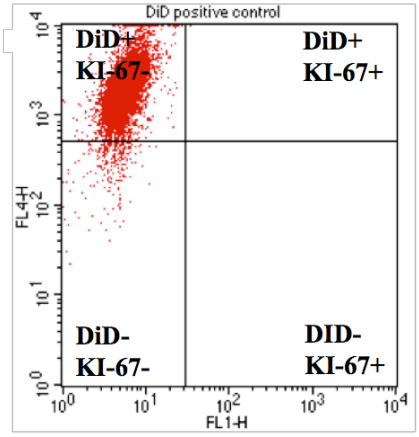

Quadrant Statistics

File: DiD positive control
Sample ID: positive
Tube: Untitled
Acquisition Date: 01-Apr-14
Gated Events: 10000
X Parameter: FL1-H (Log)
Quad Location: 29, 514

Log Data Units: Linear Values
Patient ID:
Panel: Untitled Acquisition Tube List
Gate: G1
Total Events: 10127
Y Parameter: FL4-H (Log)

Quad	Events	% Gated	% Total	X Mean	X Geo Mean	Y Mean	Y Geo Mean
UL	9717	97.17	95.95	5.92	5.64	2338.31	2070.83
UR	3	0.03	0.03	32.56	32.49	9910.46	9910.46
LL	280	2.80	2.76	4.13	3.78	329.67	290.40
LR	0	0.00	0.00	***	***	***	***

B.

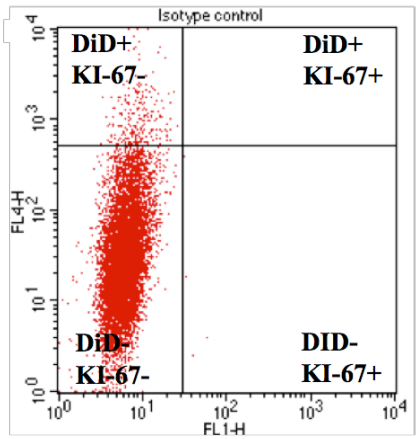

Quadrant Statistics

File: Isotype control
Sample ID: Isotypes
Tube: Untitled
Acquisition Date: 19-Mar-14
Gated Events: 10079
X Parameter: FL1-H (Log)
Quad Location: 29, 514

Log Data Units: Linear Values
Patient ID:
Panel: Untitled Acquisition Tube List
Gate: G1
Total Events: 10172
Y Parameter: FL4-H (Log)

Quad	Events	% Gated	% Total	X Mean	X Geo Mean	Y Mean	Y Geo Mean
UL	239	2.37	2.35	9.44	8.67	1426.05	1092.39
UR	1	0.01	0.01	29.96	29.96	8505.26	8505.26
LL	9835	97.58	96.69	6.34	6.01	55.56	28.62
LR	4	0.04	0.04	40.31	39.15	101.69	16.14

Figure 3.15 Gating of the KI-67 positive population

A. A positive control of 10,000 DiD stained PC-3NW1 cells was used to set the DiD positive gate to determine the DiD positive fraction on day 14. **B.** An IgG isotype control was used to set the gate to determine cells that were positive for the Ki-67 antibody and therefore in a proliferative state.

A.

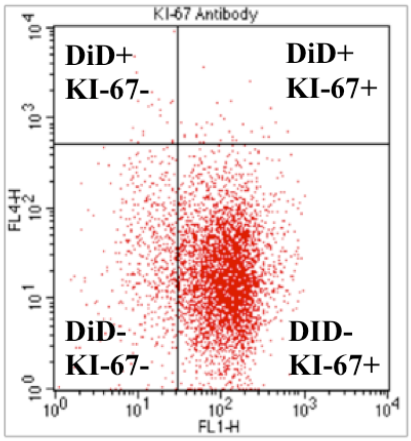

Quadrant Statistics

File: KI-67 Antibody
Sample ID: KI67 3
Tube: Untitled
Acquisition Date: 02-Apr-14
Gated Events: 4920
X Parameter: FL1-H (Log)
Quad Location: 29, 514

Log Data Units: Linear Values
Patient ID:
Panel: Untitled Acquisition Tube List
Gate: G1
Total Events: 5100
Y Parameter: FL4-H (Log)

Quad	Events	% Gated	% Total	X Mean	X Geo Mean	Y Mean	Y Geo Mean
UL	21	0.43	0.41	16.38	15.09	1705.20	1205.32
UR	32	0.65	0.63	153.97	110.77	923.86	815.87
LL	521	10.59	10.22	15.99	13.75	63.15	28.31
LR	4346	88.33	85.22	138.64	113.67	33.12	16.88

B.

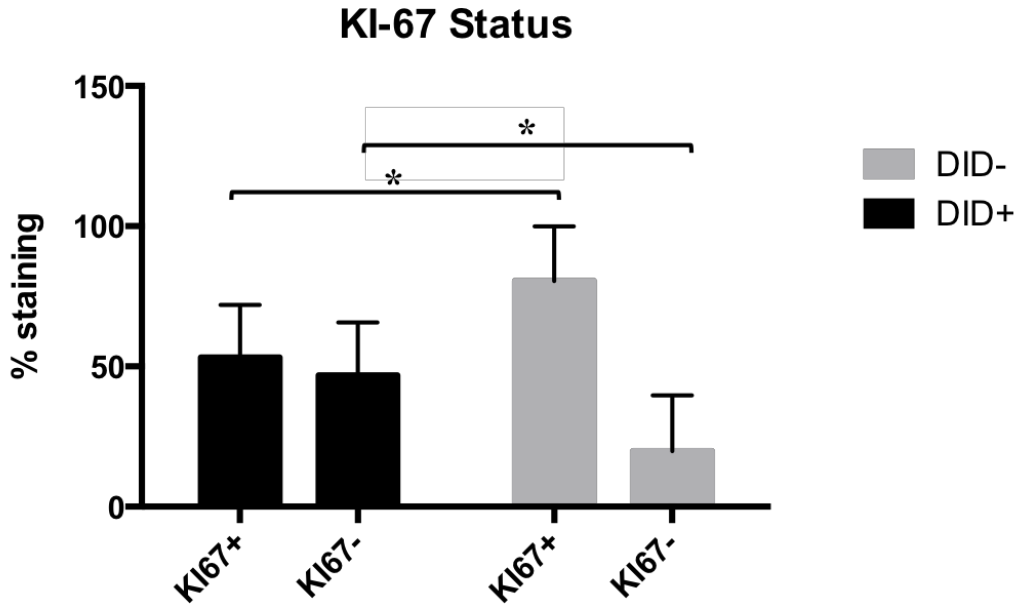

Figure 3.16 The Ki-67 status of the DiD positive PC-3NW1 cells on day 14

A. A representative dot plot and the accompanying statistical output of a sample on day 14. **B.** The bar chart shows the Ki-67 status of DiD negative cell in grey and DiD positive cells in black. The bar represents the mean value of three biological repeats. The error bars represent standard deviation (Unpaired T-test, DiD+ Ki-67+ vs. DiD- Ki-67+ P=0.015) (Unpaired T-test DiD+ Ki-67- vs. DiD- Ki-67- P=0.015)

3.4.7.3 Qualitative assessment of KI-67 status in the dormant cell sub-population by immunofluorescence

This result was qualitatively evaluated by immunofluorescence. PC-3NW1 cells stained with DiD were grown on a Permanox® microscope chamber slide for 14 days. At day 14 after DiD staining the cells were fixed and stained with a AlexaFluor® 488 Mouse anti-Human Ki-67 (BD Pharmingen™) monoclonal antibody overnight at 4°C (Methods 2.5.2). A matched isotype and no treatment were also done to control for non-specific binding or auto-fluorescence. A representative image at 20 x magnification is shown in **Figure 3.17**. The image shows DiD retaining cells were both Ki-67 positive and negative, reflecting the quantitative Flow cytometry result

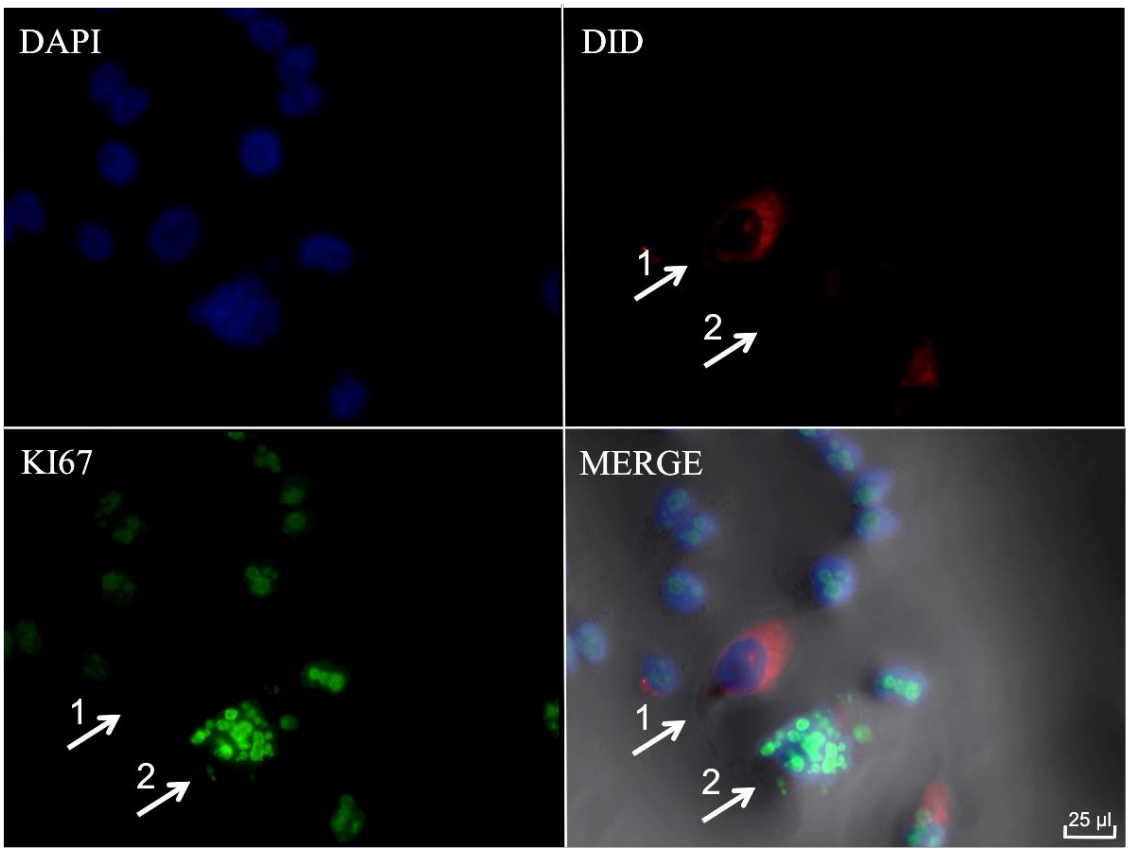

Figure 3.17 Immunofluorescence to detect Ki-67 status
A fluorescent image taken at 40x magnification following immunofluorescent staining with an alexa 488 conjugated anti-human mouse monoclonal antibody to Ki-67 (Abcam). Ki-67 is present in the nucleus of dividing cells. The nucleus was counterstained with DAPI in blue (top left). The far-red Y5 channel detects DiD positive cells in red (top right). The N3 channel was used to detect the AlexaFluor 488 conjugated Ki-67 antibody in green (lower left). The merged image (lower right) shows an example of two DiD positive cells in the centre that were Ki-67 negative (arrow 1) and Ki-67 positive (arrow 2).

3.4.7.4 P.I assay

Propidium iodide (P.I) can be used to determine the DNA content of a cell, and so determine which stage of the cell cycle it is in, by intercalating with DNA bases and emitting a fluorescent signal when exited by a 535 nm laser. To gain more information about what stage of the cell cycle the DiD positive cells were in, flow cytometry analysis of Propidium iodide staining was used to evaluate cell DNA content in the DiD positive fraction at day 14 after staining.

$1x10^6$ PC-3NW1 cells on day 14 after DiD staining were prepared and stained for P.I following Methods section 2.5.3. A negative control of unstained PC-3NW1 cells stained with P.I was used to establish the cell cycle profile (dot plot **Part A, Figure 3.18** and its corresponding cell cycle histogram **Part B, Figure 3.18**). PC-3NW1 cells stained with DiD and immediately processed were used to set the DiD positive gate and to ensure that dye addition would not affect the P.I fluorescent signal (**Parts C and D, Figure 3.18**). No change was observed with DiD addition.

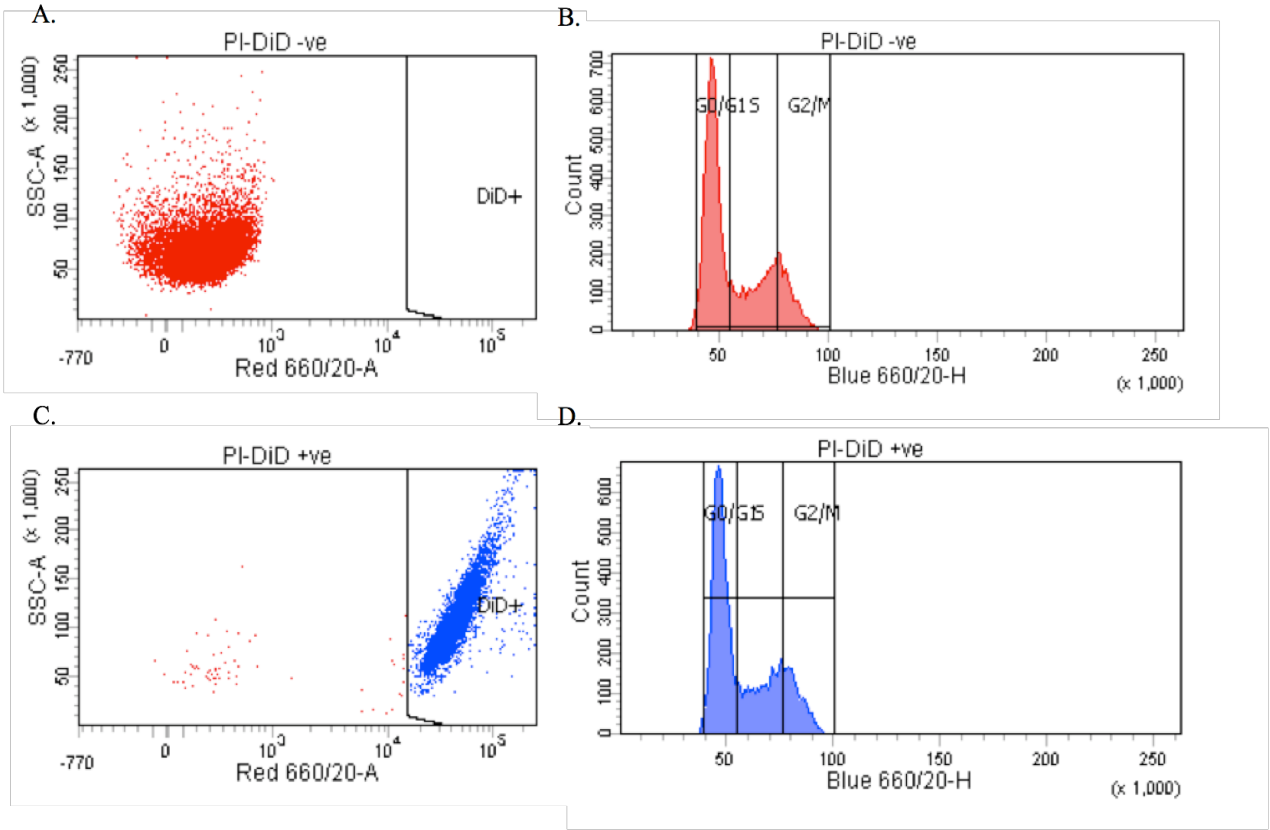

Figure 3.18 Setting the P.I gate

A. A dot plot of DiD negative PC-3NW1 cells. **B.** The cell cycle status of these cells determined by PI staining of DNA content. **C.** A dot plot of DiD positive PC-3NW1 cells. **D.** The cell cycle status of these cells show that dye addition has no affect on P.I staining.

These controls allowed the DiD positive fraction to be gated and analysed. The dot plot shows the expected percentage of DiD positive cells (1.52%) (**Part A, Figure 3.19**) and allowed the cell cycle status of the DiD negative cells to be assessed. 88.03% of the DiD negative cells were in G0/G1, 2.90% in S and 8.83% in G2/M (**Part B).** The DiD positive fractions showed that 51.56% of cells were in G0/G1, 10.43% in S and 38.01% in G2/M (**Part C**). There were significant differences between the DiD+/- cells in cell cycle distribution (**Part B, Figure 3.19**).

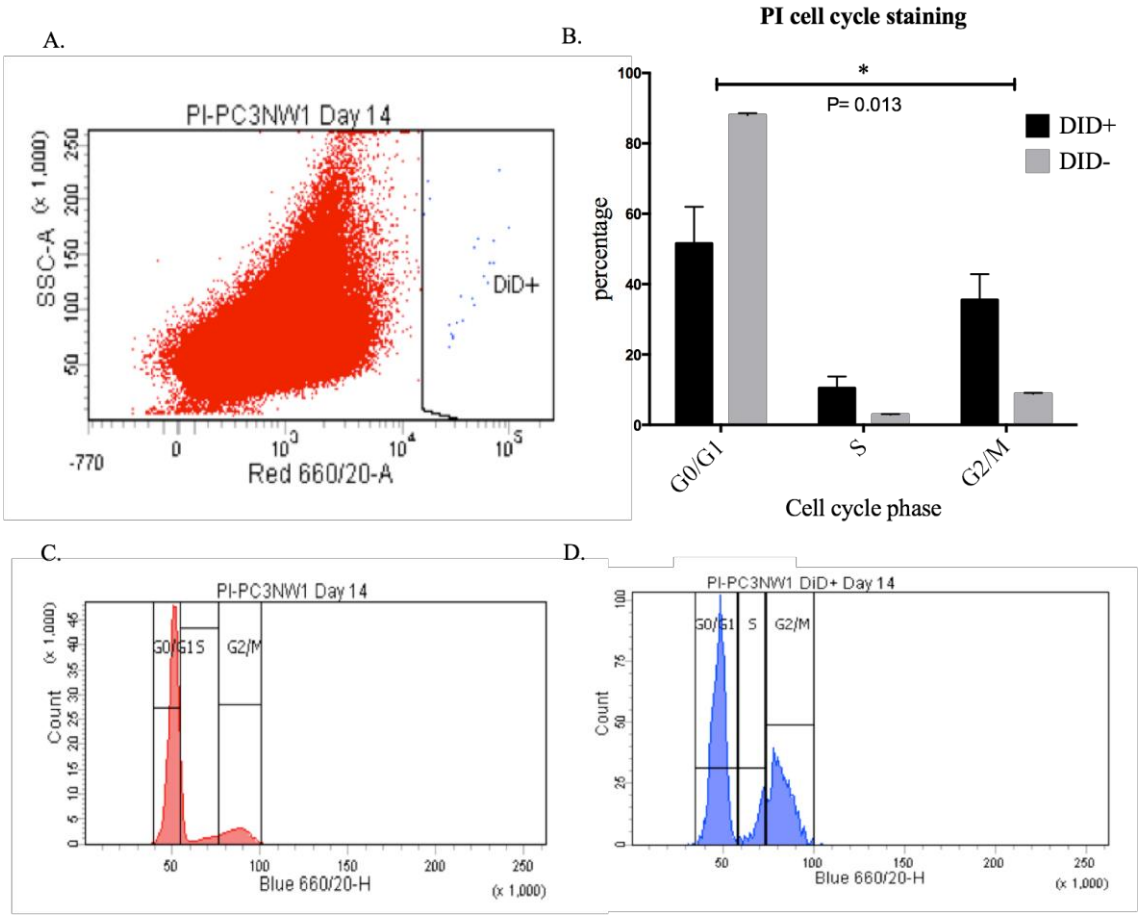

Figure 3.19 P.I cell cycle staining of the DiD positive cell population

A. A representative dot plot showing the gating of the day 14 population. **B.** The bar chart shows the cell cycle status of the DiD negative (grey) and DiD positive (black) populations. N= three biological repeats. **C.** A representative histogram showing the cell cycle status of the DiD negative population on day 14. **D.** A representative histogram showing the cell cycle status of the DiD positive population on day 14.

3.5 Discussion

The growth characteristics of the PC-3 cell line and sub-strains were evaluated in standard and ½ maximum growth conditions as well as low serum (1%). All the strains shared the classic sigmoidal (S-shaped) growth curve: a lag phase, followed by steep exponential growth and, finally, a 'plateau' as growth rates decline. The differences in doubling time were unlikely to be a result of experimental error as each of the growth curves were repeated three times and are more likely to reflect inherent differences in the cell strains. It is sometimes expected that cells that have undergone a transfection may have a reduced growth rate, due to toxicity of the transfection reagent, compared to the parental cell line (in this case PC-3). However, the difference between PC-3 and its sub-strains is minimal (PC-3=27.25 hours, PC-3RFP=31.36, PC-3GFP=32.30). The PC-3NW1 strain was routinely grown in 10% FBS and had the fastest doubling time overall (27.25 hours) in this media but this increase could be due to the higher serum concentration (10% FBS vs. 5% FBS for PC-3). It is interesting to note that each cell line reached its ½ maximum at 2% FBS, despite the difference in the original or 'standard' growth conditions (10% FBS DMEM for PC-3NW1; 5% FBS for PC-3 and PC-3RFP/GFP).

All growth curves were performed in quadruplet in a minimum of three biological repeats. Each repeat was performed within three passages of each other which explains the overall consistent growth rate with only slight variation between repeats. These growth curves highlighted differences in the three prostate cancer cell lines that will be used in subsequent experimental chapters: PC-3NW1, LNCaP and C42B4. Although there is little evidence that doubling time correlates with tumourigenicity (Stiles et al., 1976), in this case PC-3NW1 with the lowest doubling time is the most tumourigenic in the *in vivo* models used by the Sheffield group. However, the opposite trend is seen in C42B4 and LNCaP as it was expected C42B4 to have a faster doubling time than its less metastatic parent strain. Establishing these growth curves early on has led to a greater understanding of what is 'normal' growth for each strain. This allows effects such as reducing the serum concentration or lipophilic dye addition to be compared to an established baseline.

The addition of CM-DiI or DiD had no significant impact on growth compared to the unstained PC-3-NW1 cell line (one-way ANOVA P=0.223). No difference in the cloning ability of stained and unstained cells was seen, therefore the use of CM-DiI and DiD in subsequent experiments could be carried out with an assurance that the basic characteristics of the cell line was not affected by dye addition.

3.5.1 Identification of a dormant cell sub-population

The identification of a dormant cell sub-population within the rapidly dividing PC-3 cell line and sub-strains is a novel finding but others have recently reported similar results to mine in this context (Yumoto et al., 2014). The population doubling time of PC-3-NW1 cells, even with the addition of CM-DiI or DiD, in culture is <28 hours in 10% FBS **Part A, Figure 3.13**. This is comparatively fast growth for a mammalian cell line and suggests that all cells should be rapidly growing. The presence of a low frequency of cells that maintain mitotic quiescence in culture, despite signals from cells dividing around them, is interesting. These cells represent an attractive candidate for further study as a divergent sub-population.

In standard culture conditions (10% FBS DMEM) the frequency of CM-DiI retaining dormant cells was 0.04% on day 21. The high X Geometric mean value at day 21 suggests that these cells are unlikely to have undertaken even a single division as some loss in CM-DiI intensity is expected as the cells are cultured over time. **Part B, Figure 3.7** shows that there is a small but not significant difference in the X Geo Mean between day 0 and day 21. This could be because CM-DiI is sensitive to bleaching by UV light; culturing flasks wrapped in foil would allow a greater degree of control for this variable.

A higher percentage of dormant cells were detected with the use of DiD (day 14 1.61%, day 21 0.37%). This is most likely due to the greater intensity of the dye both upon staining and over time compare to CM-DiI (**Part B, Figure 3.7**). This is reflected at the level of fluorescent microscopy making DiD a more desirable dye to use in subsequent experiments.

It is unclear why a sudden drop in dormant cell frequency and X Geo Mean occurs between day 3 and day 7. This could be due, however, to an extended lag phase after staining in which the cells are recovering from the process. Growth and divisions then

pick up and the dye is rapidly lost as the population expands. Evidence for this was seen when the growth curves of PC-3-NW1 with and without the addition of CM-DiI/DiD was compared. At first the growth of PC-3-NW1 with dye addition fell behind that of cells without the dye. The curve then sharply increased and coincided with that of the PC-3-NW1 cells without dye addition. It is also possible that the sensitivity of the FACS calibur machine may be insufficient at high levels of DiD loading of cells to detect only a small amount of dye reduction as result of cell division immediately after DiD staining i.e. the FACS detection is 'saturated' at high dye levels on cells and DiD levels need to fall before differences can be identified.

3.5.2 Dormancy in multiple cell lines

My studies showed that the dormant cell sub-population was present in multiple PC-3 sub-strains including the parental PC-3 cell line itself. This might be expected for variants of the same strain with roughly the same growth characteristics. The discovery of a dormant sub-population in two separate prostate cancer cell lines (LNCaP and C42B4) was an interesting result.

The consistent percentage of the dormant sub-populations present when different cell lines are cultured in the same conditions, suggests that dormancy may be a result of factors in the culture environment. The effects of the environment on dormancy will be explored in subsequent results chapters. It remains possible that this is an intrinsic population in prostate cancer, since the low numbers of these cells, fits with the paradigm of a cancer stem cell-like sub-population (Collins et al., 2005). The notion that cells exist within a tumour that are stem cell like in nature, and solely responsible for the initiation and maintenance of the cancer, remains a controversial hypothesis (see Introduction). Indeed, recent research has indicated the presence of a cancer stem cell (CSC) sub-population in prostate cancer, with a unique expression signature (Collins et al., 2005). The presence of this signature in the dormant sub-population will be explored in the third results chapter.

3.5.3 Resistance to Doxorubicin

It is perhaps not surprising that the dormant cell sub-population was insensitive to Doxorubicin as, like many chemotherapeutics, it targets rapidly dividing cells. This effect was illustrated *in vivo* by Naumov et al., 2003, who showed that Doxorubicin was

ineffective in targeting single dormant cells *in vivo* and could not prevent the subsequent ability of these cells to form metastases (Naumov et al., 2003). Whether the DiD retaining cells can form colonies after Doxorubicin treatment is an import factor to consider and will be tested in the following results chapter.

3.5.4 Cell cycle status

It was important to determine that DiD retaining cells represented a sub-population of dormant and not senescent cells which was shown using the Senescent detection kit from Abcam. Qualitative image analysis found that DiD positive dormant cells at day 14 were not senescent as they did not positively stain for SA-beta-galactosidase at pH 6.0. Although the specificity of SA-beta-galactosidase in senescent cells has been debated, it is still the most widely used tool to assess cellular senescence. Lee et al. (2006), hypothesise that SA-beta-galactosidase activity at pH 6.0 is due to an increase in lysosomal beta-galactosidase. As it has been hypothesised that lysomsomal size and content increases in ageing cells, this could account for the increase in activity at sub-optimal pH (pH 6.0) that is seen in senescent cells. The negative staining result seen with the Senescent detection kit supported the hypothesis that the dormant sub-population was not senescent. It was therefore important to look at the cell cycle profile of this sub-population in more detail.

The results of the Ki-67 status experiments showed that the dye retaining cells did exist in a Ki-67 positive state. However the percentages of cells that were Ki-67 negative and dye retaining was significantly higher (P=0.015) than cells that have lost the dye after 14 days in culture. Despite this, over 50% of DiD positive cells were positive for Ki-67 despite retaining DiD which has been confirmed in previous experiments to be retained after growth arrest (Figure 3.3.11) Although this seems counter intuitive it could be that these cells are suspended in a prolonged G1 stage in which they will appear Ki-67 positive but will not progress past this stage for an extended period of time. This is a concept that was explored in ‘The Ki-67 Protein: From the Known and the Unknown’ (Scholzen and Gerdes, 2000). This review explores the difficulty of defining the non-proliferative state and that cells can exist in a range of intermitotic times in which quiescent cells can be Ki-67 positive.

Indeed although Ki-67 is an established marker of proliferating cells van Oijen et al. showed that, by using synchronizing inhibitors to arrest cells, osteosarcoma cells were

positive for Ki-67 even when arrested in G1/S or G2/M (van Oijen et al., 1998). This result seems in agreement to my own and could also explain the variation in cell cycle stage when using Propidium iodide.

Propidium iodide was used to evaluate cell DNA content to gain more information about what stage of the cell cycle dye retaining cells are in. This experiment showed that dormant dye-retaining cells could exist in all stages of the cell cycle from G0/G1 through S phase to G2/M. The cell cycle profile of the DiD negative fraction showed a high percentage of cells in the G1/G0 compartment which could be due to sub-optimal culture conditions at the cells reach maximum confluence at day 14. However, as the use of PI cannot differentiate between cells in G0 between cells in G1, based on DNA content, it is not possible to distinguish cells in G0 from those on the brink of division. An interesting set of experiments could look at whether the variation in DNA content in the dormant sub-population is due to variation in ploidy, which may reveal differences at the chromosomal level using karyotype analysis. Changes in karyotype number may give clues as to the origin of dormant cells. Spontaneous fusion in prostate cancer cell lines has been hypothesised to be a source of heterogeneity in tumours (Pesce et al., 2011). Cell fusion may account for the delay in growth as the cell reorganises after fusion however this would need to be shown at the karotype and perhaps microscopy level before being considered as a hypothesis.

3.5.5 Conclusion

In conclusion a dormant cell sub-population has been identified in three human prostate cancer cell lines. These cells were slow-cycling and dye retaining. They were KI-67 positive and negative and Propidium iodide staining showed these cells to be in all stages of the cell cycle. Cells following a growth arrest with Mitomycin C retained CM-DiI and DiD at high frequency supporting the use of these dyes as markers of slowly dividing cells. The senescence detection kit showed that DiD positive cells at day 14 do not stain for β-galactosidase suggesting they may retain the ability to divide and form colonies.

An important factor to consider is whether dormancy is reversible and to consider in more detail how the culture environment affects dormancy. The following results chapter investigates the effects of altering the culture environment on the frequency of

the dormant phenotype including how serum and seeding density can change the frequency of dye retaining cells. It is important to investigate the mechanisms underpinning entry/exit of cells from dormancy. This will be the subject of the next chapter.

Chapter 4: Investigating dormancy in prostate cancer cell lines: exploring conditions that affect entry and exit into this state *in vitro*

4.1 Introduction

As discussed in the previous results chapter there can be a prolonged period of disease 'dormancy' between initial diagnosis, treatment and potential remission to the presentation of skeletal metastases. This is extensively reviewed in Ruppender et al. 2013, which makes the important distinction between micrometastastic, angiogenic and conditional dormancy. Micrometastastic dormancy refers to groups of disseminated tumour cells that lack the proliferative over apoptotic potential to form a growing lesion i.e. the rate of proliferation is equal to the rate of cell death, whereas, angiogenic dormancy refers to a group of tumour cells forming a microscopic lesion (often <1mm in size) that cannot proliferate further without a blood supply. These cells are held in a dormant state as they lack a supply of oxygen and nutrients that would be provided by the angiogenic network. Conditional dormancy, on the other hand, involves single cells or very low numbers of cells that are held in a dormant state due to lack of cues from the environment to begin cell division (Ruppender et al., 2013). It is also important to make the distinction between tumour and metastatic dormancy; this concept is discussed in a recent review by Giancotti (2013). Tumour dormancy refers to the initial lag in growth of the primary tumour, during tumour initiation where cells sequentially acquire additional mutations to over rule apoptotic signalling and evade host immunity. In addition, the level of neoangiogenesis is also important, as the tumour reaches a critical mass it remains dormant until spouting a vascular network. Metastatic dormancy, on the other hand, refers to the prolonged phase of cell cycle arrest which can occur as disseminated tumour cells adapt to their new environment. In our own studies there is evidence that disseminated cells are present as single cells for prolonged periods of time in potential metastatic sites (as shown by DiD retention in cells in the bone marrow up to 8 weeks after injection) and in other groups (Goodison et al., 2003).

The previous results chapter identified DiD dye retaining cells in three prostate cancer cell lines after long term culture *in vitro*. The dye retaining cells were by definition non-dividing or at least dividing very slowly over a prolonged period of time (14-21 days). Recent studies in our research group have found that this dormant cell sub-population *in vitro* i.e., PC-3NW1 cells that have retained DiD for 14 days after staining, were more metastatic *in vivo* than PC-3NW1 cells that were DiD negative after 14 days. After isolated by FACS Aria, $5x10^3$ DiD positive (dormant) cells were injected intracardiac

into athymic mice and the presence of lesions in the bone, as measured by IVIS imaging, was compared to $5x10^3$ injected DiD negative (rapidly dividing) cells. We found that the DiD positive cells formed more skeletal tumours and specifically more long bone tumours than their DiD negative counterparts. This is particularly interesting as long bone tumours more accurately epitomize the disease in human patients. This result suggests that cellular dormancy confers an as yet unknown colonising or survival advantage that results in a greater bone metastatic ability. Dye retention will be used as a model to study dormant (or DiD+) cells in order to investigate the factors that modulate this state.

Little is know about the mechanisms that hold prostate cancer cells in a dormant state in the bone metastatic niche. It has been suggested that prostate cancer cells can express markers of haematopoietic stem cells (HSC) in order to hijack the HSC niche and gain 'footholds' in the bone marrow (Shiozawa et al., 2011b) until receiving, as yet unknown, signals to divide. Shiozawa et al. 2011, presented data that suggested prostate cancer cells utilise CXCR4 to gain entry into the HSC niche. CXCR4 is a chemokine receptor for CXCL12 that is highly expressed in HSCs. This group showed that disrupting this interaction by AMD3100 led to a reduction of these cells in the bone marrow. Although the HSC niche is hypothesised to be a site of DTCs seeding it is not yet know how it may play a role in the mechanisms of dormancy. The expression of HSC markers by the dormant cell sub-population, previously identified, will be explored in Chapter 5.

There is a clear need to develop methods to study dormancy *in vitro* but due to the small number of dormant cells found *in vivo* it is difficult to isolate and culture these cells in order to investigate their phenotype. Indeed in the book Tumor Dormancy, Quiescence, and Senescence, Volume 1: Aging, Cancer, and Non cancer Pathologies, it states that due to the importance of dormancy in cancer and the difficulty of obtaining cells from *in vivo* models "The development of cell culture models of dormancy is therefore highly needed to facilitate the investigation of the mechanisms underlying the dormant state" (Hayat, 2013).

Our *in vivo* studies also suggested that early colonising cells in metastatic sites (after DiD staining and intracardiac injection) were mitotically dormant as measured by long

term DiD retention by multiphoton imaging. This situation is similar to that encountered by cells seeded at clonal density where growth is often slow and some cells never form colonies. Due to the difficulties of investigating dormancy *in vivo*, cells held in a dormant state by cell culture conditions (dye retention over 14 days and in colony assays) was used as a model for dormancy and the factors that control this.

The studies in this chapter will focus on investigating cellular dormancy *in vitro* using the PC-3NW1 cell line, a prostate cancer cell line that was original isolated from the bone environment from a skeletal tumour. The conditions that affect clonal growth in monolayer and whether dormancy in these conditions is reversible will be assessed. Whether the DiD retaining dormant sub-population is regulated by the culture environment i.e. is not an intrinsic stem cell like population, and whether dormancy in this sub-population can be manipulated will also be assessed. This chapter aims to investigate dormancy in a broad sense focussing on dormancy at the cellular level, as opposed to tumour or metastatic dormancy. These studies were designed to coincide with *in vivo* experiments in our research group but also aimed to increase understanding of how cell lines behave in terms of cell division and the basis of growth arrest.

4.2 Chapter Aims, Hypothesis and Objectives

4.2.1 Aims

The aim of this study is to explore the culture conditions that affect cellular dormancy and assess whether dormancy is an intrinsic characteristic or whether this sub-population emerges under permissive conditions.

To address these aims the following hypothesis will be tested

4.2.2 Hypothesis

The dormant sub-population is not intrinsic to prostate cancer lines but is induced by culture conditions and can re-emerge or disappear under environmental influence.

4.2.3 Objectives

To test the above hypothesis the following objectives will determine whether:

7. Conditions in culture can affect cellular growth in monolayer clone assays.
8. Cells held in a dormant state can be stimulated to form colonies.
9. The dormant phenotype (as defined by DiD dye retention after 14 days in culture) can re-emerge in rapidly diving populations.
10. Culture conditions such as serum concentration and seeding density can affect the frequency of the DiD retaining dormant sub-population.

4.3 Results

4.3.1 Conditions that affect cellular growth in monolayer clone assays

4.3.1.1 The effects of serum on colony growth

In these studies cloning ability at low density in monolayer was tested. This tests the ability of cells to survive in relative isolation and to form colonies, characteristics required by tumour cells that survive in low numbers in metastatic sites. To assess if the concentration of FBS could affect clonal growth in standard clone assays in monolayer (Methods 2.1.11), PC-3NW1 cells were stained with DiD and seeded at clonal density ($1x10^3$ cells) into 60mm petri-dishes in quadruplet. Each quadruplet was seeded into 6 ml of either 10%, 2% or 1% FBS in DMEM+ antibiotics (1% concentration penicillin-streptomycin: PenStrep). After incubation for 14 days colonies were fixed, stained and counted as outlined in Methods 2.1.11. The number of colonies formed in 10% FBS was significantly higher than in 2% FBS (Unpaired T-test, P=0.0025). No colony formation was found in 1% FBS (**Figure 4.1**). Each experiment was repeated 3 times.

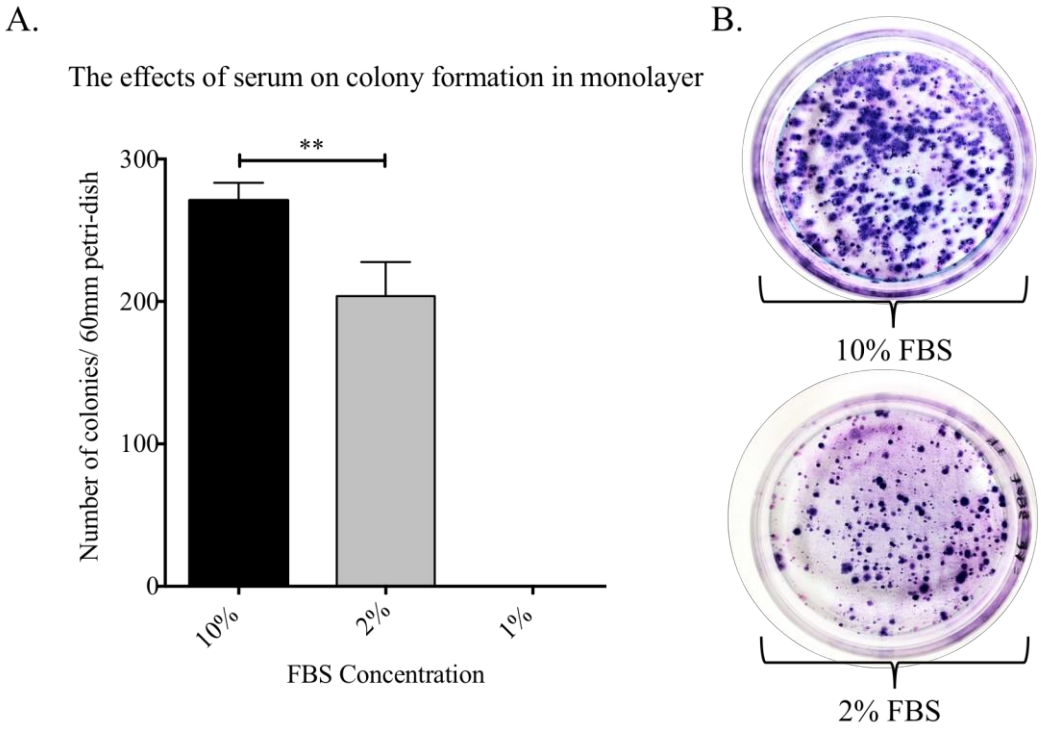

Figure 4.1 The effects of serum on colony growth

A. The bar graph shows significantly more colonies were formed in 10% FBS media compared to 2% FBS media (Unpaired T-test, P=0.0025). No colonies were formed in 1% FBS media. **B.** A representative image of colonies formed in 10% FBS media (top) after fixing and staining with Giemsa shows more colonies (seen as purple circles) than in the lower image of colonies in 2% FBS media. N= 4 petri-dishes/ media type in 3 biological repeats.

These cells did not form colonies in 1% FBS but by using DiD dye, the number of single cells that had not divided, and therefore retained the dye, could be counted by fluorescent microscopy (**Figure 4.2**). On average 87.77 cells were present after seeding in 1% serum at day 14. This suggests that although these cells do not have the potential to form colonies at low serum when seeded at clonal density, a fraction can survive and be held in a dormant state for up to 14 days. The potential of these cells, held in an apparently dormant state, to be stimulated to divide will be presented in results section 4.3.3.1.

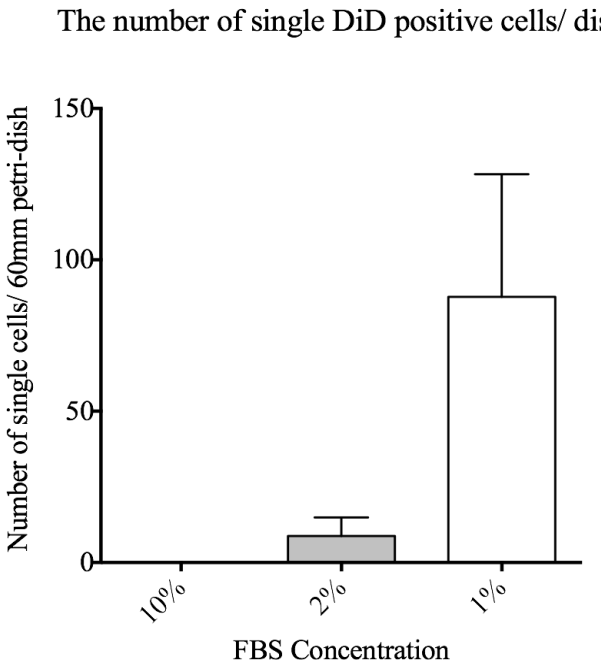

Figure 4.2 DiD positive single cells were present in colony assays at low serum
The bar graph shows that in 10% FBS serum there were no DiD retaining single cells. A small number of DiD retaining single cells were counted in 2% FBS media and a high number of single cells were found in 1% FBS. N= 4 petri-dishes/ media type in 3 biological repeats.

It was found in the previous results chapter that cell growth can occur at low serum conditions when cells are seeded in 10% FBS and transferred to lower serum after 48 hours (as in the serum titration experiments **Figure 3.3**), To test whether cells were intrinsically unable to grow in 1% serum at clonal density, the above experiments were repeated seeding 1,000 PC-3NW1 cells into 6 mL 10% FBS DMEM and, after washing with PBS, transferred into 6 mL of either 2% (10-2%) or 1% (10-1%) FBS DMEM after 48 hours. A significantly higher number of colonies was formed after transfer into 1% serum compared to 2% serum (Unpaired T-test, P= 0.0001) (**Figure 4.3**).

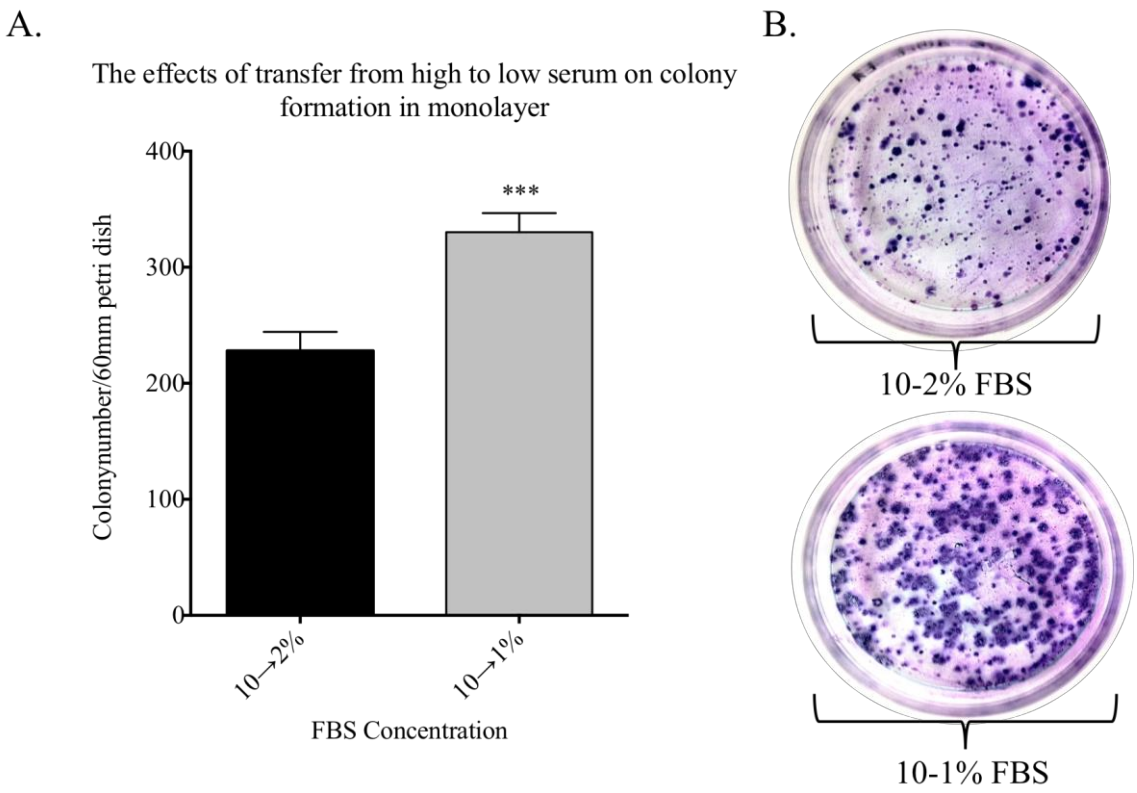

Figure 4.3 PC-3NW1 cells can form colonies after transfer from 10% FBS to 1% FBS media

A. The bar graph shows that after initial seeding in 10% FBS cells retain the ability to form colonies after transfer into low serum. A significantly higher number of colonies were formed after transfer from 10% to 1% serum than after transfer from 10% to 2% FBS in colony assays (Unpaired T-test, P= 0.001). **B.** A representative image after fixing and staining with Giemsa of colonies formed after transfer into 2% FBS media (top) shows fewer colonies (seen as purple circles) than in the lower image of colonies in 1% FBS media. N= 4 petri-dishes/ media type in 3 biological repeats.

4.3.1.2 The effects of seeding density on colony growth

The previous results chapter also showed that PC-3NW1 cells could grow in growth curve experiments when directly seeded into 1% serum when seeded at a density of 10,000 cells per well in a 12 well plate (approximately 2,631 cell/cm^2). Therefore, to determine whether PC-3NW1 cells could ever form colonies when seeded directly into 1% serum the seeding density for colony assays was increased up to about half of this value (32x10^3 cells/60mm petri dish is equal to approximately 1,132 cell/cm^2). 1x10^3, 2x10^3, 4x10^3, 8x10^3, 16x10^3 and 32x10^3 PC-3NW1 cells were seeded per 60mm petri dish in 6 mL of 1% FBS media and cultured undisturbed for 14 days. Colony formation was then assessed as above.

At a seeding density of $32x10^3$ cells/60mm petri dish it was not possible to discern colonies by Giemsa staining as the dish had been filled to 100% confluence. Below this amount, the number of colonies increased with seeding density increase (as expected). Interestingly, increasing the seeding density to only double the number that did not form colonies (1,000 to 2,000 cells) allowed colony formation in 1% FBS. As in previous experiments, no colonies were detected when cells were seeded at clonal density in 1% FBS (**Figure 4.4**).

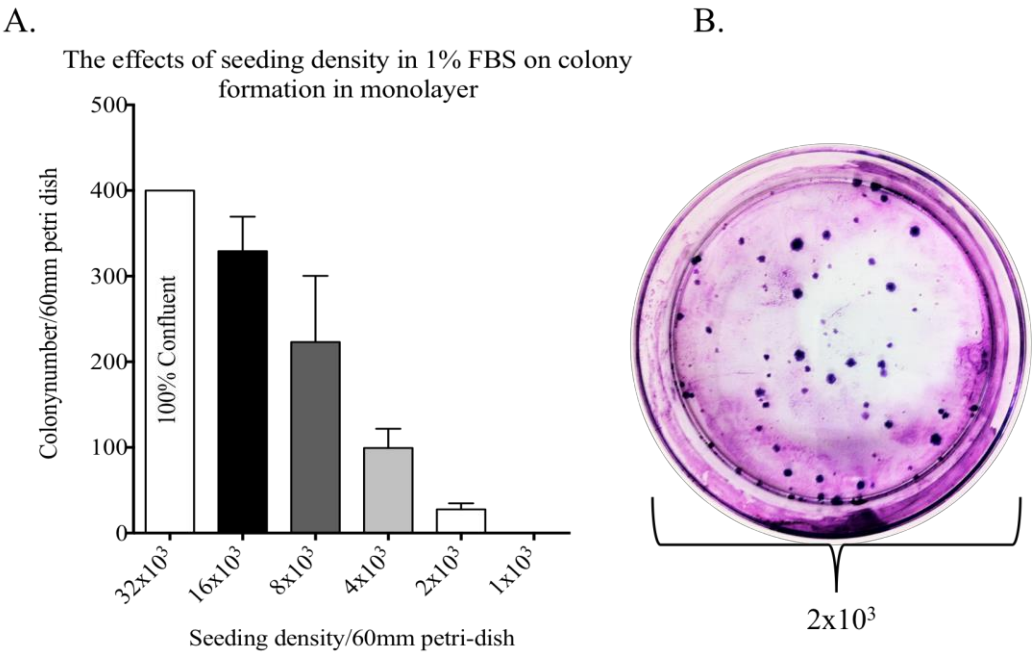

Figure 4.4 Increasing the seeding density of colony assays in 1% FBS media allows colony formation

A. 100% confluence was seen when $32x10^3$ were seeded in 1% FBS. As the seeding density increased the number of colonies increased (as expected). PC-3NW1 cells could form colonies in 1% FBS when clonal density was doubled to $2x10^3$ cells/dish. **B.** A representative image of fixed and stained colonies present when $2x10^3$ were seeded in 1% FBS media showing the small number of colonies that were present after 14 days in culture. N= 4 petri-dishes/ seeding density in 3 biological repeats.

4.3.2 The effects of serum and seeding density on LNCaP and C42B4 colony growth

4.3.2.1 The LNCaP cell line did not readily form colonies in monolayer assays

The LNCaP cell line formed very few colonies in colony assays in monolayer in either 10% or 2% FBS, no colonies were formed in 1% FBS media (**Part A, Figure 4.5**). As before, the cells were stained with DiD before seeding so that the number of single cells on day 14 could be determined. A much lower number of single cells was present in 1% FBS than in the PC-3NW1 cell line but a higher number of single cells were detected in 2% FBS in the LNCaP compared to the PC-3NW1 cell line. Unlike the results in 10% FBS for the PC3-NW1 cell line, there were single cells in 10% FBS in LNCaP (**Part B, Figure 4.5**). These results suggest that LNCaP cells were held in a dormant state in colony assays regardless of the serum concentration and they have very limited cloning ability and do not survive well in 1% FBS at clonal density.

To test whether LNCaP cells could form colonies in 1% FBS at higher seeding densities, the experiments in 4.4.1.2 were repeated with the LNCaP cell line. At higher seeding densities in 1% FBS the LNCaP cell line grew as a *monolayer*, filling the dish at increasing confluence as seeding density increased, represented by a percentage confluence on the graph in **Figure 4.5**. Discernible colonies were only detected, and at a small number, when $4x10^3$ cells were seeded. No colonies were detected when $2x10^3$ cells were seeded/ dish (**Part C, Figure 4.5**).

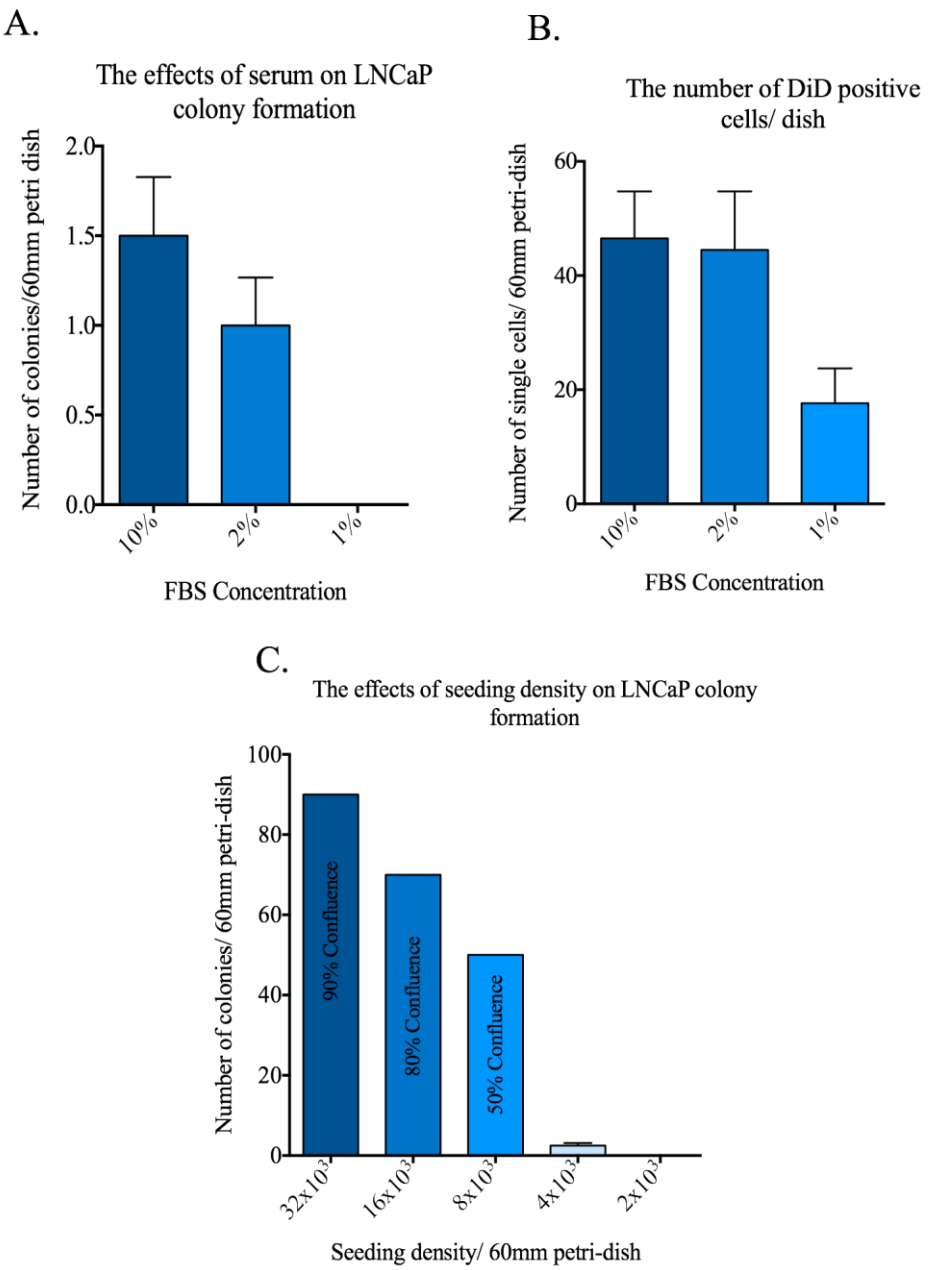

Figure 4.5 The colony forming ability of the LNCaP cell line in monolayer
A. The LNCaP cell line produced very few colonies in 10% or 2% FBS media when seeded at clonal density. No colonies were detected in 1% FBS media. **B.** A much lower number of DiD positive single cell were detected at any serum concentration than in the PC-3NW1 cell line. Single cells were present in 10% FBS media. **C.** In colony assays in 1%, LNCaP cells formed monolayer cultures, with varying coverage of the petri dish (represented as a percentage). When 4x103 cells were seeded a small number (<10) of colonies were detected. N= 4 petri-dishes/ media type or seeding density in 3 biological repeats.

4.3.2.2 The C42B4 cell line has an increased ability to form colonies in monolayer than its parental strain

The C42B4 cell line also formed very few colonies in either 10% or 2% FBS media. C42B4 did produce colonies in 1% FBS media when seeded at clonal density ($1x10^5$ cells/dish). However, this was only a result of two colonies being found in a single dish in one repeat. (**Part A, Figure 4.6**). The numbers of DiD positive single cells were counted after 14 days and similar results to the LNCaP cell line were found. Fewer cells survived as single cells overall, compared to the PC3-NW1 cell line, and there was a higher number in 10% FBS media than in the PC-3NW1 cell line (**Part B, Figure 4.6**). These results suggest that, like the LNCaP cell line, C42B4 cells have limited cloning ability and do not survive well in 1% FBS at clonal density.

To test whether seeding density could affect colony formation in 1% in the C42B4 cell line the experiments in section 4.4.1.2 were done with the C42B4 cell line. It was interesting to find that at higher seeding densities in 1% FBS, the C42B4 cell line produced a high number of colonies, when the seeding density exceeded $4x10^3$ cells/dish, in similar numbers to the PC-3NW1 cell line. However, no colonies were formed when $2x10^3$ cells were seeded/ dish (**Part C, Figure 4.6**).

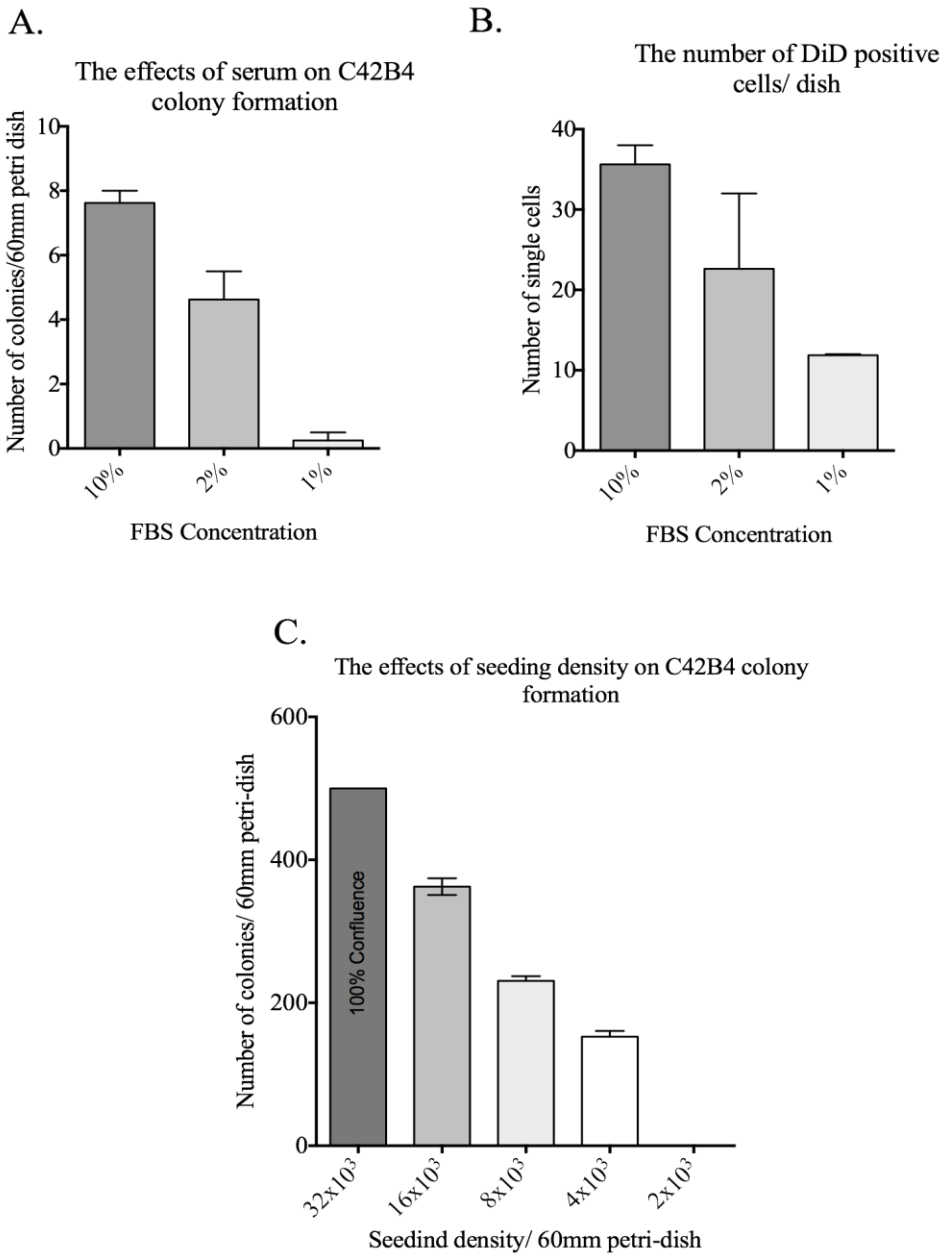

Figure 4.6 The colony forming ability of the C42B4 cell line in monolayer

A. C42B4 cells produced very few colonies in 10% or 2% FBS media when seeded at clonal density. Only 2 colonies were detected in 1% FBS media in a single dish. **B.** A much lower number of DiD positive single cell were detected at any serum concentration than in the PC-3NW1 cell line. Single cells were present in 10% FBS media. **C.** In 1% FBS C42B4 cells readily formed colonies to a similar number as those formed in the PC-3NW1 cell line. N= 4 petri-dishes/ media type or seeding density in 3 biological repeats.

4.3.3 Cells held in a dormant state can be stimulated to form colonies

4.3.3.1 Cells seeded at clonal density (1,000 cells/60mm petri-dish) in 1% FBS can be stimulated to form colonies

To assess if cells that have been held in a dormant state in clone assays for 14 days when seeded at clonal density in 1% FBS, retain the ability to form colonies, 1,000 PC-3NW1 cells were cultured in colony assays for 14 days in 1% FBS media then transferred into 2% or 10% FBS media or 1% FBS conditioned media (Methods 2.1.12). To make conditioned media, $3.5x10^5$ PC-3NW1 cells were seeded into three T175 tissue culture flasks (approximately equivalent to 2,631 cell/cm^2, the initiating seeding density of growth curves) with 20 mL of 10% FBS DMEM+ 1% PenStrep. After 6 days in culture, i.e. mid-exponential growth as determined from growth curve experiments in Chapter 3, the media was removed and the flasks were washed with PBS. 20 mL of 1% FBS DMEM+ 1% PenStrep was then added to the flasks and cultured for 24 hours. After 24 hours the media was removed, centrifuged to pellet any contaminating cells or debris and finally filtered through a 0.2 μm mesh. The resulting 'conditioned media' could then be added to petri-dishes of the dormant cells at clonal density. A control set was also transferred into fresh 1% FBS media that had also been centrifuged and filtered. Each treatment or control was carried out in quadruplet and each experiment was repeated 3 times.

After the initial colony assay at 14 days in 1% FBS all surviving cells retained DiD, the number of these cells in each well was counted by fluorescent microscopy. This was to ensure that no treatment set had significantly more cells that may naturally lead to more colonies after treatment. There was no significant difference between the number of single cells in any well in all 3 repeats (**Part A, Figure 4.7**). The media could then be changed into either 2% FBS, 10% FBS, 1% conditioned media or 1% FBS control and cultured undisturbed for 14 days. Significantly more colonies were formed after transfer into 2% FBS than in the control (Unpaired T-Test, P=0.044) and significantly more colonies were formed in 10% FBS than in either the 1% control (Unpaired T-test, P= <0.0001) or 2% FBS (P= 0.022).

The effects of transfer into conditioned media were more variable, as can be seen from the error bars, however the increase in colony formation was significantly increased

compared to the 1% control (P= 0.027). No significant difference in colony formation was seen between 1% conditioned media and 10% FBS (**Part B, Figure 4.7**).

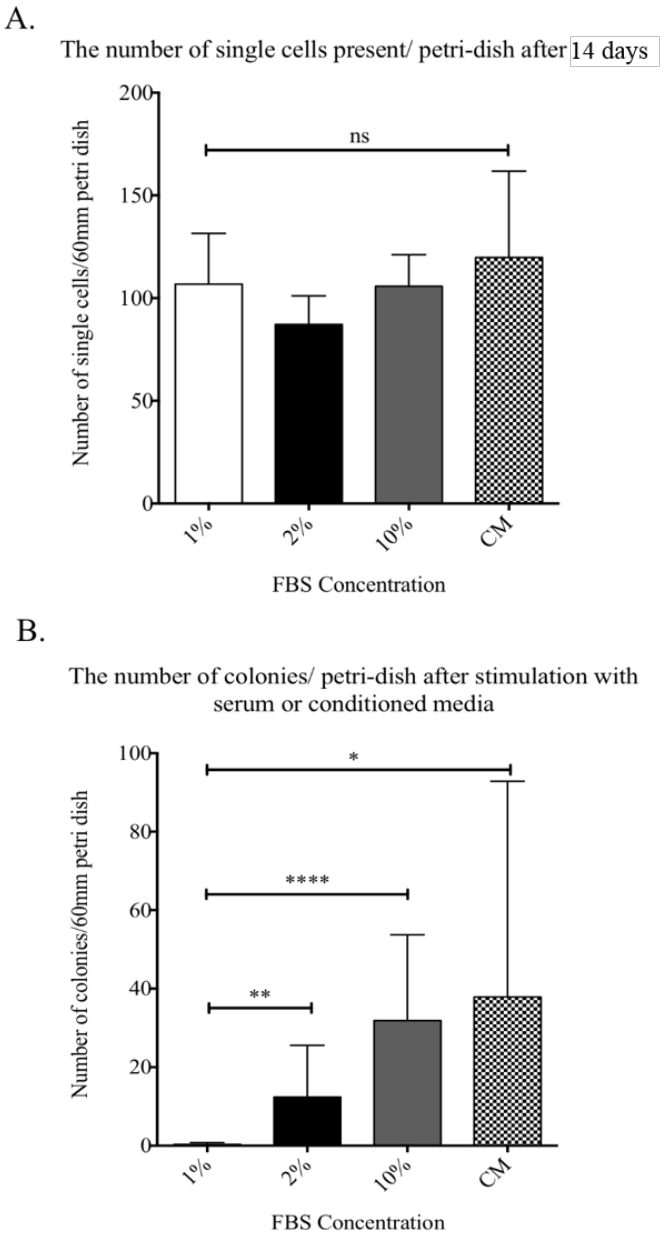

Figure 4.7 Cells that were dormant after seeding at clonal density in 1% FBS retain the ability to form colonies

A. No significant difference in DiD retaining single cell number was seen after the initial 14 days in 1% FBS media. After this was confirmed the appropriate new media could be added. **B.** After 14 days in culture in the new media type a significant increase in colony number was seen after the addition of 2% FBS (Unpaired T-test, P= 0.044), 10% FBS (Unpaired T-test, P= <0.0001) and 1% conditioned media (CM) (Unpaired T-test, P= 0.027) compared to the 1% control. N= 4 petri-dishes/ media type in 3 biological repeats.

4.3.3.2 Cells that are isolated at 14 days after DiD staining in standard culture can form colonies when stimulated

To test if the dormant cell sub-population in the PC-3NW1 cell line, as identified by DiD retention after 14 days, could form colonies in monolayer, this sub-population was isolated and tested by standard clone assays in varying serum concentrations. After following the staining and culture protocol in Methods **Table 2.6**, three T175 flasks were sorted by FACS Aria on day 14 after staining. This allowed the isolations of pure populations of either the DiD negative (DiD-) rapidly dividing cells alone or DiD positive (DiD+) dormant cells alone.

After FACS sorting 1,000 DiD+ or DiD- cells were seeded into 60mm petri-dishes in either 10% FBS, 1% FBS or 10% FBS with transfer into 1% FBS media at 48 hours. These dishes were cultured undisturbed for 14 days. Colony formation was tracked by fluorescent microscopy every 24 hours to determine when dormant cells began to divide. After 14 days colonies were fixed, stained and counted as described previously.

Both DiD+ and DiD- cell types were able to form colonies after isolation. The onset of cell division in the DiD positive population was 48 hours (2 days) after seeding (**Part B, Figure 4.8**) whereas the DiD negative cells begun to divide <24 hours after seeding (not shown).

The DiD positive cells had an increased ability to form colonies in 10% FBS compared to the DiD negative cells (Upaired T-test, P= 0.029). This affect was increased when cells were seeded into 10% FBS and transferred into 1% FBS at 48 hours (Unpaired T-test, P= 0.022). Neither cell type produced colonies when directly seeded into 1% FBS. This experiment was done in quadruplet dishes and repeated 3 times.

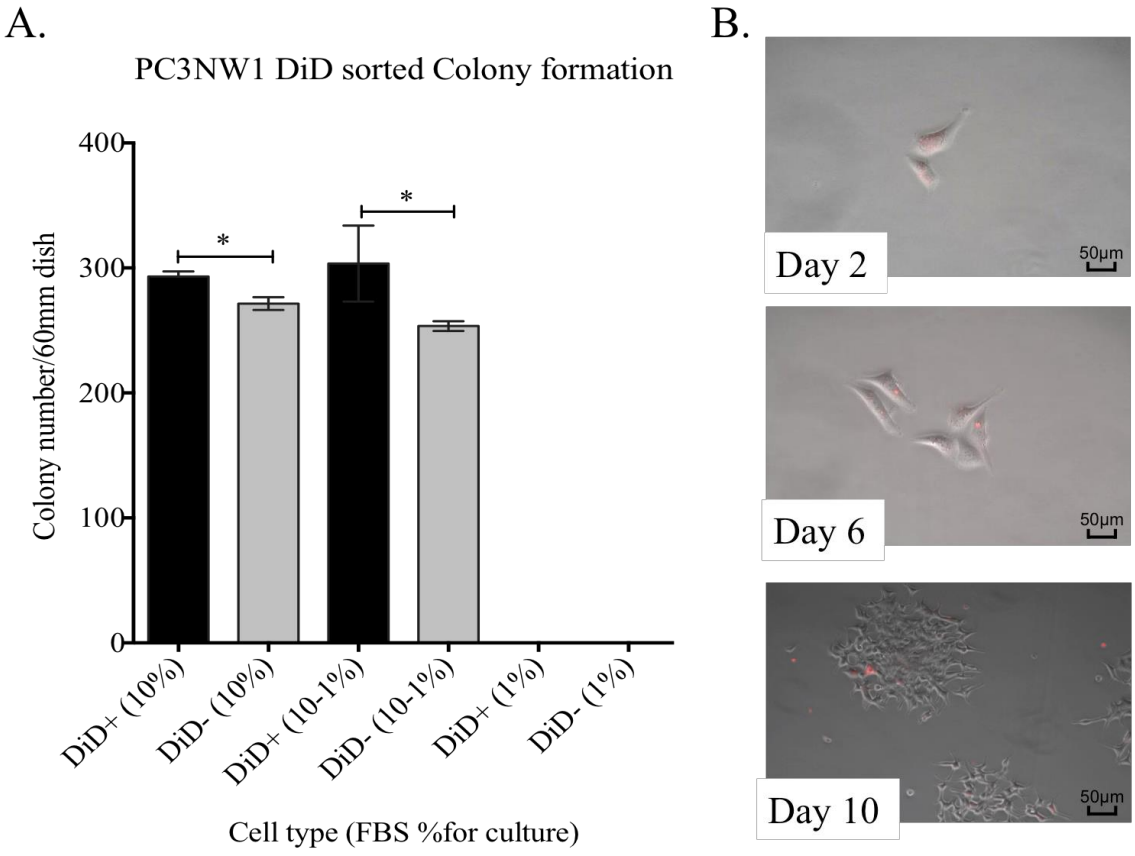

Figure 4.8 DiD positive dormant cells were more clonogenic in monolayer than DiD negative cells

A. When seeded in colony assays the isolated DiD positive cell sub-population, at day 14 after staining, formed significantly more colonies in 10% FBS serum (Upaired T-test, P= 0.029) and when transferred from 10% to 1% FBS (Unpaired T-test, P= 0.022) than their DiD- counterparts. **B.** Representative fluorescent microscopy images taken every 24 hours for 14 days. DiD positive cells began to divide 48 hours after seeding and formed discernible colonies at day 10. N= 4 petri-dishes/ media type in 3 biological repeats.

4.3.3.3 Cells that survive long term Doxorubicin treatment do not form colonies in 10% FBS media

Following experiments in Chapter 3 (section 3.4.6) the DiD positive and DiD negative cells that had survived Doxorubicin treatment for 14 days were washed with PBS and fresh 10% FBS media without Doxorubicin was added. These plates were cultured for 14 days undisturbed and then fixed and stained following the method previously described. No colonies were detected in any wells after 14 days (graph not shown). This experiment was carried out in triplicate wells and repeated 3 times.

4.3.4 The dormant cell sub-population can re-emerge in rapidly dividing cultures

To assess whether all cells within the PC-3NW1 cell line have the ability to enter into a dormant state, the DiD retaining dormant sub-population at day 14 was removed by FACS Aria. 14 days after DiD staining a single T175 flask was sorted by FACS Aria to remove the DiD positive sub-population and retain only those cells that had lost DiD due to successive divisions. Due to the high yields of this fraction the resulting DiD negative cells could be re-sorted through the FACS Aria to ensure that a pure population of DiD negative cells was given (**Part A Figure 4.9**). This was to ensure that if the dormant cell sub-population did re-emerge it was not derived from any contaminated DiD positive cells that may act as a source of more dormant cells.

After re-staining with DiD these cells were cultured and assessed by FACS Calibur for 21 days (as outlined in Methods 2.3.1). It was found that a DiD retaining subpopulation did re-merge in re-stained cultures at a frequency of 0.82% at day 14 and 0.03% at day 21 (**Part B, Figure 4.9**). There was no significant difference between the percentage of the DiD positive population between the original stain, after the initial 14 day culture period (graph legend PC-3NW1+DiD), and the re-stained cells (graph legend PC-3NW1 DiD- Restain) which had been cultured for the initial 14 days sorted as DiD negative, re-stained and cultured for a further 14 days (Paired T-test, P=0.095).

A.

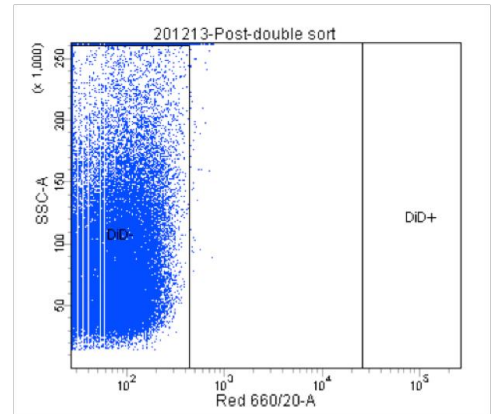

Tube: Post-double sort

Population	#Events	%Parent	%Total
All Events	111,263	####	100.0
FSC SSC	101,335	91.1	91.1
DiD+	0	0.0	0.0
DiD-	99,901	98.6	89.8

B.

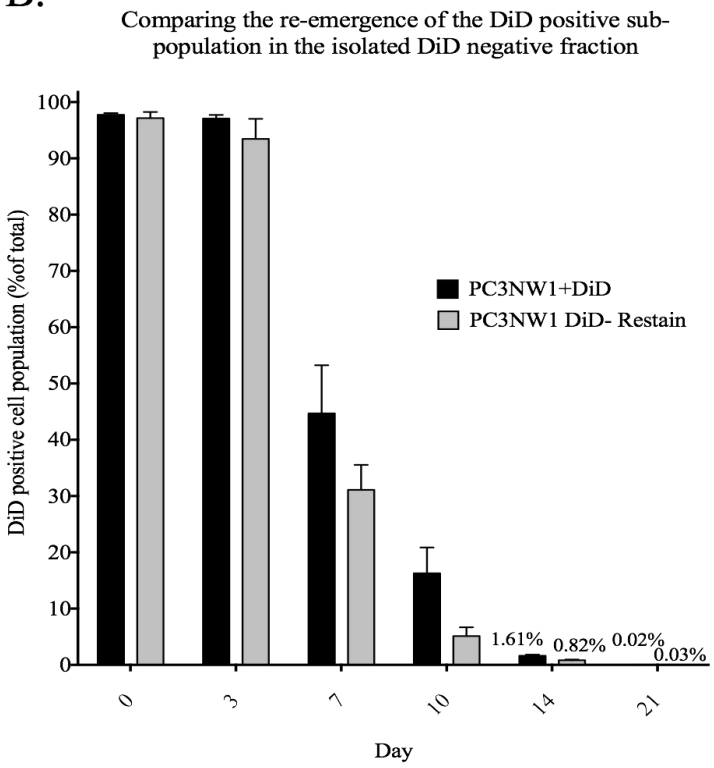

Figure 4.9 The dormant cell sub-population can re-emerge in DiD negative cultures after re-stain

A. The dot plot confirms that a pure negative population is obtained after double sorting of the DiD negative cells on day 14. Shown below is the resulting statistical output, 0% of the cell were DiD positive. **B.** The bar chart shows that after re-staining with DiD the dormant cell sub-population can re-emerge in the rapidly dividing population and there is no significant difference in the frequency of this population compared to the original stain (Paired T-test, P=0.095). N= 3 biological repeats.

4.3.5 Conditions in the culture environment can affect the dormant cell sub-population

4.3.5.1 Serum effects on the dormant cell sub-population

It was necessary to determine whether the frequency of the DiD retaining dormant cell sub-population could be altered by a reduction in FBS concentration. To do this PC-3NW1 cells were stained with DiD, as previous described, and transferred directly into T25 flasks with either 5%, 2% or 1% FBS DMEM+ 1% PenStrep. These cells were cultured and the DiD retaining sub-population was assessed following the protocol in Methods **Table 2.6.**

Using a two-way ANOVA to compare the effect of serum on DiD percentage, it was found that changes in serum concentration had a significant effect on the dormant cell sub-population (P= <0.0001). The DiD retaining sub-population was reduced overall in 5% FBS but increased in 1% and 2% FBS (Day 7 onwards shown, **Figure 4.10**).

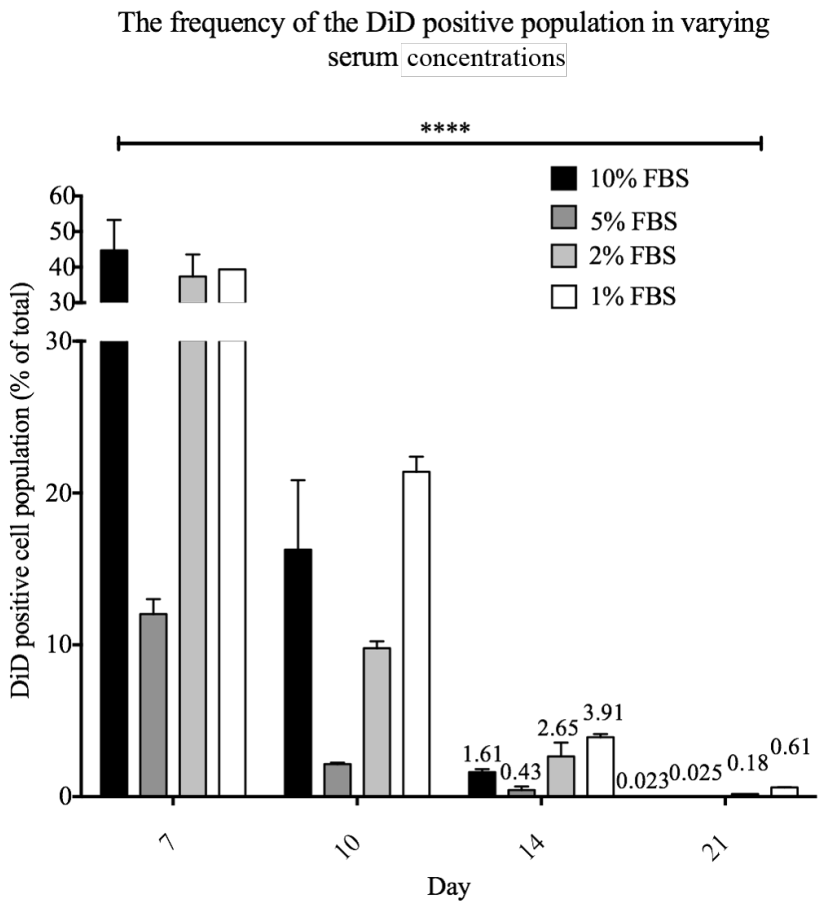

Figure 4.10 The effects of serum on the percentage of the dormant sub-population

Overall serum had a significant effect on the frequency of DiD retaining dormant cells (P= <0.0001). Culture in 5% FBS media reduced the frequency of the dormant sub-population, whereas at lower serum concentrations (1% and 2% FBS) the sub-population was increased. N= 3 biological repeats.

4.3.5.2 The effects of seeding density on the dormant cell subpopulation

As with the above colony assays, it was deemed of interest to determine whether the frequency of the DiD retaining dormant cell sub-population could be altered by changing the initial seeding density of cells after staining. After noticing that the culture flasks were close to 100% confluence at the time of passage, the seeding density of the flasks was reduced to assess the affects of contact inhibition on the dormant sub-population. After staining, $25x10^3$, $10x10^3$ and $5x10^3$ cells were seeded into 5x T25 flasks. These cells were cultured, passaged and analysed as normal (as outlined in Methods table 2.6). The frequency of the DiD retaining sub-population at these reduced seeding densities was then compared to the control, $1x10^5$ cell seeding density that was standard for all previous experiments (**Figure 4.11**).

Seeding density had a significant effect on the frequency of the DiD retaining sub-population by two-way ANOVA (P= <0.0001). The DiD retaining sub-population was reduced in all three of the lower seeding densities tested.

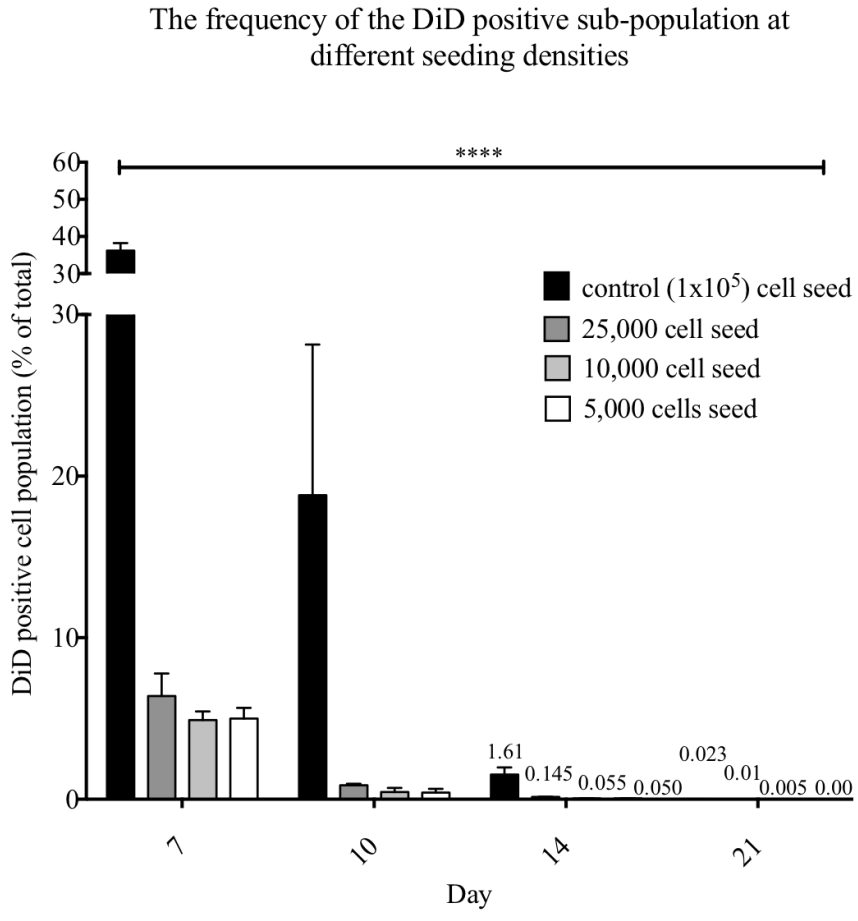

Figure 4.11 The effects of seeding density on the percentage of the dormant sub-population
Overall seeding density had a significant effect on the frequency of DiD retaining dormant cells (P= <0.0001). Decreasing the seeding density appeared to reduce the frequency of the dormant cell sub-population. N= 3 biological repeats.

4.3.6 Hypoxia: A potential mechanism for dormancy in the PC-3NW1 cell line

The above experiments indicated that factors in the culture environment could be responsible for inducing the presence of dormant sub-populations. As this sub-population was reduced when seeding density was decreased, it was hypothesised that induction of the dormant state was due to lack of available nutrients or hypoxia resulting from overcrowding in the flask. It was decided to look at Hif1α (hypoxia-inducible factor 1α) as an indicator of hypoxia.

Hif1α is present in the cytoplasm of all cells in normoxia and is translocated to the cell nucleus under hypoxia, where is acts as a transcription factor to several downstream genes to regulate cell response to environmental stress. At 14 days after DiD staining, a single T175 flask was prepared and cytospun as in Methods 2.7.1. Immunofluorescence was used to detect Hif1α nuclear translocation using a primary rabbit monoclonal anti-Hif1α antibody with a matched IgG isotype control followed by a Goat anti-Rabbit IgG AlexaFluor® 488 (all life technologies) following the protocol in Methods 2.7.2.

To test the affinity of the purchased Hif1α antibody, a positive control of DMOG treated PC-3NW1cells (14 days after DiD staining) was done. DMOG is a cell permeable prolyl-4-hydroxylase inhibitor, which up-regulates Hif1α nuclear translocation and can be used as a hypoxia mimetic (Chan et al., 2002). 0.1mM DMOG was added in the media of these cells for 6 hours before harvesting; 6 hours was determined as the optimum incubation time after optimisation tested 4 hours, 6 hours and 8 hours. (**Figure 4.12**).

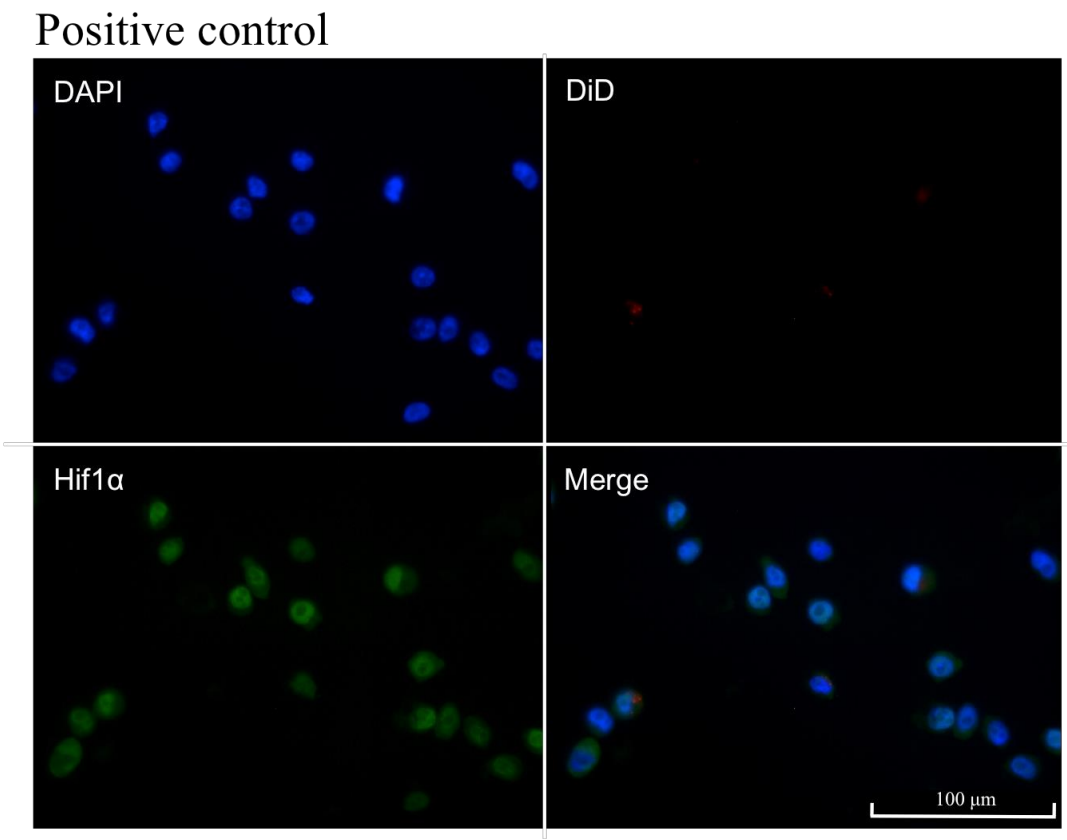

Figure 14.12 DMOG treatment as a positive control to test the Hif1α antibody
DiD stained PC-3NW1 cells at day 14 were treated with 0.1mM DMOG for 6 hours before harvesting for the immunofluorescence. The L5 channel (green) shows the Alexa488 conjugated Hif1α antibody. All cells were positive for nuclear translocation.

Using the tile scan system on the Leica microscope, 25 tiled images at 40x magnification of the central section of the cytospin were automatically captured. Using both the phase contrast, DAPI, DiD and AlexaFluor® 488 channels the DiD status of cells could be correlated to Hif1α status. Representative images of an isotype control and an antibody stained image are shown in **Parts A and B** of **Figure 4.13**, respectively. The white arrows show the DiD positive cells that were strongly positive for the presence of nuclear Hif1α. This is shown by the positive correlation of green AlexaFluor® 488 staining for Hif1α and the blue Dapi stain for the cell nucleus.Nuclear translocation was scored by eye for all cells in each image and the percentage of Hif1α nuclear translocation for DiD negative (DiD-) and DiD positive dormant (DiD+) cells was plotted. A significantly higher percentage of DiD positive cells had Hif1α nuclear translocation than DiD- cells (Unpaired T-test, P=0.026) (**Figure 4.14**).

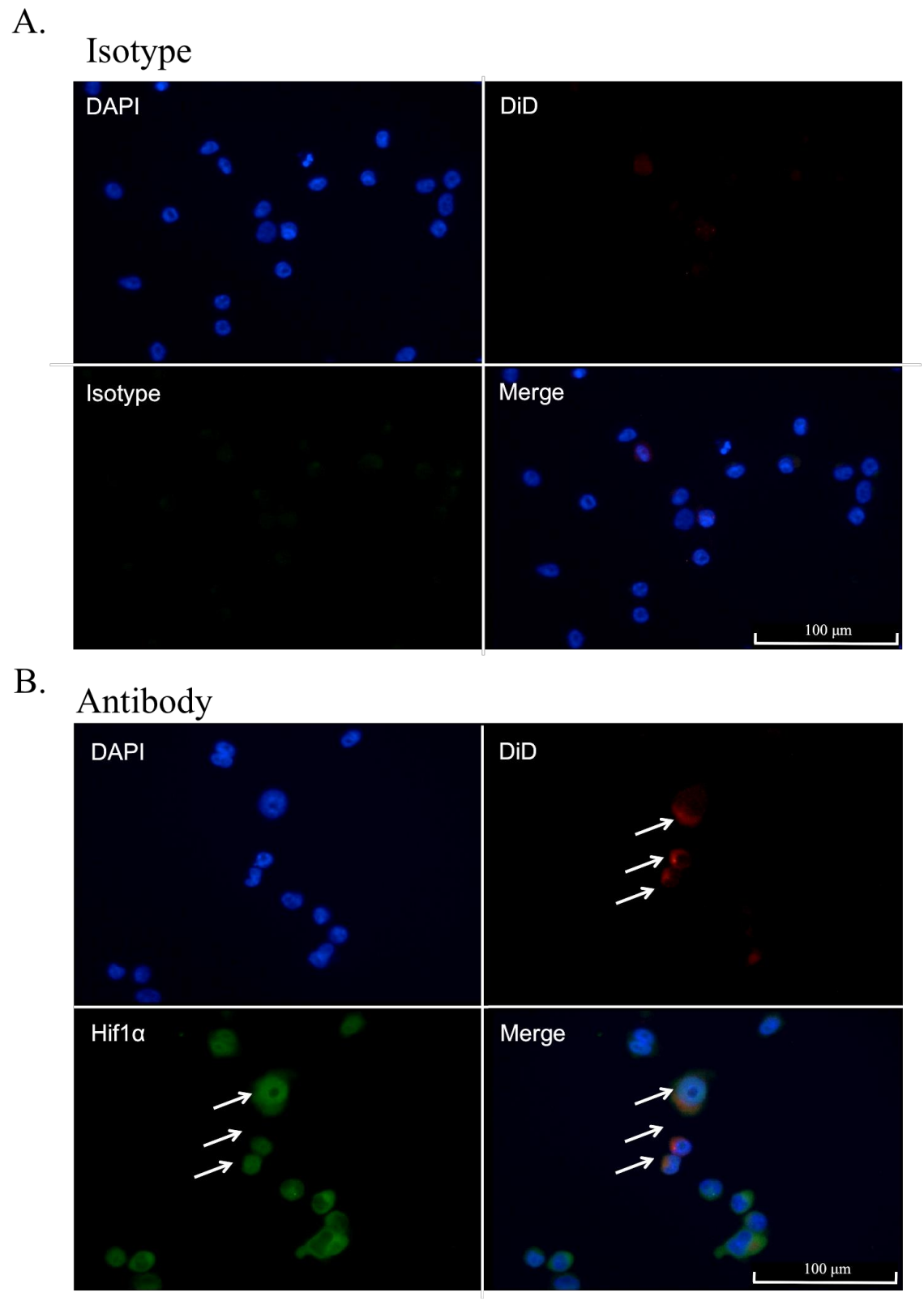

Figure 4.13 Representative images of the immunofluorescent assay to detect Hif1α nuclear translocation

A. The isotype control shows the A4 (blue) DAPI channel, the Y5 (far red) DiD channel, the L5 (green) Alexa 488 channel and the merged image. There is only a very small amount of background when using the isotype. **B.** The antibody image shows the A4 (blue) DAPI channel, the Y5 (far red) DiD channel, the L5 (green) channel and the AlexaFluor® 488 merged image. The white arrows show DiD positive cells that have clear Hif1α nuclear translocation**.**

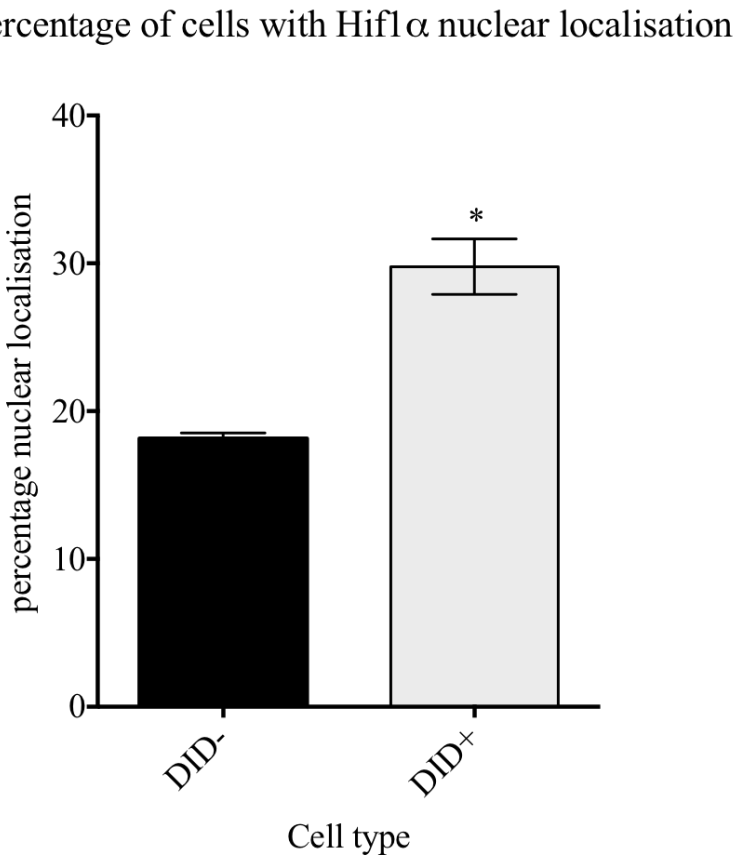

Figure 4.14 The dormant cell sub-population has a higher percentage of cells with Hif1α nuclear translocation

The percentage of cells with Hif1α nuclear translocation was significantly higher in the DiD positive (DiD+) cell sub-population compare to the DiD negative (DiD-) cells (Unpaired T-test, P=0.026)

4.4 Discussion

4.4.1 Analysing cell growth in colony assays

The PC-3NW1 cell line was found to be highly clonogenic in monolayer in both 10% and 2% FBS. These cells did not form colonies in 1% FBS but survived in a mitotically dormant state for up to 14 days, as measured by the retention of DiD dye by fluorescent microscopy. However, PC-3NW1 cells could form colonies in 1% FBS serum at clonal density when seeded in 10% FBS for 48 hours and then transferred into 1% FBS. This result is interesting and suggests that after the initiation of growth in favourable conditions, i.e. 10% FBS, cell growth and colony formation is independent of the culture conditions. This may be of particular importance in consideration of tumour growth *in vivo* and suggests that targeting the initiation of growth/loss of dormancy, to prevent colony initiation in the early stages of the metastatic cascade, might be more effective than preventing autonomous growth once initiated. Another interesting result of this experiment was that cells transferred into 1% FBS from 10% FBS at 48 hours, formed more colonies than cells transferred into 2% (conditions previously shown to support clonal growth). This could be due to the selection of a more aggressive phenotype after transfer into 1% FBS which, once established, has an increased clonogenic potential. It would be interesting to test the tumourigenic ability of cells treated in this way in xenograft models. Alternatively it is likely that FBS contains a mix of clone promoting and apoptotic factors and that different concentrations of FBS in media allow these competing additives to be more or less effective: at 1% the balance favours colony formation, at 2% apoptotic factors may be more effective. Increasing the seeding density in 1% FBS allowed the formation of colonies in the PC-3NW1 cell line at densities as low as only double clonal density ($2x10^3$ cells/ dish). The LNCaP and C42B4 had a much lower cloning ability in monolayer.

It was found that LNCaP cells did not readily form colonies either at high FBS concentration (10% FBS media) or when seeded at high density in low FBS media (1%). They instead preferred to grow as monolayer cultures at high density and did not form discernible colonies that could be counted. This may reflect high motility within higher densities, with cells proliferating and spreading rather than forming colonies. However, studies published by Havard et al., 2011 found that the clonogenicity of the

LNCaP cell line is increased when cultured in RPMI. They found that LNCaP cells produced 100-1,000 times more colonies when cultured in RPMI +10% FBS compared to DMEM +10% FBS. They hypothesised that this effect was due to the higher osmotic pressure of DMEM media making it slightly hyper-tonic (360 Osm/L) compared to RPMI (310 Osm/L), as when osmotic pressure is reduced in DMEM the ability of LNCaP cells to form colonies increased. Interestingly, Havard et al. also found that the LNCaP cells were held in a dormant state in DMEM+ 10% FBS and had a similar cell cycle profile as the PC-3NW1 dormant cell sub-population (characterised in Chapter 3) by Propidium Iodide staining. They found that LNCaP cells that could not form colonies in DMEM, but remained in a dormant state, were found in both G2/M and G0/G1 phases as well as at a low frequency in S-phase (Havard et al., 2011). Future work could look at the cell cycle profile of the PC-3NW1 cells held in a dormant state when seeded at clonal density in 1% FBS but this would be difficult as the number of these cells was low.

The C42B4 cell line, although weakly clonogenic at high serum concentration, formed colonies when seeded at higher density in 1% FBS media. This suggests that, like the PC-3NW1 cells, when cells are kept at low density in an unfavourable environment they lack signals to divide. However, when the number of cells is increased there is a trigger, possibly an accumulation of growth signals, which allows cells cultured in close proximity to divide and form colonies.

To test the ability of the PC-3NW1 cell line to provide clonogenic signals to dormant cells, conditioned media from rapidly growing cultures in 1% FBS (to remove any serum effects) was added to cells seeded in 1% at clonal density at day 14. Conditioned media was very carefully eluted from rapidly growing flasks and centrifuged for 10 minutes at 300 x g to prevent any cells being transferred to the dish, so we could be sure that any colonies were a result of the originally seeded cells. This caused cells that had previously been held in a dormant state, at clonal density in 1% FBS media, to be triggered out of dormancy and stimulated to form colonies. It was also found that increasing the serum concentration, by the addition of 10% and 2% FBS media at day 14, could stimulate dormant cell to form colonies. These results suggest that it is possible for these cells to exist as solitary dormant cells for long periods of time whilst retaining the ability to divide under favourable conditions. This is interesting and in

agreement to what is seen *in vivo* studies. Our group (unpublished) have shown that metastases in the bone marrow arise from low numbers of initiating cells, often a single clone that has remained dormant for varying periods of time that is then triggered (by unknown factors) to form a colony.

The effects of serum increases were less variable than the effect of conditioned media, which may be due to the variability of factors released by conditioning cells. Despite the fact that 1% FBS media was conditioned over a known number of cells for the same period of time it is not possible to re-create the exact environment in every flask so some variability between repeats is to be expected. It is not know what the exact component present in conditioned media stimulated cell growth in my study. This was explored in Havard et al., 2001, who found that LNcaP cells remained mostly dormant when seeded at clonal density in 10% FBS DMEM. Havard et al. seeded LNCaP cells at clonal density in DMEM+10% FBS that had been conditioned over rapidly diving cells and found that colonies were formed. After screening several metabolites, they narrowed this effect down to citric acid and showed that an increase in citric acid in un-conditioned 10% FBS DMEM could promote LNCaP cells to produce colonies (Havard et al., 2011). Future work could look at the levels of citric acid in the PC-3NW1 conditioned media to determine if this had the same effect in this cell line.

The reversal of dormancy at clonal density provided a framework to test whether dormancy was reversible in the dormant cell sub-population that was characterised in Chapter 3.

4.4.3 Assessing the plasticity of the DiD retaining dormant cell sub-population

4.4.3.1 Dormancy is reversible

Following FACS Aria sorting at day 14 after DiD staining, $1x10^3$ DiD positive cells were seeded per 60mm petri-dish in 1% and 10% FBS media. Following the results obtained with the earlier clone assays, cells were also seeded into 10% FBS media to be transfer into 1% FBS media at 48 hours. As a comparison $1x10^3$ DiD negative cells were also set up under the above conditions.

It was significant to find that not only did the dormant DiD retaining cells produce colonies, they did so at a higher rate than the DiD negative 'rapidly dividing' cells. This clearly shows that the dormant DiD+ cells retained the ability to form colonies once placed in conditions favourable for colony formation. That they did so more effectively than the DiD- cells seems counter intuitive, it is possible that the DiD retaining sub-population is better able to survive when plated at clonal density than the DiD- cells. This was not tested here. This also indicates that the dormant state is reversible and is a state that prostate cancer cells can move in and out of depending on their environment. To explore this further, whether dormancy could be induced in the PC-3NW1 cell line as well as reversed was tested.

4.4.3.2 The dormant phenotype can re-emerge

Evidence that rapidly diving cells i.e. cells that have lost the DiD dye after 14 days in culture can enter into the dormant state (shown by DiD dye retention after a further 14 days) suggests that previously non-dormant cells have the ability to become dormant and that dormancy is not an intrinsic characteristic of a defined population. This suggests that the dormant sub-population may not be stem cell-like in nature and may not be the same as the proposed CSC sub-population in prostate cancer (Collins et al., 2005). This will be investigated in the following results chapter.

4.4.4 Dormancy is driven by the culture environment

It was also shown that the dormant cell sub-population can be increased or decreased in response to factors in the culture environment i.e. serum and seeding density. The frequency of the dormant subpopulation, as a proportion of the total, increases at high seeding density and at lower serum concentrations. This strongly suggests that entry/exit from dormancy is driven by culture conditions: when cells are at high density, the competition for factors/nutrients may result in deprivation for some cells which then switch from proliferation to dormancy. Conversely, when serum levels are low, the factors required to stimulate transition from dormancy to proliferation are in short supply. To investigate the mechanism that may be responsible for dormancy, that could be increased at high density, hypoxia in the cells was assessed. The experiments in section 4.3.6 provided evidence that Hif1α nuclear translocation was increased in DiD

retaining cells. It has previously been shown that Hif1α specifically, can act as an up regulator of $p21^{cip1}$, which provides a break to cell division resulting in cellular dormancy (Koshiji et al., 2004). It is tempting to speculate that this could be responsible for the DiD retaining phenotype however, more studies at the molecular level are required to further evaluate hypoxia as a driver of dormancy.

4.4.5 Conclusion

Clonogenic assays have proved useful to study dormancy *in vitro*. These indicate that at clonal density, cells seeded in low serum concentrationscan be maintained in a dormant state but that this state can be reversed by stimulation with FBS or conditioned media. Cells characterised as dormant by the retention of DiD at 14 days also have the ability to exit from the dormant state when transferred out of their usual culture conditions and stimulated with 10% FBS. These experiments provide evidence that cells that were DiD retaining at day 14, and were 'dormant' as distinct from senescent, since they have the ability to re-enter the cell cycle and begin division. Dormancy appears to be regulated by the environment and the studies provide evidence that hypoxia, as measured by Hif1α nuclear translocation, is part of the mechanism that drives entry into this state.

The molecular mechanisms that induce/suppress dormancy have been extensively studied. For example, studies have indicated the importance of uPaR and EGFR (epidermal growth factor receptor) as drivers of dormancy (Almog, 2010). Although these molecular determinants are important, the following results chapter will use qRT-PCR in the form of individual TaqMan assays and custom designed low density arrays (LDAs) to define the gene expression profile of the dormant cell sub-population in order to use these differences as a marker set to *identify* dormant cells.

Chapter 5: Gene expression profiling of the dormant cell sub-population: defining a gene signature for dormancy

5.1 Introduction

In an attempt to define the metastasis initiating phenotype, the majority of studies have focused on profiling circulating tumour cells (CTCs). This is in part due to the availability of these cells from patient blood samples compared to the availability of bone marrow aspirates. However, a number of studies have looked at the molecular mechanisms of disseminated tumour cells (DTCs) in the bone marrow of prostate cancer patients. Weckerman et al., 2009 found that DTCs had significantly more chromosomal aberrations than in cells isolated from the primary tumour by comparative genomic hybridisation (CGH). This suggests that in order to survive in the bone marrow a number of genetic alterations must take place for cells to have the potential to metastasize.

A number of groups have also investigated the specific gene alterations that characterise tumour dormancy and also the switch from this state to rapid growth. Almog et al., 2013 found that microRNA 190 can be responsible for the initiation of tumour dormancy in glioblastoma and osteosarcoma cell lines. Over expression of MicroRNA 190 was found to induce tumour dormancy in an orthotopically injected rapidly growing glioblastoma cell line. However, after long periods it was found that this cell line did eventually form rapidly growing tumours similar to the parental strain (Almog et al., 2013). Almog et al., 2009 also published what they consider to be a consensus fingerprint of tumour dormancy *in vivo*. Using genome-wide transcriptional analysis they identified genes that were significantly altered in four slow growing cell lines *in vivo* compared to their rapidly growing counterparts. They found that the most significant alterations were seen in angiogenesis related genes that seemed to characterise the 'switch' from tumour dormancy to rapid growth (Almog et al., 2009). This work, although comprehensive focused on *tumour* dormancy *in vivo* and did not use any prostate cancer cell lines.

Despite it's clinical relevance, metastatic dormancy has not been extensively researched. However, recently, a number of groups have published experiments that have provided evidence for the importance of the bone microenvironment in the mechanisms that control metastatic dormancy. Specifically molecular factors, such as stress signalling (Aguirre-Ghiso et al., 2001) or osteoblast/tumour cell signalling

(Taichman et al., 2013) have been highlighted to regulate how disseminated tumour cells survive and grow in the bone marrow. As previously mentioned, results in our laboratory suggest that the DiD retaining dormant sub-population are more metastatic *in vivo* as when injected intracardiac DiD positive cells at day 14 formed more skeletal tumours than DiD negative cells at day 14. This result was significant and it was therefore deemed crucial to assess the molecular characteristics that distinguish this dormant phenotype in order to gain information about their behaviour *in vivo*.

The following studies will look specifically at the molecular profile of the dormant sub-population in the PC-3NW1 cell line. This is in order to establish a phenotypic 'signature' of cellular dormancy. By using individual TaqMan arrays and two custom designed low density array cards, the gene expression profile of the PC-3NW1 dormant cell sub-population will be analysed. Although genetic alterations may highlight potential mechanisms for dormancy in this sub-population, the primary aim is to characterise a marker set that is associated with dormancy. The aim is that this can then be used to compare cells under various conditions of dormancy i.e., dormant cells grown at clonal density in 1% FBS. It is also aimed that these LDA cards can also be used to assess the gene expression profile of early colonising cells *in vivo*.

It has been hypothesised that the bone metastatic niche is similar to the HSC niche and shown that prostate cancer cells 'compete' with HSCs for access to this niche in the bone marrow (Shiozawa et al., 2011a). It has also been argued that prostate cancer cells may interact with the niche in order to remain dormant until activation (Pedersen et al., 2012). RT-qPCR, using individual TaqMan assays, will be used to assess gene expression differences of HSC niche related factors in the dormant vs. rapidly dividing cell lines in the PC-3NW1 cell line.

Building on this, a 96 gene custom Low Density Array (LDA) card from Applied Biosystems was designed to cover five areas of interest that may define differences in the PC-3NW1 dormant cell sub-population and the rapidly dividing cells. These were HSC niche related markers, stem cell markers, osteomimetic markers, markers of epithelial to mesenchymal transition (EMT) and endocrine or miscellaneous markers (A full list of the genes studied with abbreviations as they appear in the Results is found in Appendix 1.1).

In the context of previous work relating to metastasis initiating cells discussed in the Introduction (1.2.1), several gene assays relating to stem cell function were included on the array. Primarily, it was important to assess whether the dormant cell sub-population differentially expressed the same gene markers as the proposed prostate cancer stem cells, CD44+/α2β1hi/CD133+ as discussed in previous chapters. However, it was also necessary to determine whether the dormant cell sub-population represented a primordial or de-differentiated population, therefore classic stem cell markers such as OCT4 (LDA card synonym POU5F1), NANOG and SOX2 were included on the card. Epithelial to mesenchymal transition (EMT) has been hypothesised to induce a more migratory phenotype in tumour cells that may lead to a heightened metastatic ability. Specifically the expression of matrix metalloproteinases (MMPs) are considered key drivers of this change (Radisky and Radisky, 2010). Another proposed mechanism that leads to an increase in, specifically bone, metastases is osteomimicry. This process describes the heightened ability of tumour cells to express markers of bone cells, for example osteocalcin and osteoprotegerin, in order to survive and grow in the bone marrow. Several other miscellaneous markers were included on the card for example genes related to hormone response (the estrogen and androgen receptor) and several proposed markers of poor prognosis in prostate cancer patients e.g. the TMPRSS-ERG fusion.

5.2 Chapter Aims, Hypothesis and Objectives

5.2.1 Aims

The aim of this study was to characterise the gene expression profile of the dormant cell sub-population in the PC-3NW1 cell line to establish a molecular signature for dormancy.

To address these aims the following hypothesis were tested

5.2.2 Hypothesis

The dormant sub-population has a unique gene expression profile compared to rapidly dividing cells.

5.2.3 Objectives

To test the above hypotheses the following objectives will determine whether:

1. The DiD retaining dormant cells express different levels of HSC niche related genes compared to rapidly dividing cells by TaqMan RT-qPCR.
2. Dormant cells have a unique gene expression profile by Low-density array (LDA) analysis.
3. LDA card analysis can be used to assess the gene expression profile of DiD labelled cells that have been injected intracardiac into mice and homed to the bone at 3 days post injection, i.e. early colonising or 'bone homing' cells.
4. This unique expression profile is the same in cells that have been forced into dormancy i.e., cells grown at clonal density in 1% FBS and in rapidly dividing cells that have been restained with DiD and retained the dye for long periods i.e., restained DiD positive cells.

5.3 Results

5.3.1 Optimising the RNA extraction method

To ensure that high quality RNA could be obtained using the Reliaprep™ RNA extraction kit from Promega, even when using low cell numbers, RNA was extracted from populations of reducing size and analysed using the 2200 TapeStation from Agilent Technologies.

PC-3NW1 cells from routine growing cultured were trypsinised and $1x10^5$, $1x10^4$, $3x10^3$ and $1x10^3$ cells were prepared for RNA extraction following Methods 2.6.1. Following extraction using the Reliaprep™ RNA extraction kit from Promega the RNA was analysed by NanoDrop (using the NanoDrop 2000 from Thermo Scientific) to check for the quantity and purity of RNA extracted. **Table 5.1** shows the values of the RNA extracted. The 260/280 ratio should be ~2.0 and the 260/230 between 2.0-2.2, but above 1.5 is generally acceptable. DEPC (Diethylpyrocarbonate) water was used as a normaliser as when using the Reliaprep™ system this is the final elution liquid.

Sample/Number of cells	Yield (ηg/µl)	260/280	260/230
Water	0.6	6.81	8.14
$1x10^5$	271.9	2.14	2.14
$1x10^4$	15.4	1.98	1.71
$3x10^3$	5.5	1.87	1.37
$1x10^3$	2.5	1.97	0.9

Table 5.1 Nanodrop values of decreasing cell number
DEPC water was used as a normaliser. A 260/280 ratio ~2.0 indicates pure RNA, a 260/230 between 2.0-2.2, but above 1.5 is acceptable.

To give a measure of the integrity of the RNA extracted i.e., to ensure that the product is good quality and not fragmented, the 2200 TapeStation from Aligent was used (Methods 2.6.3). The TapeStation analyses the RNA product by gel electrophoresis after it is loaded into the complimentary R6K screentape platform. This allows for fully automated electrophoresis and the generation of an objective measure of RNA quality, the RNA integrity number equivalent (RIN^e). The RIN^e is used as a measure of the amount of RNA degradation between 1 and 10, where a RIN^e value of 10 is completely

intact RNA. This value is calculated based on the ribosomal RNA 28:18s ratio calculated from the electrophoresis gel and also the corresponding electrophrenogram (not shown).

Figure 5.1 shows the gel electrophoresis result. A ladder was loaded into A0 and the four samples were compared, from left to right E1=$1x10^3$ cells, F1=$3x10^3$ cells, G1=$1x10^4$ cells and H1 =$1x10^5$ cells. A first look at the RNA gel showed that most of the RNA was good quality as there was a roughly 2:1 ratio of the 28:18s bands and there was 'smearing' between and above the ribosomal RNA but not below. There were also no low molecular weight species towards the bottom of the gel. This result showed that high quality RNA was extracted from as little as 3,000 cells (RIN^e=9.7) but below this value (1,000 cells) the quality was low despite a good 260/280 ratio by Nanodrop.

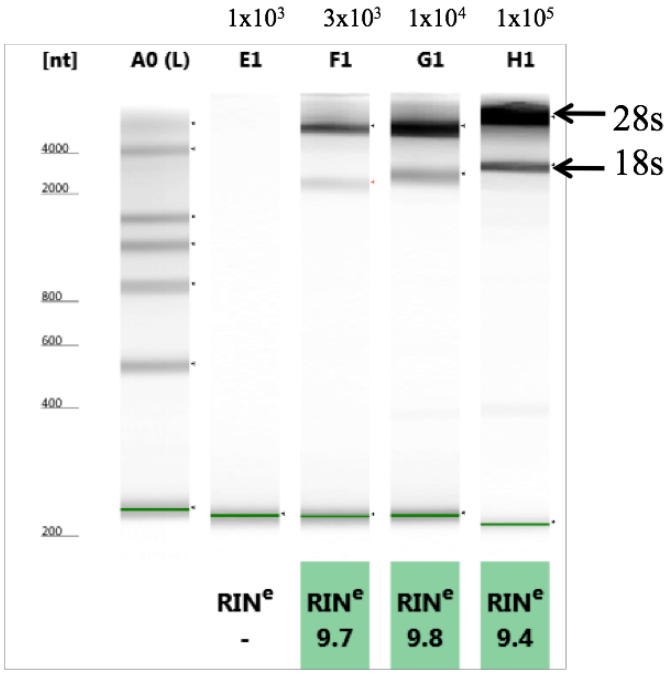

Figure 5.1 TapeStation gel electrophoresis result

The ladder (A0) shows the nucleotide (nt) length of the bands. The samples run from left to right E1 is $1x10^3$ cell, F1 $3x10^3$, G1 $1x10^4$ and H1 $1x10^5$. A RIN^e value ~ 10 denotes intact RNA. Intact RNA can be extracted from as little as $3x10^3$ cells (RIN= 9.7).

5.3.2 Investigation of HSC niche related gene expression in the PC-3NW1 dormant sub-population

To test if dormant cells, i.e., PC-3NW1 cells that have retained DiD after 14 days in culture, expressed higher levels of genes related to the HSC niche individual Taqman assays were done using primers for Angiopoietin 1 (ANGPT1), N-cadherin (CDH2), Chemokine (C-X-C Motif) Ligand 12 (CXCL12), Chemokine (C-X-C Motif) Receptor 4 (CXCR4), Jagged 1 (JAG1), Notch-1 (NOTCH1) and Endothelial Tyrosine Kinase (TEK). On day 14 after DiD staining 3 T175 flasks of PC-3NW1 cells were sorted by FACS Aria to separate the DiD positive dormant cell sub-population and the DiD negative rapidly dividing cells. RNA extraction was done using the ReliaPrep™ RNA Cell Miniprep System from Promega. cDNA was generated using Superscript® III RT enzyme from life technologies™ following Methods 2.2.4.

RT-qPCR was done using an Applied Biosystems 7900 Real-Time PCR machine. The results were entered into Prism to generate bar charts to compare the delta Ct values. Each graph represents three biological repeats consisting of two replicate wells for each assay. A superscript negative control was run in each plate, for each sample, and was negative in all experiments. Three housekeeper genes were used to normalise the data and generate delta Ct values (The Ct value of the assay minus the Ct value of the housekeeper) to compare expression levels. On all bar charts, the lower the bar the higher the gene expression level as a low Ct (cycle threshold) means a more abundant gene transcript as fewer cycles are needed to reach the fluorescent threshold.

These assays showed that the expression of CXCR4 was significantly up-regulated in the DiD positive dormant cell sub-population (graph legend DiD+) compared to the DiD negative rapidly dividing population (graph legend DiD-). This result was significant using all three housekeepers as the normalisation method (GAPDH Unpaired T-test, P=0.009, HPRT11 P=0.0001, Beta-actin P=0.035) (GAPDH shown **Figure 5.2**). There were no other significant differences between the DiD+ and DiD- populations in the expression of putative HSC niche genes although there was a trend towards increased expression of Jag 1 in the DiD+ population using these individual RT-qPCR assays.

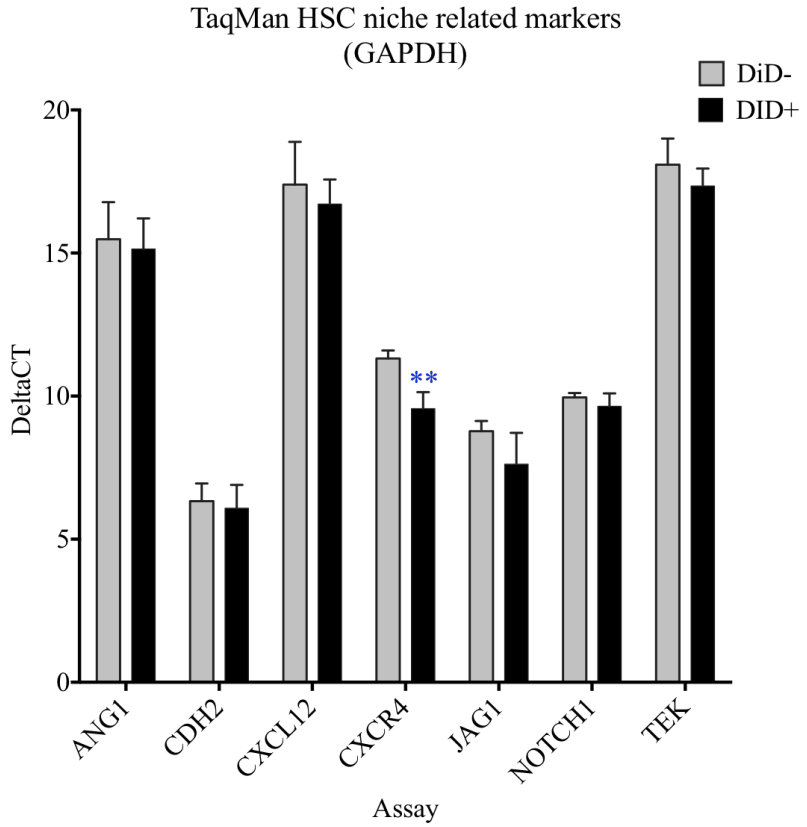

Figure 5.2 Investigation of HSC niche related gene expression by individual TaqMan assays
CXCR4 was significantly up-regulated in the dormant cell sub-population by RT-qPCR (Unpaired T-test, P=0.009). The mean value of 3 biological repeats with standard deviation is plotted.

5.3.3 Low Density Array technology to investigate the PC-3NW1 dormant cell sub-population

Three housekeeper genes were assigned to the LDA card GAPDH, HPRT1 and Beta-actin as well as the standard 18s housekeeper included by Applied Biosystems. DataAssist™ software from life technologies was used to analyse the data and select the most stable housekeeper to use as an endogenous control. GAPDH was shown to be the most stable, having the lowest standard deviation amongst the three repeats (negative/positive 1-3) by Pairwise comparisons and was therefore selected as the control for all subsequent analyses (GAPDH: 0.47, HPRT1: 0.56, 18s: 0.57, Beta- actin: 0.74) (**Figure 5.3**).

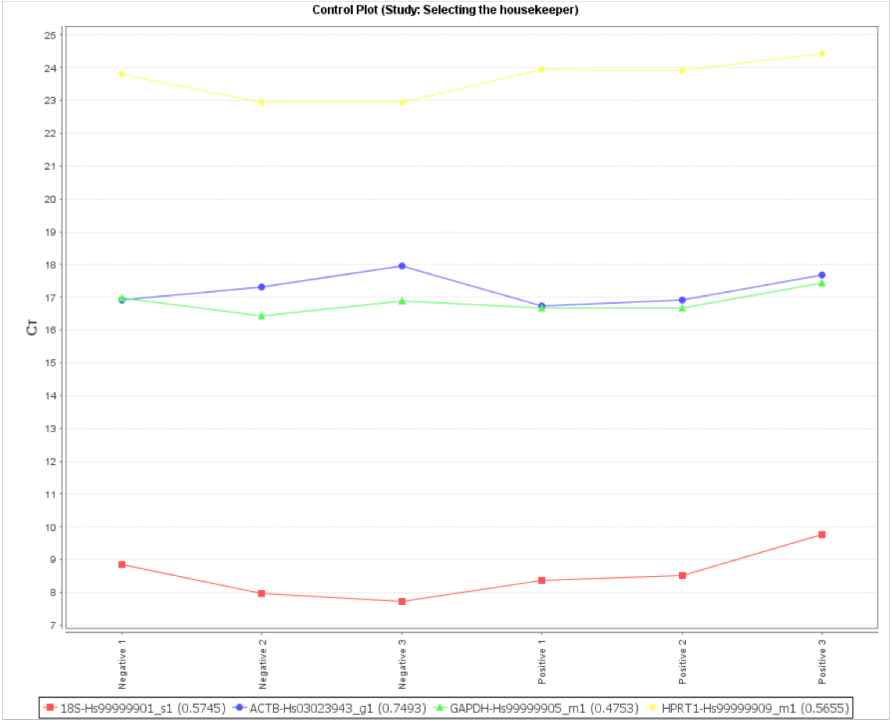

Figure 5.3 Selection of the most stable housekeeper
Across the three biological repeats GAPDH had the lowest standard deviation and was selected as the housekeeper to use for normalisation. (Standard deviation of GAPDH: 0.47 (green line), HPRT1: 0.56 (yellow line), 18s: 0.57 (red line), Beta- actin: 0.74 (blue line)). N=3 biological repeats.

As detailed above RNA was extracted from isolated PC-3NW1 DiD positive cells and DiD negative cells and cDNA was generated to perform RT-qPCR. Each card (considered as one biological repeat) had 8 'fill ports' allowing DiD positive and DiD negative samples to be run alongside each other in replicate. Each experiment was repeated 3 times. Genes that had a Ct value >35, due to low expression, and were therefore undetected at this sensitivity level are not plotted on the graphs (A complete table of the genes included in this LDA card (LDA card 1) and their gene expression values is found in **Appendix 1.1 and 1.2**). The following sections will present the results obtained in each of the five areas of interest. Heat Maps were generated using DataAssist™ software. In all graphs the mean value of 3 biological repeats with standard deviation is plotted.

5.3.3.1 Differences in the expression of HSC niche related markers in the dormant cell sub-population

LDA card analysis showed that by Unpaired T-test the expression of CXCR4 was significantly up-regulated in the PC-3NW1 dormant cell sub-population (DiD+) compared to the rapidly dividing cells (DiD-) (P= 0.038). This result is in agreement with the original Taqman assay. A significant up regulation in Jagged 1 (JAG1) expression was seen in the dormant cell sub-population (Unpaired T-test, P= 0.001). This increase was not significant at the level of individual TaqMan assays however the trend is the same.

By Unpaired T-test a significant down regulation in the gene expression of melanoma cell adhesion molecule (MCAM) was found in the dormant cell sub-population (P=<0.0001) (**Part A, Figure 5.4**). The Heatmap (**Part B, Figure 5.4**) shows the gene expression levels of the dormant DiD positive cells (positive) and the rapidly dividing DiD negative cells (Negative). The scale bar to the right (shown only in this figure) represents delta Ct values, which are given a colour based on their value. The lower the delta Ct, and therefore the higher expressed the gene, the closer to the red end of the scale the gene is. High delta Ct values denote low gene expression and are closer to the blue end of the scale. The mid-point (shown by the grey arrow at delta Ct 12) represents the median delta Ct value across all three biological repeats for all genes and is used as the mid-point for all analyses.

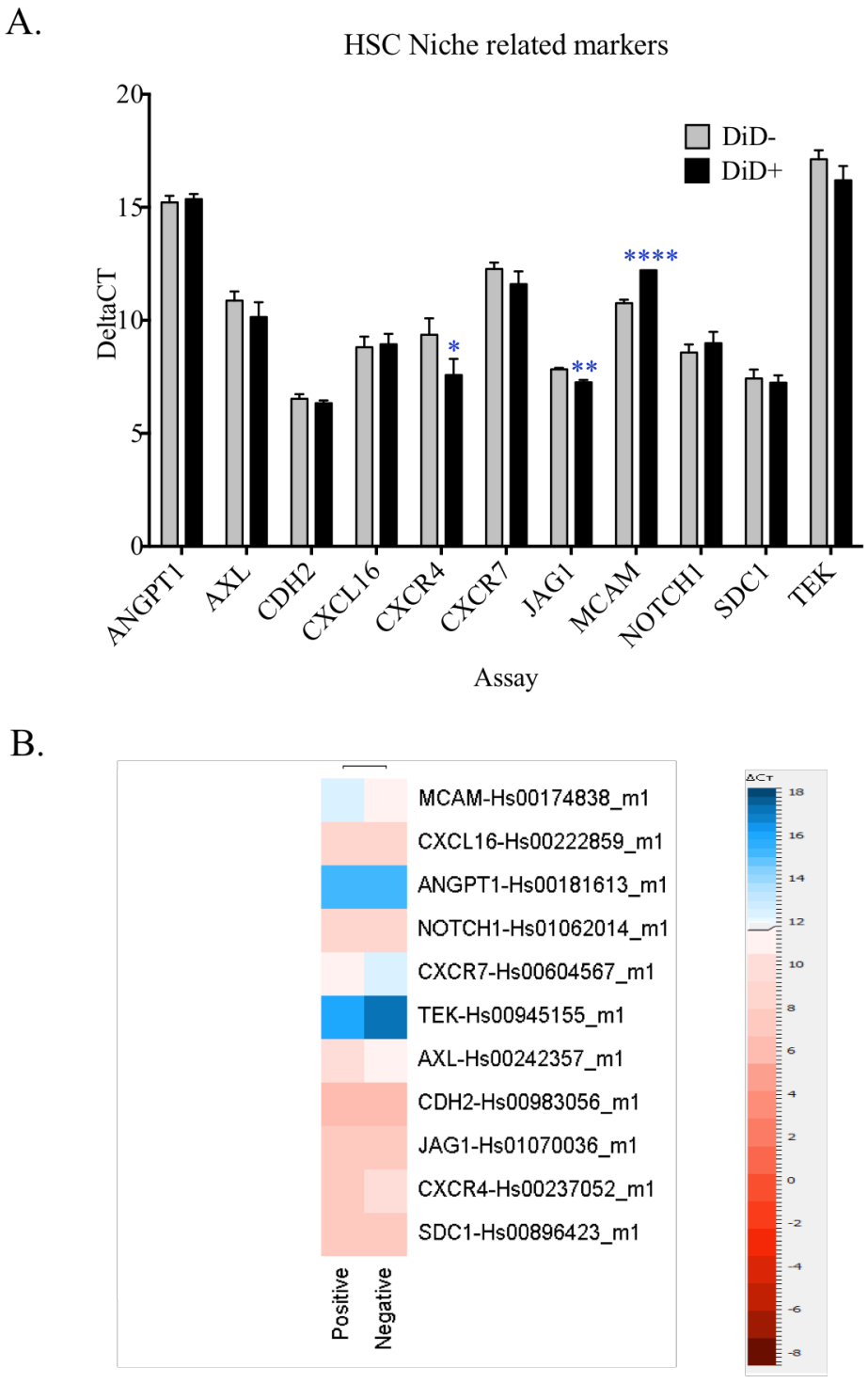

Figure 5.4 Investigation of HSC niche related genes by LDA card analysis
A. The bar chart shows the differences in the delta Ct values of the dormant (DiD+) cell sub-population compared to the rapidly dividing (DiD-) cells. CXCR4 (P=0.038) and JAG1 (P=0.001) were both significantly up-regulated in the DiD + cells. MCAM was significantly down regulated in the dormant cells (P=0.0001). **B.** The heat map shows the gene expression difference between the dormant DiD positive (Positive) cell sub-population and the rapidly dividing DiD negative cells (Negative). N= 3 biological repeats.

5.3.3.2 Differences in the expression of stem cells markers in the dormant cell sub-population

The dormant cell sub-population did not differentially express the proposed prostate cancer stem cell phenotype, CD44+/α2β1hi/CD133+. Although integrin α_2 (ITGA2) was significantly up-regulated in the dormant cells, the P value was weak (0.048) and these cells do not express significantly higher levels of integrin β_1 (ITGB1) or CD44 or CD133 (**Figure 5.5**).

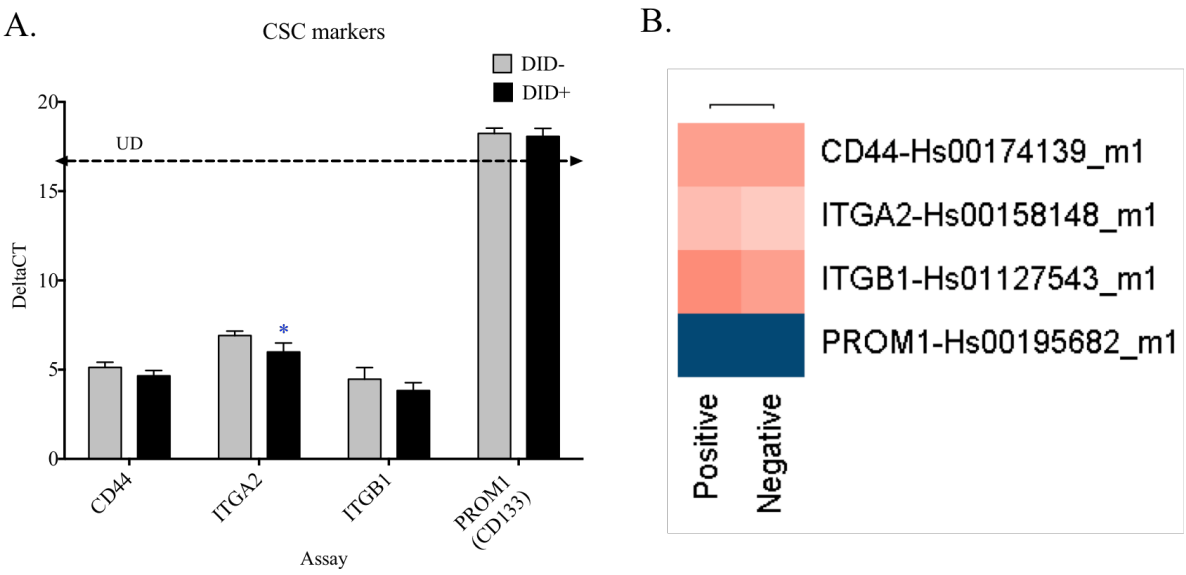

Figure 5.5 Investigation of proposed cancer stem cell (CSC) markers by LDA card analysis

A. The bar chart shows that only integrin α_2 (ITGA2) was significantly up-regulated in the dormant cells (P=0.048)**. B.** The differences in gene expression by heat map. N= 3 biological repeats.

However, other proposed stem cell markers were differentially expressed by the dormant cells. By Unpaired T-test the expression of Annexin 2 (ANAX2) (P=0.001), CD24 (P= 0.006) and Prostate stem cell antigen (PSCA) (0.0004) were significantly up-regulated in the dormant cell sub-population. A significant down regulation in the expression of Lactate Dehydrogenase B (LDHB) and Nestin (NES) was seen in the dormant cells (P= 0.014 and 0.013, respectively) (**Figure 5.6**).

A.

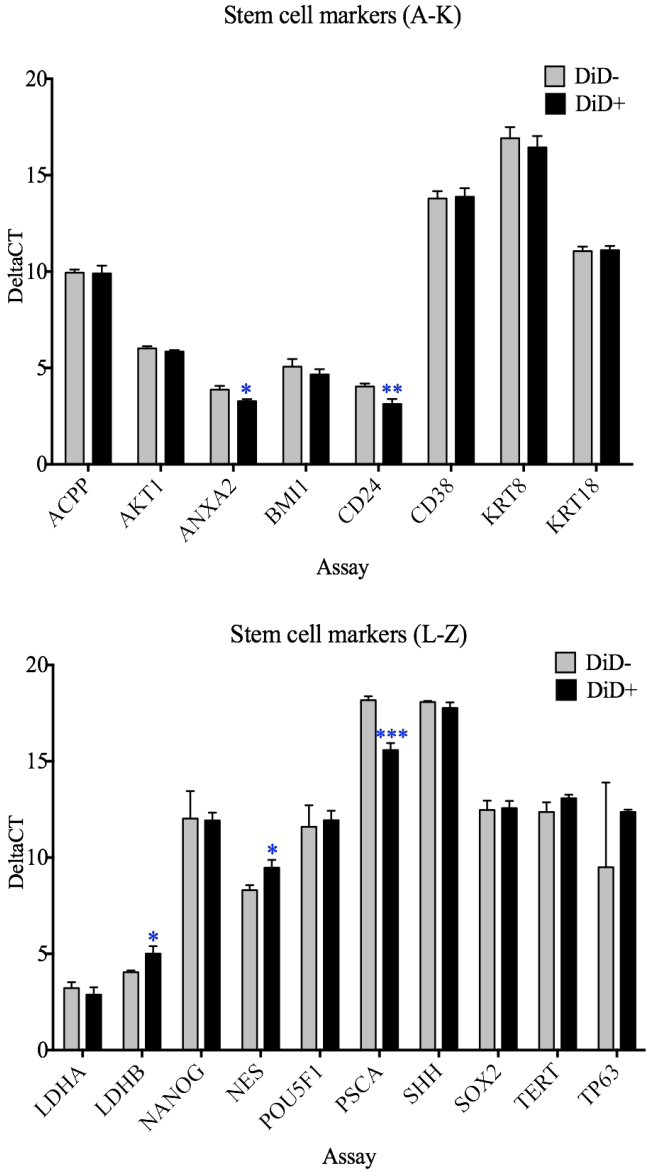

B.

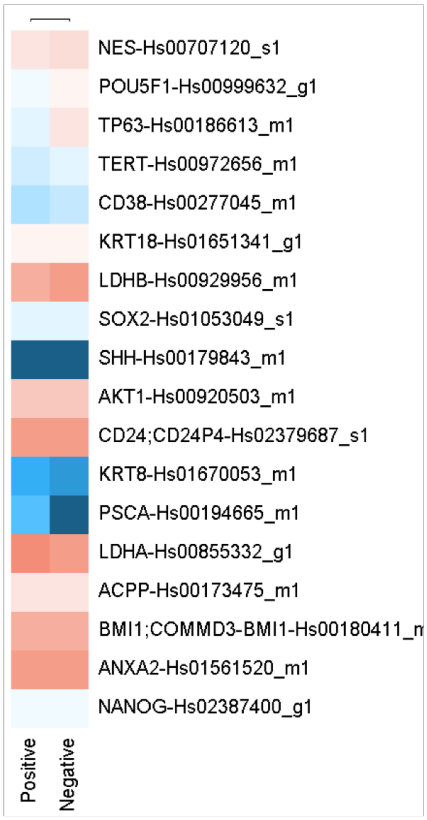

Figure 5.6 Investigation of Stem cell markers by LDA card analysis

A. The bar chart shows the differences in the delta Ct values of stem cell marker genes in the dormant (DiD+) vs. the rapidly dividing cell population (DiD-). ANAX2 (P=0.001), CD24 (P=0.006) and PSCA (P-0.0004) were all significantly up-regulated in the dormant sub-population. LDHB and NES were both significantly down regulated in the dormant cells (P= 0.014 and 0.013, respectively) **B.** The heat map shows the differences in delta Ct values. N= 3 biological repeats.

5.3.3.3 Differences in the expression of markers of EMT in the dormant cell sub-population

The dormant cell sub-population had increased gene expression levels of several proposed drivers of epithelial to mesenchymal transition (EMT). These were CXCL1 (Kuo et al., 2012), P=0.0002 by Unpaired T-test. MMP2 and MMP3 (Radisky and

Radisky, 2010), P= 0.004, <0.0001 respectively. Tenasin C, another proposed driver of EMT in tumours (Takahashi et al., 2013) was also significantly up-regulated (P=0.007) as well as markers of mesenchymal/fibroblast cells; fibroblast growth factor 2 (FGF2) (P=0.037), fibronectin (FN1) (P=0.0004) and vitronectin (VTN) (P=0.043) (**Figure 5.7**).

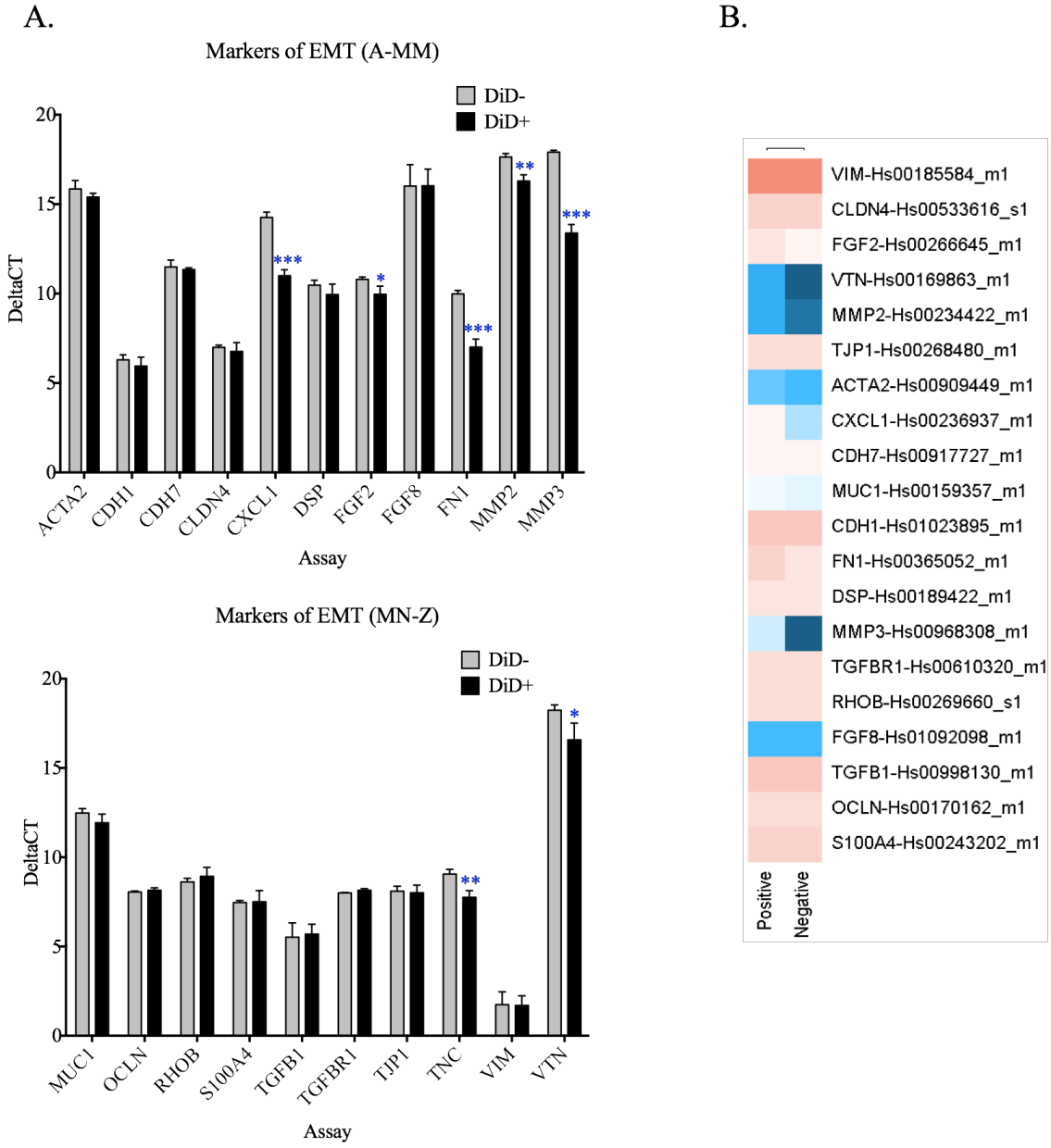

Figure 5.7 Investigation of markers of EMT by LDA card analysis

A. The bar chart shows the differences in the delta Ct values of markers of EMT in the dormant (DiD+) vs. the rapidly dividing cell population (DiD-). A number of markers of EMT transition were significantly up-regulated in the DiD positive cells by Un-paired T-test: CXCL1 (P=0.0002), MMP2 (P=0.004), MMP3 (P=<0.0001), TNC (P=0.007), FGF2 (P=0.037), FN1 (P=0.0004) and VTN (P=0.043). **B.** The heat map shows the differences in delta Ct value in the dormant DiD positive (Positive) vs. DiD negative (Negative) cells. N= 3 biological repeats.

5.3.3.4 Differences in the expression of osteomimetic markers in the dormant cell sub-population

It has been hypothesised that cancer cells can acquire features of bone cells, in particular osteoblasts, that allow them to survive and proliferate in the bone (Rucci and Teti, 2010). It was found that only BMP7 was significantly up-regulated in the dormant cells (P=0.030) (**Figure 5.8**).

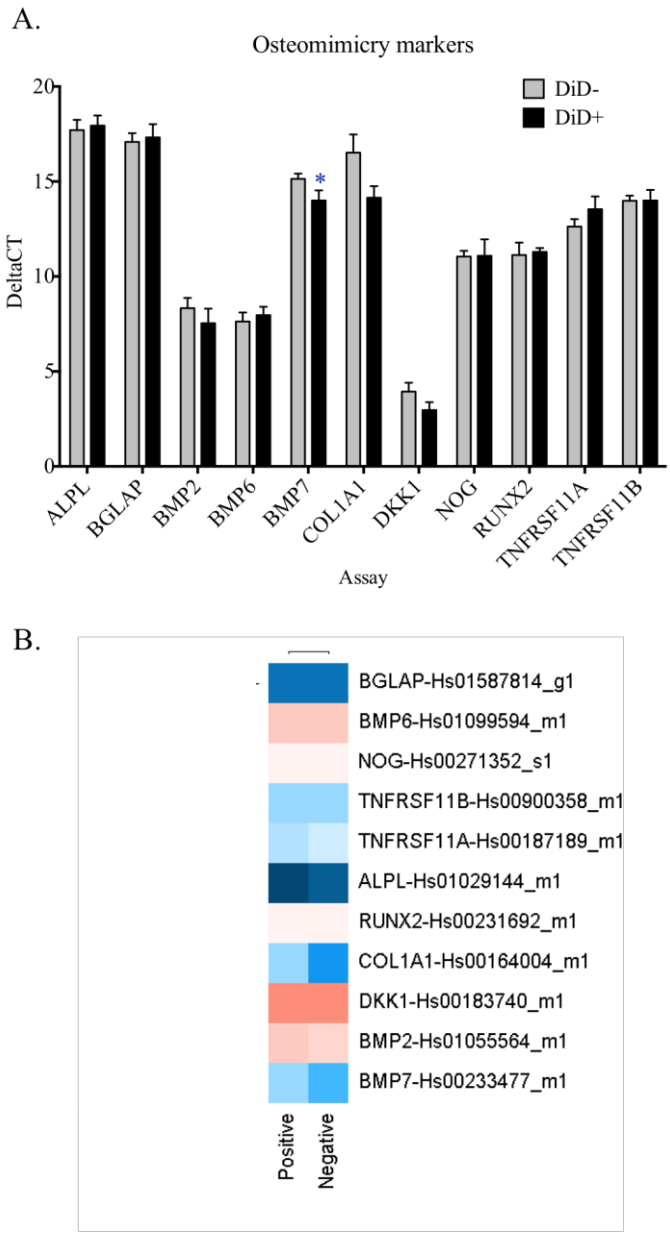

Figure 5.8 Investigation of osteomimetic markers by LDA card analysis

A. The bar chart shows that only BMP7 was significantly up-regulated in the dormant cell sub-population (P=0.030). **B.** The heat map shows the differences in delta Ct value in the dormant DiD positive (Positive) vs. DiD negative (Negative) cells. N= 3 biological repeats.

5.3.3.5 Differences in the expression of endocrine and miscellaneous markers in the dormant cell sub-population

The final spaces on the LDA card were used to investigate several markers of interest that had either been proposed by members of the lab group or had recently appeared in the literature (**Figure 5.9**).

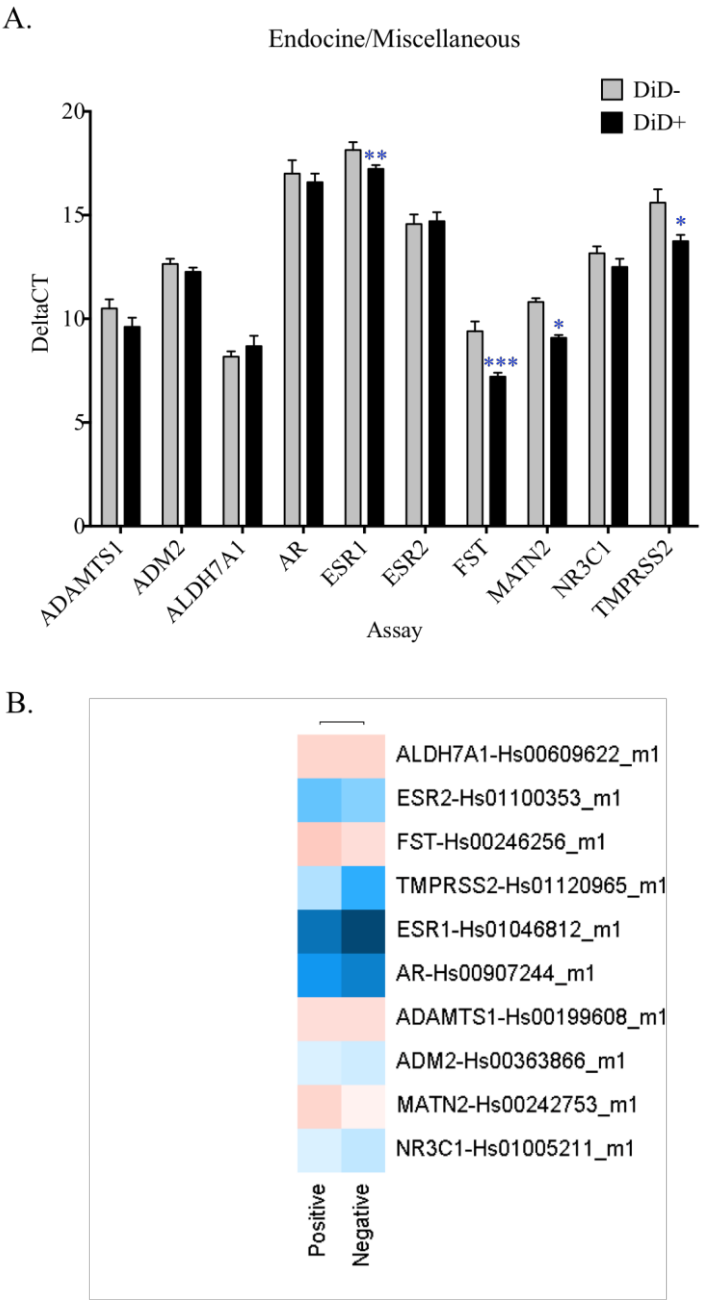

Figure 5.9 Investigation of endocrine / miscellaneous markers by LDA card analysis
A. The bar chart shows that FST (P=0.001) as well as MATN2 (P=0.0001), ESR1 (P=0.020) and TMPRSS2 (P=0.010) were significantly up-regulated in the dormant sub-population **B.** The heat map shows the differences in delta Ct value in the dormant DiD positive (Positive) vs. DiD negative (Negative) cells. N= 3 biological repeats.

Follistatin (FST) was significantly up-regulated in the dormant sub-population (P=0.001). Along with Matrillin 2 (MATN2) (P=0.0001) and the estrogen receptor 1 (ESR1) (P=0.020). Expression of the androgen regulated gene TMPRSS2 was significantly increased in the dormant cell sub-population (P=0.010), however expression of the TMPRSS2-ERG fusion was not detected in either sub-population (Ct value >35, not shown on the graph). The negative presence of the TMPRSS2-ERG fusion was expected for a sub-strain of the PC-3 cell line.

5.3.4 Assessment of the *in vivo* bone homing DiD positive population

As previously mentioned, recent work in our lab has found that PC-3NW1 cells can survive in a dormant state for long periods of time in the bone marrow of mice. These cells can remain DiD positive up to 8 weeks after intracardiac injection. It is not yet known whether these cells represent the same sub-population as those identified *in vitro*, by DiD retention for 14-21 days.

The first aim of this study was to use LDA card analysis to assess the genetic profile of cells that had homed to the bone in xenograft models. $1x10^5$ PC-3NW1 cells were stained with DiD and immediately injected into balb/c nude mice via intracardiac. After 7 days, the mice were culled and their hind limbs were dissected to remove the tibia and femur. These bones were 'flushed' following the protocol in Methods 2.8.1. The cells were retained for FACS sorting based on DiD retention to isolate the human PC-3NW1 cells for RNA extraction. These cells would represent the early colonising population. The aim of this was to use this profile to compare these cells to those that were dormant *in vitro* and, eventually, cells that were dormant *in vivo*, i.e. DiD retaining 8 weeks after intracardiac injection.

The bones from three mice were prepared for bone marrow flush and the resulting cell suspensions were each individually sorted by FACS Aria to retrieve the DiD positive cell fraction. However, despite increasing the positive gate to sort cells that had low DiD intensity but still remained outside of the negative control gate, very low yields of DiD positive cells were obtained (Figure 5.10). It was therefore decided that quality RNA could not be isolated from these cells for LDA card analysis.

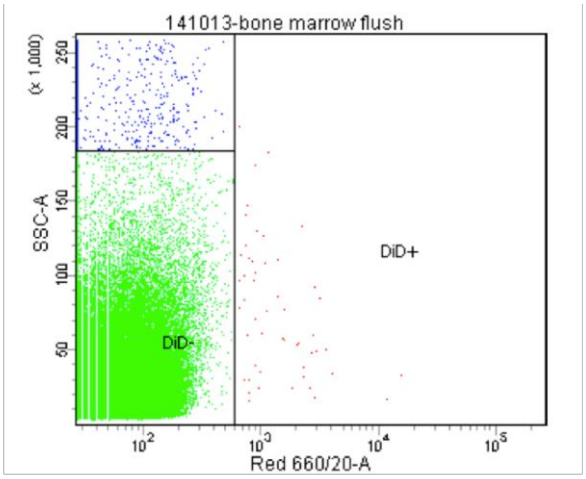

Tube: bone marrow flush

Population	#Events	%Parent	%Total
All Events	1,348,610	####	100.0
FSC SSC	1,254,172	93.0	93.0
DiD-	1,253,471	99.9	92.9
DiD+	52	0.0	0.0

Figure 5.10 FACS analysis following the bone marrow flush The flow cytometry plot and statistical output. The plot shows the gated DiD+ population, which is drawn just outside of the DiD- gate. The upper square of blue 'dots' represents large events, which could be doublets or dead cells and were excluded from analysis. 7 days after intracardiac injection of DiD stained PC-3NW1 cells the hind limbs of 3 mice were dissected and the tibia and femur 'flushed' to remove the marrow. The cells were sorted by FACS Aria. Only a very small number of DiD positive cells were retrieved in this way 52 out of 1,253,172, which was deemed insufficient for LDA card analysis.

5.3.4 Using the LDA card information to create a signature for dormancy

The previous results show that there were significant gene expression differences between the PC-3NW1 dormant cell sub-population and rapidly dividing cells. The next stage was to test whether these differences were also seen in other dormant cells i.e., PC-3NW1 cells grown at clonal density in 1% FBS media (referred to as Clonal dormancy) and rapidly dividing PC-3NW1 cells that had lost DiD after the initial stain but retained it after FACS sorting and re-staining (referred to as Restained dormant cells). A second LDA card was designed, containing 22 genes of interest plus the endogenous control GAPDH and 18s (Applied Biosystems standard). These included a number of genes that were identified in the previous section as significantly different but also novel genes added after group discussion (a full gene list of this LDA card (LDA card 2) is shown in Appendix 1.3). This smaller card allowed the direct comparison of different cell sub-populations as multiple samples could be loaded per card.

5.3.4.1 LDA card 2 analysis of the original PC-3NW1 dormant cell sub-population

To clarify the markers identified with the first LDA card (LDA card 2), PC-3NW1 cells stained with DiD and cultured for 14 days were sorted by FACS Aria to separate the

dormant (DiD+) and rapidly dividing (DiD-) populations. The delta Ct values were compared and it wad found that eight genes were significantly up-regulated (none were down regulated) in the dormant cell sub-population by Unpaired T-test. These were CD34 (P=0.020), CXCL1 (P=0.039), CXCR4 (P=0.024), DKK1 (P=0.0127), MMP3 (P=0.012), SOSTDC1 (P=0.0112) TNC (P=0.037) and VTN (P=0.043) (**Figure 5.10**). The bars that pass above the perforated UD (undetected) line represent genes that had a CT value of above 35 and are therefore undetected (UD) at this level. The results from LDA card 2 were consistent with the first LDA card in the overlapping genes analysed.

5.3.4.2 LDA card 2 analysis of dormancy in restained PC-3NW1 cultures

Following Methods 2.3.2 and 2.6 PC3-NW1 cells that had retained DiD after restaining were sorted by FACS Aria to separate the now dormant restained DiD positive cells and the rapidly dividing restained DiD negative cells for RNA extraction and LDA card analysis i.e. cells that were all initially classed as fast growing by loss of detectable DiD after 14 days were stained a second time with DiD which, after a further 14 days in culture, allowed the identification of a DiD retaining sub-population of cells within the previously rapidly growing population that had 'switched' to the dormant phenotype. The gene expression differences of these cells ('Restained+') compared to cells in the same cultures that had lost DiD, after the second staining, ('Restain-') was then compared by LDA card 2 analysis.

By Un-paired T-test seven genes were significantly up-regulated in the restained DiD retaining dormant cells (graph legend: 'Restain+') compared to restained DiD negative, consistently rapidly dividing cells (graph legend: 'Restain-'). These were DKK1 (P=0.029), FN1 (0.044), MMP3 (0.003), SOSTDC1 (0.012), TNC (P=0.017), TP63 (0.014) and VTN (P=0.044) (**Figure 5.11**). There was a trend towards increased CXCR4 expression in the restained DiD+ cells (Restain+) compared to the DiD- cells (Restain-) but this failed to reach significance. Although slight differences were seen between the PC-3NW1 dormant cells and the restained dormant cells by two-way ANOVA overall there was no significant difference between these cell types (P=0.651). There is also no significant difference by two-way ANOVA between the PC-3NW1 DiD negative cells and the DiD negative cells after re-staining (P=0.277) across the complete gene set.

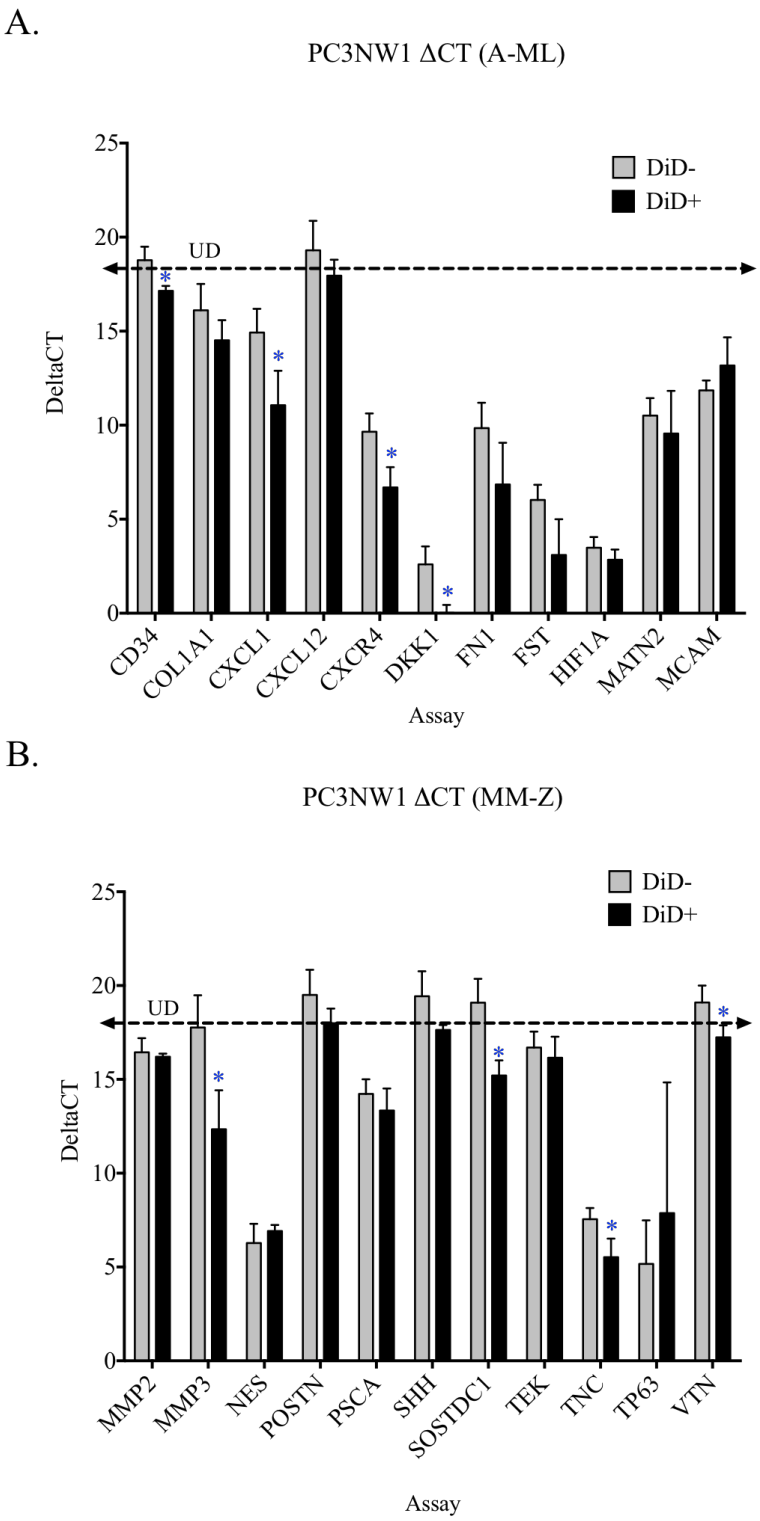

Figure 5.10 Investigation of a signature for dormancy in the PC-3NW1 cell line
CD34 (P=0.020), CXCL1 (P=0.039), CXCR4 (P=0.024), DKK1 (P=0.0127), MMP3 (P=0.012), SOSTDC1 (P=0.0112) TNC (P=0.037) and VTN (P=0.043) were all significantly up-regulated in the dormant cell sub population (DiD+) compared to the rapidly dividing cells (DiD-). N= 3 biological repeats.

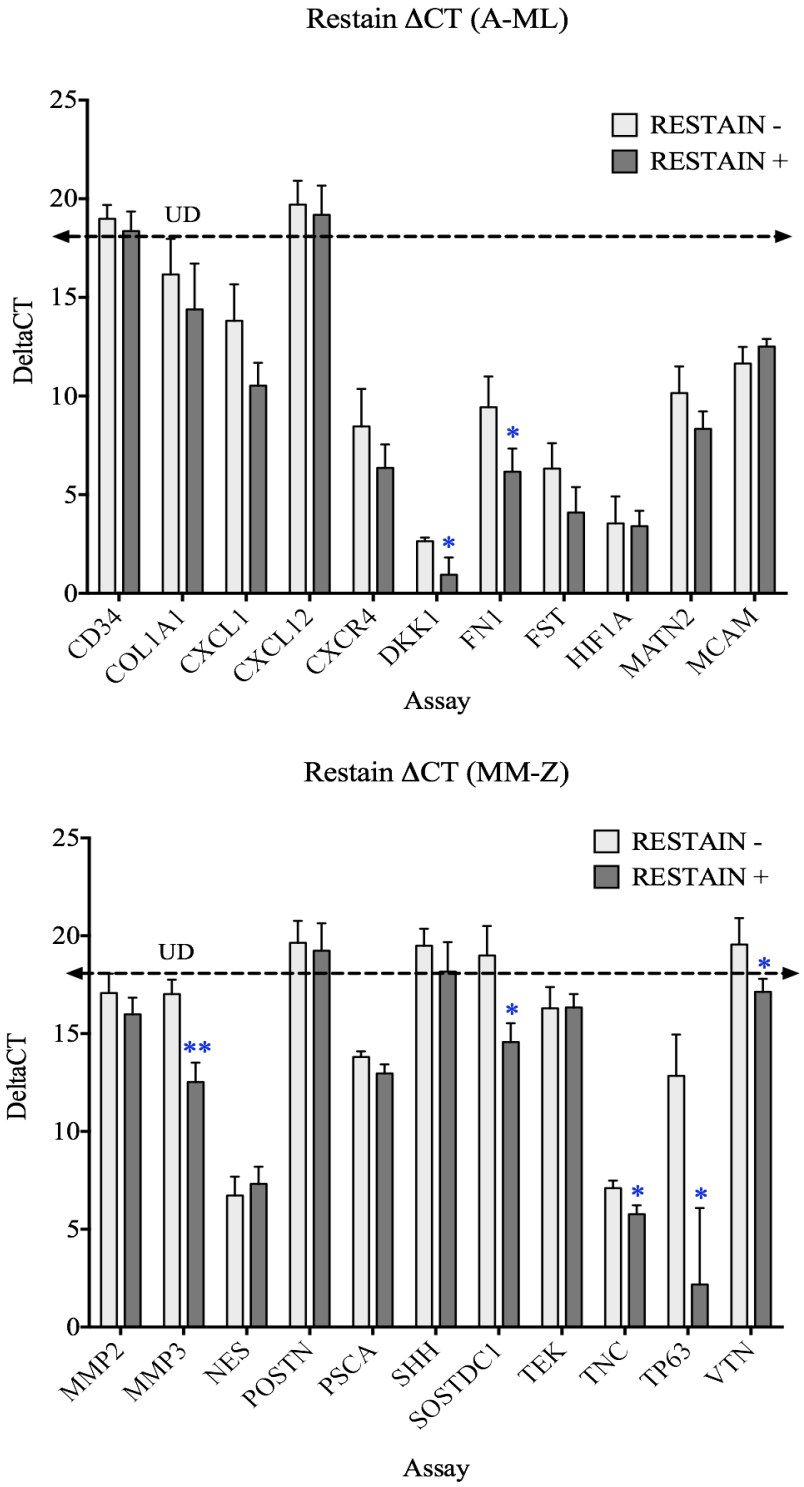

Figure 5.11 Investigation of a signature for dormancy in dormant restained cells
DKK1 (P=0.029), FN1 (0.044), MMP3 (0.003), SOSTDC1 (0.012), TNC (P=0.017), TP63 (0.014) and VTN (P=0.044) were all significantly up-regulated in the dormant cell sub population (DiD+) compared to the rapidly dividing cells (DiD-). N= 3 biological repeats.

5.3.4.3 LDA card analysis of clonal dormancy

To investigate whether dormant single cells grown at clonal density in 1% FBS differentially expressed these same markers, cells isolated from these conditions were compare by LDA card 2 analysis to a control population. The 'Control' population consisted of DiD stained PC-3NW1 cells that were seeded at clonal density into 10 x T175 flasks in 10% FBS DMEM + 1% PenStrep and harvested after 14 days to be used as a comparison. These cells formed growing clones and were used as a reference population (graph legend: 'Control'). In order to gain enough cells for RNA extraction, to investigate the dormant single cells at clonal density (graph legend: 'Clonal'), the experiments performed in Chapter 4.3.1 had to be scaled up. $6x10^3$ DiD stained PC-3NW1 cells were seeded into 10 x T175 flasks with 37 mL of 1% FBS DMEM + PenStrep (equivalent to the conditions used in the colony assays, 35.3 cells /cm^2 and 0.21 mL of media/cm^2). These flasks were cultured for 14 days, after which RNA was extracted and cDNA was generated for RT-qPCR.

By Unpaired T-test, seven genes were significantly up-regulated in the Clonal dormancy cell sub-population compared to the Control. These were CXCL1 (P=0.011), CXCR4 (P=0.034), MMP3 (0.002), PSCA (0.006), SHH (0.011), TNC (0.042) and VTN (0.008) (**Figure 5.12**). Although there were a number of differences between cells that were dormant at clonal density and cells that have retained DiD due to dormancy after 14 days by two way ANOVA there was no significant difference between the two cell types (P=0.723) across the complete gene set.

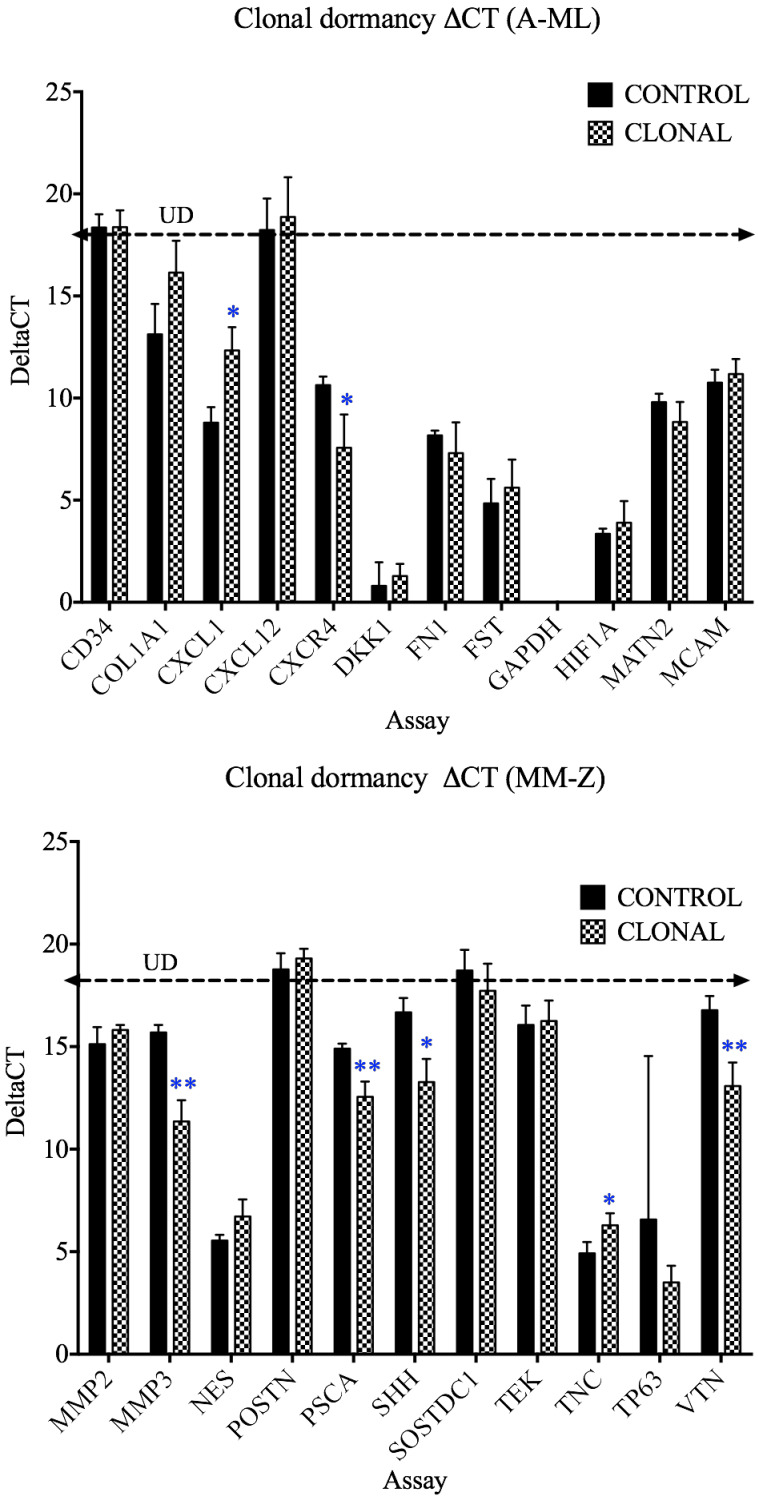

Figure 5.12 Investigation of a signature for dormancy in dormant cells cultured at clonal density in 1% FBS media compared to cells growing in colonoies (Control)
CXCL1 (P=0.011), CXCR4 (P=0.034), MMP3 (0.002), PSCA (0.006), SHH (0.011), TNC (0.042) and VTN (0.008) were all significantly up-regulated in the dormant cell sub population (DiD+) compared to the rapidly dividing cells (DiD-). N= 3 biological repeats.

5.3.5 Comparisons of gene expression under different conditions of dormancy

LDA card 2 analysis was useful to investigate the gene expression differences between dormant cell sub-populations and their rapidly dividing counterparts. To compare the gene expression signature of the three different dormant sub-populations, i.e. between sub-populations that were initially dormant (PC3NW1 DiD+) to cells that had re-emerged as dormant (Restain+) and cells that survived as single dormant cells under clonal conditions (Clonal), the Ct value information was pooled in order to construct a heat map. This was also useful to compare the three different sub-populations of DiD-/ rapidly dividing cells. As reported, two way ANOVAs had shown that there was no significant difference between dormant cells identified under any of the three conditions mentioned above. This suggests that dormancy, as a phenotype, is characterised by common gene expression alterations of the assays included on LDA card 2.

A full heat map to show the comparisons between all cell types is shown in **Figure 5.13.** The scale bar to the right shows the mid-point (the grey arrow), which is placed at 12, the median delta Ct value of all samples for all repeats. The DiD positive dormant cells in the PC-3NW1 cell line (PC-3NW1+) were compared to their rapidly dividing counterpart (PC-3NW1-) as well as with single cells maintained as dormant grown in 1% FBS media (Clonal) and their proliferating counterpart growing as clone colonies (Control) and also PC-3NW1 cells that have re-emerged as dormant after re-staining (Restain+) and their rapidly dividing counterpart (Restain-). The perforate black line indicates the divide between the ‘dormant’ sub-population and the ‘non-dormant’ / rapidly dividing populations. This highlights the key patterns of gene expression that were different between the two groups. For example, the heat map demonstrates lower gene expression (indicated by colours of paler red or towards the blue end of the spectrum) to the left of the perforated line in the ‘non-dormant’ populations for key genes such as CXCR4, MMP3 and SOSTDC1 compared to higher gene expression in the ‘dormant’ cell sub-populations to the right of the perforated line.

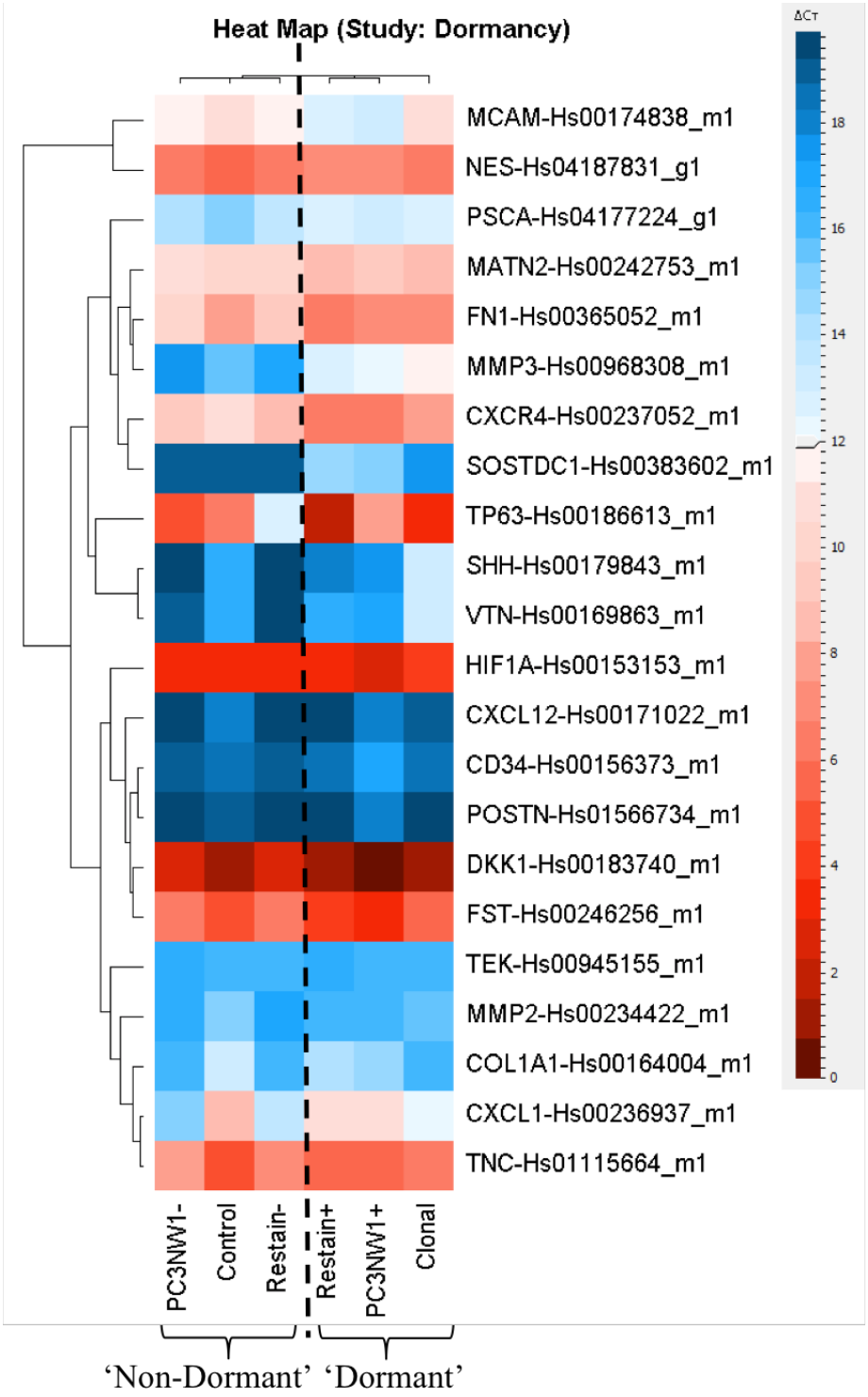

Figure 5.13 A full heat map to show investigation of a dormant cell signature
The heat map shows the differences in delta Ct values of the dormant cell sub-populations in the PC-3NW1 cell line (PC3NW1+ = sorted DiD positive cells after 14 days), restained dormant cells (Restain+ = sorted DiD positive cells, that were initially DiD negative but were restained with DiD and emerged as DiD retaining and therefore dormant) and clonal dormant cells (Clonal = single cells held in a dormant state when seeded at clonal density in 1% FBS media) compared to rapidly dividing cells (PC3NW1-= sorted DiD negative cells after 14 days), Restain- (sorted DiD- cells, that rapidly lost DiD a second time after restaining) and Control (cells growing in colonies when seeded at clonal density in 10% FBS media).

5.4 Discussion

The aim of this study was to characterise a molecular signature for dormancy. Using TaqMan assays and two LDA cards the gene expression profile of the dormant cell sub-population in comparison to rapidly dividing cells was assessed. Initially individual TaqMan assays revealed a significant up regulation of CXCR4 expression in the dormant sub-population. This result was replicated using the first LDA card and LDA card 2.

The initial LDA card highlighted a number of other interesting markers that were up-regulated in the dormant cell population. In particular, PC-3NW1 dormant cells have an increase in gene expression of several stem cell markers including prostate stem cell antigen (PSCA). High PSCA expression, although not unique to cancer cells, has been linked to higher Gleason grade tumours and bone metastases (Gu et al., 2000). It has been suggested that PSCA could be used as a potential prognostic indicator of more aggressive tumours but its link to dormancy is as yet unclear. It is interesting to note that the isolated PC-3NW1 dormant cells do not differentially express markers of the proposed prostate CSC sub-population, apart from ITGA2. However, CD24, a proposed marker of a CSC sub-population in Nasopharyngeal Carcinoma (Yang et al., 2014a), was significantly up-regulated in the dormant cells of the PC-3NW1 cell line. Therefore, although dormant cells have many characteristics of stem cells at the gene expression level as well as other CSC like features such as high cloning ability and increased chemotherapeutic resistance, they were distinct from the previously identified prostate CSCs although they may be a sub-set of these cells.

A clear up-regulation in markers of EMT was seen in the dormant cell sub-population in the initial LDA card analysis. This was verified in LDA card 2. MMP3, a proposed driver of EMT (Radisky and Radisky, 2010), was significantly up-regulated in all three dormant cell sub-populations by LDA card 2 analysis. It has been proposed that EMT can act as a driver of a more migratory phenotype in cancer cells but in order for this de-differentiated phenotype to initiate metastasis, MET (mesenchymal to epithelial transition) must take place (see Introduction for a more detail discussion of this). In a review by Thiery (2009), it is hypothesised that EMT is needed to act as a suppressor of proliferation in order to promote a more invasive phenotype that has an increased

resistance to cell death and drug treatment but once in the bone marrow this is reversed to allow proliferation and metastatic growth (Thiery et al., 2009). The role of EMT as a driver of cellular dormancy still remains unclear and in order to build on the work presented here, knockdown studies of EMT drivers would be needed to see if the dormant phenotype was affected.

The only osteomimetic marker that was significantly up-regulated in the dormant cell sub-population, by LDA card 1 analysis, was BMP7. The link between BMP7 as a driver of dormancy has already been published by Kobayashi et al., 2011 who found that BMP7 secreted from bone stromal cells induces 'reversible senescence' in prostate cancer cells by the activation of P38, P21 and NDRG1 (Kobayashi et al., 2011). As this was the only marker of its kind to be significantly altered in my studies, and it had previously been linked to dormancy, it was not including on LDA card 2. Interestingly however, studies by Buijs et al., 2007 indicated that increased BMP7 correlated to increased E-cadherin and reduced vimentin in prostate cancer cells, which, the authors suggest, indicates a role for BMP7 in inducing an epithelial rather than mesenchymal phenotype (Buijs et al., 2007). These results appear to be in disagreement to my own, that suggested that in the dormant cells increased BMP7 correlates to a more mesenchymal phenotype. The reason for this could be however, that Buijs et al. looked at the E-cadherin : vimentin ratio as an indicator of an epithelial or mesenchymal phenotype while these experiemnts looked at a broader range of markers of EMT and while there was no significant differences in the gene expression of E-cadherin (LDA card synonym CDH1) or vimentin between the DiD+ and DiD- sub-populations, there was increased levels of other markers of mesenchymal cells such as FGF2 and MMP2 and 3. This suggests that while BMP7 could have an effect on the levels of E-cadherin and vimentin, increased BMP7 in my studies appeared to correlate to increased expression of other mesenchymal markers. Furthermore, the results reported in Buijs et al. stated that the PC-3 cell line did not show detectable BMP7 mRNA expression while my studies reported detectable levels, although low, of BMP7 in both the DiD+ and DiD- sub-populations in the PC-3NW1 cell line. This could suggest differences in the specificity of the assays used or could reflect inherent differences in the PC-3 parental cell line and the transfected PC-3NW1 derivative.

It was interesting to find that although PC-3 cell are widely considered to be androgen receptor (AR) negative, the presence of AR RNA was detected in both the dormant and rapidly dividing PC-3NW1 cell populations. It has previously been shown that AR mRNA is present in the PC-3 cell line by RT-PCR at high cycle number (30 cycles) and present as AR protein at a low level by western blot (Alimirah et al., 2006). However, as this was not differentially expressed by the dormant cells so it was not included on the second LDA card. Furthermore, western blot analysis would be needed to determine whether AR RNA in this cell line was translated to protein.

5.4.1 A signature for dormancy

Three markers were significantly up-regulated in all three dormant cell sub-populations by LDA card 2 analysis. These were MMP3, TNC and VTN. As mentioned above MMP3 and TNC are both proposed drivers of EMT, while VTN is a known marker of fibroblast cells. It is tempting to speculate that cellular dormancy in the PC-3NW1 cell line is a result of EMT induction in a subset of cells that have become more mesenchymal as a result. However, as mentioned previously, further research is needed to investigate the role of EMT and dormancy in these conditions. It is significant to note, however, that by LDA card analysis there were commonly up-regulated genes in cells with a dormant phenotype in different culture conditions.

CXCR4 expression was consistently up-regulated to significance in the PC-3NW1 dormant cell sub-population by individual TaqMan assays and LDA card 1 and 2. CXCR4 was also significantly up-regulated in the dormant cell population grown at clonal density in 1% FBS media. CXCR4 expression was also higher in the restained dormant population but failed to reach significance. CXCR4 and its potential as a marker of dormancy will be investigated in the following results chapter. Although PSCA was significantly up-regulated in the PC-3NW1 dormant sub-population by LDA card 1 analysis, this failed to reach significance using LDA card 2 but the trend was the same. It was interesting to note that in the dormant cells population grown at clonal density, PSCA and SHH were significantly up-regulated.

Although Hif1α expression was not significantly up-regulated in any of the dormant cell sub-populations, as Hif1α acts at the protein level as a transcription factor it would be

more useful to look at genes that are targets of Hif1α such as glut1 (Chen et al., 2001) to determine whether hypoxia could still be a potential driver of dormancy.

Overall LDA card 2 analyses showed that the gene expression signature of all three dormant cell sub-populations was not significantly different by two-way ANOVA. This suggests that as well as the three genes that were significantly up-regulated in all three cell types (MMP3, TNC and VTN) there is an overall consensus gene expression signature of dormancy. By two-way ANOVA the gene expression signature of the PC-3NW1 dormant sub-population was significantly different (P=0.0001) from the PC-3NW1 rapidly dividing cells using LDA card 2 analysis. The restained DiD positive dormant cells were also significantly different (P=0.0001) from the restained DiD negative rapidly dividing cells by two-way ANOVA. However, no significant difference was seen between clonal dormant cells and the control by two-way ANOVA (P=0.116) but a significant difference was seen between clonal cells and PC-3NW1 rapidly dividing (P=<0.0001). This suggests that the gene expression profile of dormancy is distinct from rapidly dividing cells.

5.4.2 Conclusion

Initial LDA card analysis revealed several differences in the gene expression levels of dormant vs. rapidly dividing cells. In particular, markers of stem cells (but not the proposed prostate CSC) as well as markers of EMT were significantly up-regulated in the PC-3NW1 dormant cell sub-population. The utilisation of a second smaller LDA card (LDA card 2) showed that under different conditions (re-stain and clonal density in 1% FBS) the gene expression profile of dormant cells is not significantly different. Indeed three key genes were highlighted (MMP3, TNC and VTN) as markers that may define the dormant phenotype. However, their functional role in dormancy is yet to be defined.

The following results chapter will utilise LDA card 2 to investigate markers of dormancy in the human prostate cancer cell lines LNCaP and C42B4. The aim of these studies is to assess whether the dormant cell sub-populations identified in these two cell lines in Chapter 3, have the same gene expression signature of the PC3-NW1 dormant phenotypes. This chapter will also investigate markers of dormancy, in particular

CXCR4, in more detail and how they could be used to identify dormant cells in patient samples that may predict poor prognosis.

Chapter 6: Defining markers of the dormant cell phenotype

6.1 Introduction

Results presented in the previous chapter indicate that cells with a dormant phenotype share gene expression modifications, as measured by LDA card 2 analysis, in sub-populations of the PC-3NW1 cell line. The studies in this chapter aim to test whether this expression profile is present in the dormant cell sub-population identified in the LNCaP and C42B4 cells lines in Chapter 3. This chapter also aims to define a marker set that will identify cells of the dormant phenotype by immunostaining techniques. This will be used to assess the frequency of dormant cells in patient samples. As discussed, results in our own lab have indicated that the dormant PC-3NW1 cell line, i.e. DiD retaining cells 14 days after staining, have a higher bone metastatic ability in xenograft models. This suggests that cells of a dormant phenotype may represent a novel metastasis initiating cell type. It was therefore consider to be of interest to identify markers of these cells that could be used as prognostic indicators of metastatic progression in patients.

Successful treatment of prostate cancer patients with radical prostatectomy is limited to those with organ confirmed disease and while prognostic tests can highlight patients who require more intensive treatment, metastatic prostate cancer is still an incurable disease. There are already several clinical tests that are used to evaluate prognosis in prostate cancer patients. Patient age, Gleason grade and TNM (Tumour, Node, Metastasis) staging are all used as clinical indicators of prognosis; as well as several biological tests that include PSA level, P53 status and Ki-67 status of tumour biopsies (Buhmeida et al., 2006).The limited routine availability of tissue samples from prostate cancer patients has hampered the development and use of prognostic markers. Realistically, the only prostate cancer samples routinely available are fixed, parrafin wax embedded, diagnostic biopsies and a small number of similarly processed radical specimens. This means that tests need to be applicable to these materials to be useful. For this reason immunohistochemistry has been widely used to assess potential prognostic markers in these sample sets. Indeed E-cadherin status in prostate cancer specimens has been shown to correlate to survival in patients. Umbas et al. (1994) used 89 snap frozen cancer specimens and stained for E-cadherin presence using an anti-E-cadherin monoclonal antibody. The authors found that the 3-year survival of patients with ‘normal’ E-cadherin staining (uniform staining confined to the cell membrane) had

a significantly higher survival rate than patients with 'aberrant' E-cadherin staining (defined as heterogeneous, cytoplasmic or negative staining). Indeed, a decrease in E-cadherin staining correlated to the presence of metastases in patients, with 76% of patients with distant metastases having 'low' E-cadherin staining compared to 33% of patients with organ confined disease at the time of biopsy (Umbas et al., 1994). More recently, Nakagawa et al. (2011) found that there was a correlation between low positive staining for E-cadherin and high Gleason grade (Nakagawa et al., 2011). These results suggest that a loss of E-cadherin staining, a characteristic of EMT, is an important prognostic indicator and further highlights the important role of phenotypic changes in cell type in the metastatic cascade.

Recently, Fisher et al. (2013) published data using samples from a large patient cohort (293 men) to support the value of Ki-67 as a prognostic indicator in prostate cancer using long term survival as the end-point. While Ki-67 status is considered the most promising biomarker for immunohistochemical analysis of prognosis in prostate cancer, many of the published studies are confusing with varying cut-off points used to define levels of staining (Fisher et al., 2013). This same research group also published promising results to support the use of loss of PTEN as an immunohistochemical marker of poor prognosis in prostate cancer. Again a large cohort of men were sampled (675 patients) with prostate cancer death used as the end-point of long-term follow-up. They found that loss of PTEN staining in prostate cancer cores was a significant predicator of prostate cancer death and that this corresponded to Ki-67 staining. However, although PTEN was shown to be a useful prognostic indicator in univariate analysis it was not additionally informative when other markers e.g. Gleason score and PSA predicted poor prognosis (Cuzick et al., 2013).

An important step of the studies presented in this chapter was to make the progression from measuring gene expression changes to protein expression changes using immunofluorescence/immunohistochemistry. It is understood that various modifications in the production processes of proteins in cells can mean that mRNA levels do not always correlate to protein levels. This can occur at the stage of translation or during post-translational modification, in which processes such as the addition of functional groups or the trafficking of proteins to their active cellular domains can be distorted.

The studies presented in this chapter will test the identified gene expression profile for dormancy in PC3-NW1 populations against those expressed in dormant populations from other prostate cancer cell lines to define a consensus set of dormancy markers. The studies will also evaluate the presence of proteins encoded by dormancy specific up-regulated genes in prostate cancer cell populations. Finally, the most consistent marker of dormancy will be assessed in prostate cancer specimens from patients and the frequency/intensity of cellular staining related to pathology and disease status at the time of biopsy.

6.2 Chapter Aims, Hypothesis and Objectives

6.2.1 Aims

The aim of this study was to identify common markers of dormancy that are differentially expressed at the gene level and present at the protein level in the dormant sub-population of all three prostate cancer cell lines previously utilised; PC-3NW1, LNCaP and C42B4.

A further aim is to determine if a marker can be utilised to identify dormant cells in primary prostate cancer patient samples and whether their presence is linked to the occurrence of metastases. To address these aims the following hypotheses will be tested.

6.2.2 Hypothesis

1. Gene expression markers of dormancy in the PC-3NW1 cell line are expressed in the dormant sub-population in LNCaP and C42B4 cell lines.
2. The differential production of these markers is present at the protein level.
3. High positive staining for a marker correlates with other prognostic indicators e.g. Gleason grade
4. High positive staining for a marker predicts the occurrence of metastases in patient samples.

6.2.3 Objectives

To test the above hypotheses the following objectives will determine whether:

1. The dormant cell sub-population in the LNCaP and C42B4 cell lines differentially express the same dormancy markers as the PC-3NW1 cell line using a low density array (LDA) card quantitative RT-PCR approach.
2. Key markers of dormancy at the RNA level are differentially present in the dormant sub-population of these cell lines at protein level using immunofluorescence.

3. The presence of a marker of dormancy correlates with Gleason grade, Gleason score and patient age.
4. Whether high positive staining for a marker is associated with progression when present in patient samples.

6.3 Results

6.3.1 LDA card 2 analysis of the dormant cell sub-population in the LNCaP cell line

To determine whether the dormant cell sub-population identified in the LNCaP cell line in Chapter 3 differentially expressed the same markers of dormancy as the PC-3NW1 cell line, LDA card 2 was repeated with RNA from LNCaP. As described in Chapter 5 for the PC-3NW1 cell line, LNCaP cells were stained with DiD and cultured for 14 days. These cells were then sorted by FACs Aria to isolate the DiD retaining cell sub-population and the DiD negative, rapidly dividing cells. RNA was separately extracted and after reverse transcription, cDNA was loaded into the LDA card 2 to compare gene expression differences in the DiD positive dormant (denoted as LNCaP+ on the graph) vs. rapidly diving populations (LNCap-). Each assay was run in replicate and 3 biological repeats (3 separate LDA cards) were performed. The graph shows delta Ct values of each assay (gene), which is the average Ct value of all repeats minus the Ct value of the housekeeper GAPDH. Bars above the perforated 'UD' line were undetected at this sensitivity level.

There was a significant up-regulation in the gene expression of CXCR4 in the dormant cell sub-population in LNCaP cell line (Unpaired T-test, P= 0.007) similar to the increase in expression seen in the PC-3NW1 dormant cells. Follistatin (FST) was also significantly up regulated in the LNCaP dormant cells (P=0.002) and although the trend was the same in PC-3NW1 the up regulation in these dormant cells was not significant (P=0.069) by LDA card 2 analysis. However, vitronectin (VTN) was significantly up regulated in the LNCaP dormant cells (P=0.006) and in the PC-3NW1 dormant cells (P=0.043). Unlike in the PC-3NW1 line MMP3, CD34, CXCL1, DKK1 SOSTDC1 and TNC were not significantly altered in the LNCaP dormant sub-population (**Figure 6.1**).

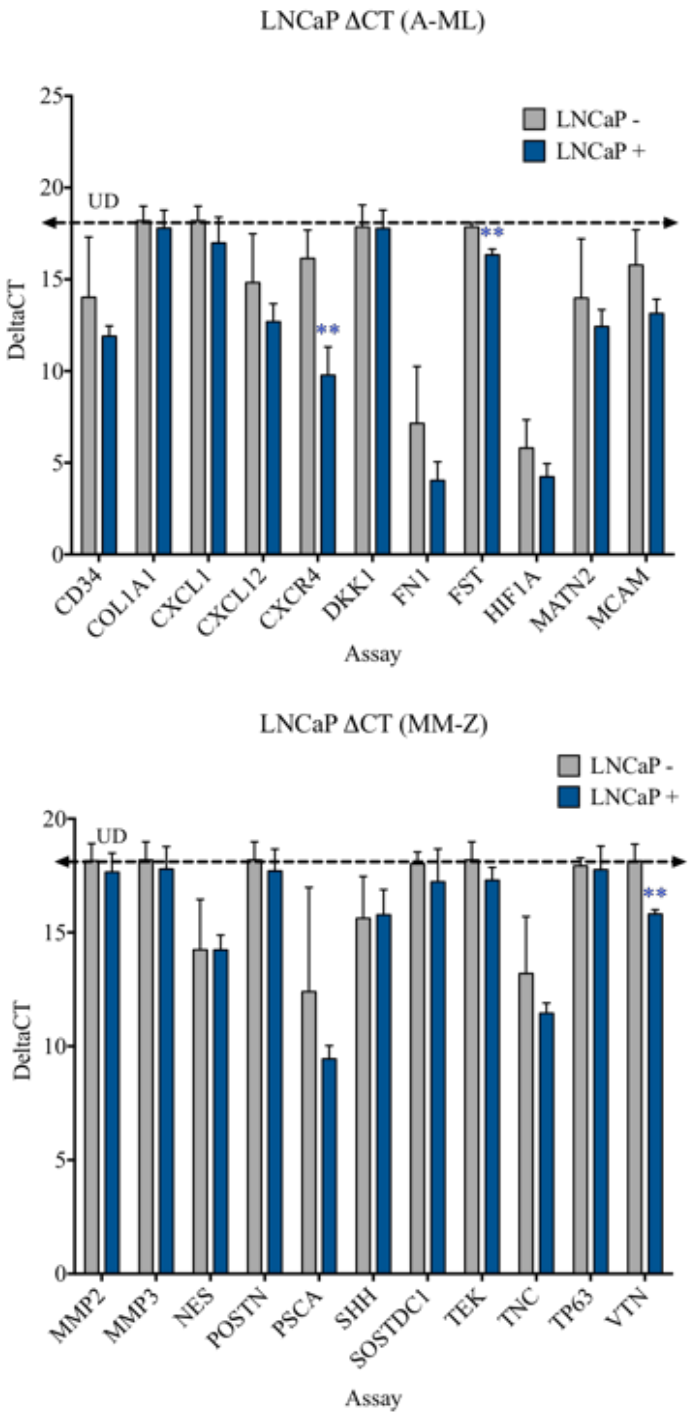

Figure 6.1 CXCR4, Follistatin and Vitronectin were significantly up regulated in the LNCaP dormant cell sub-population

Gene expression analysis of dormant, DiD retaining LNCaP (LNCaP+) cells compared to non-dormant, DiD negative (LNCaP-) cells assessed by low density array (LDA2) showed that CXCR4 and Follistatin (FST) were significantly up regulated in the LNCaP dormant cells (LNCaP+) by Unpaired T-test (P= 0.007 and P=0.002 respectively) compared to rapidly dividing cells (LNCaP-). Vitronectin (VTN) was also significantly up regulated in the LNCaP dormant cells (P=0.006). The graph represents three biological repeats; error bars represent standard deviation. Delta CT values relative to GAPDH are presented so that lower values indicate higher levels of gene expression. Top panel shows alphabetical list of genes A-ML and lower, genes MM-Z.

6.3.2 LDA card 2 analysis of the dormant cell sub-population in the C42B4 cell line

cDNA prepared from the dormant and rapidly dividing populations in the C42B4 cell line was also compared by LDA card 2 analysis. There was a significant up-regulation in the gene expression level of CXCR4 in the dormant cell sub-population in the C42B4 cell line (C42B4+) compared to the DiD negative rapidly dividing cells (C42B4-) (Unpaired T-test, P=<0.001). Unlike the LNCaP or PC-3NW1 cell lines no other significant up or down regulations in gene expression was detected in the dormant cell sub-population in C42B4. Although not significant, increases in the expression of DKK1 (P=0.0064), Follistatin (FST) (P=0.057), Tenascin (TNC) (P=0.079) and Vitronectin (VTN) (P=0.068) were detected in the C42B4 dormant sub-population. This follows the same trend as that seen in the PC-3NW1 cell line (**Figure 6.2**). The graph shows delta Ct values of each assay, which was normalised, to the housekeeper GAPDH.

Statistical analysis to compare the gene expression levels of the LNCaP dormant cell sub-population to the PC-3NW1 dormant cell sub-population, found that by LDA card 2 analysis these cell types were significantly different by two-way ANOVA (P=0.0069). This suggests that although these sub-populations share phenotypic dormancy the gene expression levels between them are not alike. However, the dormant cell sub-population in the C42B4 was not significantly different from the PC-3NW1 dormant cell sub-population by two-way ANOVA (P=0.446) and, interestingly, the C42B4 and LNCaP dormant cell sub-populations were not significantly different from each other by two-way ANOVA (P=0.135).

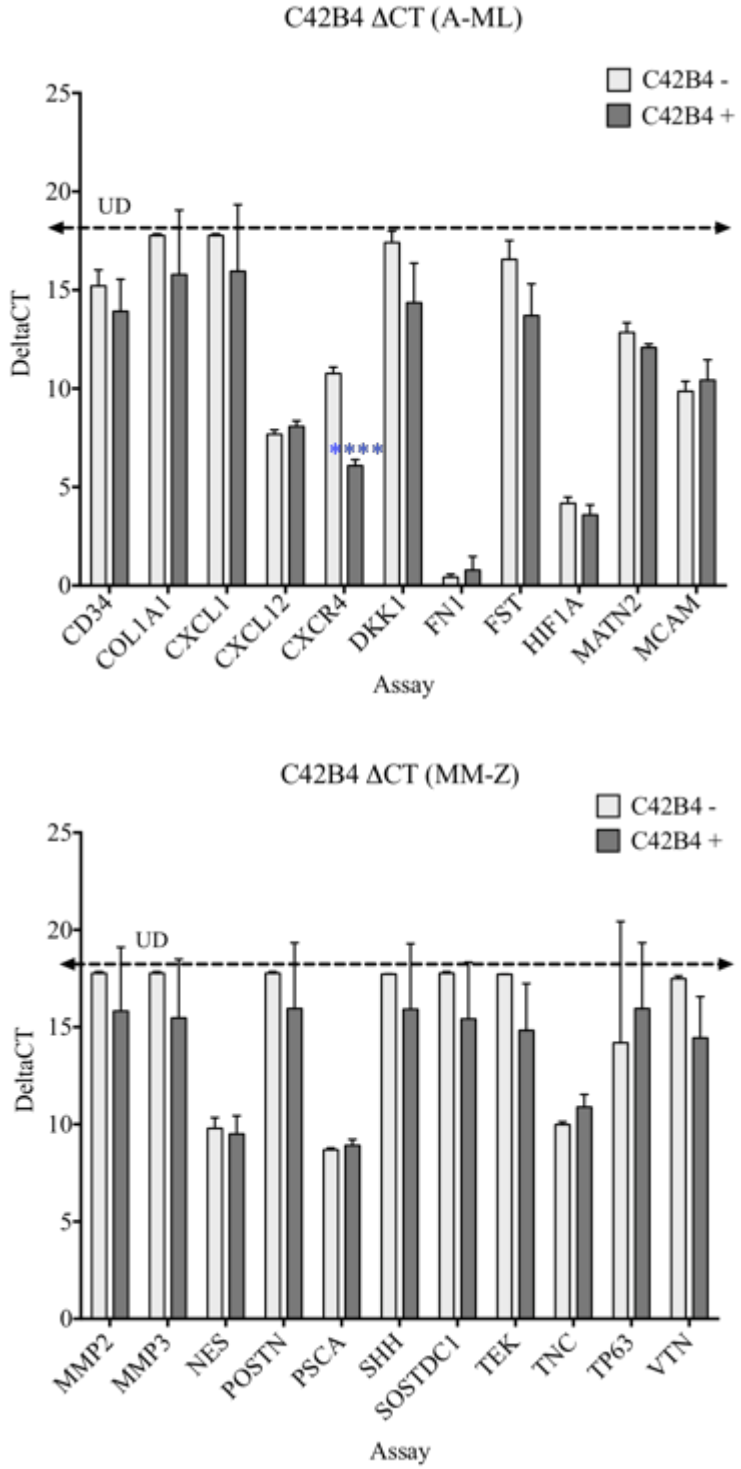

Figure 6.2 CXCR4 was significantly up-regulated in the C42B4 dormant cell sub-population

Gene expression analysis of dormant, DiD retaining C42B4 (C42B4+) cells compared to non-dormant, DiD negative (C42B4-) cells assessed by low density array (LDA2) showed that CXCR4 was significantly up regulated in the C42B4 dormant cells by Unpaired T-test (P=<0.001) compared to rapidly dividing cells. The graph represents three biological repeats; error bars represent standard deviation. Delta CT values relative to GAPDH are presented so that lower values indicate higher levels of gene expression. Top panel shows alphabetical list of genes A-ML and lower, genes MM-Z.

As a result of these experiments, CXCR4, DKK1, FST and MMP3 were selected to investigate at the protein level by immunofluorescence as possible markers of dormancy. CXCR4 was the most attractive candidate as it was significantly up regulated at the gene level in the dormant cell sub-population of all three cell lines. DKK1, was significantly up regulated in the PC-3NW1 cell line and was increased in the C42B4 cell line, although this did not reach significance. The gene expression level of FST was significantly increased in the dormant cell sub-population of the LNCaP cell line and significantly up regulated in the dormant cells in the PC-3NW1 cell line by LDA card 1 but not LDA card 2 analysis. MMP3 was significantly up-regulated only in the PC-3NW1 cell line but the fold change ($2^{\Delta\Delta Ct}$) increase was the highest of all assays, 45.29 fold higher than in the rapidly dividing cells, which made it an attractive candidate for study. As CXCR4 was significantly up regulated in all three cell lines, dual staining using the CXCR4 antibody and either the DKK1, FST or MMP3 antibody was performed in each experiment.

6.3.3 Antibody optimisation for immunofluorescence

Monoclonal Anti-Human CXCR4-Phycoerythrin conjugated antibody was purchased from R&D systems. Phycoerythrin (PE) is a red fluorescent protein that is excited at 480/565 nm and emits at 578 nm. This allows the excitation of the PE conjugated CXCR4 protein to be visualised with minimal cross over into the DiD channel (excitation 644 nm, emission 665 nm) allowing each to be visualised separately and also merged. Mouse monoclonal antibodies against Human DKK1, MMP3 and Follistatin were purchased from Abcam. As no directly conjugated anti-human products were available each primary was matched with the AlexaFluor® 488 Goat Anti-Mouse IgG secondary antibody from Abcam. AlexaFluor® 488 (excitation 499, emission 519nm) is distinct from both the DiD and PE channels allowing all three fluorescent tags to be detected in a single image. Fluorescence SpectraViewer from life technologies was used to select fluorophores with the desired wavelength. An image is shown in **Figure 6.3**. An IgG isotype control was done for each antibody and the optimum concentration was determined using a positive control.

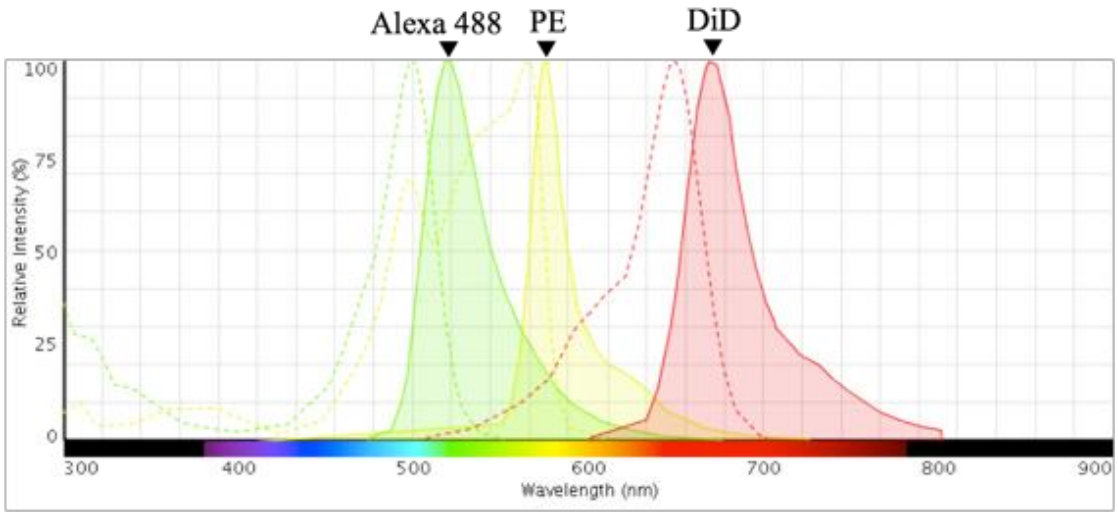

Figure 6.3 Excitation/emission profiles and of different fluorescently tagged antibodies
The two antibodies AlexaFluor 488 and PE are distinct in their excitation (perforated peak) and emission peaks to allow visualisation by fluorescent microscope together and alongside DiD.

6.3.3.1 CXCR4 optimisation

The use of the Anti-Human CXCR4-Phycoerythrin antibody (purchased from R&D systems) has previously been published to show a high level of protein presence in the LNCaP cell line. Growing stocks of LNCaP were used to determine the appropriate antibody concentration to use in subsequent experiments. $1x10^5$ LNCaP cells (without DiD staining) were prepared and cytospun onto slides as described in Methods 2.7.1. Cytospinning allows the fixation of a high density of cells to be adhered to a microscope slide after being directly removed from culture. The cytospin generates a cell "spot" that can be treated much in the same way as a tissue core section without the need for de-waxing and antigen retrieval. A 1:100, 1: 50 and 1:20 dilution of both the antibody and matched isotype control (also conjugated to Phycoerythrin) were tested following Methods 2.7.2. A 1: 50 dilution was determined as the optimum, which gave a bright uniform stain with minimal signal using the isotype (**Figure 6.4**).

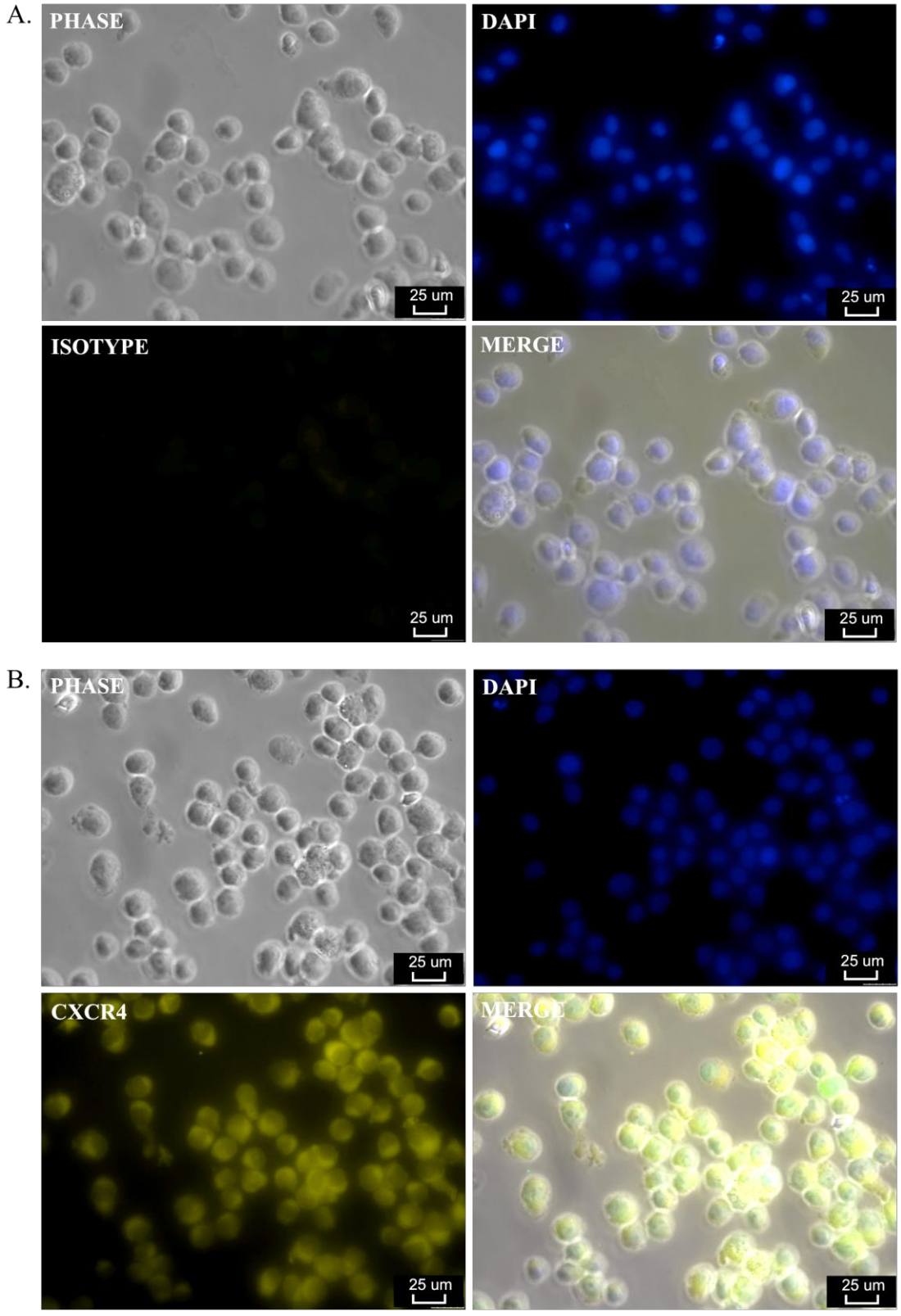

Figure 6.4 Immunofluorescent staining with CXCR4 antibody (showing the optimum antibody dilution, using the positive control: LNCaP)
A. $1x10^5$ LNCaP cells were treated with a 1:50 dilution of a PE conjugated isotype control. **B.** $1x10^5$ LNCaP cells were treated with a 1:50 dilution of a PE conjugated Anti-CXCR4 antibody (yellow).

6.3.3.2 DKK1 optimisation

The MCF-7 human breast cancer cell line was used as a positive control to determine the optimum concentration of the mouse monoclonal Anti-DKK1 antibody. MCF-7 cells show a high degree of DKK1 staining when using this antibody as demonstrated on the Abcam data sheet online. Following the protocol outlined in Methods 2.7.1 and 2.7.2, $1x10^5$ MCF-7 cells were cytospun onto superfrost slides and two different concentrations of primary antibody were tested (1:200, 1:100) in combination with two different concentrations of the matched secondary Goat Anti-Mouse IgG H&L (Alexa Fluor® 488) antibody (1:200, 1:100).

The optimum combination was determined as a 1:200 dilution of the primary Anti-DKK1 antibody with a 1:200 dilution of the secondary. This allowed for a bright uniform stain with minimal isotype staining (**Figure 6.5**).

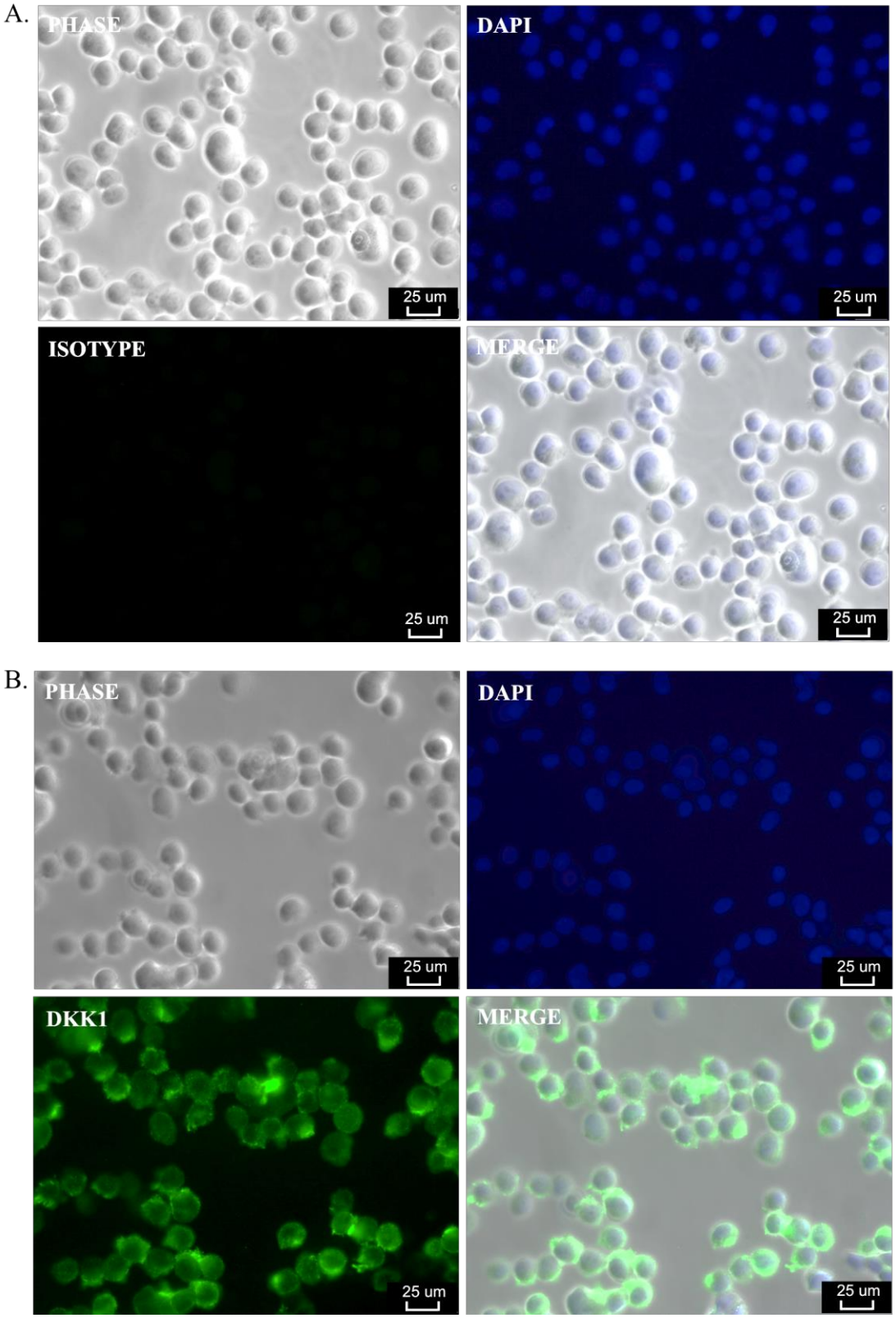

Figure 6.5 Immunofluorescent staining with DKK1 antibody (showing the optimum antibody dilutions, using the positive control: MCF-7)

A. 1x10^5 MCF-7 cells were treated with a 1:200 dilution of isotype control with a 1:200 dilution of Alexa Fluor® 488 conjugated secondary. **B.** 1x10^5 MCF-7 cells were treated with a 1:200 dilution of Anti-DKK1 antibody with a 1:200 dilution of Alexa Fluor® 488 conjugated secondary (green).

6.3.3.3 MMP3 optimisation

Mouse monoclonal Anti-MMP3 antibody was purchased from Abcam and optimised using HeLa cells as a positive control, as recommended by Abcam. Following the protocol in Methods 2.7.2, a 1:200 and 1:100 dilution of the Anti-MMP3 primary was tested in combination with a 1:200 and 1:100 dilution of the Goat Anti-Mouse IgG H&L (Alexa Fluor® 488) antibody.

The optimum combination was determined as a 1:100 concentration of the primary Anti-MMP3 antibody with a 1:200 dilution of the secondary. This showed a bright uniform stain with minimal isotype signal (**Figure 6.6**).

6.3.3.4 Follistatin optimisation

A mouse monoclonal Anti-FST antibody was purchased from Abcam and optimised using HeLa cells as a positive control, as recommended by Abcam. A 1:200 and 1:100 dilution of the Anti-FST primary was tested in combination with a 1:200 and 1:100 dilution of the Goat Anti-Mouse IgG H&L (Alexa Fluor® 488) antibody following the protocol in Methods 2.7.1.

The optimum combination was determined as a 1:100 concentration of the primary Anti-FST antibody with a 1:200 dilution of the secondary. This showed a bright uniform stain with minimal isotype background signal (**Figure 6.7**).

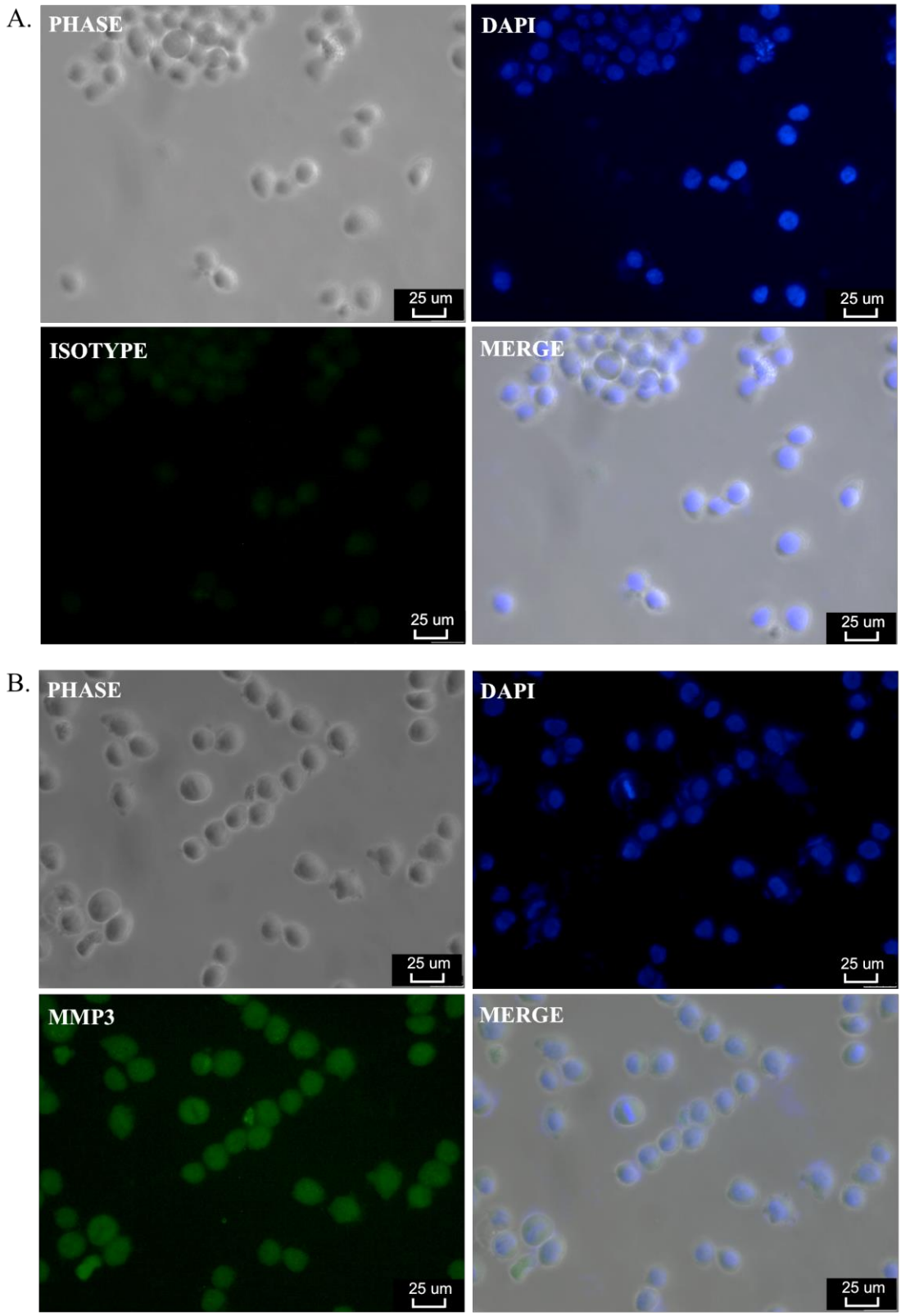

Figure 6.6 Immunofluorescent staining with MMP3 antibody (showing the optimum antibody dilutions, using the positive control: HeLa cells)

A. $1x10^5$ HeLa cells were treated with a 1:100 dilution of isotype control with a 1:200 dilution of Alexa Fluor® 488 conjugated secondary. **B.** $1x10^5$ HeLa cells were treated with a 1:100 dilution of Anti-MMP3 antibody with a 1:200 dilution of Alexa Fluor® 488 conjugated secondary (green).

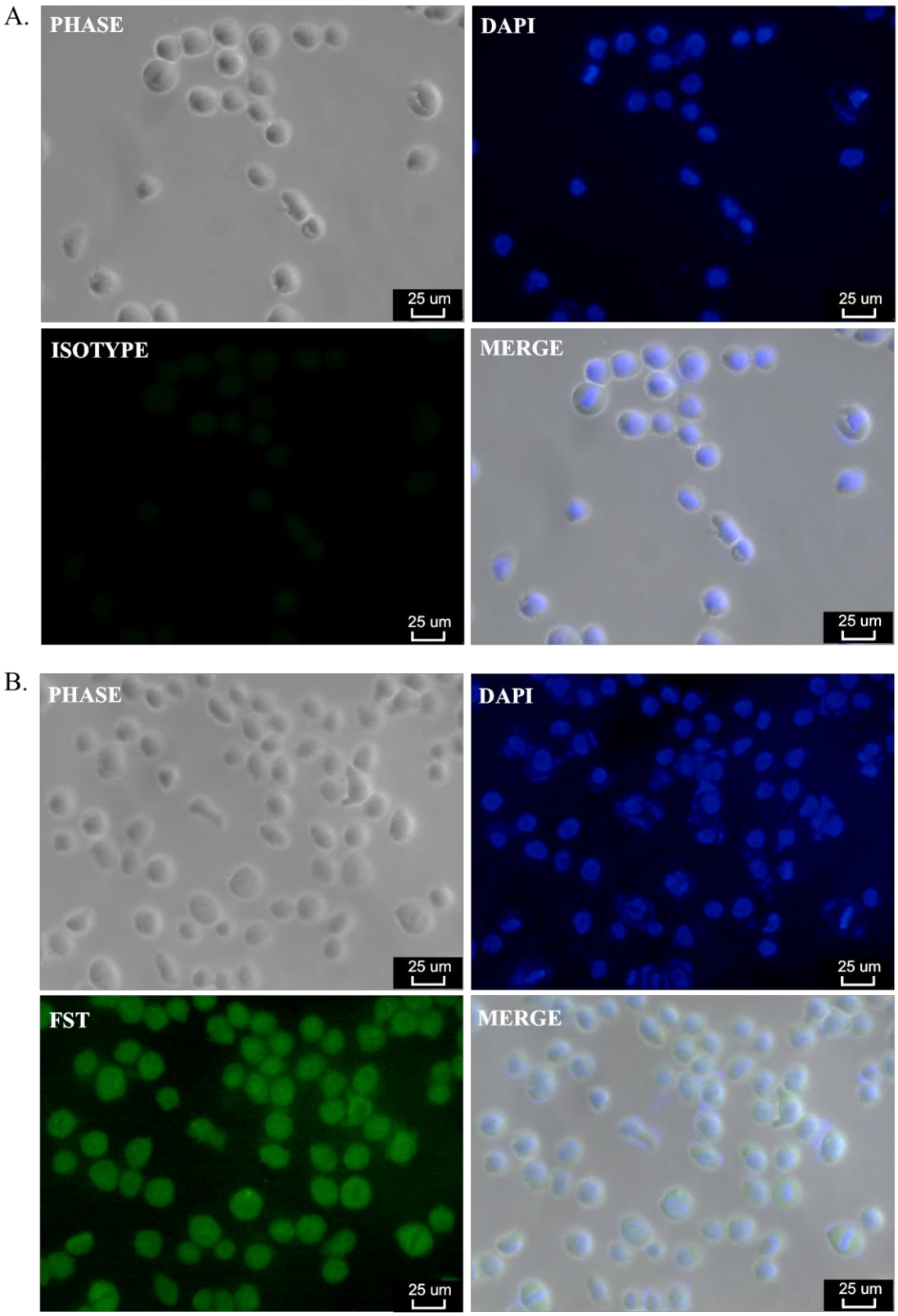

Figure 6.7 Immunofluorescent staining with FST antibody (showing the optimum antibody dilutions, using the positive control: HeLa cells)

A. $1x10^5$ HeLa cells were treated with a 1:100 dilution of isotype control with a 1:200 dilution of Alexa Fluor® 488 conjugated secondary. **B.** $1x10^5$ HeLa cells were treated with a 1:100 dilution of Anti-FST antibody with a 1:200 dilution of Alexa Fluor® 488 conjugated secondary (green).

6.3.4 CXCR4 protein levels were significantly up regulated in the dormant cell sub-population in all three cell lines

The level of CXCR4 protein presence was significantly up regulated in the dormant cell sub-population (DiD+) in all three cell lines. After DiD staining PC-3NW1 cells, LNCaP and C42B4 cells were cultured for 14 days. $1x10^6$ cells were harvested at this time point and prepared for cytospinning (full protocol Methods 2.7.1 and 2.7.2). After fixing in formalin and washing in PBS $1x10^5$ cells were cytospun onto superfrost slides. The slides were then permeabilised and dual stained for either CXCR4 and DKK1, CXCR4 and MMP3 or CXCR4 and FST. This was to test the hypothesis that multiple markers of dormancy (as shown by LDA card) could identify dormant cells by immunofluorescence. Three slides per cell line were prepared in this way so that a no treatment control slide, an isotype antibody treated control slide and a specific antibody, antibody treated slide could be generated for each biological repeat.

25 images were taken using the Leica AF6000 time lapse microscope per slide and the antibody staining intensity was evaluated by imageJ. As the Leica AF600 allows imaging using multiple channels the far red (DID) channel could be imaged in combination with both the red (Phycoerythrin conjugated CXCR4) channel and the green (Alexa Fluor® 488 secondary antibody to DKK1, MMP3 and FST) channel. Using the tile scan function on the Leica, 25 images could be captured from a defined region in the central quadrant of the cell "spot" using a fully automated system which reduced observer bias during image capture. These images were than analysed in ImageJ which gave a score of the antibody intensity per cell which was then correlated to the presence or absence of DiD staining. In this way the average antibody intensity of these proteins could be compared between the DiD+ dormant cells and the DiD- rapidly dividing cells.

When considered on its own, the level of CXCR4 (as measured by Mean antibody intensity per cell, Y-axis) was significantly higher in the dormant (DID+) sub-population compared to rapidly dividing (DID-) cells for all three cell lines tested. This is shown in **Part A**, **Figure 6.8**. The graph represents three biological repeats (error bars show standard deviation), each repeat took the average of three biological replicates which consisted of the CXCR4 with DKK1, CXCR4 with MMP3 and CXCR4 with

FST. CXCR4 presence when considered on its own is shown on the graph. The mean intensity of CXCR4 antibody staining was significantly higher by Paired T-test in the DiD+ dormant cells in the PC-3NW1 cell line compared to the DiD- rapidly dividing cells (P=0.011). CXCR4 staining intensity was also significantly higher in the dormant sub-population (DiD+) in both the LNCaP and C42B4 cell lines (P=0.017, P=0.006 respectively). This result was in agreement with the significant up regulation in CXCR4 expression in the dormant cell sub-population of all three cell lines by LDA 2 card analysis. A representative image of CXCR4 (yellow) presence in combination with the DiD stain (red) in the PC-3NW1 cell line is in shown in **Part B, Figure 6.8.**

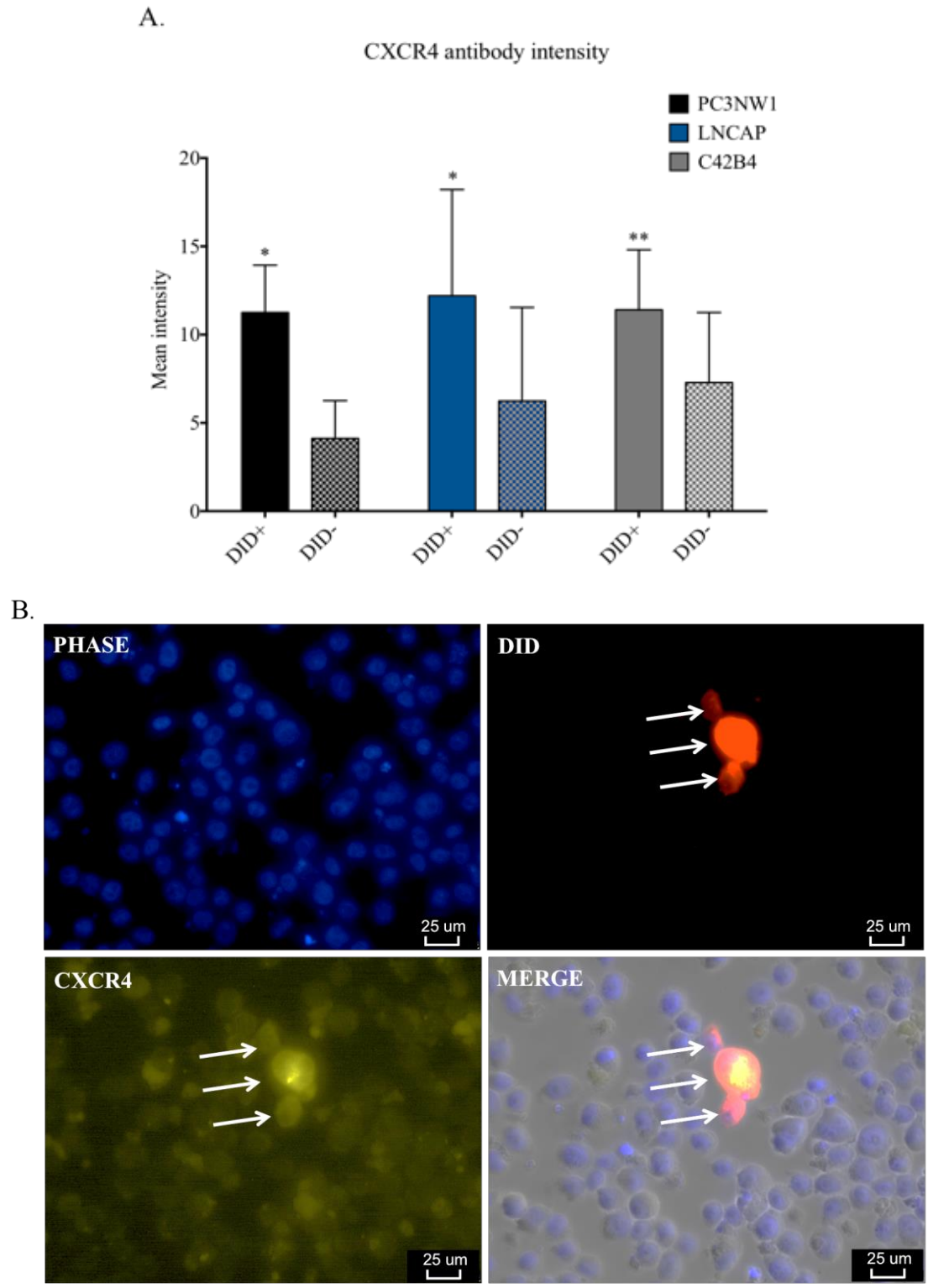

Figure 6.8 CXCR4 protein was significantly up regulated in the dormant compared to non-dormant cells

A. The presence of CXCR4 as measured by antibody staining intensity per cell (Y-axis, Mean intensity) was significantly higher in the dormant (DiD+) sub-population of all three cell lines compared to rapidly dividing cells (DiD-) by Paired T-test (PC-3NW1 P=0.011, LNCaP P=0.017, C42B4 P=0.006). N=3 repeats. **B.** A representative image of the PC-3NW1 cell line shows DiD positive cells at day 14 (white arrows) have a higher intensity of CXCR4 staining (yellow) than the DiD negative cells that surround them.

6.3.5 There were no significant differences in the level of DKK1 protein in the dormant vs non-dormant cell sub-populations isolated from each cell line.

When scored in combination with CXCR4 intensity there was no significant up-regulation in DKK1 present in the dormant (DiD+) cell sub-populations in the LNCaP or C42B4 cell lines **Part A, Figure 6.9**. This could be expected as no significant up regulation in DKK1 gene expression was detected by LDA card 2 analysis in these cell lines.

However, DKK1 was significantly up regulated in dormant cells at the gene expression level by LDA card 2 analysis in the PC-3NW1 cell line but no significant difference was detected at the protein level by immunofluorescence. A representative image of DKK1 staining (green) in the PC-3NW1 cell line shown in combination with CXCR4 (yellow) and DiD staining (red) is shown in **Part B, Figure 6.9.** The graph represents the mean antibody staining (Mean intensity, Y-axis) of the DKK1 antibody in three biological repeats; error bars show standard deviation.

6.3.6 There were no significant differences in the level of MMP3 protein in the dormant vs non-dormant cell sub-populations isolated from each cell line

In all three cell lines tested there was no significant up regulation in MMP3 using the anti-MMP antibody in the dormant cell sub-population (DiD+) compared to rapidly dividing cells (DiD-) **Part A, Figure 6.10**. The graph represents three biological repeats; error bars show standard deviation. This is despite the observation that MMP3 was significantly up regulated in the dormant cell sub-population of the PC-3NW1 cell line by LDA card 2 analysis and has a very high fold change when compared to rapidly dividing cells (>40 times). A representative image of MMP3 staining (green) in the C42B4 cell line shown in combination with CXCR4 (yellow) and DiD staining (red) is shown in **Part B, Figure 6.10.**

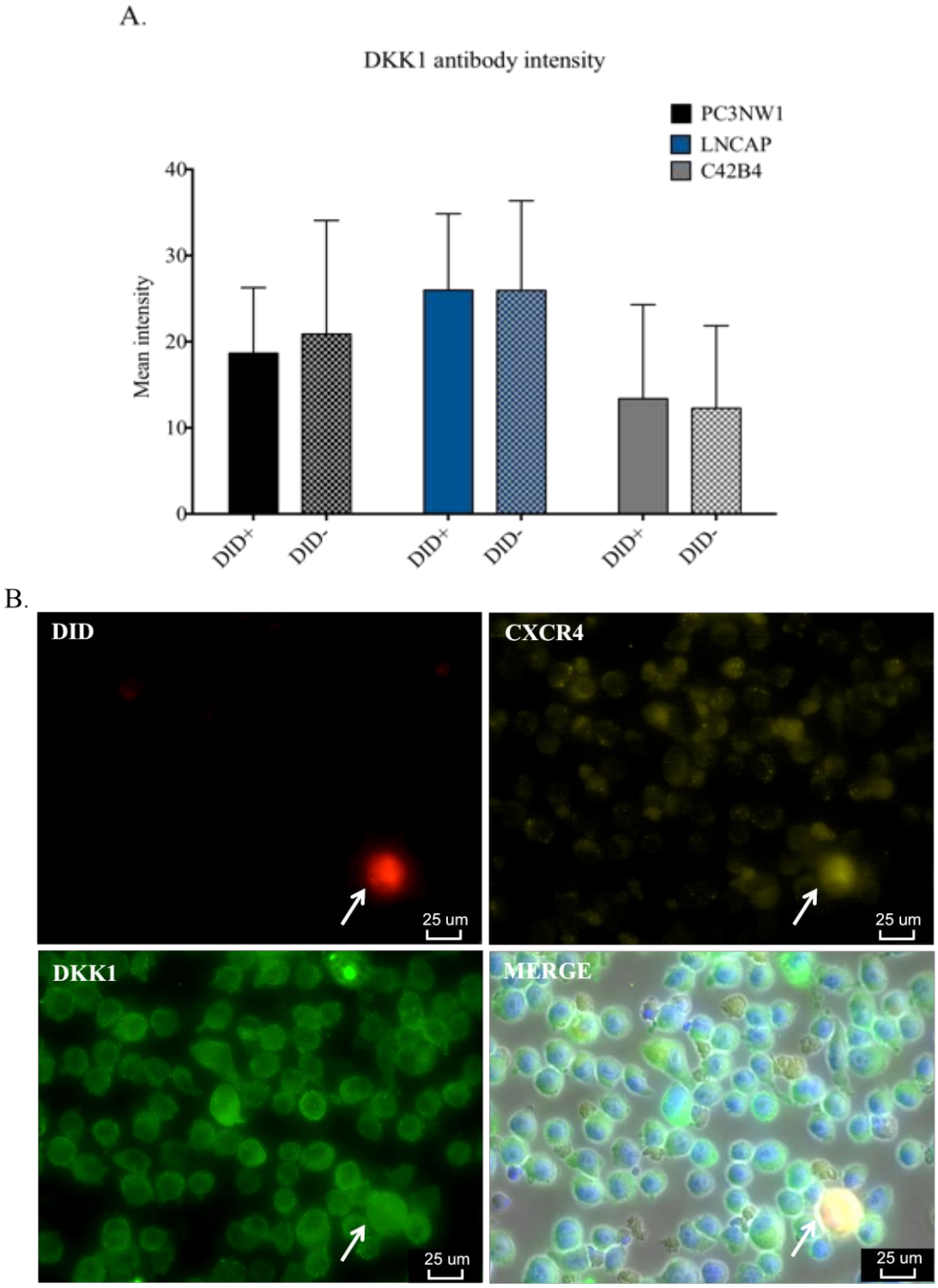

Figure 6.9 There was no significant difference in DKK1 protein in the dormant compared to non-dormant cells

A. The presence of DKK1 as measured by antibody staining intensity per cell (Y-axis, Mean intensity) was not significantly higher in the dormant (DiD+) sub-population of any cell line compared to rapidly dividing cells (DiD-). N=3 repeats. **B.** A representative image of the PC-3NW1 cell line shows a DiD positive cells at day 14 (white arrow) has a high intensity of CXCR4 staining (yellow) but not a higher intensity of DKK1 stain (green) compared to the DiD negative cells that surround it.

A.

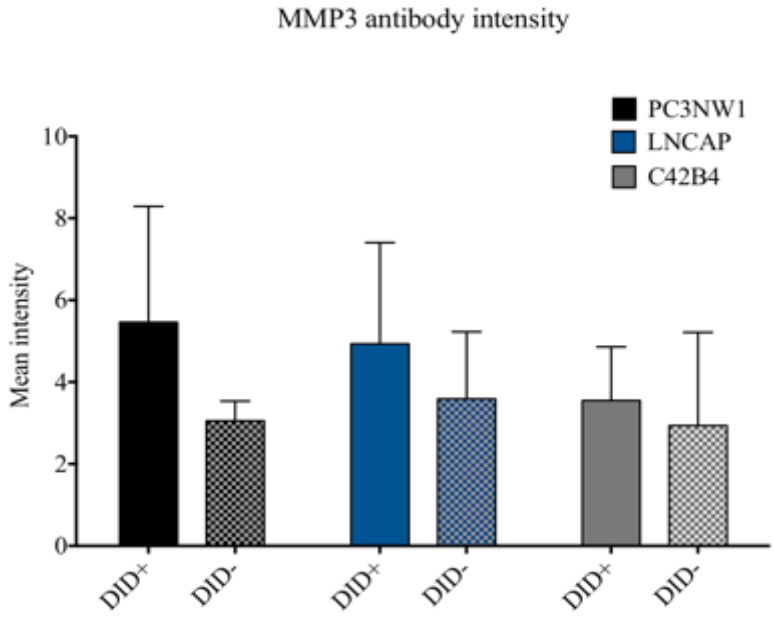

B.

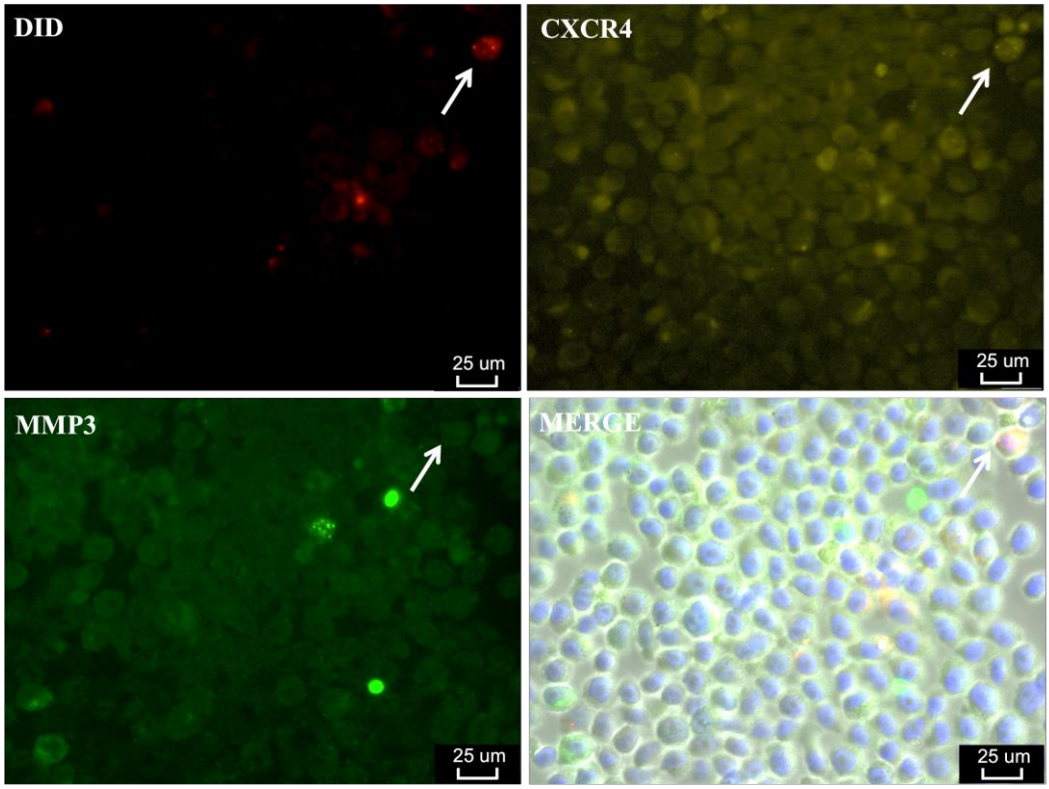

Figure 6.10 There was no significant difference in MMP3 protein in the dormant compared to non-dormant cells

A. The presence of MMP3 as measured by antibody staining intensity per cell (Y-axis, Mean intensity) was not significantly higher in the dormant (DiD+) sub-population of any cell line compared to rapidly dividing cells (DiD-). N= 3 repeats **B.** A representative image of the C42B4 cell line shows a DiD positive cells at day 14 (white arrow) which has a higher level of CXCR4 staining (yellow) than many DiD- cells, but a low level of MMP3 staining (green) which is comparable to the DiD negative cells that surround it .

6.3.7 There was a significant increase in FST protein in the dormant cells in the LNCaP cell line compared to non-dormant cells but not in dormant cells in the PC3NW1 or C42B4 cell lines compared to their respective non-dormant populations

By immunofluorescence, Follistatin (FST) was detected at a significantly higher level in the DiD positive dormant sub-population in the LNCaP cell line, by Paired T-test (P=0.018), but not in the PC-3NW1 or C42B4 cell lines. This is in agreement with the LDA card 2 results; FST was significantly up regulated at the gene expression level in the dormant compared to the non-dormant LNCaP sub-population but not the dormant PC-3NW1 or C42B4 cell lines compared to their respective non-dormant population. The graph represents the mean staining intensity (Mean intensity, Y-axis) of the FST antibody in three biological repeats; error bars show standard deviation (**Part A, Figure 6.11**). A representative image of FST staining (green) in the LNCaP cell line shown in combination with CXCR4 (yellow) and DiD staining (red) is shown in **Part B, Figure 6.11.** This result suggests that FST and CXCR4 together can be used to identify dormant cells but this is only applicable to the LNCaP cell line.

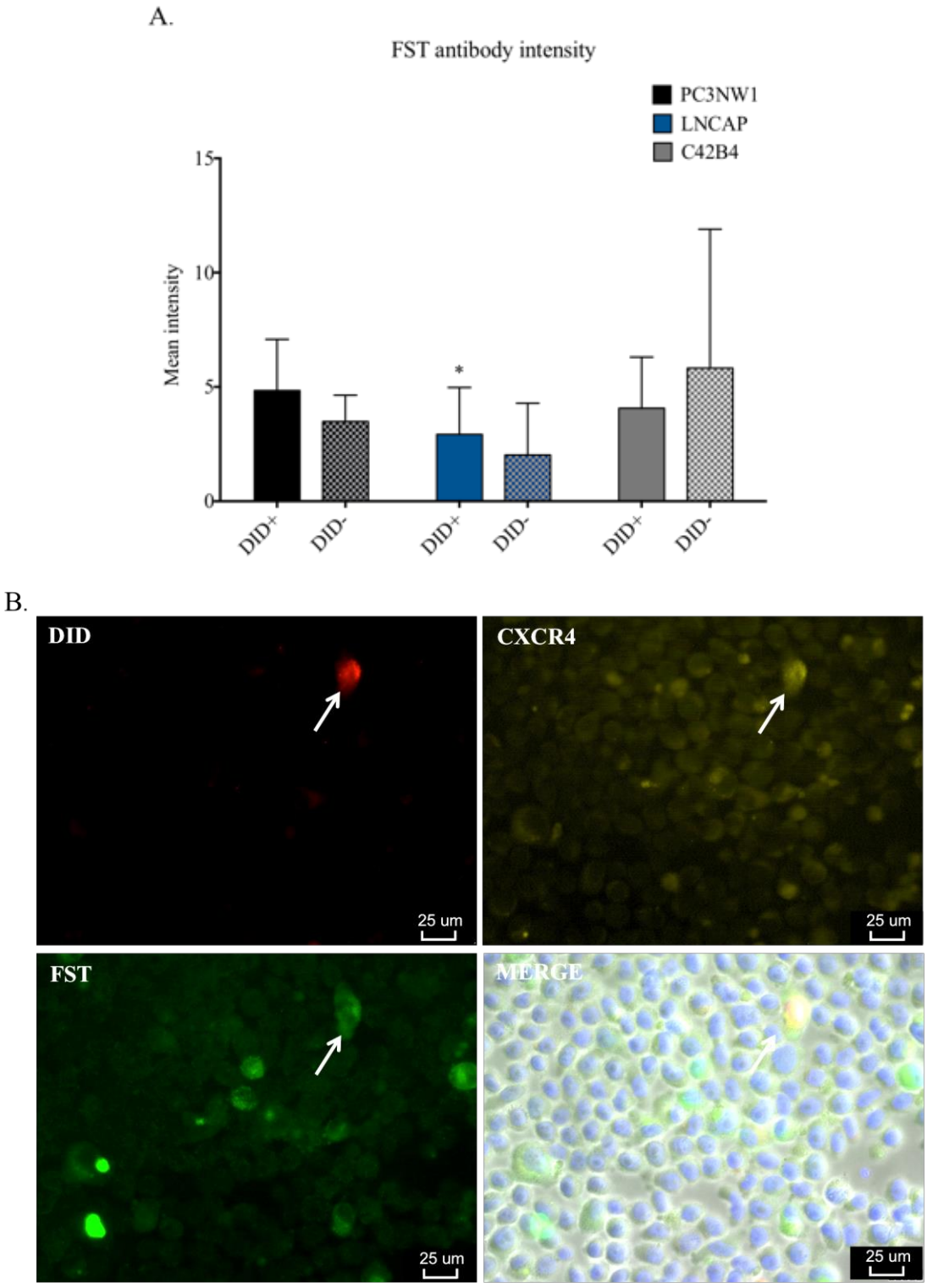

Figure 6.11 There was a significant increase in the level of Follistatin protein in the LNCaP dormant compared to the non-dormant cell sub-population

A. The presence of FST as measured by antibody staining intensity per cell (Y-axis, Mean intensity) was not significantly higher in the dormant (DiD+) sub-population of the PC-3NW1 or C42B4 cell lines compared to rapidly dividing cells (DiD-). However, FST was significantly increased in the dormant cell sub-population in the LNCaP cell line (Paired T-test, P=0.018) N= 3 repeats **B.** A representative image of the LNCaP cell line shows a DiD positive cell at day 14 (white arrow) has a high intensity of CXCR4 staining (yellow) and a high intensity of FST stain (green).

6.3.8 An assessment of CXCR4 presence in primary prostate cancer samples

CXCR4 was the only marker that was significantly higher in the dormant cell sub-population of all three cell lines. It was therefore decided that increases in CXCR4 protein were the most likely to be useful in identifying this sub-population in patient samples and potentially in predicting disease progression.

A primary prostate tissue microarray was purchased from US Biomax, Inc. The PR752 array consisted of 75 cores representing 75 patients with Prostate carcinoma and hyperplasia (64 cases of adenocarcinoma, 11 hyperplasia (BPH)), single core per case. The provided specification sheet included information about the Gleason grade, Gleason score and TNM stage of each core. It was therefore known which primary prostate samples were taken from patients with metastases. No follow up clinical information was available, therefore the information only showed which patients had developed metastases at the time of biopsy. It was therefore not possible to assess the use CXCR4 to predict the development of node or distant metastases but only to correlate the amount of CXCR4 staining to the presence of existing metastases. These experimenst were also designed to test the hypothesis that an increase in CXCR4 protein in a primary patient sample, as assessed by immunohistochemistry, predicted the presence of metastases in these patients and to evaluate whether this parameter was dependent/independent of Gleason scores.

The array slide was dewaxed, hydrated and stained following the protocol in Methods 2.7.4. For antibody optimization, a number of the recommended test slides from US Biomax, Inc (product code: T125b) were purchased and it was found that the optimum antibody concentration was 1:500 with a 1:200 dilution of the biotinylated secondary. This protocol had also previously been optimized by Jenny Down (now at the Garvan institute, Sydney, Australia) and published in Eaton et al. 2011. A Mouse monoclonal anti human CXCR4 (purchased from R&D) and matched Mouse IgG2A Isotype Control were used in each experiment. The isotype showed minimal to zero background staining.

After staining the array was scored by Dr. Colby Eaton and an independent and experienced pathologists (Professor Simon Cross) who were each blinded to the clinical

information provided with the array. Each core was given a percentage of CXCR4 staining; <10% was considered weak, 10-50% moderate, 50-90% strong and 100% very strong. A representative image of the scoring system is shown in **Figure 6.14**. Only two cores were excluded from the analysis as the histology could not be scored due to high background.

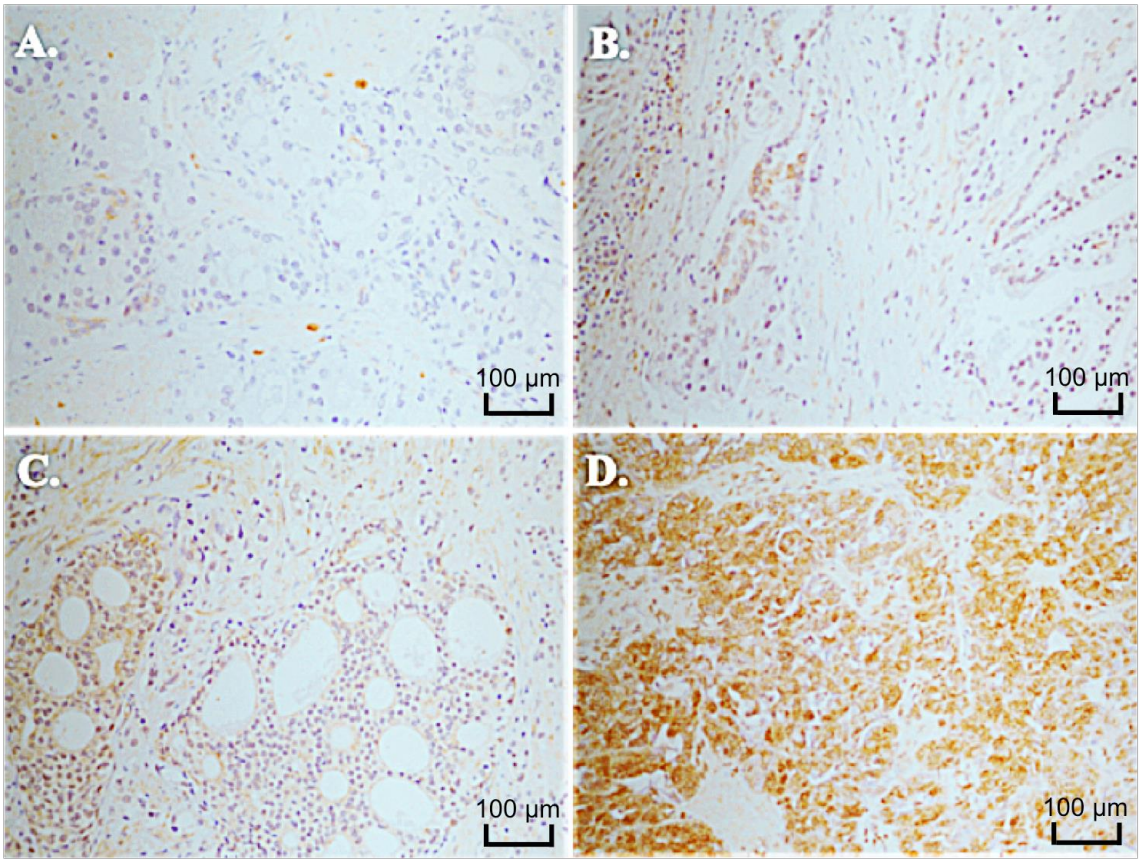

Figure 6.14 Immunohistochemistry for CXCR4 in human primary prostate cancer specimens: examples of scoring system
A. Weak <10%. B. Moderate 10-50%. C. Strong 50-90%. D. Very strong 100%.

The array showed that CXCR4 staining was significantly stronger in the 62 prostate cancer samples (adenocarcinomas) compared to the 11 BPH samples by Mann-Whitney non-parametric test (P=0.0003) (**Part A, Figure 6.15**). CXCR4 staining was also significantly stronger in higher Gleason grade tumours (Grades 3 and 4) compared to low Gleason grade tumours (Grade 2) (Mann-Whitney test P= 0.043 Grade 2 vs. Grade 3, P= 0.016 Grade 2 vs. Grade 4). Although Grade 5 tumours showed the same trend, the variation was much greater and this result was not significant (P=0.37) (**Part B, Figure 6.14**). CXCR4 staining also corresponded to Gleason score (the sum of the two most common cell grades in the sample). Only 24.0% of low Gleason score tumours (a

combined score of ≤ 6) had strong-very strong CXCR4 staining compared to 55.5% and 47.4% strong-very strong staining in intermediate (Gleason score 7) and high (8-10) Gleason score tumours, respectively. A lower age at diagnosis is often associated with poor prognosis and is often an indicator that patients should receive radical surgery. 66.6% of patients under the age of 50 had strong-very strong staining for CXCR4. This result was the same in the 50-60 age group, 66.6% strong-very strong staining and very slightly higher in the 61-70 age group, 69.23%. However, this reduced slightly to 50% strong-very strong staining in the ≥71 age group.

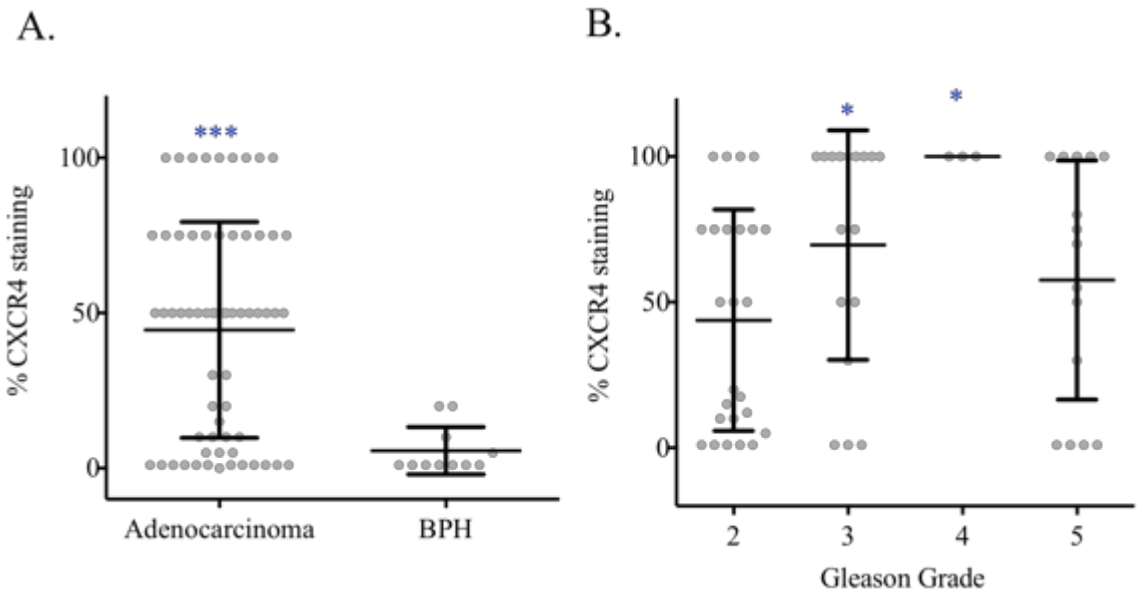

Figure 6.15 Positive CXCR4 staining was significantly stronger in higher grade tumours

A. Positive CXCR4 staining was significantly higher in prostate cancer samples (adenocarcinoma) than in Benign Prostatic hyperplasia (BPH) samples (Mann-Whitney test, P= 0.0003). **B.** Positive CXCR4 staining was significantly higher in Gleason grade 3 and 4 samples than in low grade (2) tumour samples (Mann-Whitney, P= 0.043 and P= 0.016 and respectively).

CXCR4 staining did not correspond to the presence of metastases at the time of biopsy. 57.69% of patients with metastases had strong-very strong CXCR4 staining compared to 63.0% strong-very strong staining in patients without metastases. However, strong-very strong CXCR4 staining was higher in patients with distant metastases (37.5%) compared to patients with node but no distant metastases (only 25% of these samples had strong-very strong staining). Overall, a strong positive CXCR4 staining did not

predict the presence of metastases better than Gleason score, as 47.5% of patients with a high Gleason score had metastases compared with only 38.4% of high CXCR4 patients with metastases. A representative image of these results is shown in **Figure 6.16** with the provided clinical information and the percentage of CXCR4 staining shown in **Table 6.1**.

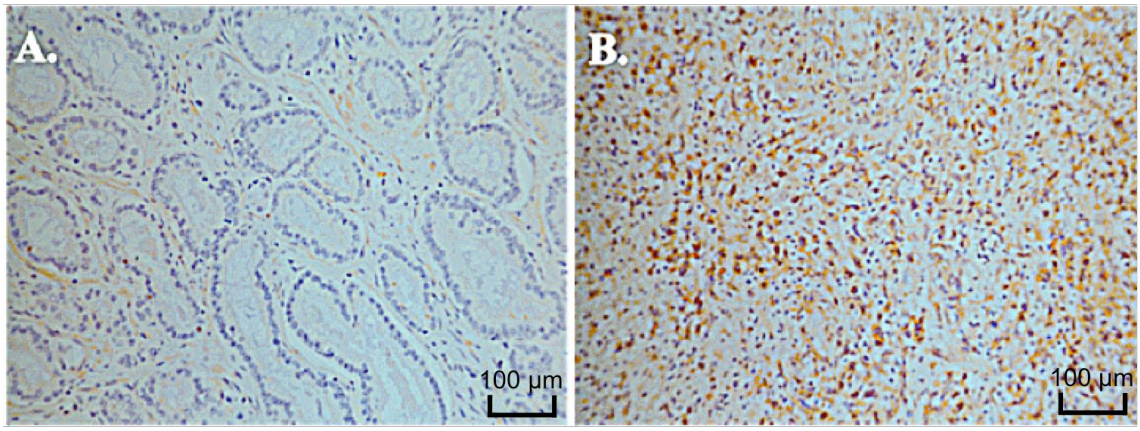

Figure 6.15 Immunohistochemistry for CXCR4 in human primary prostate cancer specimens: Example of Gleason grade vs CXCR4 staining

A. A low grade 2 Gleason grade tumour sample with weak CXCR4 staining indicated by the low amount of brown DAB stain. **B.** A high grade 4/5 Gleason grade tumour with strong CXCR4 staining indicated by the high amount of strong brown DAB stain.

Number	Gleason grade	Gleason Score	Total score	TNM	CXCR4 staining
1	2	2+4	6	T3aN0M0	weak
2	2	2+4	6	T4N1M1c	weak
3	2	2+2	4	T2N0M0	weak
4	2	3+4	7	T2N0M0	weak
5	3	3+4	7	T2aN0M0	weak
6	2	2+4	6	T3N1M1	weak
7	2	2+4	6	T2N0M0	moderate
8	2	2+4	6	T2N1M1b	weak
9	2	2+4	6	T2N0M0	weak
10	2	2+4	6	T2aN0M0	weak
11	Excluded	-	-	-	-
12	2	2+4	6	T4N1M1	strong
13	3	3+3	6	T2N0M0	weak
14	2	2+4	6	T2N0M0	strong
15	3	3+4	7	T2N0M0	very strong
16	2	2+4	6	T4N1M1c	moderate
17	3	2+5	7	T2N1M1c	strong
18	3	3+4	7	T3N1M1b	moderate
19	3	3+4	7	T2aN0M0	strong
20	2	2+4	6	T2N0M0	strong
21	3	2+5	7	T3N2M1	weak
22	2	2+4	6	T3N1M0	strong
23	3	2+5	7	T2N0M0	strong
24	3	2+5	7	T3N0M1	very strong
25	5	4+5	9	T3N1M0	strong
26	2	2+4	6	T2N0M0	strong
27	3	2+5	7	T3N2M1	weak
28	3	2+5	7	T3N2M1	very strong
29	2	2+4	6	T3N0M1b	weak
30	2	2+4	6	T2N0M0	weak
31	3	2+5	7	T3N0M1	weak
32	2	2+4	6	T2N0M0	strong
33	3	2+5	7	T3N0M0	very strong
34	3	2+5	7	T2N0M0	very strong
35	3	2+5	7	T2N0M0	very strong
36	2	2+4	6	T3N0M0	moderate
37	2	2+4	6	T3N0M0	very strong
38	2	2+4	6	T3N1M1b	strong
39	2	2+4	6	T3bN0M0	strong
40	2	2+4	6	T3N1M0	moderate

41	2	2+4	6	T2N0M0	strong
42	3	2+5	7	T3aN0M0	moderate
43	Excluded	-	-	-	-
44	5	5+5	10	T4N1M1	weak
45	5	5+5	10	T4N1M1c	weak
46	5	5+5	10	T2N0M0	strong
47	5	5+5	10	T4N1M1c	strong
48	5	5+5	10	T3N0M0	weak
49	5	5+5	10	T2N0M0	very strong
50	5	5+5	10	T2N0M0	strong
51	4	4+5	9	T2aN0M0	very strong
52	4	4+5	9	T2N0M0	strong
53	5	5+5	10	T2N0M0	strong
54	5	5+5	10	T2N0M0	moderate
55	2	2+4	6	T2N0M0	weak
56	5	4+5	9	T2N1M1	weak
57	3	2+5	7	T2N1M1c	very strong
58	4	4+4	8	T2N1M1b	strong
59	3	2+5	7	T4N0M1	moderate
60	2	2+4	6	T3N1M1b	strong
61	5	5+5	10	T3N1M0	weak
62	5	5+5	10	T3aN0M0	weak
63	5	5+5	10	T2N0M0	moderate
64	5	5+5	10	T2N0M1	strong
65	BPH	–		–	weak
66	BPH	–		–	weak
67	BPH	–		–	weak
68	BPH	–		–	weak
69	BPH	–		–	weak
70	BPH	–		–	weak
71	BPH	–		–	weak
72	BPH	–		–	weak
73	BPH	–		–	weak
74	BPH	–		–	weak
75	BPH	–		–	weak

Table 6.1 The summary clinical information and level of CXCR positive stain for each patient sample on the PR752 array.

6.4 Discussion

6.4.1 Markers of dormancy in multiple prostate cancer cell lines

Low density array (LDA) card 2 analysis revealed that the expression of CXCR4 was significantly increased in the dormant cell sub-population (DiD retaining cells at day 14) in both the LNCaP and C42B4 cell lines. This was in agreement to the increase seen in the PC-3NW1 cell line. CXCR4 is an alpha-chemokine receptor, which binds to the ligand stromal-derived-factor-1 (SDF-1 also called CXCL12). In addition to the increased expression of this receptor in dormant cells, CXCR4 was the only protein to have a significant increase in staining in the DiD+ sub-population in all three cell lines. It is widely accepted that an increase in CXCR4 increases the migratory potential of a cell towards its chemoattractant ligand CXCL12 (SDF-1) (Teicher and Fricker, 2010). CXCL12 is abundantly present in multiple locations in the body, including the lung, liver and bone marrow. Indeed, the presence of CXCR4 on HSC allows the trafficking of these cells to the HSC niche in the bone marrow. CXCR4-CXCL12 signalling via PIK3 and MAPK is hypothesised to increases cell migration as well as survival and proliferation (Teicher and Fricker, 2010). The presence of CXCR4 in prostate cancer, as well as its role in the disease particularly its link to metastasis, has been explored in many published *in vitro* and *in vivo* studies and there is multiple evidence that CXCR4/CXL12 signalling promotes metastasis in experimental models. Xing et al. (2008) demonstrated that prostate cancer cells had increased invasion through matrigel in response to the CXCL12 ligand, and that invasion was decreased following a down regulation of CXCR4 by siRNA (Xing et al., 2008). Sun et al (2005) provided evidence that the neutralisation of CXCR4 by targeted antibodies, reduced the size of skeletal tumours when PC-3 cells were injected directly into the tibia of NOD/SCID mice (Sun et al., 2005). Schiozawa et al. (2011) demonstrated that prostate cancer cells utilise CXCR4 in order to home to and establish 'footholds' in the bone marrow of xenograft mouse models. Although these studies have indicated that CXCR4 is present in prostate cancer cell lines and that its presence may confer a heightened metastatic ability, the results presented in this chapter present a novel hypothesis in which CXCR4 expression/presence is not uniform across the cell line and that a specific sub-population, characterised by dormancy, has a significant higher level of this protein. It is tempting to speculate that these cells, with elevated CXCR4, will have a greater

ability to home to the bone marrow and therefore have an increased ability to form skeletal tumours. Although experiments in our group have shown the increased metastatic ability of the dormant cell sub-population, further *in vivo* imaging studies would be required to assess whether DiD+ cells have a greater ability to arrive in the bone or whether their high tumourigenic ability is determined at another stage of the metastatic cascade.

Many molecules have been implicated in the molecular basis for cancer dormancy in the bone marrow, including growth-arrest specific 6 (GAS-6) (Shiozawa et al., 2010b). Although CXCR4 presents an attractive candidate as a driver of dormancy, the primary aim was to assess the value of this marker as a prognostic indicator. It was important to determine whether CXCR4 staining correlated to other prognostic indicators such as Gleason grade and Gleason score. A further aimwas to determine if an increase in CXCR4 staining in primary prostate cancer samples was an indicator of the presence of metastases by correlating the level of CXCR4 staining to the known TNM stage of the patients screened.

LDA card 2 analysis also showed that Follistatin (FST) and Vitronectin were both significantly increased in the LNCaP dormant cell sub-population compared to their rapidly dividing (DiD negative at day 14) counterparts. VTN is a marker of EMT as it is associated with mesenchymal/fibroblast-like cells. This increase was significant in the PC-3NW1 sub-population but not in the C42B4, however the trend was the same but the increase failed to reach significance (P= 0.093). FST is a glycosylated protein that binds to and neutralises members of the TGF-ß family including Activin. FST-Activin signalling is hypothesised to be involved in the normal development and homeostasis of the prostate gland. Therefore, aberrant expression of FST is linked to prostate cancer progression and poor prognosis (Sepporta et al., 2013). Indeed an increase in FST expression in the androgen responsive LNCaP cell line is linked to progression towards a more malignant androgen-insensitive phenotype. Vaarala et al. (2000) compared the gene expression differences by microarray of LNCaP cells to an engineered androgen insensitive variant (LNCaP-). The authors found that FST was significantly increased in the LNCaP- variant (Vaarala et al., 2000). It would therefore be of interest to assess the androgen receptor status of the DiD+ LNCaP cells to see if an increase in FST in my studies correlates to a switch to androgen insensitivity.

FST was also increased in the dormant cell sub-population, by LDA card 2 analysis, in both the C42B4 and PC-3NW1 cell lines however this did not reach significance (P=0.0578 and 0.0698 respectively). Interestingly, FST expression was on average higher in the androgen insensitive PC-3 and C42B4 cell lines than in the LNCaP cell line which may again suggest androgenic involvement in its expression.

Interestingly, an increase in FST was also detected at the protein level by immunofluorescence in the LNCaP DiD retaining cells alone. This suggests that in the androgen sensitive LNCaP cell line an increase in FST is associated with a more dormant, and perhaps more malignant, cell phenotype. Whether the dormant phenotype is androgen sensitive re: proliferation has yet to be tested.

No significant increase was detected in the presence of DKK1 protein in the dormant cell sub-population of any of the cell lines tested. Although, a difference in the LNCaP or C42B4 cell lines was not expected, it was predicted that DKK1 levels would be increased in the DiD+ cells in the PC-3NW1 cell line. DKK1 staining was detected at a very high intensity in this cell line so that subtle differences between the dormant and rapidly growing populations may not have been measurable.

Similarly, there was no significant difference in the presence of MMP3 in the dormant cell sub-population of any of the cell lines tested. Again, it was predicted that an increase in staining would only be observed in the PC-3NW1 DiD+ population. A non-significant increase in staining in the DiD+ vs. DiD- PC-3NW1 cells was observed and it may be that increasing the number of repeats would allow differences to reach significance.

In cases where increased expression of genes were identified using the LDA analyses but where protein levels were not altered in dormant vs. non-dormant comparisons, there could be several reasons for lack of correlation between RNA and protein production. Firstly, and as mentioned previously, the role of transcription and post-translational modifications are not to be underestimated which may account for the high variability. In a review by Vogel and Marcotte (2012), it is suggested that only around 40% of the variation in protein concentration can be explained by knowing mRNA

levels. This can also be attributed to the variation in protein half-life that can mean the degradation time of different proteins can vary between minutes and days (RNA has a more uniform rate of degradation between 2 and 7 hours) meaning that within an experiment the detectable protein levels may change (Vogel and Marcotte, 2012). Furthermore, the turnover rate of these proteins may be high and differences may not have been captured in the time frame of this experiment. Furthermore, the level of protein detection is reliant on the efficiency of the fluorescent microscope used to detect antibody fluorescence and also by the experimenter to set the exposure times and light intensity based on the controls. Perhaps a less subjective measure of protein levels would have been achieved by western blot but the low number of cells retained after FACs would be insufficient for protein extraction for this method. Another major issue of antibody based techniques is whether the proteins are cell surface or secreted, if the protein is cell surface i.e. retained by the cell correlations would be more likely. This is the case for the membrane bound CXCR4 protein. If the protein is secreted i.e. lost from the cell as is the case with MMP3, FST and DKK1, then correlation with gene expression could be lost since the protein is no longer there to be seen by IHC. This means that secreted markers are often less useful to apply to tissue sections as prognostic markers.

6.4.2 CXCR4 as a prognostic indicator in primary patient samples

The value of CXCR4 as a prognostic indicator in prostate cancer has previously been investigated by a number of groups. However, the published data to date has not assigned a definitive role for CXCR4 in predicting patient outcomes and there are many conflicting results. The first study to consider this interaction was published in 2004 by Mockizuki and colleagues which provide evidence that a higher rate of CXCR4 staining (following immunohistochemistry on 25 prostate cancer samples and 9 non-malignant prostate samples) was detected in patients with bony metastases compared to patients without bone metastases (Mochizuki et al., 2004). The authors concluded that high positive staining for CXCR4 was a better predictor of metastases than Gleason score. In a similar study, Jung et al. (2011), assessed CXCR4 in 57 prostate cancer patients and correlated staining to age, PSA (pre-treatment), Gleason score, Tumour stage, biochemical recurrence, local recurrence and distant metastases. They also found evidence that a high level of CXCR4 staining was associated with the presence of

distant metastases as well with local recurrence but none of the other parameters measured (Jung et al., 2011). In contrast to this result, Lu et al. (2013) published data to suggest that CXCR4 staining correlated only to tumour residue at the primary site and was not associated with metastases. This work was however, carried out on the smallest sample set (36 patients consisting of 8 normal, 28 prostate cancer samples) (Lu et al., 2013). Akashi et al. (2008) used 52 patient samples that all had evidence of bone metastases to measure the correlation between high CXCR4 staining and other clinical parameters. All 52 patients had metastatic prostate cancer and were receiving hormone therapy. The level of CXCR4 staining was assessed by immunohistochemstry on primary prostate biopsies taken prior to treatment; the level of staining was evaluated by two independent pathologists. Strong positive CXCR4 staining was not associated with pathological grade, extent of bony metastasis, or clinical response to hormonal therapy. However, high CXCR4 staining did correlate to poor cancer-specific survival (Akashi et al., 2008).

The patient array utilised in my studies comprised of the larger patient sample set than the previous published work (75 cores: 64 cases of prostate cancer, 11 hyperplasia). The array showed that a significantly stronger amount of positive CXCR4 staining was detected in prostate adenocarcinoma samples compared to samples of hyperplasia (Mann-Whitney, P= 0.0003). Lu et al. (2013) also showed that positive CXCR4 staining was higher in prostate cancer samples compared to 'normal' prostate tissue. However, the latter was sampled from the peritumoural normal prostate, not from independent BPH specimens, as was the case in my array studies. The collection of tumour associated normal tissue would require a high degree of accuracy and may not always exclude tumour tissue which may confound the results.

Unlike any of the previously mentioned studies, my study showed that strong positive CXCR4 staining was associated with a higher Gleason score and a higher Gleason grade compared to lower grade tumours. However, this was not significant at the highest grade (Grade 5), nevertheless this could be attributed to the increase in variation seen in very poorly differentiated cancers. This result was in conflict to the results published in Jung et al. (2011), who found that CXCR4 did not correlate to any of the other prognostic parameters investigated. The results published in Jung et al. are also the only other study that looked at the correlation between patient age and CXCR4 staining and

again they found conflicting results to my own. The source of this variation could be in the antibody used. These experiments utilised a mouse monoclonal CXCR4 antibody from R&D, which ensured love background. The antibody used by Jung et al. was a polyclonal Goat antibody that could have produced increased background due to its polyclonal nature. Furthermore, the blocking solution used in Jung et al. and in what concentration was not specified. The importance of the right blocking solution when detecting CXCR4 is highlighted in Eaton et al. (2010) who provided evidence that the wrong blocking serum may produce false positives.

My array suggested that a lower age at the time of biopsy correlated to higher CXCR4 staining. This result was only marginal and the value of age as a prognostic indicator in prostate cancer has come under scrutiny. Therefore, the fact that younger patients have higher CXCR4 may not be an indicator of poor prognosis. However, perhaps when used in combination with age, CXCR4 staining may be useful in assigning prognosis but this would require a larger series than that presented here.

Strong positive CXCR4 staining in this study could not be used as an alternative to Gleason grading to predict TNM status as while 38.4% of high CXCR4 samples had metastases compared to 47.36% of high Gleason grade tumours with metastases. This suggests that CXCR4 is not additionally informative when poor prognosis is already predicted by other factors but may contribute to prognosis in multivariate analysis.

A limitation of this study was that no follow up clinical information was available for the patients sampled on the array. The presence of metastases at the time of biopsy was the only information provided, therefore it was impossible to know whether patients with high CXCR4 staining would go on to develop metastases in later years. Therefore, although the level of positive CXCR4 staining did not correlate to the TNM stage of patients in this sample set, this does not exclude a use for CXCR4 as a marker to predict later occurring metastases in patients with apparently better prognosis based on stage/grade at the time of diagnosis. Given the association of CXCR4 with dormancy in my experimental studies, it is perhaps in the context of identifying patients with very early disease, apparently confined to the prostate but who present at a later date with metastases that CXCR4 staining as a predictor of later metastasis would be most useful.

This requires further investigation with different panels of patient samples with good follow up over 5-10 years.

It was also interesting that CXCR4 was higher in patients with distant metastases than in patients with node metastases without distant metastases suggesting that high CXCR4 is associated with a more migratory phenotype once it has invaded the lymph nodes. The suggestion that CXCR4 does not correlate to metastases in this study is in agreement with the work published by Lu et al. (2013) and counters the claims made in Mochizuki et al. (2004) and Jung et al. (2011). However, as mentioned without follow up clinical information it was impossible to tell whether strong CXCR4 staining would predict the onset of later metastases.

Other limitations include those that are typical of most immunohistochemical stains. It is expected that a certain amount of variability exists between experimenters performing the assay and even between experimental 'runs'. There is also the caveat of inter-observer variation when is came to scoring CXCR4 staining. However, as two experienced scientists scored the samples independently this bias is reduced. There is also the limitation that only one core per patient was provided on the array and as prostate cancer is known to be a very heterogeneous disease it is not expected that this single core will represent the disease. Although Biomax provides information on their website that argues that as the 1.5 mm diameter cores used are 6.3 x bigger than 0.6 mm standard size cores and therefore represent a better representation of the disease it does not account for variation within different regions of the tumour. This would require sampling from multiple sites of the prostate to allow a better representation. There were however, several advantages to using the commercially available arrays from Biomax which reduced other common limitations such as variable processing time and time in formalin as Biomax ensures that all of their samples are processed within 15-30 minutes of surgical resection and are fixed in formalin for 24 hours. This suggests that the results obtained in my experiments should be highly reproducible when using Biomax arrays as they are all prepared in a controlled, uniform way.

6.4.3 Conclusion

CXCR4 has been shown to be a common marker of the dormant phenotype in three human prostate cancer cell lines. DiD retaining dormant cells in the PC-3NW1, LNCaP and C42B4 cell lines had a significantly higher level of CXCR4 at the gene (as measured by RT-qPCR) and protein level (as measured by immunofluorescence). Although CXCR4 did not correlate to the TNM status of patients in the tissue microarray examined, as measured by immunostaining, high CXCR4 did correlate to higher Gleason grade and Gleason score. A positive link between CXCR4 staining and Gleason grade and score has previously been contested, however the array used in this study had the largest patient sample examined and this may account for these differences. It remains a possibility that CXCR4 could have a role as a prognostic marker in some important settings but this will require further studies with better patient sample sets with more complete clinical histories.

Chapter 7: Discussion

7.1 Discussion

7.1.1 Identifying the presence of a dormant cell sub-population in multiple prostate cancer cell lines

Staining with the lipophilic membrane dyes CM-DiI and Vybrant® DiD revealed the presence of a low frequency dye retaining sub-population in the PC-3NW1 cell line. Vybrant® DiD (DiD) was selected to be used in subsequent experiments due to its higher fluorescent intensity as measured by flow cytometry (X geometric mean) and fluorescent microscopy. Mitomycin C treatment of PC-3NW1 cells to induce mitotic arrest, showed that DiD was retained at high frequency following a growth suppression treatment. This indicated that dye retention was an accurate measure of cell dormancy.

Dormancy, in this project, was defined as cells that have retained lipophilic dyes past 14 days in *in vitro* culture. Dye retaining cells at day 14 in the PC-3NW1 cell line were subject to cell cycle analysis by KI-67 and P.I staining. From these experiments it was decided that DiD positive cells would be classified as 'dormant' and not quiescent as they existed in all stages of the cell cycle from S phase to G2/M and not exclusively G0/G1: a characteristic of cells in quiescence, and were both KI-67 positive and negative suggesting growth arrest had occurred outside G0. This definition is in agreement to that published in Fehm et al. (2008), which stated that dormant cells are characterised by cell cycle arrest (not specifically in G0) and that dormant cells do not undergo apoptosis or proliferation until changes in the microenvironment, or at the gene expression level, prompt them to do so (Fehm et al., 2008). In other studies however, GO/G1 cell status is used as a marker of 'dormant' circulating tumour cells (CTCs) or disseminated tumour cells (DTCs) in patients, as discussed in a review by Aguirre-Ghiso (2007) . In these studies G0/G1 status is often used to identify cells in a quiescent state that are then labelled as 'dormant' that are present in patients and not as a definition of cells that have a dormant phenotype. My studies aimed to observe the dormant *phenotype* (defined as long term DiD retention) and *then* look at the cell cycle profile. This is different from traditional methods that have used cell cycle status: GO/G1 as a marker of dormancy, which is then used to identify these cells in experimental models in order to study 'dormancy'.

There is also debate as to whether 'dormant cells' detected in patients represent quiescent (retaining the ability to proliferate) or senescent cells (Aguirre-Ghiso, 2007). The results presented in my own studies suggest that dormant cells in this context are not senescent. A senescence detection kit was used to assess whether 'dormant' cells were senescent and it was shown that DiD positive cells at day 14 after staining did not stain positively for blue Senescent Associated-beta-galactosidase activity which is thought to be a marker of senescent cells. Further evidence that the DiD retaining cells represented a dormant and not senescent sub-population was provided by experiments in Chapter 4 which showed that DiD retaining dormant cells isolated at day 14 after staining were capable of forming colonies in monolayer clone assays. This was an important distinction as in the development of cancer the avoidance of senescence after the accumulation of mutations in the cell is seen as an important step in tumourogenesis and that senescence, as opposed to dormancy, does not result in disease relapse (Aguirre-Ghiso, 2007). This does not rule out the possibility that dormancy is a result of a perturbed senescent pathway but this requires further study.

It was significant to find that the presence of a DiD retaining population was not limited to the PC-3 cell line or the tested PC-3 variants (PC-3NW1, PC-3RFP and PC-3GFP) but was present in both the LNCaP and C42B4 cell lines. Whether the presence of this sub-population is exclusive to cancer cell lines remains to be tested. Future experiments would be required to assess DiD dye retention in normal human primary prostate epithelial cells or in immortalised 'normal' prostatic epithelium such as PNT2 or in a BPH (benign prostatic hyperplasia) cell line such as BPH-1 (Hayward et al., 1995) to test this. However, the identification of a dormant population in prostate cancer cell lines may reflect the observed clinical manifestations of the disease in patients where many have prolonged periods where they appear to be disease free after diagnosis and removal of the primary cancer until they present with incurable bone metastases. This implies the presence of relatively indolent cells taking up residency in the skeleton at an early stage in the disease and remaining 'dormant' for many years until triggered to proliferate. The use of lipophilic dyes presents a novel protocol to investigate dormancy, which may enable us to gather more information relevant to the dormant phenotype, its drivers and mechanisms for activation.

The use of DiD to identify dormant cells *in vivo* and *in vitro* has been published by Yumoto et al. (2014) since the start of this thesis. The authors provide further support that DiD can be used to identify cells with limited proliferation, as measured by EdU incorporation during DNA synthesis. However the authors have not looked at the use of this dye to investigate the mechanisms that regulate dormancy or the characteristics of the DiD retaining population. The use of this type of technology has however been demonstrated in other cancers. For example, and as discussed in Introduction 1.4.13, retention of the lipohilic cell membrane dye PKH67 was used by Kusumbe and Bapat (2009) to identify dormant cells in the A4 ovarian cancer cell line. The authors stained A4 cells with PKH67 and injected cells sub-cutaneous into NOD/SCID mice. They found that a $PKH67^{High}$ population was present after long-term incubation. In agreement to my studies this dye retaining sub-population had, upon isolation, a higher clonogenic ability in monolayer and also an increased ability to form tumours when re-injected into immunocompromised mice. My studies provide support to the hypothesis presented in Kusumbe and Bapat that dye retaining cells were not characterised by G0/G1 cycle status as in experiments similar to my own, the authors found that a percentage, albeit a small one, of dye retaining cells were KI-67 positive by flow cytometry and that PKH^{High} cells when stained with Propidium Iodide also have a variable cell cycle profile that includes S-phase and G2/M as well as G0/G1.

7.1.2 Mechanisms that regulate dormancy

The experiments presented in Chapter 4 aimed to use DiD to investigate dormancy and assess the factors that may regulate entry and exit into this state. Clone assays in monolayer showed that altering the serum concentration of the culture media affected the cloning ability of the PC-3NW1 cell line and the C42B4 cell lines (LNCaP cells did not readily form colonies in monolayer). Low serum (2% FBS) decreased the ability of these cell lines to form colonies compared to routine serum (10% FBS) and, 1% FBS prevented colony formation entirely at clonal density in all cell types. DiD staining before plating indicated that these cells, seeded in 1% FBS at clonal density, were maintained in a dormant state after 14 days in culture. This suggested that cells could be 'forced' into dormancy and prompted the further characterization of these cells in more detail in Chapter 5. These results perhaps go against the previously accepted paradigm of hierarchical tumour cell organisation. In which, a small sub-population of stem cell-

like cells give rise to uni-directional tumour heterogeneity. However, more research into cancer cell plasticity and the role of the microenvironment on cell phenotype has led to a greater appreciation of the fluidity of cancer cell properties regardless of hierarchical organisation (Meacham and Morrison, 2013). Further experiments in Chapter 4 showed that the re-staining of cells that had lost DiD at day 14 after initial DiD staining, and were therefore considered to be rapidly dividing, could give rise to slow cycling cells that were DiD retaining. This suggests that in the PC-3NW1 cell line, cells can transit between rapid growth and dormancy so that phenotypes are 'plastic' rather than intrinsic. This result is in agreement to research published by Roesch et al. in 2013. The authors identified a slow-cycling sub-population in Melanoma cell lines that was characterised by the retention of the PKH26 cell dye. This sub-population was characterised by high expression of the H3K4 histone demethylase JARID1B. Interestingly the authors found that the expression of JARID1B was dynamically regulated and that cells that were JARID1B^{low} could give rise to cells of a JARID1B^{high} phenotype and vice-versa. Furthermore, the authors found that JARID1B expression and the subsequent accusation of the slow-cycling phenotype was temporally regulated by the environment (Roesch et al., 2010). This again has parallels to my own work which indicated that the acquisition of the dormant phenotype was regulated by the environment, as changes in the FBS concentration and initial seeding density of the culture environment were found to have altered the frequency of the dormant cell sub-population. The decrease in the frequency of the dormant sub-population in less crowded cultures may suggest that dormancy results from environmental stress and suggested the hypothesis that hypoxia was a driving force for dormancy. This hypothesis was also considered by Roesch et al. (2013) who found that JARID1B expression was enhanced at low oxygen (3 days, 1% pO2) but reverted to normal under atmospheric oxygen. Although, immunofluorescence studies in Chapter 4 provided evidence that Hif1α nuclear translocation was increased in the DiD retaining sub-population in my experiments, which serves as a marker for hypoxic conditions, more evidence would be required to add support to this hypothesis. Hypoxia as a driving force for cancer cell quiescence was considered mathematically in a theoretical paper published by Alarcon et al. (2004). The authors postulate that through increased p27 expression, cancer cells can enter quiescence in response to increasing levels of hypoxia which would be lethal to a normal cell (Alarcon et al., 2004). The effect of hypoxia on cancer cell proliferation was demonstrated experimentally by Heddleson et al. (2009).

The authors found that hypoxia induced a more 'stem cell-like' phenotype in Glioblastoma cells that was characterised by reduced proliferation in the short-term, followed by increase proliferation after long-term culture. The authors did not consider the effect of cell cycle proteins but did find that cancer cells exposed to hypoxia had increased expression of traditional stem cell markers including Nanog and Oct4 (Heddleston et al., 2009). Although this appears in disagreement to my own studies, that found no significant difference in the expression of these markers in the dormant cell sub-population, other stem cell markers such as PSCA were increased in the dormant cell subpopulation and furthermore the DiD retaining cells were not directly exposed to extreme hypoxia, hypoxia was only considered as a result of overcrowded culture conditions. Therefore an interesting set of experiments could investigate the effect of hypoxia exposure on stem cell marker gene expression and how it differs between DiD retaining and rapidly dividing cells.

Further investigations into cell growth were done in Chapter 4 to measure serum factors and cloning ability. To assess whether cells were intrinsically unable to form colonies in 1%, PC-3NW1 cell were seeded at clonal density in 10% FBS then transferred to 2% FBS and 1% FBS. It was found that more colonies were detected as a result of transfer into very low serum (1%) than transfer into 2% FBS. This could be due to a reliance on one set of factors in serum for the initiating stages of colony formation after which, transfer into low serum provides conditions that favour the expansion of cells that have already begun to grow. Serum contains both growth inhibitory/differentiating and mitogenic factors and cell fates are driven by this combination of influences which will vary with serum concentration. Furthermore, transfer into 1% FBS may select for a more resilient, autonomously growing cell type, than cells that survived transfer into 2%, which once established have a higher clonogenic ability.

Interestingly, increasing the seeding density in 1% FBS allowed increased colony formation in both the PC-3NW1 and C42B4 cell lines and the LNCaP cells to rapidly form monolayer cultures at varying confluence. This suggested that factors generated by the cells themselves, that are released into the culture media at sufficient concentrations when cells where at high density, could stimulate colony formation. To test this, and also to determine whether dormancy when induced at clonal density in 1% FBS was reversible, dormant cells at clonal density were treated with different media types at day

14 after seeding in 1% FBS. It was found that 10%, 2% FBS and conditioned media containing 1% FBS (media conditioned over rapidly growing cells at high density) could stimulate colony formation in previously dormant cultures. This suggested that dormancy is reversible and cells retain the ability to divide despite long term inactivity and that cells themselves were able to generate signals that initiated colony formation if present in high enough numbers. What these signals are remains to be determined, however, this was explored in Havard et al. (2011). The authors found that citric acid when added to unconditioned media was able to reproduce the stimulating growth effect observed when conditioned media was added to growth arrested LNCaP cells in monolayer clone assays. Furthermore, experiments published in 1983 by Hamburger et al. demonstrated that although increased serum promoted the cloning ability of tumour cells in soft-agar, the addition of growth factors including EGF and insulin were able to support anchorage-independent growth when the serum concentration was reduced (Hamburger et al., 1983). These studies support my own hypothesis and suggest that although serum is required for tumour cell growth there are other independent factors in the environment that can support clonal ability.

Chapter 4 also showed that DiD retaining dormant cells at day 14 had a higher clonogenic ability than their rapidly dividing counterparts. As mentioned, this not only adds further support to the hypothesis that dormant cells are not senescent cells but also indicates that the DiD retaining cells may represent a more resilient cell phenotype, able to survive under different conditions. This is supported by *in vivo* evidence in our laboratory, that this sub-population is more metastatic in xenograft models.

In order to investigate what is mediating the switch to mitotic dormancy an investigation of the presence/levels of cell cycle regulators could be performed. P27Kip1 and P21 are both inhibitors of CDKs (cyclin-dependent kinases), which are required for normal progression through cell division. RT-qPCR and/or immunofluorescence could investigate the presence of P27Kip1 and P21, as well as other regulators of the cell cycle, in the DiD+ population to assess the role these factors play in dormancy.

7.1.3 Dormancy is characterised by changes in gene expression levels

RT-qPCR (reverse transcriptase-quantitative PCR) was used to assess relative gene expression differences between DiD retaining dormant cells and DiD negative rapidly dividing cells. Initial studies using stand-alone TaqMan assays showed that the expression of CXCR4 was significantly increased in the dormant cell sub-population compared to rapidly dividing cells. Using the Promega Reliaprep™ kit high quality RNA was extracted from as little as $3x10^3$, as measured by 2200 TapeStation, which allowed me to proceed with low density array card work using relatively low yields of cells obtained from FACS Aria sorting.

LDA card 1 analysis showed that the PC-3NW1 dormant cell sub-population had a number of significantly altered gene expression values. CXCR4 was significantly up-regulated in the DiD+ population compared to the DiD- cells, which confirmed the TaqMan result. Markers of EMT including Fibronectin, Vitronectn and MMP2 and 3 were also significantly increased in the dormant cell sub-population. Expression of a number of stem cell markers were also up-regulated in the dormant cell type, including CD24, ANAX2 and PSCA. PSCA has been shown to be highly expressed in prostate cancer compared to normal tissues and has been associated with tumor progression (Gu et al., 2000). However, traditional stem cells markers such as SOX2, Nanog and Oct4 (TaqMan alias POU5F1) were not significantly up-regulated. This is in contrast to the studies published by Bapat and Kusumbe (2009), who found that slow-cycling PKH67 retaining cells were characterised by an increase in expression of OCT4 and also Nanog. Interestingly, it was found that Nestin was one of the only genes that had reduced gene expression in the dormant sub-population whereas Bapat and Kusumbe found Nestin was increased in their dye retaining cells. This result is perhaps not surprising as the difference in Nestin expression may reflect inherent differences in the prostate cell lines used in my studies and the ovarian cell lines used by Bapat and Kusumbe.

It has previously been proposed that a CSC sub-population is present within prostate cancers with the expression signature CD44+/α2β1hi/CD133+ (Collins et al., 2005). It is hypothesised that this sub-population of cells have an increased self-renewal capacity and the ability to recapitulate the heterogeneity of the parental tumour. Gene expression

analysis in Chapter 5 revealed that the DiD+ sub-population did not differentially express these markers (with the exception of alpha 2 integrin which was significantly up-regulated with a P value of 0.048). This result suggests that although the DiD+ dormant sub-population shares CSC-like characteristics such as increased clonogenic ability and expression of some prostate CSC markers, the DiD retaining population may be completely distinct from the previously proposed prostate CSC phenotype or a previously undefined subset of such a population. This result was perhaps not surprising as the CD44+/α2β1hi/CD133+ was also characterised as having a high proliferative potential *in vitro* (Collins et al., 2005). However, differences in experimental approaches may explain this. The authors measured proliferation by colony formation in clonogenic assays in monolayer rather than growth curves or loss of cell membrane dyes, which is in agreement to the higher clonogenic ability of the DiD+ cells observed in Chapter 4. They also used combinations of adhesion assays and flow-cytometry analysis of antibodies against CD44, CD133 and α2, β1 integrin to reveal a CD44+/α2β1hi/CD133+ sub-population while here I used gene expression analysis using the LDA. Repeating the above flow-cytometry studies with the DiD retaining cells could clarify the relationship between dormant cells described here and prostate cancer stem cells, but it should be noted that expression of CD133 was beyond detection in my dormant cells therefore detection by flow-cytometry may not provide any additional information. Interestingly, studies by Guzman-Ramirez et al. (2009) found that cells isolated from prostate cancer patients that had a heightened ability to form prostaspheres (a measure of a stem cell-like phenotype) had a wide distribution of marker expression suggested both a stem cell like phenotype (CD44+ and other traditional markers such as OCT4) but also a basal like phenotype (CK5+/CK14+). The authors argue this suggests a heterogeneous cell composition and found that cells that had high self-renewal capacity (as measured by sphere formation) were both CD133+ and CD133-. It is therefore tempting to speculate that the dormant cells isolated in my studies may represent a fraction of the proposed prostate CSC sub-population that has lost CD133 and has an increased ability to form metastases *in vivo*. Considering the results in Guzman-Ramirez et al. it would be useful to asses the sphere forming ability of the dormant cells vs. the rapidly dividing bulk population in the three cell lines tested in my studies.

Following LDA card 1 analysis a second LDA card was designed (LDA card 2) with a more limited number of assays, which allowed the number of samples that could be investigated per card to be increased. The aim of this card was to assess whether key gene expression differences that were present in the PC-3NW1 DiD+ population, by LDA card 1 analysis, were also present in cells grown at clonal density in 1% FBS and cells that were initially considered to be rapidly dividing which then retained DiD after restaining.

The most significant result of LDA card 2 experiments was that the gene expression profile of the PC-3NW1 dormant sub-population was not significantly different from cells that have been 'forced' into dormancy by culture in 1% FBS at clonal density. This suggested that cells with a dormant phenotype share gene expression characteristics, regardless of how dormancy was acquired. This is potentially of value, since studying the drivers of dormancy and release of cells from this state could now be modelled using induced dormancy in these models.

To investigate this further, as shown in Chapter 6, LDA card 2 was used to assess the gene expression levels of dormant cells in the LNCaP and C42B4 cell lines. It was found that the DiD retaining sub-population in the C42B4 cell line was not significantly different from the DiD retaining PC-3NW1 sub-population at the gene expression level across the assays tested. Although DiD+ LNCaP cells were significantly different to DiD+ PC-3NW1 cells, they were not significantly different from DiD+ C42B4 cells. Interestingly, the dormant cell sub-population in all three cell lines was characterised by a significant increase in the gene expression of CXCR4 compared to rapidly growing cells in the same populations. The level of CXCR4 expression in prostate cancer cell lines has previously been investigated by PCR. Mochizuki et al., (2004) found that CXCR4 was expressed at a high level in PC-3, LNCaP and DU-145 cells. However, Engl et al., (2006) found that CXCR4 expression in the LNCaP cell line was only moderate when compared to the DU-145 cell line. Engl et al. used end-point PCR whereas Mochizuki et al. used real-time PCR so this perhaps accounts for the variability in results. Although high CXCR4 expression in prostate cancer cell lines is not a new finding, to the best of my knowledge, the results demonstrated in Chapter 6 present a novel hypothesis that CXCR4 is *differentially* expressed in prostate cancer cell lines and

that a high CXCR4 sub-population exists within these cell lines that is characterised by a dormant phenotype.

Significantly this result was also observed at the protein level by immunofluorescence. ImageJ analysis showed that DiD+ cells in all three prostate cancer cell lines had significantly higher positive staining for CXCR4 than their rapidly dividing DiD- counterparts. This result was perhaps not surprising as CXCR4 is hypothesised to not only induce HSC homing to the bone marrow, but also regulate HSC quiescence once in contact with the niche to maintain the HSC pool (Sugiyama et al., 2006). Using an induced CXCR4 knockout mouse model (MxCre-CXCR4$^{flox/null}$), the authors found evidence that CXCR4 null mice were more sensitive to drugs that target cycling HSCs (5-FluroUracil specifically). CXCR4 null mice also had a decreased fraction of KI-67- HSCs as measured by FACS Aria flow cytometry. CXCR4 presents an attractive candidate as a driver of dormancy in prostate cancer cell lines. In order to investigate this further conditional knockdown studies could be utilised to assess if when the CXCR4 gene is silenced, or removed, cells retain the ability to enter into the dormant state.

There are numerous studies suggesting that CXCR4/CXL12 signalling promotes metastasis in prostate cancer. It would therefore be interesting to design experiments to define the drivers for CXCR4 increase in the dormant cells specifically and identify mechanisms to target this in these cells. As mentioned in Chapter 5 discussion, CXCR4 is a target of the Hif1∝ transcription factor, which is translocated to the nucleus under hypoxic conditions (Ishikawa et al., 2009). Immunofluorescent analysis suggested that Hif1∝ nuclear translocation was increased in the DiD+ sub-population compared to DiD- cells. However, Hif1∝ is not the only transcription factor with the ability to bind to the CXCR4 promoter. The androgen regulated gene ERG has also been shown to act as an inducer of CXCR4 via the binding of ERG to specific ERG/Ets bindings sites in the CXCR4 promoter (Chinni et al., 2013). However, the gene expression level of ERG in the PC-3NW1 cell line was undetected, i.e. it had a Ct value of above 35, suggesting this affect would be minimal. It would be interesting to assess the epigenetic profile of the dormant cells as CXCR4 has been shown to be regulated by DNA methylation (Ramos et al., 2011). The authors used sodium bisulphite sequencing to determine the methylation status of CpG dinucleotides in the promoter region of the CXCR4 gene. By

using a combination of high and low CXCR4 expressing MDA cell lines (breast cancer cell lines), they found that low CXCR4 expression was linked to hypermethylation whereas high CXCR4 expression was linked to low methylation.

Although CXCR4 may present a mechanism by which prostate cancer cells switch into dormancy, the final results chapter aimed to test whether high CXCR4 protein presence in primary prostate cancer samples was linked to metastasis. Work in our lab has shown that PC-3NW1 DiD+ cells formed more metastases *in vivo* compared to DiD- cells, identifying these cells in tissue microarrays may allow us to predict the presence of metastases. As the TNM stage was known, the amount of CXCR4 staining, after independent analysis by Dr. Colby Eaton and an independent and experienced pathologist (Professor Simon Cross), could be correlated to the disease status. A further aim was to assess whether CXCR4 status correlated to other prognostic factors such as age and Gleason stage.

7.1.4 Patient samples

So far in the published literature, the value of CXCR4 as a prognostic indicator in prostate cancer has been conflicting and inconclusive. My work indicated that strong positive staining for CXCR4 was linked to a higher Gleason grade and Gleason score in patient samples. CXCR4 did not accurately correlate to tumour, lymph node, metastasis (TNM) status but was higher in patients with distant metastases than with lymph node metastasis. This data suggests that CXCR4 may contribute to the staging of patients with prostate cancer as more poorly differentiated cancers stained higher for CXCR4. CXCR4 could possibly be used in combination with other clinical parameters to decide if radical treatment is needed.

As previously mentioned no follow-up clinical information was available to test whether patients with high CXCR4 staining but with low-grade tumours and no metastases at biopsy, progressed more frequently than patients in this group with low CXCR4. Similarly no survival data was available to test whether high CXCR4 was linked to poor survival. Interestingly of the studies discussed in Chapter 6 (Discussion 6.4.1), that also measured the value of CXCR4 as a prognostic indicator, only Jung et al. (2011) stated a follow-up time (which was on average 36 months). These authors found

that CXCR4 was linked to the recurrence of tumours at the primary site and also to the development of distant metastases. It is hoped that the data provided in this thesis may be used to set up a clinical collaboration to test CXCR4 staining in a larger prostate cancer patient cohort with long-term clinical follow up. Such sample sets are currently not available but may be in the near future via UK collections (PROMPT). CXCR4 has been associated with poor clinical outcome in triple-negative breast cancer as measured by reduced 5-year survival in patients with elevated CXCR4 staining (Yu et al., 2013). Building on this Yang et al. (2014) showed that silencing of CXCR4 in MDA-MB-231 cells reversed EMT, increased apoptosis and reduced the incidence of lung metastases in xenograft models (Yang et al., 2014b). CXCR4 had also been indicated as a prognostic marker in ovarian cancer. A recent meta-analysis that compiled evidence from 7 published studies found that increased CXCR4 was associated with both poor overall survival and low progression free survival (Liu et al., 2014). These studies support further research into the investigation of CXCR4 as a prognostic indicator in prostate cancer on a larger scale to the experiments presented here. The experience in the Sheffield group suggest that there is also scope for developing better assays for CXCR4 (Eaton et al., 2010).

7.2 Future work

Although it was not possible to characterise the dormant sub-population *in vivo* i.e. DiD retaining cells in the bone marrow of mice after intracardiac injection due to insufficient cell numbers, it would be important to determine whether this sub-population represents the same dormant sub-population as that identified *in vitro* in my studies. The experiments in Chapter 5 need to be repeated with a much larger cohort of mice to increase the DiD+ cell yield for RNA extraction and so that the presence of proteins in sorted cells can be assessed in cytospun cells by immunofluorescence. Xenograft models in our group have been used to show that a small number of cells arrive in the bone marrow after injection (500-1,000 out of $1x10^5$ cells injected) and that these cells can persist in a mitotically dormant state for up to 8 weeks. These studies also indicated that these cells are located close to osteoblast rich regions (Wang et al., 2014) and may therefore be held in a specific niche controlling dormancy. Future work should focus on defining this niche and the potential role it plays in tumour cell homing, attachment and dormancy.

Looking forward it would be important to extend the studies described in Chapter 4 to further define the role of the cell culture environment in maintaining dormancy. It is also important to determine the specific factors that trigger release of cells from dormancy. As mentioned this could involve knockdown studies to discover whether inhibition of CXCR4 prevented the dormant phenotype. As well as performing ELISAs to determine the components of the culture media in which dormant cells exist (as shown in Chapter 4, cells seeded at $1x10^5$ cells per T25 flask and cultured for 21 days) compared to conditions where the dormant phenotype is not present or in which cells have been newly released from dormancy (Chapter 4, cells seeded at $5x10^3$ cells per T25 flask and cultured for 21 days). Although it is generally suggested that CXCR4/CXCL12 signalling can regulate cell proliferation (Teicher and Fricker, 2010), Mochizuki et al., in their 2004 study found that although CXCL12 stimulated the migration of prostate cancer cells through a transwell chamber via the interaction with CXCR4, CXCL12 had no effect on the proliferation of cells as measured by MTT assay after incubation with increasing concentrations of the ligand.

Although the experiments in Chapter 4 indicated that dormancy is not an intrinsic characteristic of a stem cell like sub-population, the acquisition of this state may still have a genetic basis. For example somatic cell fusion could underlie the dormant phenotype. Previous work has indicated that spontaneous fusion between prostate cancer cells leads to the development of a fused cell phenotype that has higher clongenic potential in anchorage independent conditions and an increased ability to form tumours in bone when injected into mouse xenograft models (Glen et al., 2011). It would therefore still be important to evaluate the dormant cell sub-population by karyotype analysis. In addition to this, with the availability of better technologies for large scale proteomic analysis, a more comprehensive evaluation of the dormant proteome would be valuable. The above approaches would refine understanding of tumour cell dormancy and potentially identify new markers for this phenotype. The latter could reveal potential targets to dormancy, to either prevent its induction to allow therapy with traditional chemotherapeutics or prevent the release of dormancy and maintain low risk patient in a state of disease rest.

7.3 Conclusion

This thesis has presented a novel hypothesis that suggests that within prostate cancer cell lines a phenotypically dormant sub-population is present which is defined by an increase in CXCR4. Further results suggest that dormancy is regulated by the environment and represents a unique sub-population that does not share the putative prostate CSC marker set. This work supports the further investigation of CXCR4 as a prognostic indicator in combination with existing clinical tests in prostate cancer patients.

Further work is required to define the mechanisms that regulate cell entry and exit from the dormant phenotype, as well as the role of the bone niche in maintaining this state. It is hoped that a greater understanding of dormancy will aid the advancement of treatment for the prevention of overt, clinically relevant metastatic prostate cancer.

References

ABATE-SHEN, C. & SHEN, M. M. (2000). Molecular genetics of prostate cancer. *Genes & development,* 14**,** 2410-2434.

AGUIRRE-GHISO, J. A. (2007). Models, mechanisms and clinical evidence for cancer dormancy. *Nature Reviews Cancer,* 7**,** 834-846.

AGUIRRE-GHISO, J. A., LIU, D., MIGNATTI, A., KOVALSKI, K. & OSSOWSKI, L. (2001). Urokinase receptor and fibronectin regulate the ERK(MAPK) to p38(MAPK) activity ratios that determine carcinoma cell proliferation or dormancy in vivo. *Molecular Biology of the Cell,* 12**,** 863-79.

AKASHI, T., KOIZUMI, K., TSUNEYAMA, K., SAIKI, I., TAKANO, Y. & FUSE, H. (2008). Chemokine receptor CXCR4 expression and prognosis in patients with metastatic prostate cancer. *Cancer Science,* 99**,** 539-542.

AL-HAJJ, M., WICHA, M. S., BENITO-HERNANDEZ, A., MORRISON, S. J. & CLARKE, M. F. (2003). Prospective identification of tumorigenic breast cancer cells. *Proceedings of the National Academy of Sciences,* 100**,** 3983.

ALARCON, T., BYRNE, H. & MAINI, P. (2004). A mathematical model of the effects of hypoxia on the cell-cycle of normal and cancer cells. *Journal of theoretical biology,* 229**,** 395-411.

ALIMIRAH, F., CHEN, J., BASRAWALA, Z., XIN, H. & CHOUBEY, D. (2006). DU-145 and PC-3 human prostate cancer cell lines express androgen receptor: implications for the androgen receptor functions and regulation. *FEBS Letters,* 580**,** 2294-300.

ALMOG, N. (2010). Molecular mechanisms underlying tumor dormancy. *Cancer Letters,* 294**,** 139-46.

ALMOG, N., BRIGGS, C., BEHESHTI, A., MA, L., WILKIE, K. P., RIETMAN, E. & HLATKY, L. (2013). Transcriptional changes induced by the tumor dormancy-associated microRNA-190. *Transcription,* 4, 177-191.

ALMOG, N., MA, L., RAYCHOWDHURY, R., SCHWAGER, C., ERBER, R., SHORT, S., HLATKY, L., VAJKOCZY, P., HUBER, P. E., FOLKMAN, J. & ABDOLLAHI, A. (2009). Transcriptional switch of dormant tumors to fast-growing angiogenic phenotype. *Cancer Research,* 69**,** 836-44.

ANDRADE, W., SEABROOK, T. J., JOHNSTON, M. G. & HAY, J. B. (1996). The use of the lipophilic fluorochrome CM-DiI for tracking the migration of lymphocytes. *Journal of Immunological Methods,* 194**,** 181-189.

ARAI, F., HIRAO, A., OHMURA, M., SATO, H., MATSUOKA, S., TAKUBO, K., ITO, K., KOH, G. Y. & SUDA, T. (2004). Tie2/angiopoietin-1 signaling regulates hematopoietic stem cell quiescence in the bone marrow niche. *Cell,* 118**,** 149-161.

ARMSTRONG, A. P., MILLER, R. E., JONES, J. C., ZHANG, J., KELLER, E. T. & DOUGALL, W. C. (2008). RANKL acts directly on RANK expressing prostate tumor cells and mediates migration and expression of tumor metastasis genes. *The Prostate,* 68**,** 92-104.

BARRY, M. J. (2001). Prostate-Specific Antigen Testing for Early Diagnosis of Prostate Cancer. *New England Journal of Medicine,* 344**,** 1373-1377.

BRENNAN, P. M. & FRAME, M. (2014). Identification of a novel cancer stem cell that might be important for glioma cell invasion. *The Lancet,* 383**,** Supplement 1, 10.

BROWN, J. M., COREY, E., LEE, Z. D., TRUE, L. D., YUN, T. J., TONDRAVI, M. & VESSELLA, R. L. (2001). Osteoprotegerin and rank ligand expression in

BUHMEIDA, A., PYRHONEN, S., LAATO, M. & COLLAN, Y. (2006). Prognostic factors in prostate cancer. *Diagnostic Pathology,* 1**,** 124.

BUIJS, J. T., RENTSCH, C. A., VAN DER HORST, G., VAN OVERVELD, P. G., WETTERWALD, A., SCHWANINGER, R., HENRIQUEZ, N. V., TEN DIJKE, P., BOROVECKI, F. & MARKWALDER, R. (2007). BMP7, a Putative Regulator of Epithelial Homeostasis in the Human Prostate, Is a Potent Inhibitor of Prostate Cancer Bone Metastasis in Vivo. *The American journal of pathology,* 171**,** 1047-1057.

BUIJS, J. T. & VAN DER PLUIJM, G. (2009). Osteotropic cancers: from primary tumor to bone. *Cancer letters,* 273**,** 177-193.

CAI, C., WANG, H., XU, Y., CHEN, S. & BALK, S. P. (2009). Reactivation of Androgen Receptor-Regulated TMPRSS2:ERG Gene Expression in Castration-Resistant Prostate Cancer. *Cancer Research,* 69**,** 6027-6032.

CANCERRESEARCHUK. (2011). *Cancer Statistics(online)* [Online]. London. Available: http://info.cancerresearchuk.org/cancerstats/ [Accessed 14.10.2011].

CHAFFER, C. L., BRENNAN, J. P., SLAVIN, J. L., BLICK, T., THOMPSON, E. W. & WILLIAMS, E. D. (2006). Mesenchymal-to-epithelial transition facilitates bladder cancer metastasis: Role of fibroblast growth factor receptor-2. *Cancer Research,* 66**,** 11271-11278.

CHAFFER, C. L. & WEINBERG, R. A. (2011). A perspective on cancer cell metastasis. *Science,* 331**,** 1559.

CHAN, D. A., SUTPHIN, P. D., DENKO, N. C. & GIACCIA, A. J. (2002). Role of prolyl hydroxylation in oncogenically stabilized hypoxia-inducible factor-1alpha. *Journal of Biological Chemistry,* 277**,** 40112-7.

CHEN, C., PORE, N., BEHROOZ, A., ISMAIL-BEIGI, F. & MAITY, A. (2001). Regulation of glut1 mRNA by hypoxia-inducible factor-1. Interaction between H-ras and hypoxia. *Journal of Biological Chemistry,* 276**,** 9519-25.

CHINNI, S., SINGAREDDY, R., SEMAAN, L., CONLEY-LACOMB, M. K., JOHN, J. S., POWELL, K., IYER, M., SMITH, D., HEILBRUN, L. K. & SHI, D. (2013). Transcriptional regulation of CXCR4 in prostate tumor cells: Significance of TMPRSS2-ERG fusions. *Molecular Cancer Research***,** 11, 1349-1361.

COLLINS, A. T., BERRY, P. A., HYDE, C., STOWER, M. J. & MAITLAND, N. J. (2005). Prospective identification of tumorigenic prostate cancer stem cells. *Cancer Research,* 65**,** 10946-10951.

COLLINS, A. T., HABIB, F. K., MAITLAND, N. J. & NEAL, D. E. (2001). Identification and isolation of human prostate epithelial stem cells based on 2 1-integrin expression. *Journal of Cell Science,* 114**,** 3865-3872.

COSMIC, S. I. (2011). *Catalogue of somatic mutations in cancer* [Online]. Available: http://www.sanger.ac.uk/perl/genetics/CGP/cosmic?action=bygene&ln=SPARC&start=1&end=304&coords=AA:AA. (Accessed on: 13.10.2011).

CROSS, N., FOWLES, A, REEVES, K, JOKONYA, N, LINTON, K, HOLEN, I, HAMDY, FC, EATON, CL. (2008). Imaging the effects of castration on bone turnover and hormone-independent prostate cancer colonization of bone. *The Prostate,* 68**,** 1707-1714.

CUZICK, J., YANG, Z., FISHER, G., TIKISHVILI, E., STONE, S., LANCHBURY, J., CAMACHO, N., MERSON, S., BREWER, D. & COOPER, C. (2013). Prognostic value of PTEN loss in men with conservatively managed localised prostate cancer. *British journal of cancer,* 108**,** 2582-2589.

DANIELL, H. W. (1997). Osteoporosis after orchiectomy for prostate cancer. *Journal of Urology,* 157**,** 439-444.

DEMICHELIS, F., FALL, K., PERNER, S., ANDREN, O., SCHMIDT, F., SETLUR, S. R., HOSHIDA, Y., MOSQUERA, J. M., PAWITAN, Y., LEE, C., ADAMI, H. O., MUCCI, L. A., KANTOFF, P. W., ANDERSSON, S. O., CHINNAIYAN, A. M., JOHANSSON, J. E. & RUBIN, M. A. (2007). TMPRSS2 : ERG gene fusion associated with lethal prostate cancer in a watchful waiting cohort. *Oncogene,* 26**,** 4596-4599.

DIAMOND, T., CAMPBELL, J., BRYANT, C. & LYNCH, W. (1998). The effect of combined androgen blockade on bone turnover and bone mineral densities in men treated for prostate carcinoma. *Cancer,* 83**,** 1561-1566.

DORAI, T., DUTCHER, J. P., DEMPSTER, D. W. & WIERNIK, P. H. (2004). Therapeutic potential of curcumin in prostate cancer - IV: Interference with the osteomimetic properties of hormone refractory C4-2B prostate cancer cells. *Prostate,* 60**,** 1-17.

EATON, C. L., COLOMBEL, M., VAN DER PLUIJM, G., CECCHINI, M., WETTERWALD, A., LIPPITT, J., REHMAN, I., HAMDY, F. & THALMAN, G. (2010). Evaluation of the frequency of putative prostate cancer stem cells in primary and metastatic prostate cancer. *The Prostate,* 70**,** 875-882.

ENGL, T., RELJA, B., MARIAN, D., BLUMENBERG, C., MuLLER, I., BEECKEN, W.D., JONES, J., RINGEL, E. M., BEREITER-HAHN, J. R. & JONAS, D. (2006). CXCR4 Chemokine Receptor Mediates Prostate Tumor Cell Adhesion through α 5 and β 3 Integrins. *Neoplasia,* 8**,** 290-301.

ERAMO, A., LOTTI, F., SETTE, G., PILOZZI, E., BIFFONI, M., DI VIRGILIO, A., CONTICELLO, C., RUCO, L., PESCHLE, C. & DE MARIA, R. (2008). Identification and expansion of the tumorigenic lung cancer stem cell population. *Cell Death and Differentiation,* 15**,** 504-514.

FEHM, T., MULLER, V., ALIX-PANABIÈRES, C. & PANTEL, K. (2008). Micrometastatic spread in breast cancer: detection, molecular characterization and clinical relevance. *Breast cancer research,* 10**,** Supplement 1.

FELDMAN, B. J. & FELDMAN, D. (2001). The development of androgen-independent prostate cancer. *Nature Reviews Cancer,* 1**,** 34-45.

FISHER, G., YANG, Z., KUDAHETTI, S., MØLLER, H., SCARDINO, P., CUZICK, J. & BERNEY, D. (2013). Prognostic value of Ki-67 for prostate cancer death in a conservatively managed cohort. *British journal of cancer,* 108**,** 271-277.

GLEASON, D. F. (1988). Histologic grade, clinical stage, and patient age in prostate cancer. *NCI Monographs***,** 15-18.

GLEN, A., LIPPITT, J., FOWLES, A., REHMAN, I. & EATON, C. (2011). Spontaneous fusion between prostate cancer cells: A driver for development of tumor heterogeneity and growth in bone. *Bone,* 48**,** S46-S47.

GOODISON, S., KAWAI, K., HIHARA, J., JIANG, P., YANG, M., URQUIDI, V., HOFFMAN, R. M. & TARIN, D. (2003). Prolonged dormancy and site-specific growth potential of cancer cells spontaneously disseminated from nonmetastatic breast tumors as revealed by labeling with green fluorescent protein. *Clinical Cancer Research,* 9**,** 3808-14.

GRANT, C. M. & KYPRIANOU, N. (2013). Epithelial mesenchymal transition (EMT) in prostate growth and tumor progression. *Translational Andrology and Urology,* 2**,** 202-211.

GRAVDAL, K., HALVORSEN, O. J., HAUKAAS, S. A. & AKSLEN, L. A. (2007). A switch from E-cadherin to N-cadherin expression indicates epithelial to mesenchymal transition and is of strong and independent importance for the progress of prostate cancer. *Clinical Cancer Research,* 13**,** 7003-11.

GU, G. Y., YUAN, J. L., WILS, M. & KASPER, S. (2007). Prostate cancer cells with stem cell characteristics reconstitute the original human tumor in vivo. *Cancer Research,* 67**,** 4807-4815.

GU, Z., THOMAS, G., YAMASHIRO, J., SHINTAKU, I., DOREY, F., RAITANO, A., WITTE, O., SAID, J., LODA, M. & REITER, R. (2000). Prostate stem cell antigen (PSCA) expression increases with high gleason score, advanced stage and bone metastasis in prostate cancer. *Oncogene,* 19**,** 1288-1296.
advanced stage and bone metastasis in prostate cancer. *Oncogene,* 19**,** 1288-96.

GUISE, T. A., MOHAMMAD, K. S., CLINES, G., STEBBINS, E. G., WONG, D. H., HIGGINS, L. S., VESSELLA, R., COREY, E., PADALECKI, S. & SUVA, L. (2006). Basic mechanisms responsible for osteolytic and osteoblastic bone metastases. *Clinical cancer research,* 12**,** 6213-6216.

GUZMAN-RAMIREZ, N., VOLLER, M., WETTERWALD, A., GERMANN, M., COSS, N,A., RENTCH, C,A., SHALKEN, J., THALMANN, G,N., & CECCHINI, M,G. (2009). In vitro propagation and characterization of neoplastic stem/progenitor-like cells from human prostate cancer tissue. *Prostate*, 15, 1683-93.

HALDI, M., TON, C., SENG, W. & MCGRATH, P. (2006). Human melanoma cells transplanted into zebrafish proliferate, migrate, produce melanin, form masses and stimulate angiogenesis in zebrafish. *Angiogenesis*, 9**,** 139-151.

HALL, C. L., BAFICO, A., DAI, J., AARONSON, S. A. & KELLER, E. T. (2005). Prostate cancer cells promote osteoblastic bone metastases through Wnts. *Cancer research,* 65**,** 7554-7560.

HAMBURGER, A. W., WHITE, C. P., DUNN, F. E., CITRON, M. L. & HUMMEL, S. (1983). Modulation of human tumor colony growth in soft agar by serum. *The International Journal of Cell Cloning,* 1**,** 216-229.

HAVARD, M., DAUTRY, F. & TCHENIO, T. (2011). A dormant state modulated by osmotic pressure controls clonogenicity of prostate cancer cells. *Journal of Biological Chemistry,* 286**,** 44177-86.

HAYAT, M., ed., (2013). *Tumor Dormancy, Quiescence, and Senescence*, Volume 1. Dordrecht: Springer.

HAYWARD, S., DAHIYA, R., CUNHA, G., BARTEK, J., DESHPANDE, N. & NARAYAN, P. (1995). Establishment and characterization of an immortalized but non-transformed human prostate epithelial cell line: BPH-1. *In Vitro Cellular & Developmental Biology-Animal*, 31**,** 14-24.

HEDDLESTON, J. M., LI, Z., MCLENDON, R. E., HJELMELAND, A. B. & RICH, J. N. (2009). The hypoxic microenvironment maintains glioblastoma stem cells and promotes reprogramming towards a cancer stem cell phenotype. *Cell Cycle*, 8**,** 3274-3284.

HOLEN, I., CROUCHER, P. I., HAMDY, F. C. & EATON, C. L. (2002). Osteoprotegerin (OPG) is a survival factor for human prostate cancer cells. *Cancer research,* 62**,** 1619-1623.

HOROSZEWICZ,. J. S., LEONG, S. S., CHU, T. M., WAJSMAN, Z. L., FRIEDMAN, M., PAPSIDERO, L., KIM, J., CHAI, L. S., KAKATI, S., ARY, S. K., & SANDBERG, A. A. (1980). The LNCaP cell line:a new model for studies on human prostatic carcinoma. *In G. P. Murphy (ed.), Models for Prostate Cancer, pp. 115-132*. New York:AlanR. Liss, Inc.

HOSHINO, H., MIYOSHI, N., NAGAI, K., TOMIMARU, Y., NAGANO, H., SEKIMOTO, M., DOKI, Y., MORI, M. & ISHII, H. (2009). Epithelial-mesenchymal transition with expression of SNAI1-induced chemoresistance in

colorectal cancer. *Biochemical and Biophysical Research Communications,* 390**,** 1061-1065.

HUMPHREY, P. A. (2004). Gleason grading and prognostic factors in carcinoma of the prostate. *Modern Pathology,* 17**,** 292-306.

HURT, E. M., KAWASAKI, B. T., KLARMANN, G. J., THOMAS, S. B. & FARRAR, W. L. (2008). CD44(+)CD24(-) prostate cells are early cancer progenitor/stem cells that provide a model for patients with poor prognosis. *British Journal of Cancer,* 98**,** 756-765.

ISHIKAWA, T., NAKASHIRO, K.-I., KLOSEK, S. K., GODA, H., HARA, S., UCHIDA, D. & HAMAKAWA, H. (2009). Hypoxia enhances CXCR4 expression by activating HIF-1 in oral squamous cell carcinoma. *Oncology reports,* 21**,** 707-712.

IZUMI, K., MIZOKAMI, A., SUGIMOTO, K., NARIMOTO, K., MIWA, S., MAEDA, Y., KADONO, Y., TAKASHIMA, M., KOH, E. & NAMIKI, M. (2009). Risedronate Recovers Bone Loss in Patients With Prostate Cancer Undergoing Androgen-deprivation Therapy. *Urology,* 73**,** 1342-1346.

JACOBSEN, B. M., HARRELL, J. C., JEDLICKA, P., BORGES, V. F., VARELLA-GARCIA, M. & HORWITZ, K. B. (2006). Spontaneous fusion with, and transformation of mouse stroma by, malignant human breast cancer epithelium. *Cancer research,* 66**,** 8274-8281.

JAMES BUCHANAN BRADY UROLOGICAL INSTITUTE, J. H. M. (2012). *The Partin Tables (online)* [Online]. Baltimore. Available: http://urology.jhu.edu/prostate/partintable.php [Accessed 27/06/2012 2012].

JEMAL, A., SIEGEL, R., WARD, E., HAO, Y., XU, J., MURRAY, T. & THUN, M. J. (2008). Cancer statistics, 2008. *CA: a cancer journal for clinicians,* 58**,** 71-96.

JOYCE, J. A. & POLLARD, J. W. (2009). Microenvironmental regulation of metastasis. *Nature Reviews Cancer,* 9**,** 239-252.

JUNG, S. J., KIM, C. I., PARK, C. H., CHANG, H. S., KIM, B. H., CHOI, M. S. & JUNG, H. R. (2011). Correlation between chemokine receptor CXCR4 expression and prognostic factors in patients with prostate cancer. *Korean journal of urology,* 52**,** 607-611.

KAIGHN ME, N. K., OHNUKI Y, LECHNER JF, JONES LW (1979). Establishment and characterization of a human prostatic carcinoma cell line (PC-3). *Investigative Urology,* 17**,** 16-23.

KANTOFF, P. W., HIGANO, C. S., SHORE, N. D., BERGER, E. R., SMALL, E. J., PENSON, D. F., REDFERN, C. H., FERRARI, A. C., DREICER, R., SIMS, R. B., XU, Y., FROHLICH, M. W. & SCHELLHAMMER, P. F. (2010). Sipuleucel-T Immunotherapy for Castration-Resistant Prostate Cancer. *New England Journal of Medicine,* 363**,** 411-422.

KOBAYASHI, A., OKUDA, H., XING, F., PANDEY, P. R., WATABE, M., HIROTA, S., PAI, S. K., LIU, W., FUKUDA, K., CHAMBERS, C., WILBER, A. & WATABE, K. (2011). Bone morphogenetic protein 7 in dormancy and metastasis of prostate cancer stem-like cells in bone. *Journal of Experimental Medicine,* 208**,** 2641-55.

KOENEMAN, K. S., YEUNG, F. & CHUNG, L. W. K. (1999). Osteomimetic properties of prostate cancer cells: A hypothesis supporting the predilection of prostate cancer metastasis and growth in the bone environment. *Prostate,* 39**,** 246-261.

KONG, D., BANERJEE, S., AHMAD, A., LI, Y., WANG, Z., SETHI, S. & SARKAR, F. H. (2010). Epithelial to mesenchymal transition is mechanistically linked with

stem cell signatures in prostate cancer cells. *PloS one,* 5**,** e12445. doi: 10.1371/journal.pone.0012445

KOSHIJI, M., KAGEYAMA, Y., PETE, E. A., HORIKAWA, I., BARRETT, J. C. & HUANG, L. E. (2004). HIF-1alpha induces cell cycle arrest by functionally counteracting Myc. *EMBO Journal,* 23**,** 1949-56.

KRISHNAN, B., SMITH, T. L., DUBEY, P., ZAPADKA, M. E., TORTI, F. M., WILLINGHAM, M. C., TALLANT, E. A. & GALLAGHER, P. E. (2013). Angiotensin-(1-7) attenuates metastatic prostate cancer and reduces osteoclastogenesis. *Prostate,* 73**,** 71-82.

KUMAR, R., SRINIVASAN, S., PAHARI, P., ROHR, J. & DAMODARAN, C. (2010). Activating Stress-Activated Protein Kinase-Mediated Cell Death and Inhibiting Epidermal Growth Factor Receptor Signaling: A Promising Therapeutic Strategy for Prostate Cancer. *Molecular Cancer Therapeutics,* 9**,** 2488-2496.

KUO, P. L., SHEN, K. H., HUNG, S. H. & HSU, Y. L. (2012). CXCL1/GROalpha increases cell migration and invasion of prostate cancer by decreasing fibulin-1 expression through NF-kappaB/HDAC1 epigenetic regulation. *Carcinogenesis,* 33**,** 2477-87.

KUSUMBE, A. P. & BAPAT, S. A. (2009). Cancer Stem Cells and Aneuploid Populations within Developing Tumors Are the Major Determinants of Tumor Dormancy. *Cancer Research,* 69**,** 9245-9253.

LAPIDOT, T., SIRARD, C., VORMOOR, J., MURDOCH, B., HOANG, T., CACERESCORTES, J., MINDEN, M., PATERSON, B., CALIGIURI, M. A. & DICK, J. E. (1994). A Cell Initiating Human Acute Myeloid-Leukemia after Transplantation into Scid Mice. *Nature,* 367**,** 645-648.

LAPOINTE, J., LI, C., HIGGINS, J. P., VAN DE RIJN, M., BAIR, E., MONTGOMERY, K., FERRARI, M., EGEVAD, L., RAYFORD, W. & BERGERHEIM, U. (2004). Gene expression profiling identifies clinically relevant subtypes of prostate cancer. *Proceedings of the National Academy of Sciences of the United States of America,* 101**,** 811.

LARSEN, J. M., CHRISTENSEN, I. J., NIELSEN, H. J. R., HANSEN, U., BJERREGAARD, B., TALTS, J. F. & LARSSON, L.-I. (2009). Syncytin immunoreactivity in colorectal cancer: Potential prognostic impact. *Cancer Letters,* 280**,** 44-49.

LARSSON, L.-I., HOLCK, S. & CHRISTENSEN, I. J. (2007). Prognostic role of syncytin expression in breast cancer. *Human Pathology,* 38**,** 726-731.

LATHIA, J., VENERE, M., RAO, M. & RICH, J. (2010). Seeing is Believing: Are Cancer Stem Cells the Loch Ness Monster of Tumor Biology? *Stem Cell Reviews and Reports,* 7**,** 227-237.

LEE, B. Y., HAN, J. A., IM, J. S., MORRONE, A., JOHUNG, K., GOODWIN, E. C., KLEIJER, W. J., DIMAIO, D. & HWANG, E. S. (2006). Senescence Associated B-galactosidase is lysosomal B-galactosidase. *Aging cell,* 5**,** 187-195.

LI, C., HEIDT, D. G., DALERBA, P., BURANT, C. F., ZHANG, L., ADSAY, V., WICHA, M., CLARKE, M. F. & SIMEONE, D. M. (2007). Identification of pancreatic cancer stem cells. *Cancer research,* 67**,** 1030-1039.

LI, S., KENNEDY, M., PAYNE, S., KENNEDY, K., SEEWALDT, V. L., PIZZO, S. V. & BACHELDER, R. E. (2014). Model of Tumor Dormancy/Recurrence after Short-Term Chemotherapy. *PLoS ONE,* 9**,** e98021. doi: 10.1371/journal.pone.0098021

LIU, C.-F., LIU, S.-Y., MIN, X.-Y., JI, Y.-Y., WANG, N., LIU, D., MA, N., LI, Z.-F. & LI, K. (2014). The Prognostic Value of CXCR4 in Ovarian Cancer: A Meta-Analysis. *PloS ONE,* 9**,** e92629. DOI: 10.1371/journal.pone.0092629.

LOGOTHETIS, C. J. & LIN, S. H. (2005). Osteoblasts in prostate cancer metastasis to bone. *Nature Reviews Cancer,* 5**,** 21-28.

LU, Y., CAI, Z., XIAO, G., KELLER, E. T., MIZOKAMI, A., YAO, Z., ROODMAN, G. D. & ZHANG, J. (2007). Monocyte chemotactic protein-1 mediates prostate cancer-induced bone resorption. *Cancer Research,* 67**,** 3646-3653.

LU, Z., QI, L., BO, X. J., LIU, G. D., WANG, J. M. & LI, G. (2013). Expression of CD26 and CXCR4 in prostate carcinoma and its relationship with clinical parameters. *Journal of research in medical sciences: the official journal of Isfahan University of Medical Sciences,* 18**,** 647-652.

MAHAJAN, K., COPPOLA, D., RAWAL, B., CHEN, Y. A., LAWRENCE, H. R., ENGELMAN, R. W., LAWRENCE, N. J. & MAHAJAN, N. P. (2012). Ack1-mediated androgen receptor phosphorylation modulates radiation resistance in castration-resistant prostate cancer. *Journal of Biological Chemistry,* 287**,** 22112-22.

MAHAJAN, N. P., LIU, Y., MAJUMDER, S., WARREN, M. R., PARKER, C. E., MOHLER, J. L., EARP, H. S. & WHANG, Y. E. (2007). Activated Cdc42-associated kinase Ack1 promotes prostate cancer progression via androgen receptor tyrosine phosphorylation. *Proceedings of the National Academy of Sciences,* 104**,** 8438-8443.

MANI, S. A., GUO, W., LIAO, M. J., EATON, E. N., AYYANAN, A., ZHOU, A. Y., BROOKS, M., REINHARD, F., ZHANG, C. C. & SHIPITSIN, M. (2008). The epithelial-mesenchymal transition generates cells with properties of stem cells. *Cell,* 133**,** 704-715.

MARKS, R. A., ZHANG, S., MONTIRONI, R., MCCARTHY, R. P., MACLENNAN, G. T., LOPEZ-BELTRAN, A., JIANG, Z., ZHOU, H., ZHENG, S., DAVIDSON, D. D., BALDRIDGE, L. A. & CHENG, L. (2008). Epidermal growth factor receptor (EGFR) expression in prostatic adenocarcinoma after hormonal therapy: A fluorescence in situ hybridization and immunohistochemical analysis. *The Prostate,* 68**,** 919-923.

MARSDEN, C. G., WRIGHT, M. J., CARRIER, L., MOROZ, K. & ROWAN, B. G. (2012). Disseminated breast cancer cells acquire a highly malignant and aggressive metastatic phenotype during metastatic latency in the bone. *PLoS ONE,* 7**,** e47587. doi: 10.1371/journal.pone.0047587

MCLENDON, R., FRIEDMAN, A., BIGNER, D., VAN MEIR, E. G., BRAT, D. J., MASTROGIANAKIS, G. M., OLSON, J. J., MIKKELSEN, T., LEHMAN, N. & ALDAPE, K. (2008). Comprehensive genomic characterization defines human glioblastoma genes and core pathways. *Nature,* 455**,** 1061-1068.

MEACHAM, C. E. & MORRISON, S. J. (2013). Tumour heterogeneity and cancer cell plasticity. *Nature,* 501**,** 328-337.

MOCHIZUKI, H., MATSUBARA, A., TEISHIMA, J., MUTAGUCHI, K., YASUMOTO, H., DAHIYA, R., USUI, T. & KAMIYA, K. (2004). Interaction of ligand,Äireceptor system between stromal-cell-derived factor-1 and CXC chemokine receptor 4 in human prostate cancer: a possible predictor of metastasis. *Biochemical and biophysical research communications,* 320**,** 656-663.

MORGAN, T. M., LANGE, P. H., PORTER, M. P., LIN, D. W., ELLIS, W. J., GALLAHER, I. S. & VESSELLA, R. L. (2009). Disseminated tumor cells in

prostate cancer patients after radical prostatectomy and without evidence of disease predicts biochemical recurrence. *Clinical Cancer Research,* 15**,** 677-83.

MUNDY, G. R. (2002). Metastasis to bone: causes, consequences and therapeutic opportunities. *Nature Reviews Cancer,* 2**,** 584-593.

NAKAGAWA, M., BANDO, Y., NAGAO, T., MORIMOTO, M., TAKAI, C., OHNISHI, T., HONDA, J., MORIYA, T., IZUMI, K. & TAKAHASHI, M. (2011). Expression of p53, Ki-67, E-cadherin, N-cadherin and TOP2A in triple-negative breast cancer. *Anticancer research,* 31**,** 2389-2393.

NAUMOV, G. N., TOWNSON, J. L., MACDONALD, I. C., WILSON, S. M., BRAMWELL, V. H., GROOM, A. C. & CHAMBERS, A. F. (2003). Ineffectiveness of doxorubicin treatment on solitary dormant mammary carcinoma cells or late-developing metastases. *Breast Cancer Research and Treatment,* 82**,** 199-206.

NELSON, J. B., NABULSI, A. A., VOGELZANG, N. J., BREUL, J., ZONNENBERG, B. A., DALIANI, D. D., SCHULMAN, C. C. & CARDUCCI, M. A. (2003). Suppression of prostate cancer induced bone remodeling by the endothelin receptor A antagonist atrasentan. *The Journal of urology,* 169**,** 1143-1149.

PATRAWALA, L., CALHOUN, T., SCHNEIDER-BROUSSARD, R., LI, H., BHATIA, B., TANG, S., REILLY, J. G., CHANDRA, D., ZHOU, J., CLAYPOOL, K., COGHLAN, L. & TANG, D. G. (2006). Highly purified CD44+ prostate cancer cells from xenograft human tumors are enriched in tumorigenic and metastatic progenitor cells. *Oncogene,* 25**,** 1696-1708.

PEDERSEN, E. A., SHIOZAWA, Y., PIENTA, K. J. & TAICHMAN, R. S. (2012). The prostate cancer bone marrow niche: more than just 'fertile soil'. *Asian Journal of Andrology,* 14**,** 423-7.

PESCE, G., GLEN, A., LIPPITT, J., FOWLES, A., REHMAN, I. & EATON, C. (2011). Spontaneous fusion between prostate cancer cells: A driver for development of tumor heterogeneity and growth in bone. *Bone,* 48**,** S46-S47.

PUNGLIA, R. S., D'AMICO, A. V., CATALONA, W. J., ROEHL, K. A. & KUNTZ, K. M. (2003). Effect of Verification Bias on Screening for Prostate Cancer by Measurement of Prostate-Specific Antigen. *New England Journal of Medicine,* 349**,** 335-342.

QUINTANA, E., SHACKLETON, M., SABEL, M. S., FULLEN, D. R., JOHNSON, T. M. & MORRISON, S. J. (2008). Efficient tumour formation by single human melanoma cells. *Nature,* 456**,** 593-598.

RABBANI, S. A., VALENTINO, M. L., ARAKELIAN, A., ALI, S. & BOSCHELLI, F. (2010). SKI-606 (Bosutinib) blocks prostate cancer invasion, growth, and metastasis in vitro and in vivo through regulation of genes involved in cancer growth and skeletal metastasis. *Molecular Cancer Therapies,* 9**,** 1147-57.

RACHKOVSKY, M., SODI, S., CHAKRABORTY, A., AVISSAR, Y., BOLOGNIA, J., MCNIFF, J. M., PLATT, J., BERMUDES, D. & PAWELEK, J. (1998). Melanoma x macrophage hybrids with enhanced metastatic potential. *Clinical and Experimental Metastasis,* 16**,** 299-312.

RADISKY, E. S. & RADISKY, D. C. (2010). Matrix metalloproteinase-induced epithelial-mesenchymal transition in breast cancer. *Journal of Mammary Gland Biology Neoplasia,* 15**,** 201-12.

RAMOS, E. A., GROCHOSKI, M., BRAUN-PRADO, K., SENISKI, G. G., CAVALLI, I. J., RIBEIRO, E. M., CAMARGO, A. A., COSTA, F. C. F. & KLASSEN, G. (201)1. Epigenetic changes of CXCR4 and its ligand CXCL12 as prognostic factors for sporadic breast cancer. *PLoS ONE,* 6**,** e29461. doi: 10.1371/journal.pone.0029461

REYA, TANNISHTHA, MORRISON, SEAN, J., CLARKE, MICHAEL, F., WEISSMAN & IRVING, L. (2001). Stem cells, cancer, and cancer stem cells : Stem cells. *Nature,* 414**,** 105-111.

RIBATTI, D., MANGIALARDI, G. & VACCA, A. (2006). Stephen Paget and the 'seed and soil' theory of metastatic dissemination. *Clinical and experimental medicine,* 6**,** 145-149.

ROESCH, A., FUKUNAGA-KALABIS, M., SCHMIDT, E. C., ZABIEROWSKI, S. E., BRAFFORD, P. A., VULTUR, A., BASU, D., GIMOTTY, P., VOGT, T. & HERLYN, M. (2010). A temporarily distinct subpopulation of slow-cycling melanoma cells is required for continuous tumor growth. *Cell,* 141**,** 583-594.

RUCCI, N. & TETI, A. (2010). Osteomimicry: how tumor cells try to deceive the bone. *Frontiers in Biosciences (Scholars Edition),* 2**,** 907-15.

RUPPENDER, N. S., MORRISSEY, C., LANGE, P. H. & VESSELLA, R. L. (2013) Dormancy in solid tumors: implications for prostate cancer. *Cancer Metastasis Reviews,* 32**,** 501-9.

SAAD, F., GLEASON, D. M., MURRAY, R., TCHEKMEDYIAN, S., VENNER, P., LACOMBE, L., CHIN, J. L., VINHOLES, J. J., GOAS, J. A., CHEN, B. & GROUP, F. T. Z. A. P. C. S. (2002). A Randomized, Placebo-Controlled Trial of Zoledronic Acid in Patients With Hormone-Refractory Metastatic Prostate Carcinoma. *Journal of the National Cancer Institute,* 94**,** 1458-1468.

SANTISTEBAN, M., REIMAN, J. M., ASIEDU, M. K., BEHRENS, M. D., NASSAR, A., KALLI, K. R., HALUSKA, P., INGLE, J. N., HARTMANN, L. C. & MANJILI, M. H. (2009). Immune-induced epithelial to mesenchymal transition in vivo generates breast cancer stem cells. *Cancer research,* 69**,** 2887.

SCHOLZEN, T. & GERDES, J. (2000). The Ki-67 protein: from the known and the unknown. *Journal of Cellular Physiology,* 182**,** 311-22.

SEPPORTA, M. V., TUMMINELLO, F. M., FLANDINA, C., CRESCIMANNO, M., GIAMMANCO, M., LA GUARDIA, M., DI MAJO, D. & LETO, G. (2013). Follistatin as potential therapeutic target in prostate cancer. *Targeted oncology,* 8**,** 215-223.

SETLUR, S. R., MERTZ, K. D., HOSHIDA, Y., DEMICHELIS, F., LUPIEN, M., PERNER, S., SBONER, A., PAWITAN, Y., ANDRON, O., JOHNSON, L. A., TANG, J., ADAMI, H.-O., CALZA, S., CHINNAIYAN, A. M., RHODES, D., TOMLINS, S., FALL, K., MUCCI, L. A., KANTOFF, P. W., STAMPFER, M. J., ANDERSSON, S.-O., VARENHORST, E., JOHANSSON, J.-E., BROWN, M., GOLUB, T. R. & RUBIN, M. A. (2008). Estrogen-Dependent Signaling in a Molecularly Distinct Subclass of Aggressive Prostate Cancer. *Journal of the National Cancer Institute,* 100**,** 815-825.

SHIOZAWA, Y., PEDERSEN, E. A., HAVENS, A. M., JUNG, Y., MISHRA, A., JOSEPH, J., KIM, J. K., PATEL, L. R., YING, C. & ZIEGLER, A. M. (2011a). Human prostate cancer metastases target the hematopoietic stem cell niche to establish footholds in mouse bone marrow. *The Journal of clinical investigation,* 121**,** 1298.

SHIOZAWA, Y., PEDERSEN, E. A., PATEL, L. R., ZIEGLER, A. M., HAVENS, A. M., JUNG, Y., WANG, J., ZALUCHA, S., LOBERG, R. D. & PIENTA, K. J. (2010). GAS6/AXL axis regulates prostate cancer invasion, proliferation, and survival in the bone marrow niche. *Neoplasia* 12**,** 116-127.

SHIOZAWA, Y., PIENTA, K. J. & TAICHMAN, R. S. (2011b). Hematopoietic Stem Cell Niche Is a Potential Therapeutic Target for Bone Metastatic Tumors. *Clinical Cancer Research,* 17**,** 5553-5558.

SIMS, N. A. & GOOI, J. H. (2008). Bone remodeling: Multiple cellular interactions required for coupling of bone formation and resorption. *Seminars in cell developmental biology,* 19**,** 444-451.

SMITH, D. C., SMITH, M. R., SWEENEY, C., ELFIKY, A. A., LOGOTHETIS, C., CORN, P. G., VOGELZANG, N. J., SMALL, E. J., HARZSTARK, A. L., GORDON, M. S., VAISHAMPAYAN, U. N., HAAS, N. B., SPIRA, A. I., LARA, P. N., JR., LIN, C. C., SRINIVAS, S., SELLA, A., SCHOFFSKI, P., SCHEFFOLD, C., WEITZMAN, A. L. & HUSSAIN, M. (2013). Cabozantinib in patients with advanced prostate cancer: results of a phase II randomized discontinuation trial. *Journal of Clincal Oncology,* 31**,** 412-419.

SMITH, M. R., EGERDIE, B., TORIZ, N. H. N., FELDMAN, R., TAMMELA, T. L. J., SAAD, F., HERACEK, J., SZWEDOWSKI, M., KE, C., KUPIC, A., LEDER, B. Z. & GOESSL, C. (2009). Denosumab in Men Receiving Androgen-Deprivation Therapy for Prostate Cancer. *New England Journal of Medicine,* 361**,** 745-755.

SOBIN, L. H. (2001). TNM, Principles, history, and relation to other prognostic factors. *Cancer,* 91**,** 1589-1592.

STEIN, S., ZOLTICK, B., PEACOCK, T., HOLROYDE, C., HALLER, D., ARMSTEAD, B., MALKOWICZ, B. S. & VAUGHN, D. J. (2001). Phase II Trial of Toremifene in Androgen-Independent Prostate Cancer: A Penn Cancer Clinical Trials Group Trial. *American Journal of Clinical Oncology,* 24**,** 283-285.

STILES, C. D., DESMOND, W., CHUMAN, L. M., SATO, G. & SAIER, M. H., JR. (1976). Relationship of cell growth behavior in vitro to tumorigenicity in athymic nude mice. *Cancer Research,* 36**,** 3300-5.

SUGIYAMA, T., KOHARA, H., NODA, M. & NAGASAWA, T. (2006). Maintenance of the hematopoietic stem cell pool by CXCL12-CXCR4 chemokine signaling in bone marrow stromal cell niches. *Immunity,* 25**,** 977-988.

SUN, Y. Ä., SCHNEIDER, A., JUNG, Y., WANG, J., DAI, J., WANG, J., COOK, K., OSMAN, N. I., KOH-PAIGE, A. J. & SHIM, H. (2005). Skeletal Localization and Neutralization of the SDF-1 (CXCL12)/CXCR4 Axis Blocks Prostate Cancer Metastasis and Growth in Osseous Sites In Vivo. *Journal of Bone and Mineral Research,* 20**,** 318-329.

SUZUKI, H., KAMIYA, N., IMAMOTO, T., KAWAMURA, K., YANO, M., TAKANO, M., UTSUMI, T., NAYA, Y. & ICHIKAWA, T. (2008). Current topics and perspectives relating to hormone therapy for prostate cancer. *International Journal of Clinical Oncology,* 13**,** 401-410.

TAICHMAN, R. S., COOPER, C., KELLER, E. T., PIENTA, K. J., TAICHMAN, N. S. & MCCAULEY, L. K. (2002). Use of the stromal cell-derived factor-1/CXCR4 pathway in prostate cancer metastasis to bone. *Cancer Research,* 62**,** 1832.

TAICHMAN, R. S., PATEL, L. R., BEDENIS, R., WANG, J., WEIDNER, S., SCHUMANN, T., YUMOTO, K., BERRY, J. E., SHIOZAWA, Y. & PIENTA, K. J. (2013). GAS6 receptor status is associated with dormancy and bone metastatic tumor formation. *PLoS ONE,* 8**,** e61873. doi: 10.1371/journal.pone.0061873

TAKAHASHI, Y., SAWADA, G., KURASHIGE, J., MATSUMURA, T., UCHI, R., UEO, H., ISHIBASHI, M., TAKANO, Y., AKIYOSHI, S., IWAYA, T., EGUCHI, H., SUDO, T., SUGIMACHI, K., YAMAMOTO, H., DOKI, Y., MORI, M. & MIMORI, K. (2013). Tumor-derived tenascin-C promotes the epithelial-mesenchymal transition in colorectal cancer cells. *Anticancer Research,* 33**,** 1927-34.

TANG, D. G. (2012). Understanding cancer stem cell heterogeneity and plasticity. *Cell research,* 22**,** 457-472.

TANNOCK, I. F., FIZAZI, K., IVANOV, S., KARLSSON, C. T., FLECHON, A., SKONECZNA, I., ORLANDI, F., GRAVIS, G., MATVEEV, V., BAVBEK, S., GIL, T., VIANA, L., AREN, O., KARYAKIN, O., ELLIOTT, T., BIRTLE, A., MAGHERINI, E., HATTEVILLE, L., PETRYLAK, D., TOMBAL, B. & ROSENTHAL, M. (2013). Aflibercept versus placebo in combination with docetaxel and prednisone for treatment of men with metastatic castration-resistant prostate cancer (VENICE): a phase 3, double-blind randomised trial. *Lancet Oncology,* 14**,** 760-8.

TEICHER, B. A. & FRICKER, S. P. (2010). CXCL12 (SDF-1)/CXCR4 pathway in cancer. *Clinical Cancer Research,* 16**,** 2927-2931.

THALMANN, G. N., ANEZINIS, P. E., CHANG, S.-M., ZHAU, H. E., KIM, E. E., HOPWOOD, V. L., PATHAK, S., VON ESCHENBACH, A. C. & CHUNG, L. W. K. (1994). Androgen-independent Cancer Progression and Bone Metastasis in the LNCaP Model of Human Prostate Cancer. *Cancer Research,* 54**,** 2577-2581.

THIERY, J. P., ACLOQUE, H., HUANG, R. Y. & NIETO, M. A. (2009). Epithelial-mesenchymal transitions in development and disease. *Cell,* 139**,** 871-90.

TOMLINS, S. A., RHODES, D. R., PERNER, S., DHANASEKARAN, S. M., MEHRA, R., SUN, X.-W., VARAMBALLY, S., CAO, X., TCHINDA, J., KUEFER, R., LEE, C., MONTIE, J. E., SHAH, R. B., PIENTA, K. J., RUBIN, M. A. & CHINNAIYAN, A. M. (2005). Recurrent Fusion of TMPRSS2 and ETS Transcription Factor Genes in Prostate Cancer. *Science,* 310**,** 644-648.

TSAI, J. H., DONAHER, J. L., MURPHY, D. A., CHAU, S. & YANG, J. (2012). Spatiotemporal regulation of epithelial-mesenchymal transition is essential for squamous cell carcinoma metastasis. *Cancer Cell,* 22**,** 725-36.

TSAI, J. H. & YANG, J. (2013). Epithelial-mesenchymal plasticity in carcinoma metastasis. *Genes and Development,* 27**,** 2192-206.

UMBAS, R., ISAACS, W. B., BRINGUIER, P. P., SCHAAFSMA, H.E., KARTHAUS, H.F., OOSTERHOF, G.O., DEBRUYNE, F.M. & SCHALKEN, J. A. (1994). Decreased E-cadherin expression is associated with poor prognosis in patients with prostate cancer. *Cancer Research,* 54**,** 3929-3933.

VAARALA, M. H., PORVARI, K., KYLLONEN, A. & VIHKO, P. (2000). Differentially expressed genes in two LNCaP prostate cancer cell lines reflecting changes during prostate cancer progression. *Laboratory investigation,* 80**,** 1259-1268.

VAN DEN HOOGEN, C., VAN DER HORST, G., CHEUNG, H., BUIJS, J. T., LIPPITT, J. M., GUZMAN-RAMIREZ, N., HAMDY, F. C., EATON, C. L., THALMANN, G. N., CECCHINI, M. G., PELGER, R. C. M. & VAN DER PLUIJM, G. (2010). High Aldehyde Dehydrogenase Activity Identifies Tumor-Initiating and Metastasis-Initiating Cells in Human Prostate Cancer. *Cancer Research,* 70**,** 5163-5173.

VAN OIJEN, M. G., MEDEMA, R. H., SLOOTWEG, P. J. & RIJKSEN, G. (1998). Positivity of the proliferation marker Ki-67 in noncycling cells. *American Journal of Clinical Pathology,* 110**,** 24-31.

VISVADER, J. E. & LINDEMAN, G. J. 2008. Cancer stem cells in solid tumours: accumulating evidence and unresolved questions. *Nature Reviews Cancer,* 8**,** 755-768.

VOGEL, C. & MARCOTTE, E. M. (2012). Insights into the regulation of protein abundance from proteomic and transcriptomic analyses. *Nature Reviews Genetics,* 13**,** 227-232.

WANG, N., DOCHERTY, F. E., BROWN, H. K., REEVES, K. J., FOWLES, A. C. M., OTTEWELL, P. D., DEAR, T. N., HOLEN, I., CROUCHER, P. I. & EATON, C. L. (2014). Prostate Cancer Cells Preferentially Home to Osteoblast-Rich Areas in the Early Stages of Bone Metastasis – Evidence from In Vivo Models. *Journal of Bone and Mineral Research***,** 29, 2688-2696.

WANG, R., CHADALAVADA, K., WILSHIRE, J., KOWALIK, U., HOVINGA, K. E., GEBER, A., FLIGELMAN, B., LEVERSHA, M., BRENNAN, C. & TABAR, V. (2010). Glioblastoma stem-like cells give rise to tumour endothelium. *Nature,* 468**,** 829-833.

WHITMORE, W. F. (1973). The natural history of prostatic cancer. *Cancer,* 32**,** 1104-1112.

WILLIAMSON, S. C., HEPBURN, A. C., WILSON, L., COFFEY, K., RYAN-MUNDEN, C. A., PAL, D., LEUNG, H. Y., ROBSON, C. N. & HEER, R. (2012). Human a2b1HI CD133+ VE epithelial prostate stem cells express low levels of active androgen receptor. *PLoS ONE,* 7**,** e48944. doi: 10.1371/journal.pone.0048944

XING, Y., LIU, M., DU, Y., QU, F., LI, Y., ZHANG, Q., XIAO, Y., ZHAO, J., ZENG, F. & XIAO, C. (2008). Tumor cell-specific blockade of CXCR4/SDF-1 interactions in prostate cancer cells by hTERT promoter induced CXCR4 knockdown: A possible metastasis preventing and minimizing approach. *Cancer biology & therapy,* 7**,** 1839-1848.

XU, M.-H., GAO, X., LUO, D., ZHOU, X.-D., XIONG, W. & LIU, G.-X. (2014). EMT and acquisition of stem cell-like properties are involved in spontaneous formation of tumorigenic hybrids between lung cancer and bone marrow-derived mesenchymal stem cells. *PLoS ONE,* 9**,** e87893. doi: 10.1371/journal.pone.0087893.

YANG, C. H., WANG, H. L., LIN, Y. S., KUMAR, K. P., LIN, H. C., CHANG, C. J., LU, C. C., HUANG, T. T., MARTEL, J., OJCIUS, D. M., CHANG, Y. S., YOUNG, J. D. & LAI, H. C. (2014a). Identification of CD24 as a Cancer Stem Cell Marker in Human Nasopharyngeal Carcinoma. *PLoS ONE,* 9**,** e99412. doi: 10.1371/journal.pone.0099412

YANG, P., LIANG, S.-X., HUANG, W.-H., ZHANG, H.-W., LI, X.-L., XIE, L.-H., DU, C.-W. & ZHANG, G.-J. (2014b). Aberrant Expression of CXCR4 Significantly Contributes to Metastasis and Predicts Poor Clinical Outcome in Breast Cancer. *Current molecular medicine,* 14**,** 174-184.

YIN, J. J., MOHAMMAD, K. S., KAKONEN, S. M., HARRIS, S., WU-WONG, J. R., WESSALE, J. L., PADLEY, R. J., GARRETT, I. R., CHIRGWIN, J. M. & GUISE, T. A. (2003). A causal role for endothelin-1 in the pathogenesis of osteoblastic bone metastases. *Proceedings of the National Academy of Sciences of the United States of America,* 100**,** 10954-10959.

YU, M., BARDIA, A., WITTNER, B., STOTT, S., SMAS, M., TING, D., ISAKOFF, S.,CICILIANO, C., WELLS, M., SHAH, A., CONCANNON, K., DONALDSON, M.,SEQUIST, L., BRACHTEL, E., SGORI, D., BASELGA, J., RAMASWAMY, S., TONER, M., HABER, D., MAHESWARAN, S. (2013). Circulating Breast Tumor Cells Exhibit Dynamic Changes in Epithelial and Mesenchymal Composition. *Science*, 339, 580-584

YU, S., WANG, X., LIU, G., ZHU, X. & CHEN, Y. (2013). High level of CXCR4 in triple-negative breast cancer specimens associated with a poor clinical outcome. *Acta Med Okayama,* 67**,** 369-75.

YUMOTO, K., BERRY, J. E., TAICHMAN, R. S., & SHIOZAWA, Y. (2014). A novel method for monitoring tumor proliferation in vivo using fluorescent dye DiD. *Cytometry Part A*, *85*, 548-555.

ZAYZAFOON, M., ABDULKADIR, S. A. & MCDONALD, J. M. (2004). Notch signaling and ERK activation are important for the osteomimetic properties of prostate cancer bone metastatic cell lines. *Journal of Biological Chemistry,* 279**,** 3662-3670.

ZHANG, J., DAI, J., QI, Y., LIN, D. L., SMITH, P., STRAYHORN, C., MIZOKAMI, A., FU, Z., WESTMAN, J. & KELLER, E. T. (2001). Osteoprotegerin inhibits prostate cancer-induced osteoclastogenesis and prevents prostate tumor growth in the bone. *Journal of Clinical Investigation,* 107**,** 1235-1284.

ZHANG, J., DAI, J., YAO, Z., LU, Y., DOUGALL, W. & KELLER, E. T. (2003). Soluble receptor activator of nuclear factor KB Fc diminishes prostate cancer progression in bone. *Cancer research,* 63**,** 7883-7890.

Appendices

Appendix 1.1

Gene Abbreviation	Gene Name
ACPP	Acid Phosphatase, Prostate
ACTA2	Actin, alpha 2
ADAMTS1	Metallopeptidase With Thrombospondin Type 1 Motif
ADM2	Adrenomedullin 2
AKT1	V-akt murine thymoma viral oncogene homolog 1
ALDH7A1	Aldehyde dehydrogenase 7 family, member A1
ALPL	Alkaline phosphatase
ANGPT1	Angiopoietin 1
ANXA2	Annexin A2
AR	Androgen receptor
AXL	AXL Receptor Tyrosine Kinase
BGLAP	Bone Gamma-Carboxyglutamate (Gla) Protein
BMI1	B lymphoma Mo-MLV insertion region 1 homolog1
BMP2	Bone Morphogenetic Protein 2
BMP6	Bone Morphogenetic Protein 6
BMP7	Bone Morphogenetic Protein 7
CD24	Cluster of differentiation 24
CD34	Cluster of differentiation 34
CD38	Cluster of differentiation 38
CD44	Cluster of differentiation 44
CDH1	E-cadherin
CDH2	N-Cadherin
CDH7	Cadherin 7, Type 2
CLDN4	Claudin 4
COL1A1	Collagen, type I, alpha 1
COX2-Mm	Murine specific Mitochondrially Encoded Cytochrome C Oxidase II
CXCL1	Chemokine (C-X-C Motif) Ligand 1
CXCL12	Chemokine (C-X-C Motif) Ligand 12
CXCL16	Chemokine (C-X-C Motif) Ligand 16
CXCR4	Chemokine (C-X-C Motif) Receptor 4
CXCR6	Chemokine (C-X-C Motif) Receptor 6
CXCR7	Chemokine (C-X-C Motif) Receptor 7
DKK1	Dickkopf WNT Signaling Pathway Inhibitor 1
DSP	Desmoplakin
ERG	V-Ets Avian Erythroblastosis Virus E26 Oncogene Homolog
ESR1	Estrogen Receptor 1
ESR2	Estrogen Receptor 2
FGF2	Fibroblast growth factor 2
FGF8	Fibroblast growth factor 8
FN1	Fibronectin
FST	Follistatin
GAPDH-Mm	Murine specific Glyceraldehyde-3-Phosphate Dehydrogenase
GAS6	Growth arrest-specific 6
ITGA2	Integrin, Alpha 2
ITGA4	Integrin, Alpha 4
ITGB1	Integrin, Beta 1

JAG1	Jagged 1
KIT	V-Kit Hardy-Zuckerman 4 Feline Sarcoma Viral Oncogene
KLK3	Kallikrein-Related Peptidase 3
KRT18	Keratin 18
KRT5	Keratin 5
KRT8	Keratin 8
LDHA	Lactate dehydrogenase A
LDHB	Lactate dehydrogenase B
MATN2	Matrilin 2
MCAM	Melanoma cell adhesion molecule (CD146)
MMP2	Matrix metalloproteinase-2
MMP3	Matrix metalloproteinase-3
MUC1	Mucin 1
NANOG	Nanog Homeobox
NES	Nestin
NOG	Noggin
NOTCH1	NOTCH1
NR3C1	Nuclear Receptor Subfamily 3, Group C, Member 1 (NR3C1)
OCLN	Occludin
PGR	Progesterone recepto
POU5F1	POU Class 5 Homeobox 1(OCT4)
PROM1	Prominin 1(CD133)
PSCA	Prostate stem cell antigen
PTEN	Phosphatase and tensin homolog
RHOB	Ras Homolog Family Member B
RUNX2	Runt-Related Transcription Factor 2
S100A4	Fibroblast-Specific Protein-1
SDC1	Syndecan 1
SHH	Sonic hedgehog
SOX2	SRY (Sex Determining Region Y)-Box 2
SPARC	Osteonectin
SPP1	Osteopontin
TEK	Tyrosine Kinase, Endothelial
TERT	Telomerase reverse transcriptase
TGFB1	Transforming Growth Factor, Beta 1
TGFBR1	Transforming Growth Factor, Beta Receptor 1
TJP1	Tight Junction Protein 1
TMPRSS2-ERG	Transmembrane Protease, Serine 2 fusion gene with ERG
TMPRSS2	Transmembrane Protease, Serine 2
TNC	Tenascin C
TNFRSF11A	Tumor Necrosis Factor Receptor Superfamily, Member 11a, NFKB
TNFRSF11B	Osteoprotegerin
TNFSF11	Tumor Necrosis Factor (Ligand) Superfamily, Member 11(RANKL)
TP63	Tumour Protein P63
VIM	Vimentin
VTN	Vitronectin

Appendix 1.2

Gene	ΔCT DiD-	ΔCT DiD+	P value
ACPP	9.94 ± 0.16	9.90 ± 0.41	0.875
ACTA2	15.85 ± 0.47	15.40 ± 0.22	0.209
ADAMTS1	10.50 ± 0.43	9.61 ± 0.44	0.068
ADM2	12.64 ± 0.24	12.27 ± 0.20	0.112
AKT1	6.02 ± 0.10	5.85 ± 0.07	0.091
ALDH7A1	8.17 ± 0.25	8.69 ± 0.50	0.186
ALPL	17.70 ± 0.53	19.76 ± 0.53	0.626
ANGPT1	15.21733 ± 0.29	15.36 ± 0.22	0.528
ANXA2	**3.87 ± 0.19**	**3.27 ± 0.11**	**0.010**
AR	17.00 ± 0.64	16.59 ± 0.42	0.403
AXL	10.87 ± 0.40	10.15 ± 0.65	0.176
BGLAP	17.08 ± 0.45	17.37 ± 0.69	0.652
BMI1	5.06 ± 0.39	4.66 ± 0.27	0.223
BMP2	8.33 ± 0.53	7.53 ± 0.77	0.215
BMP6	7.62 ± 0.47	7.96 ± 0.44	0.421
BMP7	**15.13 ± 0.27**	**14.00 ± 0.53**	**0.030**
CD24	**4.04 ± 0.15**	**3.13 ± 0.26**	**0.007**
CD34	UD	UD	UD
CD38	13.79 ± 0.38	13.88 ± 0.45	0.810
CD44	5.12 ± 0.29	4.66 ± 0.30	0.125
CDH1	6.29 ± 0.28	5.95 ± 0.50	0.359
CDH2	6.53 ± 0.19	6.33 ± 0.12	0.213
CDH7	11.48 ± 0.38	11.34 ± 0.10	0.560
CLDN4	6.99 ± 0.11	6.77 ± 0.49	0.480
COL1A1	**16.51 ± 0.96**	**14.15 ± 0.61**	**0.023**
COX2-Mm	UD	UD	UD
CXCL1	**14.25 ± 0.29**	**11.00 ± 0.34**	**0.0002**
CXCL12	17.99 ± 0.65	21.53 ± 0.45	0.865
CXCL16	8.80 ± 0.47	8.94 ± 0.46	0.742
CXCR4	**9.35 ± 0.72**	**7.58 ± 0.71**	**0.038**
CXCR6	UD	UD	UD
CXCR7	12.27 ± 0.27	11.60 ± 0.56	0.138
DKK1	3.93 ± 0.46	2.97 ± 0.41	0.055
DSP	10.47 ± 0.27	9.95 ± 0.58	0.231
ERG	UD	UD	UD
ESR1	**18.14**	**17.23 ± 0.19**	**0.020**
ESR2	14.56 ± 0.46	14.71 ± 0.43	0.726
FGF2	10.79 ± 0.12	9.96 ± 0.45	0.037
FGF8	16.00 ± 1.19	16.03 ± 0.93	0.983
FN1	**9.98 ± 0.19**	**7.01 ± 0.44**	**0.0004**
FST	**9.39 ± 0.47**	**7.21 ± 0.19**	**0.0017**
Gapdh-Mm	UD	UD	UD
GAS6	UD	UD	UD
ITGA2	**6.91 ± 0.25**	**5.99 ± 0.45**	**0.048**
ITGA4	*UD*	*UD*	*UD*
ITGB1	4.46 ± 0.65	3.83 ± 0.44	0.233
JAG1	**7.83 ± 0.05**	**7.26 ± 0.10**	**0.0010**

KIT	UD	UD	UD
KLK3	UD	UD	UD
KRT18	11.06 ± 0.23	11.11 ± 0.22	0.819
KRT5	UD	UD	UD
KRT8	16.91 ± 0.57	16.44 ± 0.59	0.368
LDHA	3.22 ± 0.30	2.88 ± 0.38	0.288
LDHB	**4.04 ± 0.09**	**5.01 ± 0.39**	**0.014**
MATN2	**10.81 ± 0.18**	**9.09 ± 0.14**	**0.0001**
MCAM	**10.76 ± 0.14**	**12.21 ± 0.004**	**0.00007**
MMP2	**17.63 ± 0.19**	**16.29 ± 0.35**	**0.0044**
MMP3	**17.91 ± 0.10**	**13.39 ± 0.48**	**0.00009**
MUC1	12.47 ± 0.24	11.93 ± 0.49	0.160
NANOG	12.02 ± 1.42	11.93 ± 0.41	0.914
NES	**8.31 ± 0.25**	**9.47 ± 0.41**	**0.013**
NOG	11.04 ± 0.30	11.09 ± 0.87	0.936
NOTCH1	8.57 ± 0.35	8.99 ± 0.50	0.310
NR3C1	13.15 ± 0.33	12.50 ± 0.40	0.093
OCLN	8.05 ± 0.05	8.15 ± 0.14	0.333
PGR	17.89 ± 0.74	18.60 ± 0.51	0.802
POU5F1	11.59 ± 1.17	11.94 ± 0.49	0.650
PROM1	UD	UD	UD
PSCA	**18.17 ± 0.19**	**15.58 ± 0.37**	**0.0004**
PTEN	*UD*	*UD*	*UD*
RHOB	8.61 ± 0.20	8.93 ± 0.50	0.375
RUNX2	11.12 ± 0.65	11.29 ± 0.21	0.703
S100A4	7.46 ± 0.11	7.51 ± 0.62	0.899
SDC1	7.42 ± 0.39	7.24 ± 0.32	0.560
SHH	18.07 ± 0.50	17.93 ± 0.29	0.142
SOX2	12.47 ± 0.48	12.57 ± 0.38	0.801
SPARC	5.80 ± 0.37	5.68 ± 0.47	0.750
SPP1	UD	UD	UD
TEK	17.12 ± 0.39	16.19 ± 0.63	0.096
TERT	12.36 ± 0.50	13.07 ± 0.19	0.083
TGFB1	5.51 ± 0.80	5.69 ± 0.09	0.770
TGFBR1	8.00 ± 0.02	8.15 ± 0.55	0.052
TJP1	8.09 ± 0.27	8.01 ± 0.09	0.773
TMPRSS2-ERG	UD	UD	UD
TMPRSS2	**15.59 ± 0.64**	**13.74 ± 0.30**	**0.010**
TNC	**9.05 ± 0.26**	**7.76 ± 0.37**	**0.007**
TNFRSF11A	12.62 ± 0.39	13.54± 0.67	0.111
TNFRSF11B	13.98 ± 0.27	14.00 ± 0.56	0.963
TNFSF11	UD	UD	UD
TP63	9.49 ± 4.39	12.37 ± 0.12	0.321
VIM	1.73 ± 0.71	1.70 ± 0.54	0.937
VTN	**18.23 ± 0.30**	**16.58 ± 0.94**	**0.043**

Appendix 1.3

Gene Abbreviation	Gene Name
CD34	Cluster of differentiation 34
COL1A1	Collagen, type I, alpha 1
CXCL1	Chemokine (C-X-C Motif) Ligand 1
CXCL12	Chemokine (C-X-C Motif) Ligand 12
CXCR4	Chemokine (C-X-C Motif) Receptor 4
DKK1	Dickkopf WNT Signaling Pathway Inhibitor 1
FN1	Fibronectin
FST	Follistatin
HIF1A	Hypoxia-inducible factor 1 alpha
MATN2	Matrilin 2
MCAM	Melanoma cell adhesion molecule (CD146)
MMP2	Matrix metalloproteinase-2
MMP3	Matrix metalloproteinase-3
NES	Nestin
POSTN	Periostin
PSCA	Prostate stem cell antigen
SHH	Sonic Hedgehog
SOSTDC1	Sclerostin Domain Containing 1
TEK	Tyrosine Kinase, Endothelial
TNC	Tenascin C
TP63	Tumor Protein P63
VTN	Vitronectin